



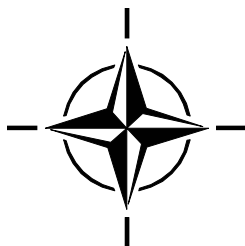
RTO TECHNICAL REPORT

TR-HFM-090

# **Test Methodology for Protection of Vehicle Occupants against Anti-Vehicular Landmine Effects**

(Méthodologie d'essais pour la protection des  
occupants de véhicules contre les effets  
des mines terrestres anti-véhicules)

Final Report of HFM-090 Task Group 25.



Published April 2007





RTO TECHNICAL REPORT

TR-HFM-090

# **Test Methodology for Protection of Vehicle Occupants against Anti-Vehicular Landmine Effects**

(Méthodologie d'essais pour la protection des  
occupants de véhicules contre les effets  
des mines terrestres anti-véhicules)

Final Report of HFM-090 Task Group 25.

---

# The Research and Technology Organisation (RTO) of NATO

RTO is the single focus in NATO for Defence Research and Technology activities. Its mission is to conduct and promote co-operative research and information exchange. The objective is to support the development and effective use of national defence research and technology and to meet the military needs of the Alliance, to maintain a technological lead, and to provide advice to NATO and national decision makers. The RTO performs its mission with the support of an extensive network of national experts. It also ensures effective co-ordination with other NATO bodies involved in R&T activities.

RTO reports both to the Military Committee of NATO and to the Conference of National Armament Directors. It comprises a Research and Technology Board (RTB) as the highest level of national representation and the Research and Technology Agency (RTA), a dedicated staff with its headquarters in Neuilly, near Paris, France. In order to facilitate contacts with the military users and other NATO activities, a small part of the RTA staff is located in NATO Headquarters in Brussels. The Brussels staff also co-ordinates RTO's co-operation with nations in Middle and Eastern Europe, to which RTO attaches particular importance especially as working together in the field of research is one of the more promising areas of co-operation.

The total spectrum of R&T activities is covered by the following 7 bodies:

- AVT Applied Vehicle Technology Panel
- HFM Human Factors and Medicine Panel
- IST Information Systems Technology Panel
- NMSG NATO Modelling and Simulation Group
- SAS System Analysis and Studies Panel
- SCI Systems Concepts and Integration Panel
- SET Sensors and Electronics Technology Panel

These bodies are made up of national representatives as well as generally recognised 'world class' scientists. They also provide a communication link to military users and other NATO bodies. RTO's scientific and technological work is carried out by Technical Teams, created for specific activities and with a specific duration. Such Technical Teams can organise workshops, symposia, field trials, lecture series and training courses. An important function of these Technical Teams is to ensure the continuity of the expert networks.

RTO builds upon earlier co-operation in defence research and technology as set-up under the Advisory Group for Aerospace Research and Development (AGARD) and the Defence Research Group (DRG). AGARD and the DRG share common roots in that they were both established at the initiative of Dr Theodore von Kármán, a leading aerospace scientist, who early on recognised the importance of scientific support for the Allied Armed Forces. RTO is capitalising on these common roots in order to provide the Alliance and the NATO nations with a strong scientific and technological basis that will guarantee a solid base for the future.

The content of this publication has been reproduced directly from material supplied by RTO or the authors.

Published April 2007

Copyright © RTO/NATO 2007  
All Rights Reserved

ISBN 978-92-837-0068-5

Single copies of this publication or of a part of it may be made for individual use only. The approval of the RTA Information Management Systems Branch is required for more than one copy to be made or an extract included in another publication. Requests to do so should be sent to the address on the back cover.



# Table of Contents

	Page
<b>List of Figures</b>	<b>vii</b>
<b>List of Tables</b>	<b>x</b>
<b>List of Symbols and Abbreviations</b>	<b>xi</b>
<b>List of Definitions</b>	<b>xiv</b>
<b>Programme Committee</b>	<b>xvii</b>
<b>Acknowledgements</b>	<b>xviii</b>
<b>Executive Summary and Synthèse</b>	<b>ES-1</b>
<b>Chapter 1 – Introduction</b>	<b>1-1</b>
1.1 Background and Problem Definition	1-1
1.1.1 Background	1-1
1.1.2 Problem Definition	1-2
1.2 The Objective and Approach of the HFM-090/TG-25	1-2
1.2.1 Objective	1-2
1.2.2 Approach	1-2
1.3 Organization of this Report	1-3
1.4 References	1-3
<b>Chapter 2 – The Mine Detonation Process and Occupant Loading</b>	<b>2-1</b>
2.1 Introduction to Mines	2-1
2.2 The Effects of an Anti-Vehicle Blast Mine Detonation	2-2
2.2.1 Local Effects	2-2
2.2.2 Global Effects	2-2
2.2.3 Drop Down Effects	2-3
2.2.4 Subsequent Effects	2-3
2.3 Occupant Loading	2-3
2.4 References	2-7
<b>Chapter 3 – Injury Criteria and Tolerance Levels</b>	<b>3-1</b>
3.1 Injury Biomechanics	3-1
3.2 Lower Leg	3-5
3.2.1 Anatomy, Loading Mechanisms and Injuries	3-5
3.2.2 Injury Risk Model	3-6
3.2.3 Conclusions	3-9
3.3 Thoraco-Lumbar Spine	3-9
3.3.1 Anatomy, Loading Mechanisms and Injuries	3-10
3.3.2 Injury Risk Model	3-11
3.3.3 Conclusions	3-14

3.4	Neck	3-14
3.4.1	Anatomy, Loading Mechanisms and Injuries to the Neck	3-14
3.4.2	Injury Criteria	3-18
3.4.3	Conclusions	3-20
3.5	Head	3-21
3.5.1	Anatomy, Loading Mechanisms and Injuries	3-21
3.5.2	Injury Assessment Models	3-22
3.5.3	Conclusions	3-22
3.6	Internal Organs	3-23
3.6.1	Anatomy, Loading Mechanisms and Injuries	3-23
3.6.2	Injury Risk Criteria	3-25
3.6.3	Conclusions	3-28
3.7	Summary on Injury Criteria and Tolerance Levels	3-28
3.8	References	3-29

## **Chapter 4 – Test Methods and Procedures** **4-1**

4.1	Human Surrogates	4-1
4.2	The Hybrid III 50 <sup>th</sup> Percentile Male Anthropomorphic Test Device (ATD)	4-1
4.3	Anthropomorphic Test Device (ATD) Positioning	4-5
4.3.1	The Position in the Vehicle	4-5
4.3.2	The Seating Posture	4-5
4.3.3	The Clothing of the ATD	4-6
4.4	Measurements with the Hybrid III ATD	4-7
4.4.1	Certification and Calibration	4-8
4.4.2	Temperature Conditions	4-8
4.5	Pressure Measurement Device	4-8
4.5.1	Pressure Measurement Device on the Chest of the ATD	4-10
4.5.2	Pressure Measurement Device at Another Position	4-10
4.5.3	Pressure Transducer Specifications	4-11
4.6	Additional Measurements	4-12
4.7	Summary	4-12
4.8	References	4-12

## **Chapter 5 – Conclusions** **5-1**

### **Annex A – Terms of Reference (TOR)** **A-1**

A.1	Origin	A-1
A.1.1	Background	A-1
A.1.2	Justification (Relevance to NATO)	A-1
A.2	Objectives	A-1
A.2.1	General Goals	A-1
A.2.2	Expected Deliverables	A-1
A.3	Resources	A-2
A.3.1	Membership	A-2
A.3.2	National and/or NATO Resources Needed	A-2

A.4	Security Level	A-3
A.5	Participation by Partner Nations	A-3
A.6	Liaison	A-3

**Annex B – Epidemiological Data on AV Mine Incidents** **B-1**

B.1	References	B-2
-----	------------	-----

**Annex C – Information Related to AV Blast Landmine Injuries** **C-1**

C.1	Introduction	C-1
C.2	Injury Scaling and Injury Risk Assessment	C-1
C.2.1	Injury Scaling	C-1
C.2.2	Injury Risk Assessment	C-2
C.3	AV Blast Mine Injuries and their Consequences	C-2
C.3.1	Injuries, Recovery and Impairment	C-3
C.3.2	Parameters that Influence the Injury Severity	C-5
C.3.3	Distance between Mine and Occupant	C-5
C.3.4	Type of Vehicle	C-6
C.3.5	Loading Conditions	C-7
C.4	Discussion and Conclusions	C-7
C.5	References	C-8

**Annex D – Mine Awareness for Vehicle Occupants** **D-1**

**Annex E – Supplemental Information on Lower Leg Injury Assessment** **E-1**

E.1	Introduction	E-1
E.2	Foot/Ankle Injury Risk Models for Pure Axial Loading	E-1
E.2.1	Yoganandan Model	E-1
E.2.2	Griffin Model	E-3
E.2.3	Kuppa Model	E-4
E.2.4	Seipel Model	E-5
E.2.5	Funk Model	E-5
E.2.6	Hirsch	E-7
E.2.7	The Lower Leg Threshold (LLth)	E-9
E.2.8	Summary, Analysis and Discussion	E-10
E.3	Other Lower Leg Injury Models	E-12
E.3.1	The Tibia Index (TI)	E-13
E.3.2	Ankle Rotation Injury Risk Models	E-13
E.4	Lower Leg Surrogates	E-14
E.4.1	Frangible Synthetic Lower Legs Surrogates: CLL and FSL	E-15
E.4.2	Post Mortem Human Subjects	E-16
E.4.3	Comparison between Hybrid III Lower Leg and Thor-Lx	E-16
E.5	The Effect of Boots on Lower Leg Protection	E-17
E.6	Effect of Leg Positioning	E-19
E.7	Conclusion	E-20
E.8	References	E-20

---

## **Annex F – Supplemental Information on Thoraco-Lumbar Spine Injury Assessment** **F-1**

F.1	Introduction	F-1
F.2	Quasi-Static Strength	F-1
F.3	Dynamic Strength	F-5
F.4	Miscellaneous	F-9
F.5	Summary	F-10
F.6	References	F-11

## **Annex G – Supplemental Information on Neck Injury Assessment** **G-1**

G.1	Introduction	G-1
G.2	Neck Injuries	G-1
G.3	Axial Compression Injury Criterion	G-2
G.4	Flexion/Extension Injury Criteria	G-3
G.5	The Neck Injury Criterion ( $N_{ij}$ )	G-4
G.6	Other Neck Injury Criteria	G-5
G.7	Summary	G-6
G.8	References	G-7

## **Annex H – Supplemental Information on Overpressure Injury Assessment** **H-1**

H.1	Introduction	H-1
H.2	Overpressure	H-1
H.3	Non Auditory Injury Assessment	H-3
H.3.1	Bowen Model	H-3
H.3.2	Stuhmiller Model	H-4
H.3.3	Axelsson Model	H-6
H.4	Summary	H-10
H.5	References	H-10

## **Annex I – Test Protocol for Occupant Safety Measurements and Injury Assessment** **I-1**

I.1	Description of the Test Set-up	I-1
I.1.1	Instrumentation for Injury Assessment	I-1
I.1.2	Description of the Anthropomorphic Test Device (ATD) Measurement	I-1
I.1.3	Hybrid III Positioning	I-5
I.1.4	Description of the Pressure Measurement Devices	I-7
I.1.5	Data Acquisition	I-9
I.1.6	Signal Processing	I-10
I.2	Description of Injury Assessment	I-11
I.2.1	Critical Body Parts	I-11
I.2.2	Injury Criteria	I-12
I.2.3	Injury Assessment	I-15
I.3	References	I-18

## List of Figures

<b>Figure</b>		<b>Page</b>
Figure 1.1	Example of Mine Detonation under a Logistic Vehicle	1-1
Figure 2.1	Time Sequence of Events during an AV Mine Detonation	2-3
Figure 2.2	Experimental and Numerical Example of Severe Leg Load Situation	2-4
Figure 2.3	Example of Axial Compression Force Signals in Tibia, Lumbar Spine and Neck for the More Local Effects Caused by a Mine Detonation under a Vehicle	2-5
Figure 2.4	Example of Axial Compression Force Signals in Tibia, Lumbar Spine and Neck for the Global Effects Caused by a Mine Detonation under a Vehicle	2-5
Figure 2.5	Loading Process in Human Body Due to Mine Detonation	2-6
Figure 3.1	Three Principle Mechanisms	3-2
Figure 3.2	Examples of Injury Risk Curves for Different Body Parts and Different Severities	3-2
Figure 3.3	The Threat Load Injury (TLI) Model	3-4
Figure 3.4	Flow Scheme to Determine Injury Tolerance Levels for Body Regions	3-4
Figure 3.5	The Lower Limb	3-5
Figure 3.6	Foot/Ankle Complex Anatomy	3-6
Figure 3.7	Experimental Set-up for MCW Dynamic Axial Impact Tests on PMHS Lower Legs	3-7
Figure 3.8	Risk of Foot/Ankle Injury as a Function of Age and Tibia Axial Force	3-7
Figure 3.9	Foot/Ankle Injury Risk Curves for 25, 45 and 65 Years Old	3-8
Figure 3.10	Lateral View of Vertebral Column and Lumbar Vertebra with Vertebral Body, Vertebral Arch and Facet Joints and Processes	3-10
Figure 3.11	DRIZ Model	3-12
Figure 3.12	Spinal Injury Risk Calculated from Laboratory and Operational Data and F-4 Operational Data Valid for AIS 2+ Injuries	3-13
Figure 3.13	Cervical Vertebrae	3-15
Figure 3.14	Anatomical Description of Head Movement	3-16
Figure 3.15	Engineering Description of Neck Loading	3-16
Figure 3.16	Injury Tolerance Curves for Axial Neck Compression Force when Using a Hybrid III 50 <sup>th</sup> Percentile Male ATD	3-19
Figure 3.17	Anatomical Structure of the Head and Brain	3-21
Figure 3.18	The Auditory System	3-23
Figure 3.19	The Respiratory System	3-24
Figure 3.20	The Gastrointestinal Tract	3-25
Figure 3.21	Single-Chamber One-Lung Model	3-26
Figure 4.1	Thor-Lx and Denton Leg Model	4-2

Figure 4.2	Size and Weight for 5 <sup>th</sup> Percentile Female and 50 <sup>th</sup> and 95 <sup>th</sup> Percentile Male Hybrid III ATD and for a Dutch Population in 2000	4-3
Figure 4.3	Size and Weight for 5 <sup>th</sup> Percentile Female and 50 <sup>th</sup> and 95 <sup>th</sup> Percentile Male Hybrid III ATD and for a Canadian Forces Population in 1997	4-4
Figure 4.4	Hybrid III ATD in a Truck before the Mine Test	4-5
Figure 4.5	Straight Seating Posture	4-6
Figure 4.6	Hybrid III ATD with Sensor Positions	4-7
Figure 4.7	BTD and Hybrid III ATD in Blast Tunnel	4-9
Figure 4.8	Example of Pressure Measurement Device on the Chest of an ATD	4-10
Figure 4.9	Example of a Flat Pressure Measurement Device	4-10
Figure 4.10	Example of a Cylinder for Pressure Measurements	4-11
Figure B.1	Overview of Mine Incidents	B-1
Figure C.1	AIS Coding Scheme	C-2
Figure C.2	APC Subjected to AV Blast Landmines	C-5
Figure C.3	Light-Armoured and Logistic Vehicles Subjected to Similar Mine Threat	C-6
Figure D.1	Illustration of Danger of Loose Objects	D-2
Figure D.2	Fire Extinguisher Impact on Occupant's Head during a Mine Test	D-2
Figure E.1	Yoganandan Experimental Set-up	E-2
Figure E.2	Risk of Foot/Ankle Injury as a Function of Age and Tibia Axial Force	E-2
Figure E.3	Yoganandan Risk Curves for Different Subject Ages	E-3
Figure E.4	Griffin Risk Curves for a 75 kg Subject and Different Loading Rates	E-4
Figure E.5	Funk Experimental Set-up	E-5
Figure E.6	Funk Risk Curves for Different Subject Age and Weight	E-6
Figure E.7	Example of Shock-Motion Terminology	E-7
Figure E.8	Tolerance of Stiff-Legged Standing Men to Shock Motion of Short Duration	E-8
Figure E.9	The LLth Acceleration-Based Injury Tolerance Curve	E-9
Figure E.10	The LLth Force-Based Injury Tolerance Curve	E-9
Figure E.11	Comparison between Yoganandan and Funk Models	E-12
Figure E.12	Ankle Joint Dorsiflexion and Inversion/Eversion Rotation Modes	E-14
Figure E.13	Thor-Lx and Standard HIII Denton Lower Leg	E-14
Figure E.14	The Canadian Lower Leg	E-15
Figure E.15	Typical CLL Injuries	E-15
Figure E.16	The Frangible Synthetic Leg (FSSL), Without and With Gelatine	E-16
Figure E.17	Exterior and Interior View of the TROSS™ Set-up	E-17
Figure E.18	Comparison between Hybrid III and Thor-Lx Tibia Axial Forces (TROSS Tests)	E-17
Figure E.19	TROSS Tests on the CLL With and Without Boot	E-18
Figure E.20	Results of Laboratory Axial Tests on the CLL With and Without Boot	E-18

Figure E.21	Example of Hybrid III Tibia Axial Force for Axial Impact Tests With and Without Boot	E-19
Figure E.22	Tracing View Using Altair Hyperworks: Crash Dummy Motion during Pure Vertical Footplate Displacement for Four Initial Positions at Two Different Loading Conditions	E-19
Figure E.23	Lower Tibia Axial Force (Fz) for MADYMO Simulation of Test db3 (Vertical Footplate Displacement) for Different Foot Positions	E-20
Figure F.1	Tolerance Curve for Vertebrae	F-5
Figure F.2	Eiband Tolerance Curve	F-6
Figure F.3	Tolerance of Seated Men to Shock Motion of Short Duration	F-7
Figure F.4	Lumbar Spine Compression Force Criterion	F-7
Figure F.5	DRIZ Model	F-8
Figure F.6	Spinal Injury Risk Calculated from Laboratory and Operational Data Supplemented with F-4 Operational Data Valid for AIS 2+ Injuries	F-9
Figure G.1	Illustration of Wedge Fractures and Burst Fracture	G-2
Figure G.2	Injury Tolerance Curves for Axial Neck Compression Force when Using a Hybrid III 50 <sup>th</sup> Percentile Male ATD	G-3
Figure G.3	N <sub>ij</sub> Risk Curves	G-5
Figure G.4	Neck Shear Injury Tolerance Curve for the 50 <sup>th</sup> Percentile Male Hybrid III	G-6
Figure G.5	Neck Tension Injury Tolerance Curve for the 50 <sup>th</sup> Percentile Male Hybrid III	G-6
Figure H.1	Typical Pressure-Time Curve for a High Explosive (Free Field)	H-2
Figure H.2	Example of Complex Overpressure Pattern inside a Vehicle Subjected to a Blast Mine	H-2
Figure H.3	Survival Curves Predicted for a 70-kg Man, Applicable to a Free-Stream Situation for Different Body Orientations with Respect to the Blast Winds	H-3
Figure H.4	Example of INJURY Program	H-6
Figure H.5	Single-Chamber One-Lung Model	H-7
Figure I.1	Examples of Hybrid III ATD in Test Vehicle	I-2
Figure I.2	Hybrid III ATD with Sensor Positions	I-3
Figure I.3	ATD Local Body Coordinate System	I-4
Figure I.4	Straight Seating Posture	I-6
Figure I.5	Example of Pressure Measurement Device on the Chest of an ATD	I-8
Figure I.6	Example of a Flat Pressure Measurement Device	I-8
Figure I.7	Example of a Cylinder for Pressure Measurements	I-9
Figure I.8	Neck Axial Compression Limit Curve	I-13
Figure I.9	Mathematical Spine Model	I-13
Figure I.10	Thorax Model	I-14
Figure I.11	Example of Defining the Maximum Duration for Two Load Levels	I-16

## List of Tables

<b>Table</b>		<b>Page</b>
Table 3.1	The Abbreviate Injury Scale	3-3
Table 3.2	Model Parameters for a 70-kg Mammal	3-27
Table 3.3	Injury Levels with Corresponding AIS Range for Each Body Region	3-27
Table 3.4	Injury Levels with Corresponding ASII and CWVP, and Estimated AIS Levels	3-28
Table 3.5	Summary of Injury Criteria and Tolerance Levels Proposed by HFM-090/TG-25 to be Used for Vehicle Mine Protection	3-29
Table 4.1	Overview of Data that Needs to be Measured	4-12
Table A.1	Time Schedule	A-2
Table C.1	Lower Leg Injuries	C-3
Table C.2	Cervical and Thoraco-Lumbar Spine Injuries	C-4
Table C.3	Head Injuries	C-4
Table C.4	Auditory and Non-Auditory Overpressure Injuries	C-4
Table E.1	Specimen Characteristics	E-10
Table E.2	Parameters Included in the Injury Risk Equations	E-11
Table E.3	Relevant Advantages and Shortcomings of the Models	E-11
Table E.4	Tolerance Levels for the Different Models	E-11
Table F.1	Breaking Mass Load ( $m_F$ ) as well as Maximum and Minimum Tolerance Level for Acceleration ( $a_F$ )	F-2
Table F.2	Breaking Mass Load ( $m_F$ )	F-3
Table F.3	Breaking Force F and Further Properties at Different Regions of the Spine	F-3
Table H.1	Model Parameters for a 70 kg Mammal	H-7
Table H.2	Injury Levels and Associated AIS Levels for the Lungs	H-8
Table H.3	Injury Levels and Associated AIS Levels for the Pharynx, Larynx and Trachea	H-8
Table H.4	Injury Levels and Associated AIS Levels for the Gastrointestinal Tract (Gas-Filled Organs)	H-9
Table H.5	Injury Levels and Associated AIS Levels for the Solid Abdominal Organs	H-9
Table H.6	Injury Levels with Corresponding ASII and CWVP and Estimated AIS Levels	H-9
Table H.7	Injury Models for Non Auditory Injury Assessment	H-10
Table I.1	Positive Polarities for the Channels at the Required Measurement Positions	I-4
Table I.2	Mandatory Criteria and Limit Values	I-12



## List of Symbols and Abbreviations

AIS	Abbreviated Injury Scale
AP	Anti-Personnel
ASII	Adjusted Severity of Injury Index
AT	Anti-Tank
ATD	Anthropomorphic Test Device
AUS	Australia
AV	Anti-Vehicular
AVP	Anti-Vehicular mine Protection
A <sub>x</sub>	Translational horizontal acceleration in x-direction
A <sub>y</sub>	Translational horizontal acceleration in y-direction
A <sub>z</sub>	Translational vertical acceleration in z-direction
BTD	Blast Test Device
CAN	Canada
CFC	Channel Frequency Class
CHE	Switzerland
CLL	Canadian Lower Leg (former name: Complex Lower Leg)
CWV(P)	Chest Wall Velocity (Predictor)
DAI	Diffuse Axonal Injuries
DEU	Germany
DGA	Direction Générale pour l'Armement
DRDC	Defence Research and Development Canada
DRIZ	Dynamical Response Index for z direction
DSTO	Defence Science and Technology Organisation (Australia)
EFP	Explosively Formed Projectile
ET	Expert Team
ETBS	Etablissement Technique de Bourges (France)
FAA	Federal Aviation Administration
FFT	Fast Fourier Transform
FRA	France
FSL	Frangible Synthetic Leg
F <sub>x</sub>	Force in x-direction (shear force)

---

Fy	Force in y-direction
Fz	Force in z-direction (axial force)
GBR	United Kingdom
GI	GastroIntestinal
HFM	Human Factors and Medicine Panel
HIC	Head Injury Criterion
HIII	Hybrid III crash test dummy
IABG	Industrieanlagen-Betriebsgesellschaft mbH (Germany)
IED	Improvised Explosives Device
IRCOBI	International Research Council on the Biomechanics of Impact
ISL	Institut de Saint Louis (France)
ISS	Injury Severity Score
LLth	Lower Leg Threshold
MADYMO	MAThematical DYNAmical MOdel
MCW	Medical College of Wisconsin (USA)
Mx	Bending moment around x-axes
My	Bending moment around y-axes
Mz	Bending moment around z-axes
NATO	North Atlantic Treaty Organisation
NISS	New Injury Severity Score
NLD	The Netherlands
NOR	Norway
PfP	Partners for Peace
PMHS	Post Mortem Human Subjects
RTI	Revised Tibia Index
RTO	Research and Technology Organisation
SAE	Society of Automotive Engineers
STANAG	NATO Standardization Agreement
SWE	Sweden
TACOM/TARDEC	Tank-automotive and Armaments Command (U.S. Army)
TCFC	Tibia Compression Force Criterion
TG	Task Group
THOR	Test device for Human Occupant Restraint

---

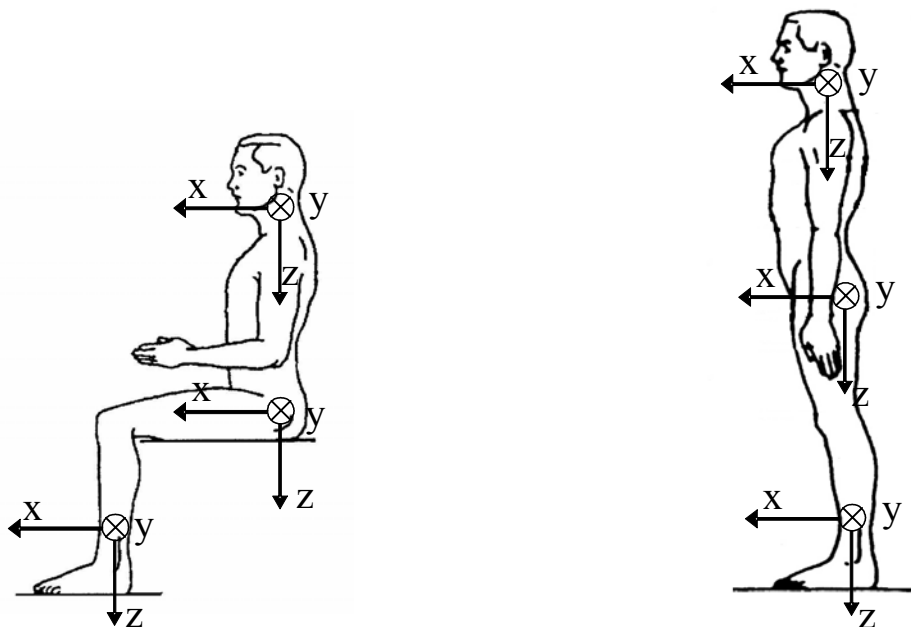
TI	Tibia Index
TNO	Netherlands Organisation for Applied Scientific Research
TNO-PML	TNO-Prins Maurits Laboratorium (recently called TNO Defence, Security and Safety)
TOR	Terms Of Reference
TROSS™	Test Rig for Occupant Safety Systems
TTCP	The Technical Cooperation Program
USA	United States of America
WSU	Wayne State University, Detroit, USA
WTD 91	The Technical Center for Weapons and Ammunition of the German Armed Forces

## List of Definitions

Anatomical scales	Described the injury in terms of anatomical location, type of injury and relative severity
Annular fibrosus	A laminar set of fibrous sheets, that surrounds the intervertebral disks
Anterior	Front part, to the front
Anterior vertebral body (vertebral) Articulate	Weight bearing part of vertebra Vertebra part for attachment of muscles
Atlas	C1 vertebra
Axis	C2 vertebra
Biofidelic response	Response resembling that of a real human
Bronchi	Part of lower respiratory system
C1-C7	First to seventh cervical vertebra
Calcaneus	Heel bone
Cerebrospinal fluid	Fluid in the spinal chord and cerebral ventricles
Cervical spine	Neck part of the spine
Coccyx	Tail bone
Cranial direction	In the direction of the head, the axial longitudinal z-axis
Cuboid	Bone in the foot
Cuneiforms	Mid foot bones
Dens	Part of C2 vertebra
Elastic injury mechanisms	Compression and tension of the body causing injury if elastic tolerances are exceeded – injury can occur in case of slow deformation of the body (crushing) as well as due to high velocity impacts
Facial cranium	Forehead, part of skull
Femur	Thigh-bone
Fibula	Calve bone
GM/FTSS foot/ankle	Company name of crash dummy foot/ankle part
Impairment	Disability and societal loss scales: Rate the long-term consequences and in relation to this, the “quality of life”
Inertial injury mechanisms	Acceleration type of loading causing tearing of internal structures due to inertia effects
Injury criterion	Physical parameter or a function of several physical parameters which correlates well with the injury severity of the body region under consideration

Injury criterion level	Magnitude of loading indicated by the threshold of the injury criterion, which produces a specific type of injury severity
Injury mechanism	Mechanism involved with the cause of injury
Injury risk curves	Define the injury risk for a given human body response
Injury scaling	Numerical classification of the type and severity of an injury
Intra-abdominal organs	Organs in abdomen, such as liver, spleen, intestines etc.
Intra-thoracic	Everything within the chest cavity
Knee clevis	Attachment part at the knee of a dummy leg
L1 – L2	First and second lumbar vertebral bodies (upper part)
Laceration	Tear in skin, muscle or organ
Laminar fractures	Fractures in longitudinal direction of bone
Larynx	Part of the lower respiratory system
Lower extremity	Lower limb
Lumbar spine	Part of the spine at the lower back
Lumbar vertebrae	Vertebrae of the lumbar spine
Metatarsals	Toe bones
Navicular	Foot bone
Neurocranium	Part of skull containing the brain
Occipityle Condyles	Attachment point of the spine to the skull
Osteoarthritis	Chronic inflammation caused by damage of cartilage
Patella	Knee bone
Pectoral	At the chest
Pedicle fractures	Fracture of a part of a vertebra
Pelvis	Hip area
Phalanges	Toe bones
Pharynx	Part of the lower respiratory system
Phrenic nerve	Responsible of the respiration functions
Physiologic scales	Describe the physiological status of the patient based on the functional change due to injury – this status may change over the duration of the injury’s treatment period
Posterior	On the back, backwards
Sacrum	Lower part of the spine
Spinal	Axial direction
Spinal cord	Extension of central nervous system in the spine
Spinous process	Bony part of the Vertebrae

T1-T12	First to twelfth thoracic vertebra
Talus	Foot bone
Tarsals	Foot bones
Thoraco-lumbar spine	Part of the spine between thoracic and lumbar region; mostly related to the lower part of the thoracic and the upper part of the lumbar vertebrae
Thoracic spine	Part of the spine at the thorax
Thoracic vertebrae	Vertebra of the thoracic spine
Thorax	Chest
Thor-Lx	Lower leg of a Thor crash test dummy
Tibia	Shin bone
Tolerance level	Magnitude of loading indicated by the threshold of the injury criterion, which produces a specific type of injury severity and risk
Trachea	Main airway of the respiratory system
Vertebrae	Parts of the spine
Viscous injury mechanisms	Impulsive type of loading causing mechanical waves in the body, which results in internal injuries if so-called viscous tolerances are exceeded



**ATD Local Body Coordinate System.**

## Programme Committee

**Mr. Piet-Jan Leerdam (Chair)**  
TNO Defence, Security and Safety  
P.O. Box 45  
2280 AA Rijswijk  
THE NETHERLANDS  
Phone: +31 15 2843463  
Email: [piet-jan.leerdam@tno.nl](mailto:piet-jan.leerdam@tno.nl)

**Ms. Marike van der Horst, Phd**  
TNO Defence, Security and Safety  
P.O. Box 45  
2280 AA Rijswijk  
THE NETHERLANDS  
Phone: +31 15 2843329  
Email: [marike.vanderhorst@tno.nl](mailto:marike.vanderhorst@tno.nl)

**Mr. Gregory Wolfe**  
US Army Tank Automotive  
Command (TACOM)  
AMSTRA-TR-R, MS 263  
Warren, MI 48397-5000  
USA  
Phone: +01 586 574 5948  
Email: [wolfeG@tacom.army.mil](mailto:wolfeG@tacom.army.mil)

**Ms. Josée Manseau**  
Defence Research and Development Canada  
(DRDC-RDDC)  
Valcartier 2459 Pie XI North  
Québec, QC G3J 1X5  
CANADA  
Phone: +1 418 844 4470  
Email: [josee.manseau@drdc-rddc-gc.ca](mailto:josee.manseau@drdc-rddc-gc.ca)

**Mr. Denis Lafont**  
DGA/DCE/ETBS  
Rocade Est-échangeur de Guerry  
18021 Bourges Cedex  
FRANCE  
Phone: +33 248 27 4334  
Email: [denis.lafont@dga.defense.gouv.fr](mailto:denis.lafont@dga.defense.gouv.fr)

**Mr. René Lemasle**  
DGA/DCE/ETBS  
Rocade Est-échangeur de Guerry  
18021 Bourges Cedex  
FRANCE  
Phone: +33 248 27 4822  
Email: [rene.lemasle@dga.defense.gouv.fr](mailto:rene.lemasle@dga.defense.gouv.fr)

**Mr. Lars Svensson**  
Defence Materiel Administration (FMV)  
Protection and Quality Management  
SE-115 88 Stockholm  
SWEDEN  
Phone: +46 8 782 6572  
Email: [lars.w.svensson@fmv.se](mailto:lars.w.svensson@fmv.se)

**Mr. Håkan Axelsson**  
Defence Materiel Administration (FMV)  
Protection and Quality Management  
SE-115 88 Stockholm  
SWEDEN  
Phone: +46 8 778 0592  
Email: [h.axelsson@privat.utfors.se](mailto:h.axelsson@privat.utfors.se)

**Mr. Frank Dosquet**  
WTD 91-450  
P.O. Box 17 64  
D-49707 Meppen  
GERMANY  
Phone: +49 5931 43 2450  
Email: [frankdosquet@bwb.org](mailto:frankdosquet@bwb.org)

**Dr. Jean Lapointe**  
Defence Research and Development Canada  
(DRDC-RDDC)  
Valcartier 2459 Pie XI North  
Québec, QC G3J 1X5  
CANADA

## Acknowledgements

The following countries participated in the HFM-090/TG-25: Germany, France, Canada, United States, The Netherlands (Chair) and Sweden as Partners for Peace (PfP).

We would like to thank Jocelyn Tremblay (DRDC Valcartier, CAN) in starting this HFM Task Group on test methodology for protection of vehicle occupants against anti-vehicular landmine effects. After the first meeting a group of experts was chosen to continue the work within HFM-090/TG-25.

Mr. P.J. Leerdam was chair of the group and did his work with great enthusiasm.

The work of the TG-25 presented in this report was conducted from January 2003 to December 2004. Two meetings a year were held.

We would like to thank following countries and their institutes for hosting the meetings of HFM-090/TG-25:

- First meeting                      France, ETBS
- Second meeting                    The Netherlands, TNO-Defence, Security and Safety
- Third meeting                      United States of America, US Army TACOM
- Fourth meeting                    Germany, WTD 91
- Fifth meeting                      Canada, DRDC Valcartier

We also would like to acknowledge the contribution of our guests:

- Oliver Nies, from WTD 91, Germany
- Marcel Müller, from IABG, Germany
- Dr Wolfgang Titius, Military Hospital, Germany
- Dr. Armand Dancer, from Institut de Saint Louis, France



---

# **Test Methodology for Protection of Vehicle Occupants against Anti-Vehicular Landmine Effects**

## **(RTO-TR-HFM-090)**

### **Executive Summary**

In the last decade, national and international projects for the improvement of the landmine protection of several military vehicles have been conducted. A landmine detonation under a vehicle causes structural deformations and sometimes vehicle hull rupture, which affect (psychologically and physically) the occupants. Following the detonation, mechanical effects like shock, structural deformation and global movement (mostly vertical), have the potential to cause injuries to the human body. Vehicle hull rupture also results into direct harming effects like fragments, fire, gases and blast overpressure.

In 2001, the NATO/RTO HFM-090/TG-25 was created in response to the NATO/RTO HFM ET-007, which identified the lack of suitable information for injury assessment of the anti-vehicle mine threat. Furthermore, the Task Group was asked to help the STANAG 4569 Team of Experts to develop an injury assessment methodology for the qualification of light-armoured and logistic vehicles (blast) landmines protection systems. Several NATO and Partner for Peace countries participated in TG-25 (CAN, DEU, FRA, NLD, SWE, USA), which was chaired by NLD (TNO Defence, Security and Safety).

Injury criteria, tolerance levels and measurement methods were proposed to assess the most vulnerable body regions to a blast mine strike under a vehicle. The tolerance levels established for these body regions are considered to represent low risk of life-threatening and disabling injuries. The results, conclusions and recommendations of the HFM-090/TG-25 work are presented in this report.

# **Méthodologie d'essais pour la protection des occupants de véhicules contre les effets des mines terrestres anti-véhicules**

## **(RTO-TR-HFM-090)**

### **Synthèse**

Au cours de la dernière décennie, des projets nationaux et internationaux ont été mis en place pour protéger les véhicules militaires contre les menaces de mines terrestres. La détonation d'une mine terrestre sous un véhicule provoque la déformation de sa structure et parfois la rupture de sa coque, affectant physiquement et psychologiquement les occupants. Suite à la détonation, apparaissent des effets de choc, de déformation structurelle et de mouvement global qui peuvent causer des blessures au corps humain. La rupture de la coque du véhicule produira également des effets directs provenant des fragments, du feu, de l'émanation de gaz et de la surpression.

En 2001, le groupe HFM-090/TG-25 de la RTO de l'OTAN a été créé en réponse au groupe HFM ET-007. Ce dernier avait identifié un manque d'information au sujet de l'évaluation des blessures causées par les mines terrestres anti-véhicules. De plus, le TG-25 a été mandaté par le groupe d'experts STANAG 4569 pour développer une méthode d'évaluation pour la qualification de systèmes de protection des véhicules blindés légers et logistiques. Plusieurs pays de l'OTAN ainsi que des Partenaires pour la Paix (l'Allemagne, le Canada, les Etats-Unis, la France, les Pays-Bas et la Suède) ont participé au groupe TG-25, qui était présidé par les Pays-Bas (TNO, Defence, Security and Safety).

Des critères de blessures, niveaux de tolérance et techniques de mesures ont été proposés pour les parties du corps les plus vulnérables. Les niveaux de tolérance pour ces différentes parties ont été établis pour correspondre à un faible risque de blessures critiques pouvant conduire à l'invalidité. Ce rapport présente les résultats du travail du HFM-090/TG-25 ainsi que ses conclusions et recommandations.

## Chapter 1 – INTRODUCTION

### 1.1 BACKGROUND AND PROBLEM DEFINITION

#### 1.1.1 Background

Mines, and specifically Anti-Tank (AT) mines, are a significant threat for military vehicles and their occupants [Radonić, 2004]. The AT mines are designed for the destruction and damage of armored and other vehicles, usually by using them in mine fields on routes used by vehicles of the enemy. These mines, with huge variation in charge mass and initiation types, a huge amount of strong explosive, and great destructive forces, can be buried in all soil types, on railroad lines, in coastal areas and river approaches, and they can be buried separately or in groups to form minefields.

The first modern antitank mines appeared in World War I as a weapon against the first armored vehicles. During World War II, technological progress in the production of antitank mines enabled their widespread tactical application. One-fourth of all German tanks were destroyed by mines in the Russia-German conflict [Mitchel, 1964; Utter, 1960]. Further technological improvement after World War II made the antitank mine one of the most efficient and least expensive lethal weapons. There are several hundred different types of antitank mines in the world today and millions of mines are left behind in several (post-war) countries. The number of antitank landmines in the world is difficult to estimate. For example, antitank mines are estimated to account 20% of the presumed total 2 millions landmines laid during the war of Croatia from 1991 to 1995 [Radonić, 2004].

In the past ten years, national and international projects for the improvement of the mine protection of several military vehicles from trucks up to main battle tanks have been performed (see Figure 1.1). Purchasers and users of military vehicles are becoming more aware that apart from vehicle integrity, personnel safety is crucial in operations where mines pose a threat. Especially, in peacekeeping and peace-enforcing operations occupant safety has the highest priority. In case of a mine detonation under a vehicle, a vehicle rupture can occur resulting into effects like fragments, fire, gases, blast overpressure as well as the mechanical shock and a vertical impulse load. All these effects will affect (psychologically and physically) the occupants inside the vehicle. In the same case, but without structural rupture, the occupants might still be affected by the mechanical effects like shock, structural deformation and the vertical impulse load.



Figure 1.1: Example of Mine Detonation under a Logistic Vehicle.

## INTRODUCTION

---

### 1.1.2 Problem Definition

NATO countries realize that the mine threat to military vehicles and their crew is of urgent and great importance. Therefore, many countries started the development of mine protection systems, which resulted into different requirements and test methods per country. Several attempts were made for standardization, for example by The Technical Cooperation Program (TTCP: a co-operation between the GBR, USA, CAN, AUS) [TTCP, 1998] and in international co-operation projects (e.g. the mine protection project of the Leopard II main battle tank involving NLD, NOR, DEU, SWE, CHN). NATO STANAG 4569 addresses the landmine problem with respect to establishing standards for protection levels for logistic and light armored vehicles.

The new HFM-090/TG-25 on test methodology for protection of vehicle occupants against anti-vehicular landmine effects was created in order to establish common injury criteria and assessment procedures for qualification.

Later, STANAG 4569 asked for assistance from the HFM-090/TG-25 for establishing the standard for protection of vehicle occupants against anti-vehicular landmine effects.

## 1.2 THE OBJECTIVE AND APPROACH OF THE HFM-090/TG-25

### 1.2.1 Objective

The mandate and objective of the HFM-090/TG-25 (see also Terms of Reference in Annex A) are:

- Describe blast mine effects resulting human physical injuries based on various countries experiences with mine incidents and tests;
- Propose injury assessment criteria and tolerance levels for occupant injuries during AV (anti-vehicular) mine strike tests; and
- Describe test methods and equipment to assess occupant injuries during AV mine strike tests.

### 1.2.2 Approach

First, the background of the mine detonation process and the consequent injuries expected were discussed. Also the discussion of the injury criteria was started. Additionally, the Terms of Reference were redefined. It was decided that each country would be responsible for a body region. This approach was followed throughout the entire process. Information was shared and each country prepared summary documents on the injury criteria and their tolerance levels. Based on these summaries discussion took place and decisions were made. Separate topics included were the measurement methods and test procedures, which were then discussed as well. The progress was presented by members of TG-25 to the STANAG 4569. Finally, this report was written with contribution from all TG-25 members.

The work by the HFM-090/TG-25 is restricted to the biomechanical effects on land based vehicle occupants (crew and troops) caused by the mechanical loading and overpressure effects occurring during an AP (Anti-Personnel) or AT (blast) mine detonation anywhere under a vehicle. Detonations in front or to the side of the vehicle are not considered here. Although not negligible, the psychological and social effects caused by a mine strike are out of the scope of this report. The work by the HFM-090/TG-25 focuses on describing criteria, tolerance levels and test methods used in occupant safety studies for mine protection qualification trials. Rather than to develop an overall criterion, the goal was to discuss and propose injury criteria and tolerance levels for all the different vulnerable body regions.

### 1.3 ORGANIZATION OF THIS REPORT

Starting with this introduction this report is built around five (5) chapters. Chapter 2 provides background information on the anti-vehicle mine detonation process and the injuries that can occur. The next chapter (Chapter 3) contains the core subject of this report: the injury criteria and tolerance levels. It is subdivided into several sections, each focusing on a body region. Chapter 3 finalizes with conclusions on the injury criteria and tolerance levels. Chapter 4 describes the measuring methods and the test set-up and procedure. Finally, the conclusions are presented in Chapter 5 along with recommendations.

Annexes supplement the main body of the report. These annexes contain mainly information that relates to the medical aspects and the injury criteria, but was too detailed for inclusion in the main text. Additionally, the Terms of References of the HFM-090/TG-25 are included in the annexes.

### 1.4 REFERENCES

Mitchell, D.W. (1964), Russian mine warfare: the historical record, *Royal United Services Institution J*, 109 32-9.

Radonić, V., Giunio, L., Biočić, M., Tripković, A., Lukšić, B. and Primorac, D. (2004), Injuries from Antitank Mines in Southern Croatia, in *Military Medicine*, Vol. 169, April, pp. 320-324.

The Technical Cooperation Program (TTCP). (1998), Protection of Soft-Skinned Vehicle Occupants from Landmine Effects. Edited by Tremblay, J., Bergeron, D.M., Gonzalez, R. TTCP, WPN/TP-1, KTA 1-29, Technical Report, August 1998.

Utter, L.N. (1960), Soviet landmine warfare, *Infantry*, 50:54-5.



## Chapter 2 – THE MINE DETONATION PROCESS AND OCCUPANT LOADING

As mentioned in Chapter 1, the HFM-090/TG-25 work focuses on the blast mine threat under vehicles (AP and AT mines). Other types of mines are excluded from the current report. After a blast mine detonation, a shock wave goes through the vehicle. Elastic and also plastic deformation (sometimes even ruptures) together with a global impulse occurs. If the integrity of the vehicle is preserved, predominantly the shock, deformation and global impulse have effect on the occupants inside the vehicle. Otherwise also primary, secondary and miscellaneous blast effects, like overpressure, secondary fragments, toxic fumes and gases, and heat radiation are threats to the occupant.

In Section 2.1, a short introduction to mines is given. In Section 2.2, the process of the effects of a blast mine detonation under a vehicle is described. In Section 2.3, the human body loadings generated by the blast mine effects are discussed.

### 2.1 INTRODUCTION TO MINES

A large variety of mines exists as mentioned in Chapter 1. These mines can be classified according to target and on damage mechanism:

- Anti-Personnel (AP) mines:
  - Blast mines
  - Fragmenting mines
- Anti-Tank (AT) mines:
  - Blast mines
  - Shaped charge mines

The **AP-mines** are used to injure hostile personnel in order to stop their activities. Most of these mines are activated by a pressure fuse, and they contain a small amount of explosives (up to 250 grams) – enough to cause severe injury to the foot, ankle and leg of someone stepping the mine. Other types of AP mines are activated by a trip wire and cause a blast and a spray of fragments. A special fragmenting type is the bounding mine. First, this mine springs approximately one meter high and then detonates. The fragments are spread 360 degrees around the mine and are very effective in killing or injuring personnel. This mine is also effective against non- or light armoured vehicles as the fragments can penetrate into the vehicle and hit the occupants. The blast load of a detonating AP mine close to a vehicle can also harm the occupants. In some cases fragmentation and blast seem to have cumulative effects.

The **AT-mines** are originally used in mine field barriers to stop the main battle tanks of the enemy. Nowadays they are used in any conflict area and against all types of vehicles. The first generation mines use a pressure fuse activated by loads of more than 200 kg from the vehicle's wheels or tracks. The large amount of explosive (up to 12 kg) causes extreme blast loads resulting in severe damage (at least a mobility kill) to the vehicle. The second generation of AT mines uses tilt rods or magnetic/seismic influence fuses so that they can also detonate under the bottom of the vehicle. These fuses are also used in combination with the shaped charge mines. These mines when detonated form a projectile or a jet (hollow charge mine), which can perforate thick (armoured) plates. A special variant is the Explosively Formed Projectile (EFP) or Self Forging Fragmenting mine (SFF). They form a big slug, which is launched at very high speeds against the target. All these types of AT mines are designed to detonate under the vehicle. The third generation of AT mines are the off-route or the top-attack mines with sophisticated fuses,

but these are out of the scope of this report. The STANAG 4569 decided to focus on the effects of blast mines under vehicles.

## **2.2 THE EFFECTS OF AN ANTI-VEHICLE BLAST MINE DETONATION**

This section describes the four types of effects of the blast mine detonation under a vehicle:

- Local effects;
- Global effects;
- Drop down effects; and
- Subsequent effects.

More background on these effects can also be found in [Dosquet, 2006]. A description of the physics of blast mines in general can be found in [RTO-TR-HFM-089, 2004].

### **2.2.1 Local Effects**

After initiation of the blast mine under a vehicle a shock wave is formed by the detonating explosive. This shock wave hits the bottom plate of the vehicle within approximately 0.5 ms and is subsequently reflected causing an extremely large peak pressure resulting in a local acceleration of the bottom plate. Within approximately 5 ms after the detonation the bottom plate bends in both the elastic and plastic regions depending on the shape, thickness, material and additional stiffeners. Sometimes the bottom plate deformation exceeds the elastic region and causes ruptures and hence, possible overpressure, fragmentation, heat and toxic effects inside the vehicle. The shock wave also causes a mechanical shock in the material of the vehicle structure, which travels with speeds up to 5000 m/s through the whole structure and causes strong vibrations in all vehicle parts. Depending on the boundary conditions, the bending bottom plate may cause deformations in the side walls of the vehicle. All parts mounted on or just above the bottom plate, like torsion bars, can be hit and accelerated in an upward direction.

### **2.2.2 Global Effects**

Due to the reflecting blast wave under the vehicle, a pressure force briefly acts on the complete bottom section of a vehicle. The total impulse load of this pressure force is a measure of the initial vertical velocity causing a jump of the complete vehicle (which follows the impulse law for rigid body motion). The jump height depends on the total mass and, for asymmetric loading, on the moments of inertia around the centre of gravity. In general, it takes about 10 to 20 ms after detonation before the complete vehicle starts moving and 100 to 300 ms before it reaches its maximum jump height.

The time sequence of the mine detonation process and of the local and global effect is presented in Figure 2.1. Some time overlap of the processes is possible.



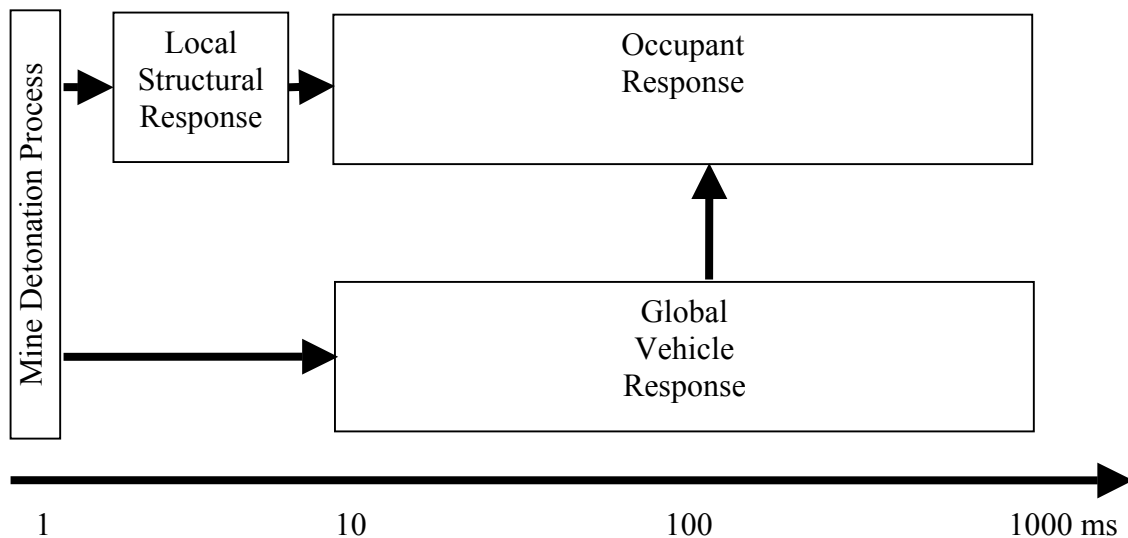


Figure 2.1: Time Sequence of Events during an AV Mine Detonation.

### 2.2.3 Drop Down Effects

After reaching its maximum jump height the vehicle will fall due to gravity. In actual incidents the vehicle is driving and will not drop down on the original place, whereas in an experimental set-up, the vehicles are tested in a static situation. Therefore, it is possible that the vehicle drops down into its own crater, which can result in higher vertical loadings than in an actual incident. Higher loads can also occur due to elements in the test set-up itself, like steel plates on the drop down surface. Experience in full-scale mine trials showed loadings that were significant during the drop down phase. Most of the time, they were not as important as the ones generated by the initial phase. If the prevention system is damaged during the initial phase, it can result in higher injuries from the impact occurring during the drop down phase.

When testing only the drop down phase, it needs to be taken into account that the initial position of the occupants is not based on the loads of the mine detonation, but on the position the occupants are placed in.

### 2.2.4 Subsequent Effects

Subsequently, incidents like roll over and frontal crashes after the mine detonation are not considered due to high variation of boundary conditions. This must be considered in crashworthiness investigations.

It should be noted that besides the blast, resulting in acceleration of the vehicle and occupants, other effects for the occupants can also occur, especially when an EFP mine or a shaped charge mine results in penetration of the vehicle. For these cases the resulting fragments, toxic fumes and gases, blast overpressure and heat are serious threats for the human body as well. However, HFM-090/TG-25 focuses on the effects of a blast mine detonation under a vehicle, and this report follows that approach.

## 2.3 OCCUPANT LOADING

The analysis of vehicle mine incidents [Medin, 1998; Radonić, 2004] is necessary in understanding the effects of blast mine detonations under vehicles on the human body. However, information is often classified, not/hardly available, or insufficiently detailed. Therefore, experimental as well as numerical research is performed to achieve this understanding. In full-scale tests, the loads on the occupants are

measured using instrumented anthropomorphic test devices (ATDs) – widely known as crash test dummies- together with other measurement equipment like sand bags, pressure gauges and accelerometers placed inside the vehicle. An ATD is able to withstand crash and vehicle mine detonation tests while simultaneously (and reproducibly) measuring the accelerations, forces and moments in different body parts. The results of these measurements may be used as input for injury assessment and for numerical studies with for example the occupant safety code MADYMO (Mathematical Dynamical Models). In this section, the occupant loading caused by a blast mine detonation under the bottom, the wheel or the track of an (armoured, light-armoured or logistic) military vehicle is described.

It is expected that once the vehicle integrity is secured, effects of fragments, overpressure, gases and heat will have minor physical effects on the occupant inside the vehicle. However, the acceleration effects still occur. The response of the occupant inside the vehicle is influenced by both the local effect (shock and deformation) and the global effect (vehicle motion) of the vehicle mine detonation process (see Section 2.1). The human body or parts of the body can be loaded directly by the shock (primary effect) or by the local deformation (secondary effect) or indirectly by the relative body motion and resulting impacts to the vehicle structure (tertiary effect) [Dosquet, 2004]. The severity of the threat, and therefore, the severity of the loads on the occupant, depend on the distance between the casualty and the detonation point as well as on the vehicle structure, the interior structure, like seat and seat mountings, and the foot plate configurations (e.g. [Radonić, 2004]). When a seat or a footrest is mounted on or close to the deforming bottom plate large loads are most likely transferred to respectively the feet, the ankles, the legs and the lumbar spine. Additionally, the chance of injury depends on initial body posture, the presence and use of personal protection equipment and restraint systems. Also age, gender, health, training, etc., may influence the injury probability.

In general, the leg and foot/ankle complex are usually in the position closest to the detonation point and the deforming structure, so they are loaded first. When the feet are placed on the bottom plate or on a floor plate close to the bottom plate, they are loaded severely and accelerated rapidly (see Figure 2.2). The loads can reach levels high enough to crush feet, ankles, legs and knees. Due to the acceleration force, the legs move upwards with the risk of hitting other vehicle parts. The leg motion may also have its influence on the lumbar spine and other body parts.

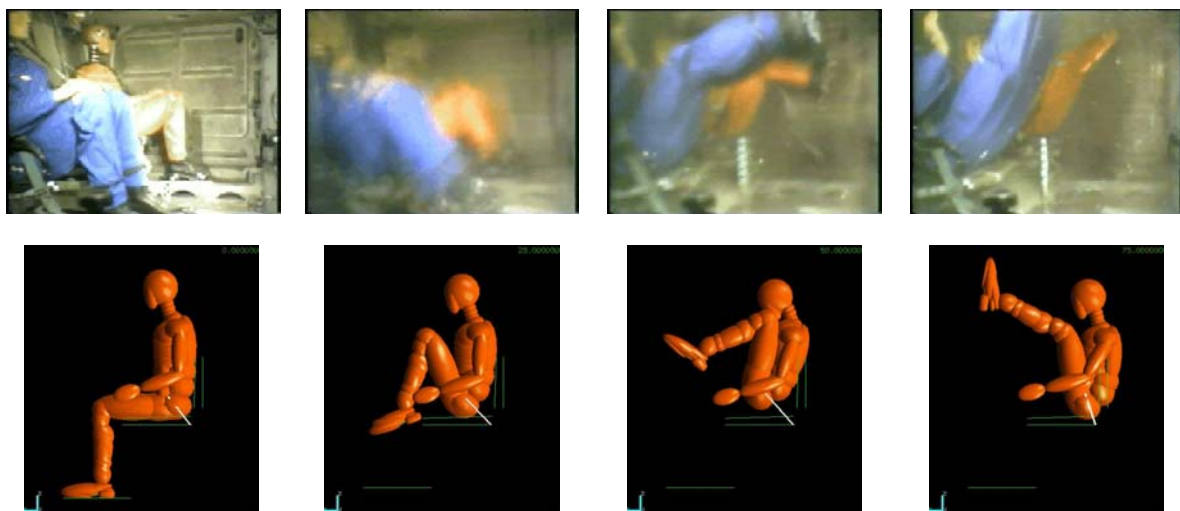


**Figure 2.2: Experimental and Numerical Example of Severe Leg Load Situation [Horst, 2002].**

The pelvis can be loaded through either the lower extremities or the seat of the vehicle. For seat mountings on the bottom plate, the pelvis will be loaded at about 10 ms after detonation, the severity depends on the

seat suspension system. When a seat is mounted to the side or the roof, the maximum acceleration is reached later (15 to 30 ms) and is usually less severe. The vertical acceleration and motion of the pelvis will cause a compression force in the lumbar spine, which can result in injury. For local effects the maximum spine force is reached at about 20 ms after detonation [see Figure 2.3 and Leerdam, 2002], for global effects the maximum will be at about 40 ms [see Figure 2.4 and Leerdam, 2002].

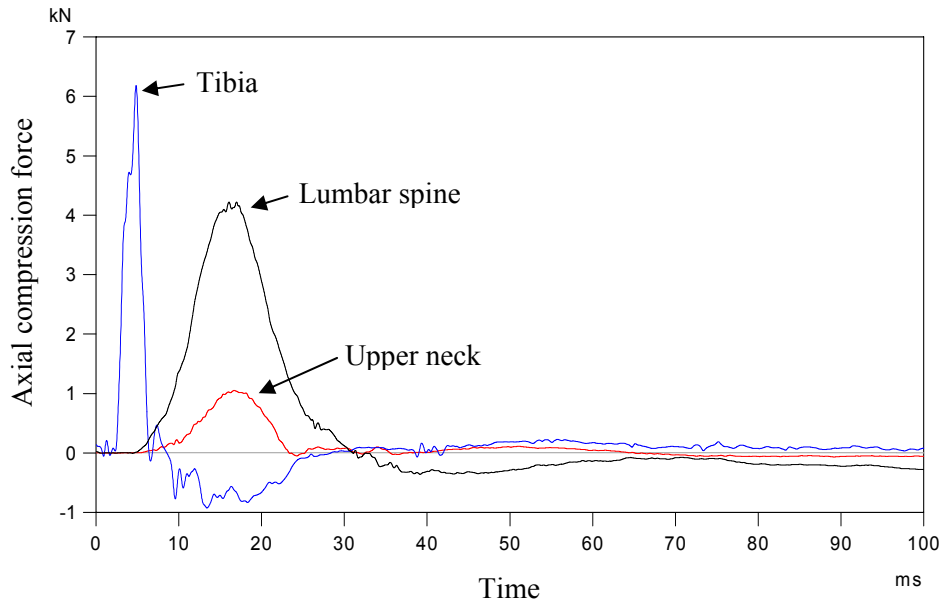


Figure 2.3: Example of Axial Compression Force Signals in Tibia, Lumbar Spine and Neck for the More Local Effects Caused by a Mine Detonation under a Vehicle.

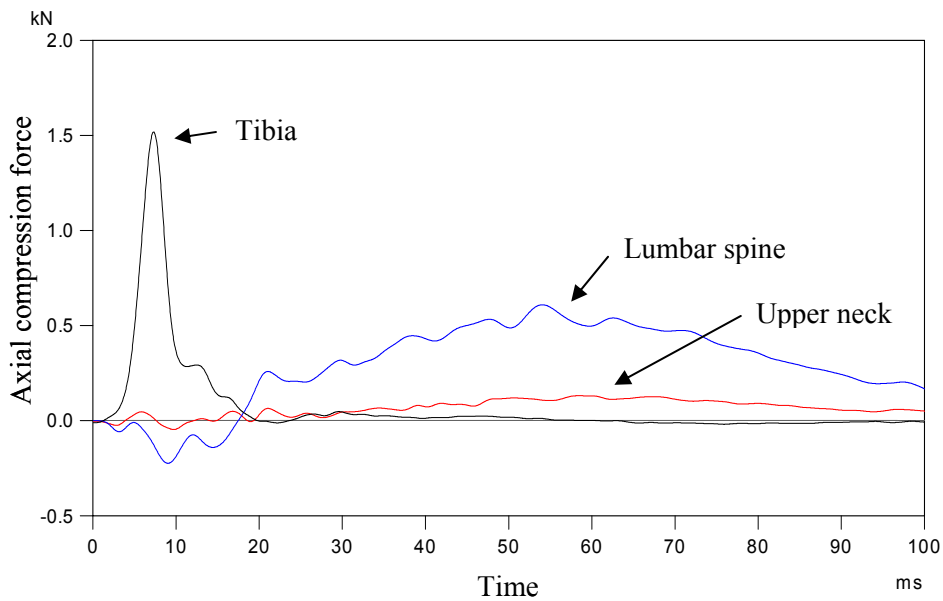


Figure 2.4: Example of Axial Compression Force Signals in Tibia, Lumbar Spine and Neck for the Global Effects Caused by a Mine Detonation under a Vehicle.

## THE MINE DETONATION PROCESS AND OCCUPANT LOADING

The pelvis acceleration and motion will also load the upper body parts, including the neck and the head. The whole body will be launched (mostly) vertically due to the seat impact. When no or inappropriate restraint systems are used, the head can hit the roof of the vehicle. Tests have proven that head contact with a stiff roof structure may cause high acceleration peaks in the head and extremely high loads in the neck. Such high neck loads are life-threatening and must be prevented.

Examples of the force signals measured using ATDs are shown in Figures 2.3 and 2.4, which show that the local effect shows higher peaks than the global effect. The peak values also occur earlier and last shorter. It should be noted that the global and local differences are difficult to distinguish for the feet, ankles and legs. The body parts mentioned in the figures are explained in Chapter 3, but it should already be mentioned that the tibia is part of the lower leg and the lumbar spine is part of the lower back.

Figure 2.5 shows in general terms the time sequence of events on the human body. The loading duration as well as the time at which the peak load occurs are presented for several body parts. This graphic is based on a database of test data for vehicle mine protection studies [Leerdam, 2002]. Over 15 tests were used for this graphic. As in Figure 2.3 and 2.4, it is seen that the duration of the global effects is longer and that the peak values occur later. Because of the difficulties in distinguishing the local and global effects for the feet, ankle and legs, only the local effects are shown.

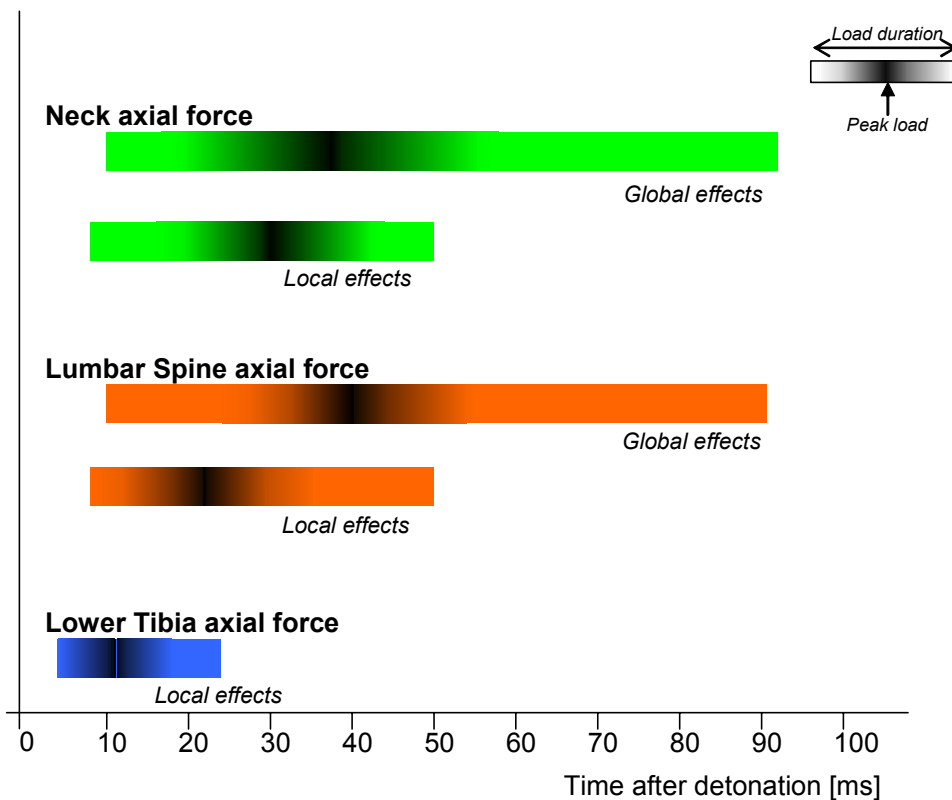


**Figure 2.5: Loading Process in Human Body Due to Mine Detonation.**  
Based on test data [Leerdam, 2002].

The initial loading effects to the human body happen within ~50 ms after detonation of the mine under the vehicle. For the global effects it takes about twice as long. Depending on the integrity of seat structure and belt system and on the free space for body motion, contacts between body parts and vehicle objects can occur as long as the entire vehicle is moving. Usually within one second after detonation the vehicle and the occupants come to rest again.

Although not the main focus of this work, the drop down phase should be taken into account also. During this vertical drop of the vehicle, the human body is loaded in the same direction, although the shape of the signal may differ from the loading of the mine detonation. Depending on the severity of this drop down phase as well as on the body posture and the damage to the vehicle just after the mine detonation additional injuries can occur. For example a specific seat system can prevent the body from serious injuries during the first phase, but after this event, the systems can be damaged and may not prevent the body for additional injuries during the drop down phase.

As mentioned at the beginning of this section, the acceleration effects are assumed to have major effects on the human body, because the other effects are considered to have minor effects when the vehicle integrity is secured – but effects resulting from toxic gases and heat may cause serious injuries when occurring [Medin, 1997]. Readers that are interested to these threats for the human body are referred to the literature for more information, e.g. [Ripple, 1990; Stoll, 1968; SFPE, 2000]. Fragments or loose objects that arise in the vehicle cabin can cause serious penetration or blunt injuries (e.g. [Sellier, 1994]). The blast overpressure effects inside the vehicle may cause injuries to auditory and non-auditory organs/systems. Although the overpressure effects are expected to be small when the vehicle integrity is secured, it was decided to include overpressure injury assessment in the proposed method. The fragmentation effects and loose objects can be neglected due to the required integrity of the hull.

In the following chapter, the injury criteria and tolerance levels for the biomechanical as well as the overpressure effects are discussed for each of the identified vulnerable body regions, which are the lower leg (leg/ankle/foot), the spine (thoraco-lumbar and cervical regions), the head and the non-auditory internal organs/systems.

## **2.4 REFERENCES**

Dosquet, F. (2004), Mine protection becoming more and more important, European Safety Symposium (original) : Minenschutz immer bedeutsamer, Europäischer Sicherheit, September 2004.

Dosquet, F. (2006), Overmatch analysis as enhancement for conventional protection analysis. Third European Survivability Workshop, Toulouse, France, May 2006.

Horst, M.J. van der and Leerdam, P.J. (2002), Experimental and Numerical Analysis of Occupant Safety in Blast Mine Loading Under Vehicles, In Proceedings of International IRCOBI conference on the biomechanics of impact. Munich, Germany, pp. 355-356, ISBN 2-9514210-3-6.

Leerdam, P.J.C. (2002), Research experiences on vehicle mine protection, First European Survivability Workshop (ESW), February, 2002, Germany.

Medin, A. (1997), Blast overpressure, gases and fumes from a HEAT warhead caused temporary incapacitation to the crews of two attacked armoured personnel carriers 302, An experience from the Swedish UN mission in Bosnia, 1994, FOA-R—97-00626-310-SE, ISSN 1104-9154.

Medin, A., Axelsson, H. and Suneson, A. (1998), The reactions of the crew in an armoured personnel carrier to an anti tank mine blast. A Swedish incident in Bosnia 1996, Defence Research Establishment Weapons and Protection Division, SE-147 25 Tumba, Sweden, FOA-R—98-00720-310—SE, ISSN 1104-9154.

Radonić, V., Giunio, L., Biočić, M., Tripković, A., Lukšić, B. and Primorac, D. (2004), Injuries from Antitank Mines in Southern Croatia, in *Military Medicine*, Vol. 169, April, pp. 320-324.

Ripple, G.R. (1990), “Predictive Criteria for Burns from Brief Thermal Exposures”; *Journal of Occupational Medicine*, Vol. 32/3, pp. 215-219.

RTO-TR-HFM-089 (2004), Test Methodologies for Personal Protective Equipment Against Anti-Personnel Mine Blast, Final Report of the NATO Research and Technology Organisation (RTO) Human Factor and Medicine Panel (HFM) Task Group TG-024, Published March.

Sellier, K. and Kneubuehl, B.P. (1994), *Wound Ballistics and the Scientific Background*, Elsevier, Amsterdam, ISBN 0-444-81511-2.

SFPE (2000), Society of Fire Protection Engineers (Ed.): “Skin Burns from Thermal Radiation – Engineering Guide”.

Stoll, A.M. and Chianta, M.A. (1968), Methods and Rating System for Evaluation of Thermal Protection, *Aerospace Medicine*, Vol. 40, pp. 1232-1238.

## Chapter 3 – INJURY CRITERIA AND TOLERANCE LEVELS

This chapter starts with a general introduction on injury biomechanics (see Section 3.1). Information on vehicle mine incidents and their injuries can be found in Annex B and C. In the research area Vehicle Mine Protection (VMP) specific body regions have been identified as the most critical ones for injuries caused by local and global effects (see Chapter 2). As mentioned in the previous chapters, it is assumed that the fragments and detonation products are not a threat to the occupants since the preservation of the integrity of the vehicle is a mandatory requirement. However, the overpressure still can affect primarily the auditory and non-auditory internal organs. Therefore these organs are discussed in this chapter as well.

The Sections 3.2 to 3.6 provide information on the different injury mechanisms and injury criteria for these specific body regions:

- Lower leg (see Section 3.2);
- Thoraco-lumbar spine (see Section 3.3);
- Neck (see Section 3.4);
- Head (see Section 3.5); and
- Internal organs (see Section 3.6).

This chapter concludes with a summary in Section 3.7.

### 3.1 INJURY BIOMECHANICS

Physical injury will take place if the biomechanical response is of such a nature that the biological system deforms beyond a tolerable limit resulting in damage to anatomical structures and/or alteration in normal function [Wismans, 1994]. The mechanism involved is called injury mechanism.

The following principal **injury mechanisms** are usually distinguished in impact (see Figure 3.1):

- **Elastic injury mechanisms:** Compression and tension of the body causing injury if elastic tolerances are exceeded. Injury can occur in case of slow deformation of the body (crushing) or in the case of high velocity impacts.
- **Viscous injury mechanisms:** Impulsive type of loading causing mechanical waves in the body, which results in internal injuries if so-called viscous tolerances are exceeded.
- **Inertial injury mechanisms:** Acceleration type of loading causing tearing of internal structures due to inertia effects.



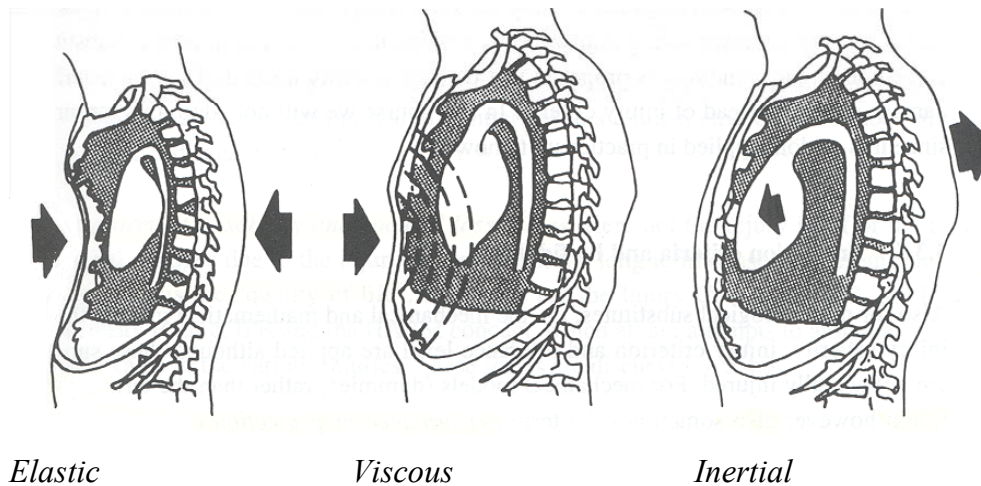


**Figure 3.1: Three Principle Mechanisms [Wismans, 1994].**

An **injury criterion** is defined as a physical parameter or a function of several physical parameters which correlates well with the injury severity of the body region under consideration. Frequently used parameters are those quantities that relatively easy can be determined in tests with human substitutes like the linear acceleration experienced by a body part, global forces or moments acting on the body or deflection of structures [Wismans, 1994].

**Injury risk curves** are used to define the injury risk for a given human body response. Examples of risk curves are shown in Figure 3.2. Along the vertical axis the injury risk is depicted, while along the horizontal axis the injury criterion is presented. The boundary conditions for which the injury criteria or models were developed are very important and will give more information about the validity of the risk curves. Sometimes, anthropomorphic factors such as age and gender, are included in the risk curves, however, the data set is usually too limited to differentiate for these factors. It should be noted that depending on the shape (which is related to the mathematical method used) of the risk curve, a small difference for the injury criterion value could result in large differences for the injury risk.

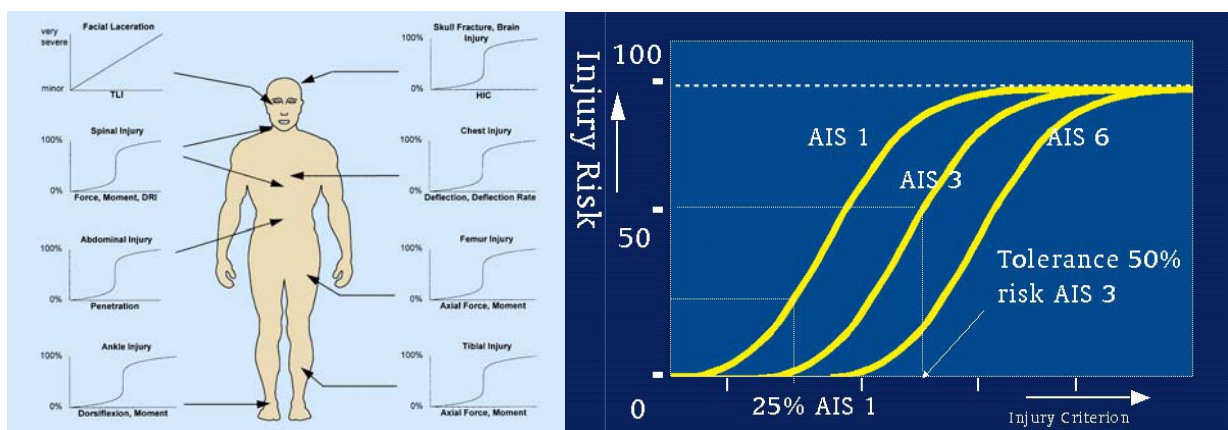


**Figure 3.2: Examples of Injury Risk Curves for Different Body Parts (left) and Different Severities (right).**

The term **tolerance level (or injury criterion level)** is defined as the magnitude of loading indicated by the threshold of the injury criterion, which produces a specific type of injury severity and risk.



Injury risk curves are mostly based on data from real case studies and experiments using animals, Post Mortem Human Surrogates (PMHS) or human volunteers. The risk curves are usually defined per body region and for specific injury severities (see Figure 3.2).

The injury severity can be defined using **injury scaling** which is defined as the numerical classification of the type and severity of an injury. The most well known anatomical scale, which is accepted world wide, is the Abbreviated Injury Scale (AIS) (see Table 3.1 and Annex C).

**Table 3.1: The Abbreviate Injury Scale [AIS, 1990]**

AIS Code	Injury Description
1	Minor
2	Moderate
3	Serious
4	Severe
5	Critical
6	Maximum (currently untreatable)
9	Unknown

The relation between threat-load-injury is presented in the TLI model by van der Horst [Horst, 2005] (see Figure 3.3). In case an injury risk curve is available, it can be used for injury assessment. This means that with information of the human body response it can be determined what the injury risk is for a specific load on that body part (Figure 3.3). Furthermore, an injury risk curve can be used to define the tolerance levels for a specific criterion (see Figure 3.4). The HFM-090/TG-25 used this method to define the tolerance levels needed for the pass/fail limits to qualify the protection level according to STANAG 4569. Based on discussions with the members of STANAG 4569 it has been decided that a 10% risk of AIS 2+ (AIS 2 or more) injuries will be accepted as pass/fail criterion for the AV mine strike tests. It should be noted that when accepting a 10% risk of AIS 2+, still a lower risk of higher severity (AIS 3+) injuries can be expected. On the other hand, this level implies a risk of more than 10% of AIS 1 injuries.

## INJURY CRITERIA AND TOLERANCE LEVELS

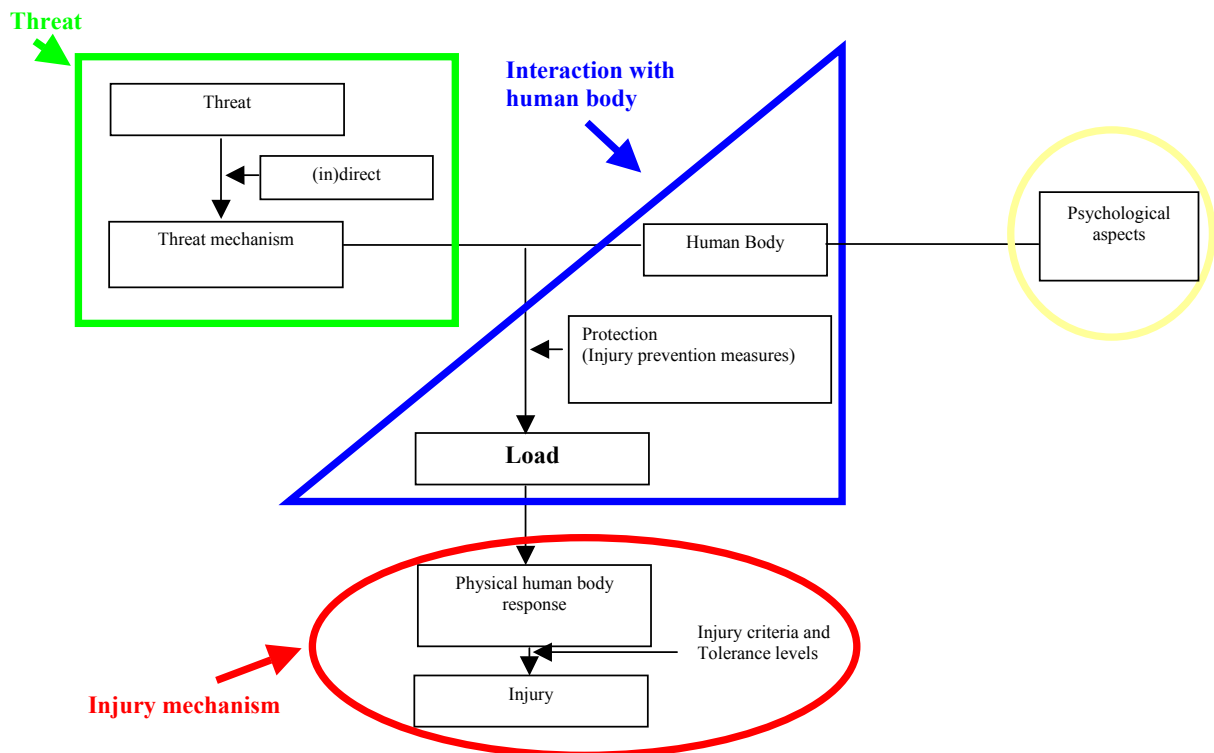


Figure 3.3: The Threat Load Injury (TLI) Model [Horst, 2005].

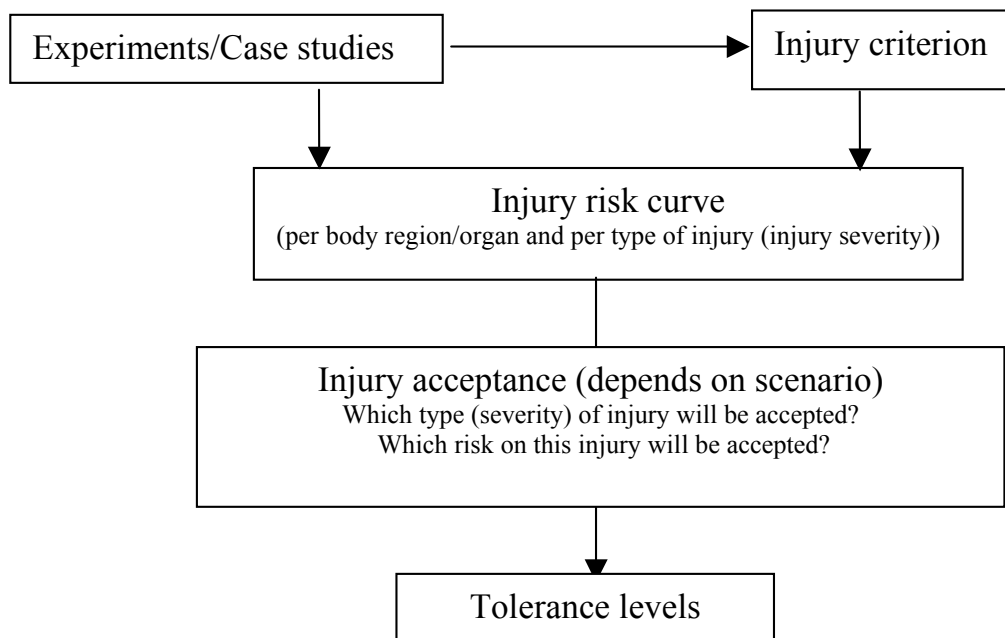


Figure 3.4: Flow Scheme to Determine Injury Tolerance Levels for Body Regions.

Standard injury criteria for the military field of application are usually not available. That is why STANAG 4569 asked HFM-090/TG-25 to define injury criteria and tolerance levels for the vehicle mine protection field. In general, the loading conditions for the occupant during a mine strike under a vehicle

are quite similar to vertical loads of pilots in an ejection seat in the aerospace, and to the loading of the human leg due to foot well intrusion in case of a frontal car impact, although higher amplitudes and shorter durations have to be expected. Criteria available from automotive and aerospace industry research areas were used by HFM-090/TG-25 as starting point to define injury criteria for the vehicle mine protection field.

### **3.2 LOWER LEG**

This section provides information on lower leg anatomy and injuries, and on the injury risk model to be used when performing AV mine protection testing. Additional information related to lower leg injury assessment is provided in Annex E.

#### **3.2.1 Anatomy, Loading Mechanisms and Injuries**

The lower limb (or lower extremity) is divided in four regions: the thigh, the knee, the leg and the foot/ankle complex. The femur is the thigh-bone, the patella is the knee bone, the tibia and the fibula are the leg bones, and the phalanges, the metatarsals and the tarsals are the bones of the foot/ankle complex (see Figure 3.5). The tibia is the larger of the two leg bones and bears most of the body weight. In this report, the term lower leg is used to designate the leg and the foot/ankle complex.

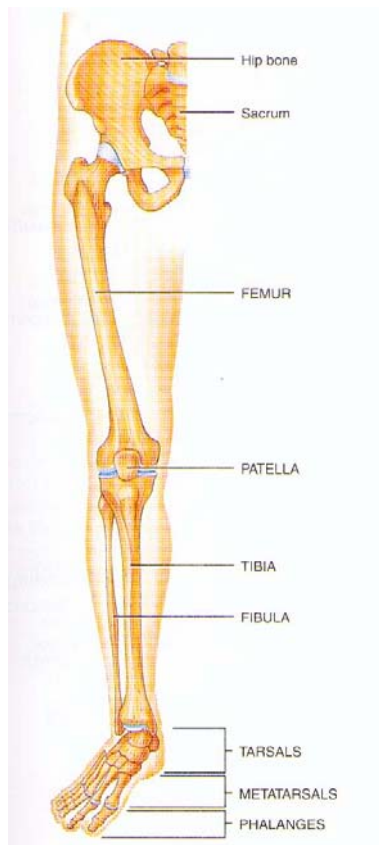


**Figure 3.5: The Lower Limb [Tortora, 2003].**

Figure 3.6 shows the medial view of the right foot. The tarsal bones (in the ankle) are the calcaneus, the talus, the cuboid, the navicular and the three cuneiforms. The talus, which is the only bone to articulate with the tibia and the fibula, transmits all the forces from the foot to the leg.

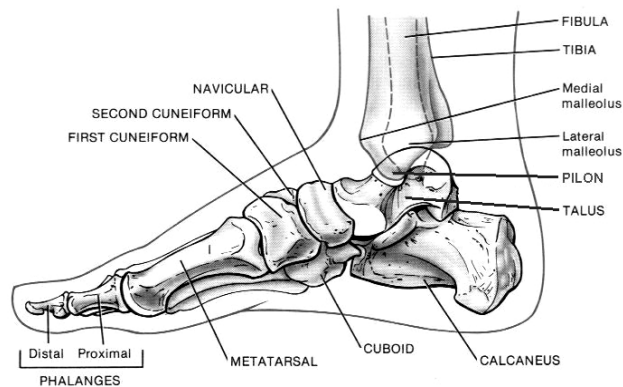


**Figure 3.6: Foot/Ankle Complex Anatomy (Modified from [Tortora, 1984]).**

When a landmine detonates under a vehicle, the movement of the structure on which the foot rests (floor, driver pedal, etc.) may cause an impact on the foot resulting in injuries to the lower leg. For example, when the foot is in direct contact with the bottom plate, its dynamic local deformation induces an important axial load to the lower leg, which may result in fractures in the foot/ankle complex. Tibia and fibula fractures and especially calcaneus fracture may also occur when the lower leg is subjected to an axial impact [Funk, 2002], but foot/ankle fractures will be predominant. Lower leg fractures have a score of AIS 2 or 3 and are not life-threatening injuries. The tendency of bone to fracture depends on their mineral density, which is strongly correlated with age, gender and body mass [Funk, 2002]. Bone density decreases with age and increases with body mass. Also, males have higher bone mineral density than females, which increases their tolerance to fracture. Soft tissue injuries (ligaments/muscles/vascular), such as sprain and contusion (AIS 1), may also occur with or without hard tissue (bones) fractures. It should be noted that complex fractures can also cause serious vascular injuries which can be of course life threatening, especially in military applications (i.e. long time till medical treatment).

Lower extremity injuries are associated with important disability and impairment. For example, fracture of the calcaneus, which is common to AV mine strikes [Medin, 1997, 1998; Radonić, 2004], often results in long-term complications such as infection and osteoarthritis [Funk, 2002]. Because the healing of calcaneus fracture is poor and is usually associated with intense pain, such injury may result in a surgical amputation of the leg.

### 3.2.2 Injury Risk Model

The loading mechanism acting on the lower leg during an AV mine strike is comparable to the one observed during frontal car crashes during which axial loading is applied via the pedal or the toepan. Therefore, literature from car crash safety research has been used here. Since seat belts and airbags significantly reduce the risk of life-threatening injuries to the head, neck, chest and abdomen, the automotive community is presently concentrating an effort towards the study of other body regions such as the foot/ankle complex. Studies on PMHS lower leg tolerance to fracture under dynamic axial impacts, such as the ones of [Yoganandan, 1996; Griffin, 2001; Seipel, 2001; Kuppa, 2001; Funk, 2002], are of strong interest in the field of mine protection research. This section focuses on the Yoganandan model and its (dis) advantages, since the TG-25 has selected this model among the available models found in the literature. Analysis of the other injury risk models is presented in Annex E.

#### 3.2.2.1 Description of Yoganandan Model

Dynamic axial impact tests were conducted by [Yoganandan, 1996], at the Medical College of Wisconsin (MCW). As shown in Figure 3.7, twenty-six intact adult lower legs were tested under dynamic loading using a mini-sled pendulum device.

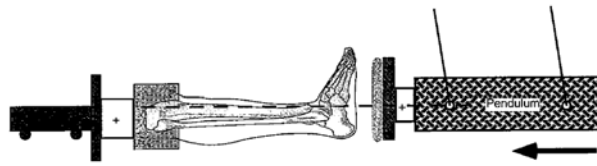


Figure 3.7: Experimental Set-up for MCW Dynamic Axial Impact Tests on PMHS Lower Legs [Yoganandan, 1996].

The forces were recorded on the pendulum impactor and at the upper end of the tibia. Statistical analysis, using the Weibull technique [Devore, 1999] was performed to derive a risk function. The probability of foot/ankle fracture is described as a function of specimen age and dynamic axial force measured at the distal end of the tibia. The pendulum maximal velocity ranged from 2.2 to 7.6 m/s and fracture tibia forces ranged from 4.3 to 11.4 kN. Results of MCW tests were combined to the ones obtained from similar studies at Wayne State University and Calpan Corporation to derive the foot/ankle injury risk equation. The model was developed using a sample of 52 specimens with an age range of 27 to 85 years old. Figure 3.8 shows the probability distribution for foot/ankle injuries as a function of age and tibia force (peak value). Plus/minus one standard deviation limits are shown in dotted lines and solid circles represent the fracture and non-fracture data points. Fractures, including extra/intra-articular (outside or inside the joint) fractures of the foot/ankle and distal tibia complex, were reported.

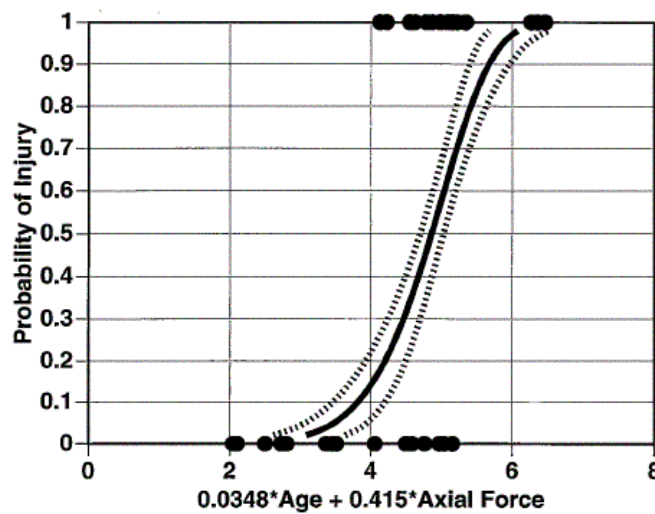


Figure 3.8: Risk of Foot/Ankle Injury as a Function of Age and Tibia Axial Force [Yoganandan, 1996].

Based on the relation given on Figure 3.8, the probability of foot/ankle fracture can be expressed as follows:

$$p(fracture) = 1 - \left[ \exp \left\{ - \left( \frac{0.0348 * age + 0.415 * force}{5.13076} \right)^{7.42582} \right\} \right]$$

where:

- $p(fracture)$  is the probability of foot/ankle fracture;

## INJURY CRITERIA AND TOLERANCE LEVELS

- Age is in years; and
- Force is the maximum tibia axial force value (in kN).

Using this Weibull probability equation presented above, the risk of foot/ankle fracture as a function of tibia force can be computed for any age. Figure 3.9 presents foot/ankle injury risk curves for 25, 45 and 65 years old.

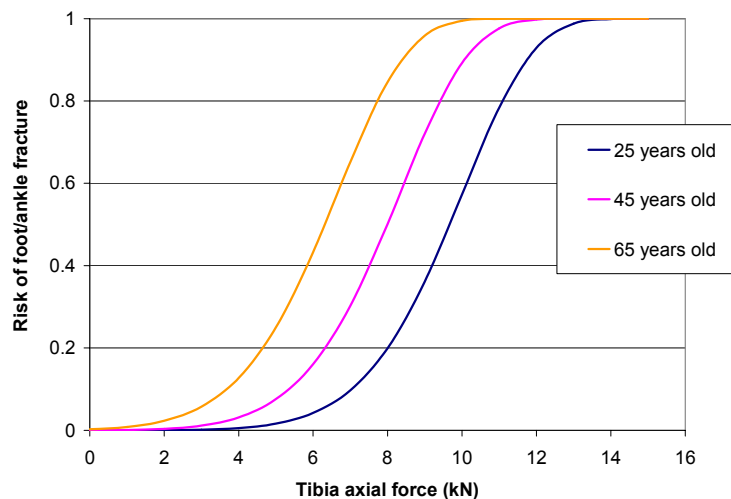


**Figure 3.9: Foot/Ankle Injury Risk Curves for 25, 45 and 65 Years Old (Based on Data from [Yoganandan 1996]).**

Based on the curves shown in Figure 3.9, the tolerance value for 25, 45 and 65 years old are respectively 7.0, 5.4 and 3.8 kN, representing 10% risk of foot/ankle fracture (AIS 2+). To protect most of the population in military vehicles (having an estimated age range of 20 to 45 years old), the tolerance value of 5.4 kN (for 45 years old) was chosen by the TG-25. Because most of the specimens used by Yoganandan were male (39 on 52) and the average specimen's weight was 75 kg, this tolerance value is applicable for mid-size males or large females [see Chapter 4, Figure 4.1 and Figure 4.2].

### 3.2.2.2 Applicability of Yoganandan Model

The Yoganandan injury risk model takes into account the most important factor affecting the lower leg tolerance to fracture: age. Because the specimens available to perform this kind of tests are usually old, the injury risk models developed without considering this factor [Seipel, 2001; Griffin, 2001; Kuppa, 2001] give very severe tolerance values. The injury risk model by Funk [Funk, 2002], including age, gender and weight, was also a satisfying model. The Yoganandan model was chosen instead of the Funk model because of the larger sample size (52 specimens) used to develop the model and the large age range (27 to 85 years old) of the specimens. Funk study was done with 30 specimens with an age range of 41 to 74 years old. However, as shown in Annex E, the Funk and Yoganandan models correlate very well for age of 45 years old which gives confidence in the lower leg injury tolerance value established by the TG-25.

### 3.2.2.3 Limitations of Yoganandan Model

The Yoganandan injury risk model, as well as all other similar models found in the literature [Kuppa, 2001; Griffin, 2001; Seipel, 2001; Funk, 2002] was developed for a pure axial loading. As shown on Figure 3.7, the lower leg was placed in a neutral position (ankle at approximately 90 degrees) and was

axially loaded. The tibia axial force was then used to compute the risk of foot/ankle complex injuries. Depending on seating configuration and footrest systems which are used in the mine strike tests the load transfer through the tibia can differ compared to this pure axial loading conditions. In that case, the risk of foot/ankle might be underestimated. A preliminary study on the effects of lower leg positioning for AV mine strike simulations was done using the multi-body/finite element software package MADYMO [Horst, 2004]. This study (summarized in Annex E), showed how the lower leg positioning can affect the tibia axial force and therefore the injury prediction when using the Yoganandan model without necessarily representing the real risk of foot/ankle injuries.

The proposed model, as well as other lower leg injury models found in the literature, is based on peak tibia axial force value and does not consider duration of the loading application. Due to the visco-elastic properties of the human tissues, their injury tolerance is believed to be time-dependant [Yoganandan, 1989]. The currently available data on injury risk models for lower legs are generated by (simulated) car crashes, which are usually slower incidents than mine strikes. Since standard Hybrid III tibia loading durations seen in AV mine strike tests are very short (can be less than 10 ms), the proposed tolerance value could be too severe. At this point, it is not known among the loading duration, the rise-time, and the impulse, which one has the strongest influence on injury tolerance. WTD 91, Meppen, Germany has started to develop a time-dependant lower leg injury criterion based on tibia loading duration, called the Lower Leg Threshold (LLth). More information about this criterion can be found in Annex E. However, so far the validation of this criterion is not available.

Finally, the use of the anthropomorphic test device (ATD) can have some limitations for injury assessment as well. As will be discussed in Chapter 4, HFM-090/TG-25 proposes to use the Hybrid III 50th percentile male ATD. The standard Hybrid III instrumented lower leg biofidelity is known to be poor based on recent PMHS tests. [Owen, 2001] showed that for non-injurious testing, when the lower leg is axially loaded on the heel, the Hybrid III tibia peak axial force is approximately 1.2 to 1.6 times higher than the one measured on PMHS tibia. Based on these results, the proposed lower leg injury criterion could be too conservative when using the standard Hybrid III lower leg. Validation for the mine loading conditions is not possible at the moment. More discussion on the choice of the ATD leg model for injury assessment is presented in Chapter 4.

### **3.2.3 Conclusions**

In conclusion, the proposed lower leg injury model is the best available in the open literature at this point. The Yoganandan model was chosen as opposed to other models because of the large sample size of lower leg PMHS within a wide age range. The mathematical model proposed by HFM-090/TG-25 is taking specimen age into account, which is the most important factor affecting the injury tolerance. Based on this parameter, it was possible to establish a realistic tolerance value for military vehicle occupants who are relatively young. The proposed tibia axial force tolerance value is 5.4 kN (10% risk of AIS2+). One major limitation of the model is that it was developed for a pure axial loading and that risk of injury may be underestimated when the lower leg is loaded differently. The other important limitation of the proposed lower leg injury assessment method could be the choice of the ATD lower leg model (see Chapter 4). Based on these limitations, further research on lower leg injury assessment methods was identified as a priority by the HFM-090/TG-25.

## **3.3 THORACO-LUMBAR SPINE**

This section provides information on thoraco-lumbar spine anatomy and injuries, and on the injury risk model to be used when performing AV mine protection testing. Additional information related to thoraco-lumbar spine injury assessment is provided in Annex F. Although pelvic injuries may also occur due to the high vertical loadings, it was assumed that thoraco-lumbar spine injuries are predominant and hence, are used as an indicator for pelvic injuries [Dosquet, 2003].



### 3.3.1 Anatomy, Loading Mechanisms and Injuries

The major functions of the vertebral column are protection of the spinal cord and stiffening for the body, and attachment for the pectoral and pelvic girdles and many muscles. The vertebral column extends from the base of the skull to the tip of the coccyx. It contains 33 discrete vertebrae and 23 intervertebral disks. These vertebrae are held together by joints and ligaments. The joints and ligaments provide stability to the spinal column while at the same time providing limited movement. There are different types of vertebrae [see Figure 3.10], and each can be easily identified by their definite physical characteristics.

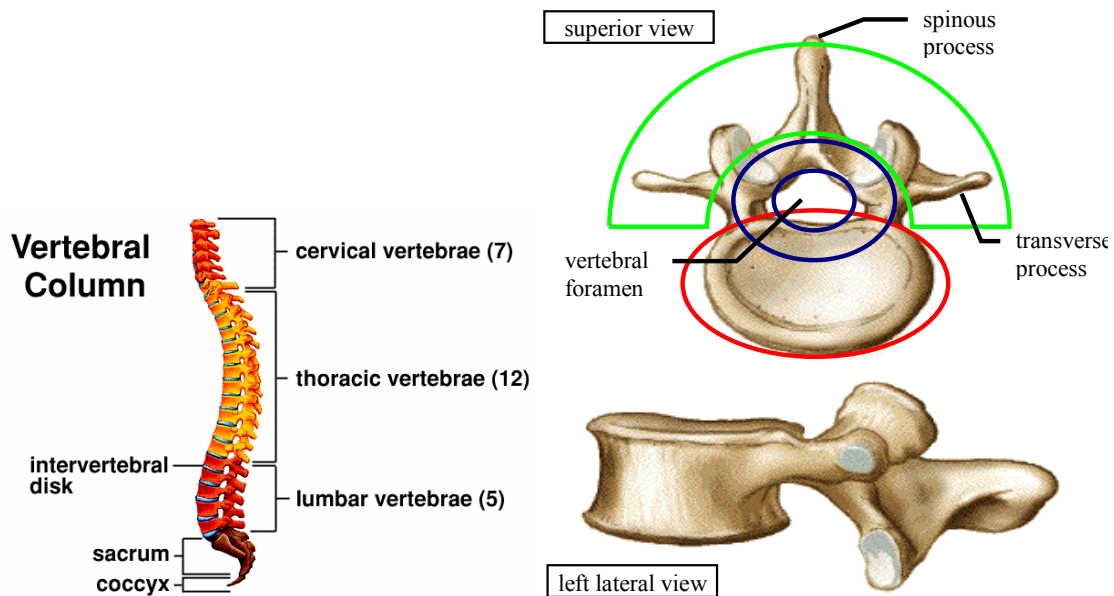


**Figure 3.10: Lateral View of Vertebral Column (left) and (on the right) Lumbar Vertebra with Vertebral Body (red), Vertebral Arch (blue) and Facet Joints and Processes (green).**

The seven cervical vertebrae have a dorsal spine and a large foramen in the transverse process. Following the cervical vertebrae are the thoracic vertebrae, which are medium in size compared to the cervical and lumbar vertebrae. The main function of the thoracic spine is to protect the organs of the chest by providing attachment for the rib cage. The range of motion in the thoracic spine is limited. The lumbar vertebrae are the heaviest and largest of the three types of individual vertebrae due to their weight bearing function of the body. They have a long transverse process and a thick dorsal spine (see Figure 3.10). The sacrum which consists of five fused vertebrae follows the fifth lumbar vertebra. At the end of the line three to five vertebrae are fused to the coccyx.

Each vertebra has three functional parts:

- The anterior vertebral body has to bear weight and withstand compressions.
- The posterior arch-shaped bone provides protection for the spinal cord.
- Muscles are attached to the posterior processes. The facet joints allow a limited backwards motion of the spine.

The spinal column is one of the vulnerable parts of crew members in vehicular mine incidents due to different loading mechanisms in cranial (axial) direction. Most critical is a direct impact of the elastic structural deformation via the seat system to the spinal column. Furthermore the transfer of the shock wave via the structure and the seat system can cause serious injuries of the spinal region.



Various types of injuries have to be expected: damage to the bony structure (i.e. vertebral fractures) as well as ligamentous and muscle injuries. Vertebral fractures cause the bone to lose height and form a wedge shape. In very severe compression fractures, the back of the vertebral body may protrude into the spinal canal putting pressure on the spinal cord. The spine can withstand an enormous amount of pressure; however, if the force is too great for the vertebra to withstand, one or more of them may break (fractures of the spinous and transverse process (AIS 2), the facet (AIS 3), the lamina (AIS 3), the pedicle (AIS 3) and the vertebral body (AIS 2-3)).

The thoraco-lumbar spine is the most vulnerable part of the spinal column when subjected to axial loading, as presented in a study of U.S. Army non-fatal helicopter crash injuries from 1979 – 1985 [Shanahan, 1989]. The lower thoracic (T12) and the upper lumbar vertebral bodies (L1 – L2), are specifically at risk because of the relation of the strength of and loads on the vertebral bodies due to the effective body weight [Dosquet, 2003].

The probability of injuries due to loading mechanisms in lateral and dorso-ventral direction are quite low because of the predominance of axial load scenarios with a mine threat. More than 50 mine protection trials with a huge variation of the boundary conditions (vehicle mass, seat adaptation, mine types, etc.) illustrated this [Dosquet, 2003].

### **3.3.2 Injury Risk Model**

Loads with durations less than 10 ms presuppose injury risk models which consider the dynamic behaviour of the thoraco-lumbar spine. Hence a dynamic function and not a constant value would reflect the requirements for an assessment criterion for mine related incidents. The Dynamic Response Index (DRIZ) model meets these requirements, whereas other available injury models for the thoraco-lumbar spine disregard the duration dependency or are not validated. In this section, only the recommended Dynamic Response Index (DRIZ) for the cranial direction (Z-axis) will be described in detail, since TG-25 decided that this DRIZ model fits the best for the injury assessment in AV mine strike tests. Other models are presented in Annex F.

#### **3.3.2.1 Description of DRI Model**

Stech and Payne [Stech, 1969] evaluated the Dynamic Response Index (DRI) as a general model to simulate the biomechanical response due to human body dynamics by using a single mass-spring-damper system (see Figure 3.11). The general model was already introduced by Latham in 1957 [Latham, 1957] to describe the impact of ejection seats to the human body. The DRIZ is the Dynamix Response Index in axial direction (z-direction).

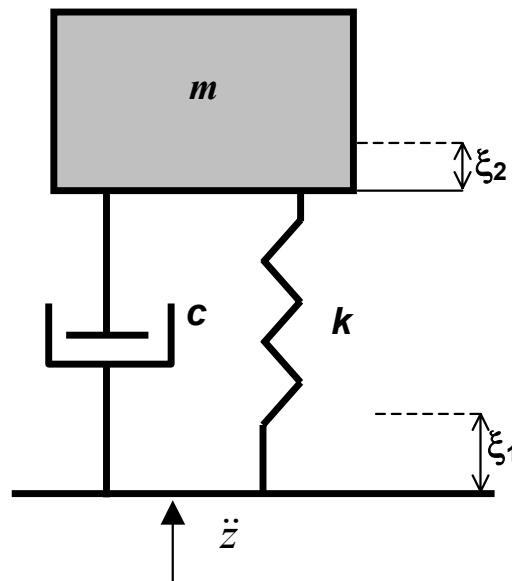


Figure 3.11: DRIZ Model [Stech, 1969].

The equation of motion for this model is:

$$\ddot{z}(t) = \ddot{\delta} + 2 \cdot \zeta \cdot \omega_n \cdot \dot{\delta} + \omega_n^2 \cdot \delta$$

where

- $\ddot{z}(t)$  is the acceleration in the vertical direction measured at the position of initiation
- $\delta$  is the relative displacement of the system with  $\delta = \xi_1 - \xi_2$ ; and  $\delta > 0 \Rightarrow$  compression
- $\zeta$  is the damping coefficient with  $\zeta = \frac{c}{2 \cdot m \cdot \omega_n}$
- $\omega_n$  is the natural frequency with  $\omega_n = \sqrt{\frac{k}{m}}$

The DRIZ is calculated by the maximum relative displacement  $\delta_{\max}$ ,  $\omega_n$  and the gravity acceleration  $g$ :

$$DRIZ = \frac{\omega_n^2 \cdot \delta_{\max}}{g}$$

The first application was a dynamic model of the human body in spinal direction by Stech and Payne (vertical compression of the spinal column). They selected the values of  $\zeta$  and  $\omega_n$ , 0.224 and 52.9 radians/s respectively, as values for a representative population of Air Force pilots with a mean age of 27.9 years. These values were estimated based on investigations on compressive individual vertebral strength by Geertz [Ruff, 1950] as well as on load-deflection curves [Yorra, 1956]. Ruff [Ruff, 1950] summarized the investigations by Geertz during WW II. The tests were made either with individual vertebrae or vertebral complexes of PMHS between 19 and 46 years of age. By using Geertz data as an indication for vertebral compression fractures, Stech and Payne related the DRIZ value to an injury risk of 50% depending on the age of the population. For an average age of 27.9 years, they calculated a DRIZ of

21.3. This value was used as a baseline to introduce the function of spinal injury risk due to compressive loads versus DRIZ values by assuming a normal distribution [Brinkley, 1970]. This function is presented in Figure 3.12 as the laboratory data curve.

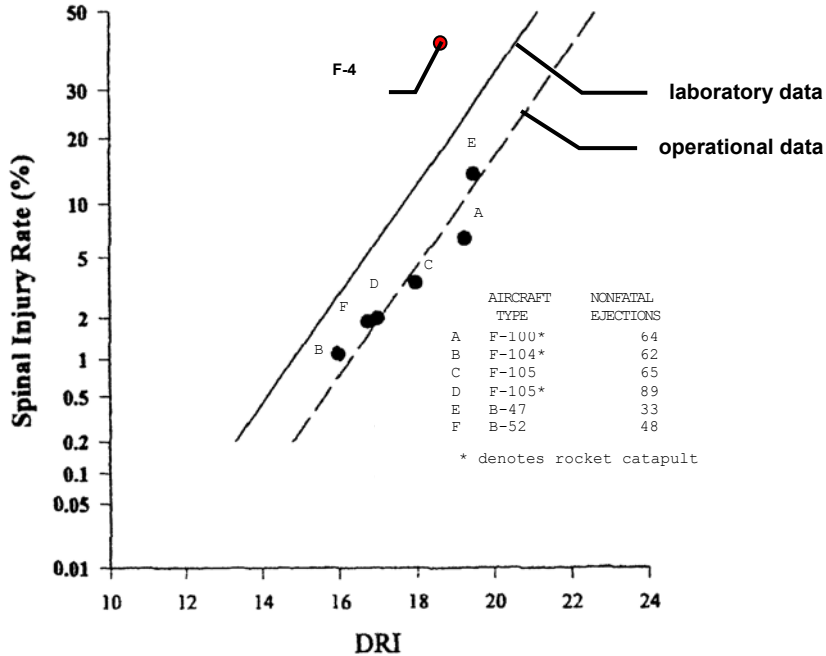


Figure 3.12: Spinal Injury Risk Calculated from Laboratory and Operational Data and F-4 Operational Data [Brinkley, 1970] Valid for AIS 2+ Injuries.

Furthermore, they presented the injury risk as a function of DRIZ based on operationally experienced non-fatal spinal injury probabilities, which were calculated in ejection seat tests (Figure 3.12 operational curve). The relation of injury risk and DRIZ is only valid for misalignments of the ejection seat compared to the catapult acceleration vector of less than 5°. Brinkley and Shaffer stated that the seat of an F-4 aircraft did not permit the crewman vertebral column to be aligned with the catapult acceleration vector as in other Air Force ejection seats; therefore, they excluded the F-4 data. When not aware of this misalignments and just using the operational curve, a risk of 9% would be predicted for these F-4 seat. However, when looking at the real data a DRIZ of 19 related to a spinal injury probability of 34% for the F-4 seat, which is much higher. Therefore, it is assumed that for higher misalignments than 5° the tolerance levels decrease, resulting in higher injury risk at the same DRIZ value.

### 3.3.2.2 Applicability of DRI Model

It should be noted that durations and maximal values of the transmitted load to the crew members varies significantly due to different threat types and vehicle concepts such as different vehicle masses, seat adaptations and seat concepts. However, the DRIZ includes a dynamic behaviour which is necessary for injury assessment of the short duration load occurring during a mine strike.

The injury model based on the laboratory data (compressive strength of vertebrae) has the pelvis as point of initiation (location where load is transferred to the model), whereas the model based on the operational data has the seat as point of initiation [Brinkley, 1970]. However, in several mine protection trials, the seat acceleration data have shown a high variation and a lack of reproducibility. Although the characteristics of the DRIZ model is comparable to a filter, the variation of the seat acceleration input has an impact to the

## INJURY CRITERIA AND TOLERANCE LEVELS

---

reproducibility of the DRIZ data, whereas the variation of DRIZ data based on acceleration measurements in the pelvis of the anthropomorphic test device (ATD) was quite low. Therefore, using the pelvis accelerations of the ATD is recommended.

Originally, the DRIZ calculations are based on seat accelerations. However, in some countries seat cushion accelerations or pelvis accelerations are used as input for the DRIZ model. Investigations on the DRIZ calculation based on acceleration data measured in a seat itself, the seat cushion and measured in the ATD pelvis in 63 tests of different test facilities demonstrated a sufficient correlation of the results [Dosquet, 2004]. The DRIZ values based on pelvic accelerations are slightly lower than the seat cushion DRIZ values, but these differences are not significant.

Based on these studies TG-25 decided that the DRIZ calculations for the mine strike trails should be based directly on measurements of the ATD pelvis.

As aforementioned, the operational data curve is not strict enough for specific boundary conditions. Some military vehicles provide misalignments of 15° and more. Furthermore, seats of protected vehicles are often adapted to the roof or the wall of the vehicle. This conceptual boundary condition causes similar effects on the load on the crew member as higher misalignments. When the misalignments of the seats are higher than 5°, the injury risk will be higher than calculated with the operational data curve, which only accounts for loads in spinal direction. Although the operational data is based on real incidents, the underestimation of the injury risk for different seat concepts resulted in the TG-25 decision to use the laboratory data curve, which is more conservative than the operational data curve. When using this curve (see Figure 3.12) the tolerance level of 17.7 for DRIZ refers to a 10% risk of AIS 2+ injuries.

### 3.3.2.3 Limitations of DRI Model

The spine injury mechanism is force driven. Using a model which is based on another physical parameter than force, e.g. the pelvis acceleration, may introduce uncertainties. However force based injury models taking the visco-elastic properties of the vertebral column into account are not available yet.

### 3.3.3 Conclusions

In conclusion, the Dynamic Response Index (DRIZ) model is at this point the best available model for thoraco-lumbar spine injury assessment. Considering relative low injury risks of spine injury due to lateral (y) and dorso-ventral (x) loads TG-25 decided to only assess spine injuries in the vertical (z) direction and use the DRIZ model. The DRIZ is to be calculated with the pelvis ATD vertical acceleration. Based on discussions on the two risk curves available in literature (see Figure 3.12), HFM-090/TG-25 decided to use the more conservative risk curve derived from laboratory data. When using this curve (see Figure 3.12) the tolerance level of 17.7 for DRIZ refers to a 10% risk of AIS 2+ injuries.

## 3.4 NECK

This section provides information on neck anatomy and injuries, and on the neck injury criteria to be used when performing AV mine protection testing. Additional information related to neck injury assessment is provided in Annex G.

### 3.4.1 Anatomy, Loading Mechanisms and Injuries to the Neck

#### 3.4.1.1 Anatomy

The cervical spine is the most important part of the neck and it comprises of seven vertebrae forming eight motion segments between the base of the skull and first thoracic vertebra (see Figure 3.13, the most upper

vertebra is denoted C1 and the lowest is C7). The cervical spine (neck) is divided morphologically and mechanically into two regions, the upper cervical and lower cervical spine. The lower cervical spine contains vertebrae C3 through C7. The upper cervical spine consists of three bony elements: the occiput (the base of the skull), the atlas (C1) and the axis (C2). Enlarged facets on the atlas allow for articulation with the base of the skull. The axis has a bony projection called the dens, or odontoid process, which projects upward and serves as the vertebral body of the atlas. The dens also serves as the axis about which the head and atlas rotate.

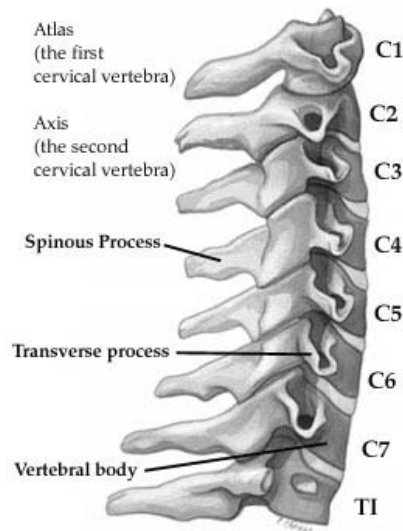


**Figure 3.13: Cervical Vertebrae [Gray, 1985].**

A number of ligaments hold the vertebral bodies together. These include the anterior and posterior longitudinal ligaments, which span the anterior and posterior portions of the vertebral bodies. There are several additional ligaments, which are named for the parts of the vertebral structure, which they connect. The vertebral bodies are connected to each other by means of an intervertebral disk. The disk is a fibrocartilaginous structure composed of a central nucleus pulposus and surrounded by the annulus fibrosus, a laminar set of fibrous sheets.

### **3.4.1.2 Loading Mechanisms**

Head and neck motion can be described anatomically as shown in Figure 3.14, which depicts these and associates terms with the movements of the head/neck complex.

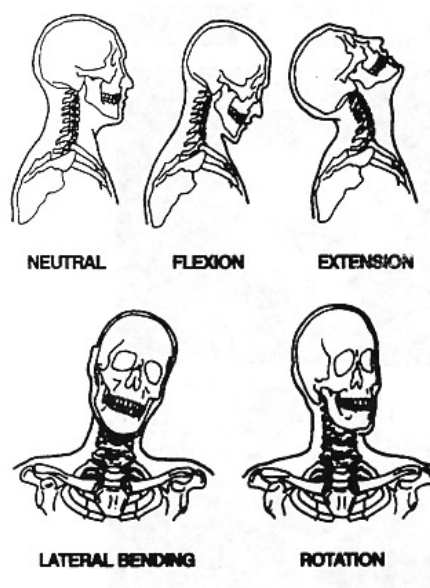


**Figure 3.14: Anatomical Description of Head Movement [McElhaney, 2002].**

A useful way to classify neck injury mechanisms is by an engineering description of loading as depicted in Figure 3.15.

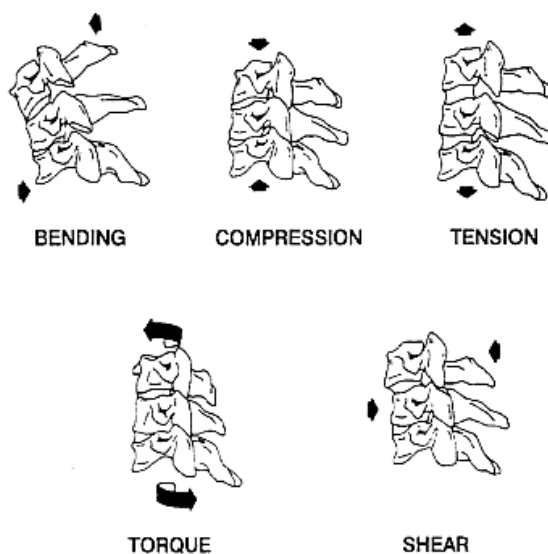


**Figure 3.15: Engineering Description of Neck Loading [McElhaney, 1993].**

The loading mechanisms described by Figure 3.15 may occur also at thoracic and lumbar region of the spine. However, neck injuries are usually more life-threatening since they may affect the phrenic nerve, responsible of the respiration functions.

In anti-vehicular (AV) mine blast incidents it is impossible to predict precisely which injury mechanism will occur. Primary location of the blast, type of vehicle, positioning of the occupant, geometry of the interior of the vehicle relative to the position of the crew member, and movement of the individual after the initial loading phase all play a part in determining what mechanism, if any, contributes to an injury.

However, the most important neck injury mechanisms expected to occur during a mine strike are the followings:

- Axial (vertical) compression;
- Forward bending (due to flexion);
- Rearward bending (due to extension); and
- Lateral bending.

In order to facilitate the reading of the next paragraphs, the following terms will be used to discuss each of these injury mechanisms mentioned above: axial compression, flexion, extension and lateral bending.

While purely compressive loading of the neck is considered to occur infrequently, many AV mine incidents may be considered to be predominantly **axial compressive loading**. With the detonation of an anti-vehicular landmine, the major component of vehicle and occupant acceleration is vertical. Many tactical vehicles have very little space between the crown (top of helmet) and the roof structure. Although the intent is to restrain the occupant to prevent excessive movement, necessary limited stretching of the upper restraints and movement of the seat complex may result in a nearly compressive strike of the occupants head into a roof structure. Based on full-scale test data, when there is no impact of the head on the roof, the axial load transmitted through the spine is not considered being important enough to cause neck injuries since the load will mainly be absorbed by the thoraco-lumbar region.

Neck injuries will usually be the result of more than one injury mechanisms. For example, automotive crash investigations indicated that compression-extension injuries resulted from head impact with the windshield, resulting in the simultaneous extension and compression on the neck, giving rise to posterior structure injuries (King, 2000). During AV mine strike, head impact on the roof will probably result in **axial compression combined with extension, flexion or lateral bending**, depending on the head position prior to impact. Finally, injury to the neck may also result of inertial loading, i.e. violent head movement without direct impact on vehicle structure.

### 3.4.1.3 Injuries

Trauma to the neck has been divided into three main categories (Pikes, 2002):

- 1) Osseous (bone) injury;
- 2) Soft tissue injury; and
- 3) Neurological injury.

**Osseous injury** refers to vertebral fractures. The severity level of these fractures will depend on: whether or not the fracture resulted in impingement of the neurological structures, and whether or not the fracture is structurally stable. For example, fracture of the atlas (C1) by compression is called the ‘Jefferson’ fracture, and may occur if the head impact the vehicle roof. Other examples of vertebra fractures are given in Annex G.

**Neurological injury** is the most severe class of neck injuries, which may result in paralysis, long-term pain and even death. They generally are the result of primary osseous or soft tissue injuries.

**Soft tissue injury** is the most common type of neck injury in vehicular crash environment. For example, neck sprain, in which the ligaments are stretched beyond their normal limits, is a result of flexion-extension (also called ‘whiplash’). Ligamentous injuries are usually minor, but when severe, they can impart severe neurological impairment.



### **3.4.2 Injury Criteria**

Numerous experimental studies, both static and dynamic, have been conducted over the past 40 years to determine injury producing loads and develop injury criteria. The well known Neck Injury Criterion (Nij), which considers combined injury mechanisms and is used as a standard for frontal car crashes, was not chosen for the reasons mentioned in Annex G. The proposed neck injury assessment method considers all injury mechanisms separately. The method includes axial compression, flexion and extension injury criteria, which are described in the next paragraphs. Due to lack of information on Hybrid III neck biofidelity and injury criteria for lateral bending, no injury criterion for this specific loading mechanism was included.

#### **3.4.2.1 Description of Axial Compression Injury Criterion**

Mertz et al. [Mertz, 1978] undertook a study to develop axial compression neck injury tolerance curves. Impact tests of a spring-loaded tackling block on football helmets [Mertz, 1978] were conducted with a 50<sup>th</sup> percentile male Hybrid III and then compared them to real accidents of high school aged football players. One player (17 years old, 1.88 m, 101 kg) suffered immediate paralysis of the arms and legs and X-rays showed fractures of C3, C4 and C5. A second 17 year old player (1.82 m, 95 kg) suffered fatal injuries including hemorrhages in the brain stem and pons (white matter nerve fibers) and subarachnoid blood (area of brain containing cerebrospinal fluid, cushioning brain from mechanical shock). In a third incident, a high school player was allegedly struck and rendered quadriplegic by the same tackling block used in Mertz's experiments.

In the tests, the Hybrid III was oriented so that the load was applied to the top of the head, loading the neck structure in compression with minimal head rotation (appropriate figure of the test set-up was not available). The configuration was chosen to produce the maximum value of neck compression force for the impact velocity chosen. The neck compression load measured by the Hybrid III was considered representative of the upper bound of maximum axial compressive load that an equivalent weight human would have experienced for the same impact velocity.

Based on this study, Mertz [Mertz, 1978] derived two injury tolerance curves based on the upper neck axial compression force measured on a 50<sup>th</sup> percentile male Hybrid III (see Figure 3.16). The coordinates of the 'Upper' curve are 0 ms and 6670 N, 35 ms and 1110 N, and greater than 35 ms, 1110 N. The coordinates of the 'Lower' curve are 0 ms and 4000 N, 30 ms and 1110 N, and greater than 30 ms, 1110 N. To evaluate neck load signal, pairs of points (force, duration) are plotted on the graph (shown in Figure 3.16) with the two injury assessment curves. The points are connected together by a series of straight lines. If any of the line segments lie above the upper curve (red), the neck axial compression force is considered to have the potential to produce serious neck injury. If any of the line segments lie above the lower curve (blue), the potential for neck injury from the axial compressive force is considered less likely. If none of the line exceeds the lower curve, the probability of neck injury from axial compressive force is considered remote.



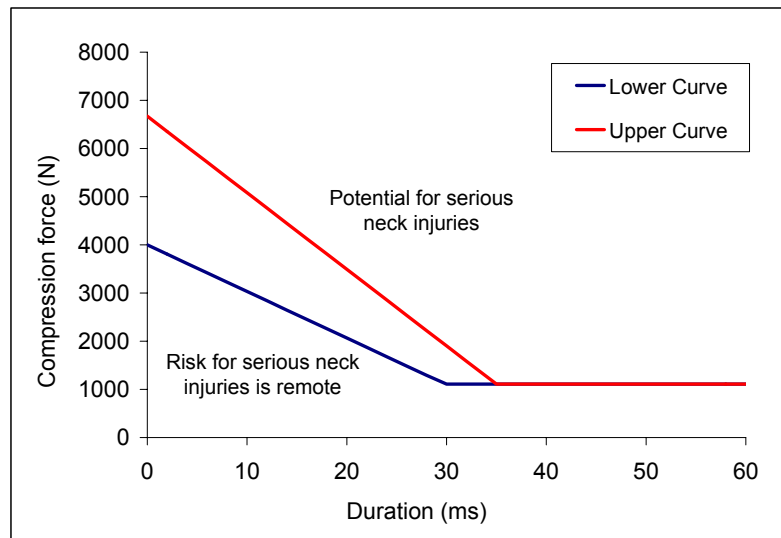


**Figure 3.16: Injury Tolerance Curves for Axial Neck Compression Force when Using a Hybrid III 50<sup>th</sup> Percentile Male ATD [Mertz, 1978].**

These levels were proposed for an adult population that was considerably older (exact age range not known) and much less conditioned than a high school football athlete. The time durations were determined from the loading times observed during the experiment, which were on the order of 30 – 40 ms.

The HFM-090/TG-25 proposed to use **the lower curve (blue)** in Figure 3.16 as the tolerance level for neck compression injuries in AV mine strike tests. Exceeding this level implies that serious neck injuries are likely.

### 3.4.2.2 Description of Flexion/Extension Injury Criteria

Mertz and Patrick [Mertz, 1971] as well as Patrick and Chou [Patrick, 1976] conducted tests on volunteers and PMHSs to determine neck reaction on the head under dynamic conditions. Human volunteers were subjected to static and dynamic tests to produce non-injurious response for neck flexion and extension. PMHSs were used to extend the data into the injury region. Their analysis of the data indicated that equivalent moment at the occipital condyles (protusions on the back of the skull which articulate with the cervical vertebra) was the critical injury parameter in flexion (forward) and extension (backward).

The dynamic tests were conducted with one human volunteer and four PMHS. The subjects were restrained in a rigid chair mounted on an impact sled (appropriate figure of the test set-up was not available). The sled was accelerated pneumatically over a distance of 2 meters to a prescribed velocity. A headrest was used to maintain the head in the upright position. After reaching the prescribed velocity the sled was stopped with a hydraulic cylinder, which produced a repeatable stroke. The occupant was restrained with a lap belt and two shoulder harnesses, which crisscrossed at the sternum. The human volunteer was subjected to 46 sled runs of various degrees of severity for four configurations of head weight. The subject attempted to achieve two different degrees of muscle tenseness, relaxed and tensed. With muscles tensed the volunteer was subjected to sled decelerations of 1.9 – 6.8 g. With weight placed above the center of mass of the head the volunteer was subjected to a 9.6 g deceleration. This particular run resulted in neck and back pain that lasted several days. The PMHS were similarly fixed so as to obtain comparisons of responses to the same sled deceleration pulses for the various configurations and head weights, and then subjected to more severe conditions. A total of 132 PMHS runs were completed using four subjects.

The volunteer withstood a static flexion moment about his occipital condyles of 35 N·m. This was without contribution from chin contact to the chest. A dynamic tolerance level for the flexion moment about the occipital condyles for the initiation of pain occurred with the maximum equivalent resisting moment of 59 Nm. The maximum dynamic flexion moment generated by the volunteer was measured to be 88 Nm. This level produced a sharp pain in the neck and upper back region with soreness persisting for several days. It was considered non-injurious, but close to the injury threshold. The PMHS were exposed to much greater decelerations. Based on the PMHS data, it was observed that the 50<sup>th</sup> percentile human could withstand equivalent flexion moments of 190 Nm without suffering ligamentous injury (AIS 1 or 2) or bone injury (AIS 2 to 6). However, it is expected that muscle injuries (AIS 1) would occur at a lower value of the flexion moment. Based on these results Mertz [Mertz, 1978] proposed an injury tolerance level of 190 Nm for neck flexion moments measured with a 50<sup>th</sup> percentile male Hybrid III. Similarly from the aforementioned study, corridors for extension were proposed with an injury tolerance level of 57 Nm [Mertz, 1978]. This level was associated with ligamentous damage (AIS 1 or 2), to a PMHS.

The HFM-090/TG-25 proposed to use the tolerance levels defined by Mertz, as described above for neck flexion (190 Nm) and extension (57 Nm). Exceeding this level implies that serious neck injuries are likely.

### 3.4.2.3 Limitations of the Proposed Injury Criteria

A first limitation of the proposed neck injury assessment method is that no injury risk curves were available such as for the lower leg and the spine. Also, the definition of the injury severity associated with the proposed injury tolerance values was not quite clear. However, based on Mertz [Mertz, 1984], exceeding the proposed tolerance levels for compression as well as flexion/extension implies that **serious** neck injuries are likely. Based on the Abbreviated Injury Scale (AIS, 1990), serious injuries have a score of 3 and according to Mertz [Mertz, 1984], a serious injury refers to AIS 2 or more.

Another limitation is that the method considers injury mechanisms separately while the loading is typically a combination of more than one injury mechanism. However, the well known Nij, which considered combined injury mechanisms, was not appropriate (see Annex G) for the current purpose. Also, only three injury mechanisms (compression, flexion and extension) were considered while many other may occur especially when the AV mine is not detonation directly under the occupant location. Three-dimensional motions of the human body and its parts may also result in lateral bending, shear, tension or torsion. Injury criteria for these other injury mechanisms are summarized in Annex G.

Finally, the proposed injury criteria were developed for the loading duration seen in automotive crash situations, while during an AV mine strike the initial loading duration could be much shorter. However, the loading durations for the global effects and the drop down phase are expected to have a similar duration.

### 3.4.3 Conclusions

Neck injury tolerance has been extensively researched by the commercial automotive industry for the past 50 years. Concern regarding head strike during front crash, whiplash in rear strike and contact injuries in rollovers has yielded criteria utilized by the European and United States regulating bodies. HFM-090/TG-25 proposed to use the criteria developed by Mertz and Patrick (1971), Patrick and Chou (1976) and Mertz (1978) for axial compression, flexion and extension. The injury tolerance values for neck compression was set to 4 kN at 0 ms and 1.11 kN at 30 ms (see Figure 3.16). If all force-duration data points fall below this tolerance limit, then the risk of serious neck injuries due to compression is unlikely. If flexion and extension bending moment peak values are below 190 Nm and 57 Nm, respectively then the risk serious neck injuries are unlikely. Although no specific information on AIS level was given for these tolerance values, they are believed to represent a low risk of AIS 2+ injuries based on information given by Mertz [Mertz, 1984].

Finally, since pure compressive or flexion/extension loadings are relatively rare (for an AV mine strike as well as for car crashes), an injury assessment method considering combined injury mechanisms, would have been more appropriate. However, the current available model (Nij) appeared not to be suitable for AV mine loading conditions. Also, it is still recommended to extend neck injury assessment to other injury mechanisms such as shear, tension and lateral bending if appropriate methods exist.

### 3.5 HEAD

This section provides a general overview on injuries, injury mechanisms and injury assessment models for the head.

#### 3.5.1 Anatomy, Loading Mechanisms and Injuries

The head can be divided into two parts: The face and the centre, and rear part of the head. The face is defined as the front part of the head, comprising the facial cranium, its skin, muscles, the blood vessels to the facial structures, as well as the facial nerves. The centre and rear part of the head include the neurocranium, its skin covering (the scalp) and its contents: the brain and meninges (Figure 3.17). The brain is connected to the spinal cord and serves as the upper, greatly expanded part of the central nervous system.

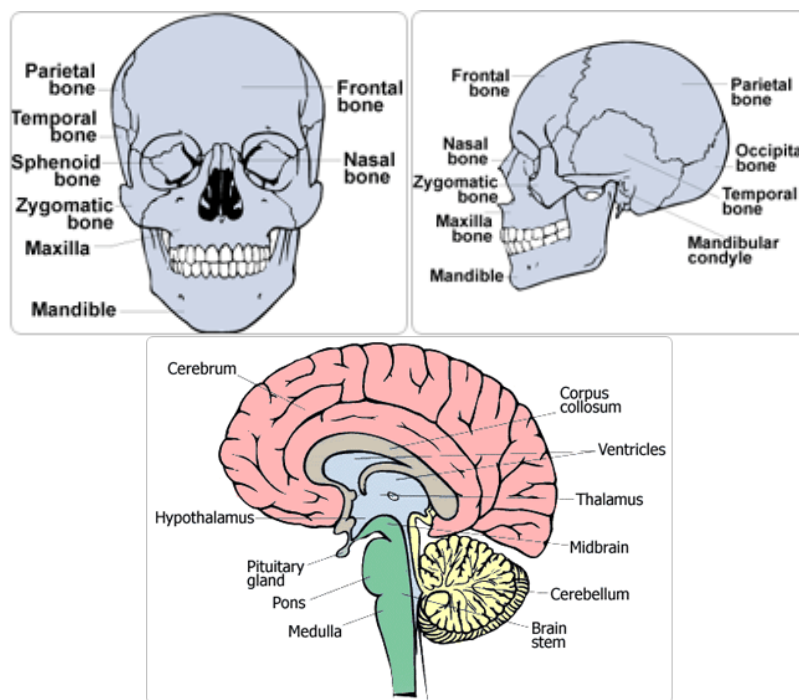


Figure 3.17: Anatomical Structure of the Head and Brain [AMA, 1998].

Head injuries were classified by Ommaya [Ommaya, 1985] as scalp, skull, extracerebral bleeding (focal or diffuse) and brain tissue damage (neural and/or vascular). Brain tissue damage can arise from concussions, contusion, intracerebral hemorrhage or brain laceration. The types of brain injury resulting from this tissue damage include focal injuries (contusions), diffuse axonal injuries (DAI) and mass lesions (hematomas).

DAI were first discovered by Sabina and Strich [Sabina, 1961]. DAIs are typically referred to as “closed head injuries”, which are damages to axons in the white matter of the brain. They are caused by both rotational and/or translational accelerations. Focal injuries are primarily due to direct impact of the head.

## INJURY CRITERIA AND TOLERANCE LEVELS

---

Mass lesions are due largely to angular accelerations suffered by the brain. Injuries to the skull include suture separation, indentation, linear fracture, depressed fracture and crushed skull.

Many current researchers in head injury biomechanics consider angular acceleration together with linear accelerations to be the principal cause of brain injury, whereas traditional biomechanical research focuses on the linear accelerations only [King, 2003]. Pressure, shear, stress, strain rate and the product of strain and strain rate are mentioned as injury mechanisms. Until now research on head injury biomechanics is still ongoing.

An AV mine strike under a vehicle will result in a global movement of the body of the vehicle occupants, which may result in violent head ‘direct’ impact (on hard surface) and may cause skull and brain injuries. Brain injuries may also result of inertial loading (no ‘direct’ impact), where as skull fracture occurs as a result of ‘direct’ impact only [Little, 1993]. The injury mechanism of impact involves a short-duration impulsive loading and a high-acceleration peak while the inertial loading is associated with linear and/or angular acceleration pulse over a significant longer time period [Little, 1993]. In case the occupants wear a protective helmet, skull injury risk is minimized. The influence of the mass of the helmet on the neck injuries is still ongoing research, however, it is not expected that for the vertical impacts of short duration the helmet will influence the risk on neck injuries significantly.

### 3.5.2 Injury Assessment Models

Most of the head injury risk models use skull fracture as a predictor of brain injuries and show that fracture is linearly related to head linear acceleration. An example of one model, the Head Injury Criterion (HIC) [Mertz and Prasad 1997], was developed to assess skull fracture and brain damage caused by frontal head impact, and is largely used in automotive and aviation testing standards. The use of the HIC in cases where there is no head impact on hard surface or when the impact location is not frontal, is presently a controversial topic in the automotive research community. Other head injury models such as the Severity Index [Gadd, 1966] and the Power Index [Newman, 2000] were developed to assess head and brain injuries in case of ‘direct’ head impact, whereas the brain injury assessment models by Ommaya [Ommaya, 1984], Thibault and Gennarelli [Thibault, 1990] and Glaister [Glaister, 1997] were developed for the inertial loading conditions and focus on the head angular accelerations. Still much research is going on with respect to head injury criteria, resulting in contradictory statements, therefore a modification of the automotive standard is not available and still the HIC is used.

Because of lack of information on the applicability of the different available head injury assessment models, the HFM-090/TG-25 decided not to include mandatory assessment of this body region. This decision was also supported by the two following assumptions:

- 1) For an AV mine strike it is assumed that in case of hard head contact the neck loads will exceed the tolerance limits as well.
- 2) For the more severe cases of head inertial loadings caused by the vertical impact on the vehicle (for e.g. impact similar to a whiplash) it is assumed that other body regions (neck and thoracolumbar spine) will exceed their injury tolerance levels first.

### 3.5.3 Conclusions

Based on the assumption that head injuries would not occur without exceeding injury risk tolerance values of other body regions and because there is actually no satisfying head injury assessment model available, HFM-090/TG-25 decided not to include head injury assessment. In the case of a ‘direct’ head impact (on hard surface), it is assumed that the neck loads will be a predictor of neck (and head) injuries and in the case of inertial loading only (no ‘direct’ impact), it is assumed that no brain injury will occur without neck or spine failure.

It is still recommended to record head linear and angular (if appropriate techniques exist) accelerations in order to understand head impact mechanisms under the strike and also to collect data for possible future research on development of head injury assessment methods. Injury assessment models presented in this section may be used, however, their limitations must be taken into consideration before interpreting the results.

### 3.6 INTERNAL ORGANS

Organs (or systems) containing air or fluids are the most sensitive to overpressure caused by blast waves. These organs (or systems) are the auditory system (ear), the respiratory system, the gastrointestinal (G. I.) tract and some solid intra-abdominal organs [Axelsson, 1996]. This section provides on internal organs and blast overpressure injuries, and on the injury risk model to be used when performing AV mine protection testing. Additional information related to overpressure injury assessment is provided in Annex H.

#### 3.6.1 Anatomy, Loading Mechanisms and Injuries

The following paragraphs give a short anatomical description of the auditory system and the non-auditory organs (respiratory system and gastrointestinal tract) vulnerable to blast overpressure. For further details on these body regions, the reader is referred to [Tortora, 2003].

##### 3.6.1.1 The Auditory System

The auditory system (ear), shown in Figure 3.18, is the most susceptible body region to blast overpressure. Overpressure may cause ear injuries at the eardrum, the middle ear or the inner ear of different degrees of severity. Tympanic membrane rupture, dislocation of ossicles (malleus, incus, stapes) and damage of cochlea hair cells are examples of ear injuries (or damage) caused by overpressure. Middle and inner ear damage usually represent a risk of hearing loss. Ear injuries have an AIS score of only 1, even when they result in permanent hearing loss. The risk of ear injuries can be reduced by wearing ear protection such as earplugs or earmuffs.

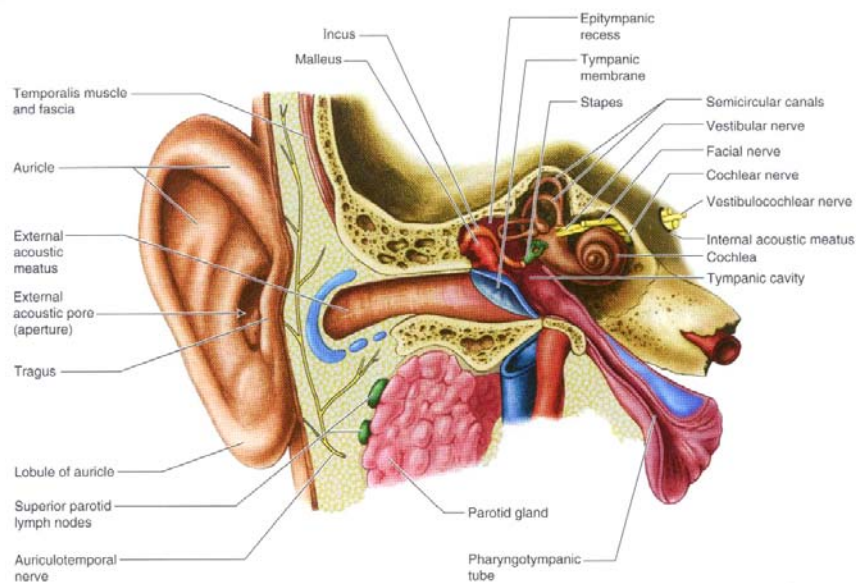


**Figure 3.18: The Auditory System [Moore, 1999].**



### 3.6.1.2 The Respiratory System

The respiratory system, shown in Figure 3.19, is divided in two parts: The upper respiratory system (including the nose and the pharynx) and the lower respiratory systems (including the larynx, trachea, bronchi and lungs) [Tortora, 2003]. The most fatal blast overpressure injuries are the ones to the lungs, because they may involve air embolisms. The air embolism is produced when the air enters the circulation from the disrupted lung tissues and may enter the brain or the heart. The *blast lung* is the most common overpressure blast injury. The term *blast lung* is used to describe the direct damage to the lung produced by the interaction of the blast-wave with the body generated by an explosion and is associated with lung hemorrhage (AIS 3 or more). The pharynx, larynx and trachea are also very vulnerable to blast overpressure, but their injuries will usually represent a lower threat to life. The severity of respiratory system injuries depends on the size of the lesion and the numbers of affected organ layers (for pharynx, larynx and trachea).

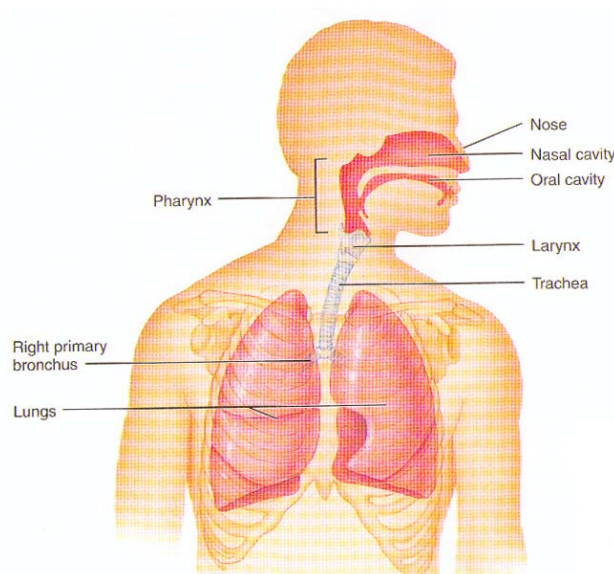
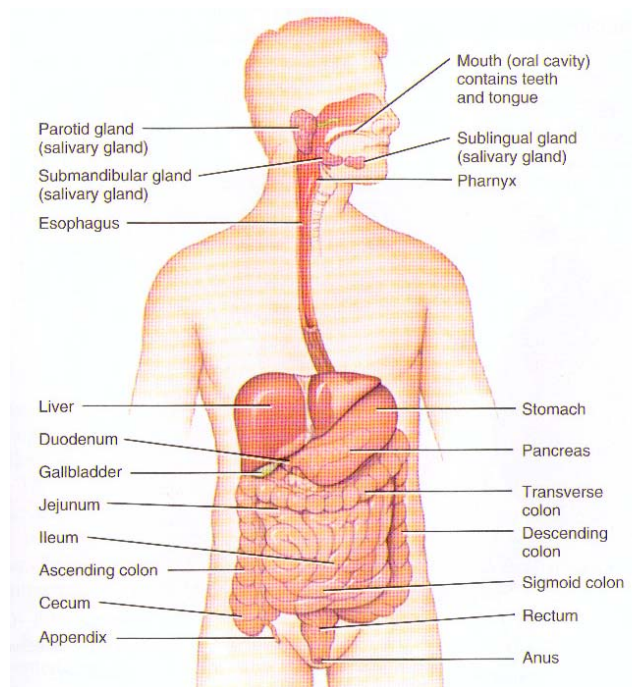


Figure 3.19: The Respiratory System [Tortora, 2003].

### 3.6.1.3 The Gastrointestinal (GI) Tract

The organs of the gastrointestinal tract (GI tract), shown in Figure 3.19, are the mouth, pharynx, esophagus, stomach, small intestine and large intestine [Tortora, 2003]. The wall of the GI tract is composed of four layers. The severity of GI tract injuries depends on the number of layers affected and the size of the lesion. Also shown in Figure 3.20, intra-abdominal solid organs such as the liver and the bladder may be injured when the body is subjected to blast overpressure.



**Figure 3.20: The Gastrointestinal Tract [Tortora, 2003].**

### 3.6.2 Injury Risk Criteria

#### 3.6.2.1 Auditory Organs

Several criteria are available for injury assessment to the auditory organs [e.g. Chan, 2001; MIL-STD-1474D, 1997; Richmond, 1992; NATO, 2003; Dancer, 1995]. However, in case of a mine detonation under a vehicle the risk of permanent auditory injuries can be minimized when proper ear protection is worn. For this reason and because ear injuries do not represent any threat to life (AIS 1), auditory injury assessment is not a mandatory criterion for the STANAG 4569.

#### 3.6.2.2 Non Auditory Internal Organs

Non-auditory overpressure injuries are not expected to occur when the vehicle structure integrity is preserved during a mine strike. However, these body regions need to be assessed in order to ensure a minimum risk of life-threatening injuries caused by blast overpressure.

Previous non-auditory blast damage risk criteria have been based on exposure of mammals to approximately ideal blast waves, typically recorded in free stream in the open. These ideal blast waves (or Friedlander waves) are characterized by a nearly instantaneous rise in pressure followed by an exponential decay leading into a negative pressure phase. The tolerance of humans to single exposure to these ideal blast waves depends on the peak overpressure and the overpressure phase duration [Bowen, 1968]. However, the actual exposure environment in many situations is of more complex nature. For example, a detonation in an enclosure or a shaped charge warhead penetrating an armoured vehicle produces a reverberant wave or complex blast wave inside. A complex blast wave typically consists of a series of multiple shocks that may be superimposed on a slow rising pressure and may cause a variety of biological effects. In an AV mine strike complex blast waves are more common.

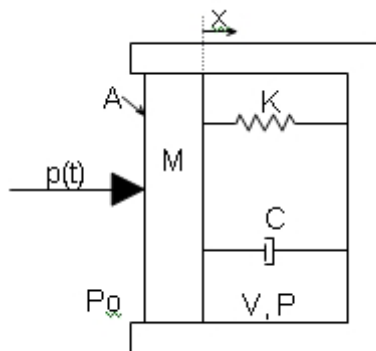
Stuhmiller et al. [Yu, 1990; Stuhmiller, 1998] as well as Axelsson & Yelverton [Axelsson, 1996] developed injury assessment models for the complex blast waves. However, Stuhmillers models focus on

the lungs only, while the model by Axelsson & Yelverton includes all non-auditory internal organs of the upper body. At this point, it is not known if the lungs are more susceptible to complex blast waves than other non-auditory internal organs. For this reason, the model of Axelsson was chosen in order to evaluate the risk of all potential injuries to the non-auditory internal organs. The model is described below, while the other models are discussed in Annex H.

**3.6.2.3 Description of Axelsson Model**

The objective of Axelsson & Yelverton study [Axelsson, 1996] was to understand the effects of complex blast waves on the human body in order to find a simple tool for vulnerability assessment. The model developed by Axelsson is based on experiments performed by Yelverton [Yelverton, 1993] in which 255 sheep and an instrumented cylinder were exposed to complex blast waves in enclosures. The instrumented cylinder (Blast Test Device) was placed where the sheep were positioned. The cylinder (described in details in Chapter 4) was an aluminium tubular test module approximating the size of a sheep. The cylinder was instrumented with four pressure gauges recording the blast loading coming from four different directions. Axelsson used data of 177 of the 255 sheep submitted to complex blast waves in Yelverton study in order to develop a transfer function between injury severity and blast loading recorded on the cylinder.

A mathematical model of the thorax was developed to predict injury severity as a function of the loading recorded by the cylinder submitted to complex blast waves in different enclosures. Initially a two-chamber spring-mass system (two lungs) was developed by Bowen [Bowen, 1965] and Fletcher [Fletcher, 1970]. The model was then simplified to a single chamber one-lung model [shown in Figure 3.21] assuming that the blast load,  $p(t)$ , is acting simultaneously on both lungs.



- A is the effective area;
- M is the effective mass;
- V is the initial gaseous volume of the lungs;
- x is the displacement;
- C is the damper coefficient;
- K is the spring constant;
- $P_0$  is the ambient pressure;
- $p(t)$  is the overpressure over the time; and
- $\gamma$  is the polytropic exponent for gas in lungs.

**Figure 3.21: Single-Chamber One-Lung Model [Axelsson, 1996].**

The model is a single degree of freedom system in which chest wall response (displacement, velocity and acceleration) and intra-thoracic (lung) pressure can be calculated for different complex blast waves and ideal blast waves as well. The equation for the model is the following

$$M \cdot \frac{d^2x}{dt^2} + C \cdot \frac{dx}{dt} + K \cdot x = A \cdot \left[ p(t) + P_0 - \left( \frac{V}{V - A \cdot x} \right)^\gamma \cdot P_0 \right]$$

with the model parameters given in Table 3.2.



**Table 3.2: Model Parameters for a 70-kg Mammal\***

<b>Parameter</b>	<b>Units</b>	<b>70-kg body*</b>
M	kg	2.03
C	Ns/m	696
K	N/m	989
A	m <sup>2</sup>	0.082
V	m <sup>3</sup>	0.00182
γ	–	1.2

\* For mammals of different body weight, scaling factors can be used as described in Axelsson, [Axelsson, 1996].

The input to the mathematical model is the measured external reflected overpressure p(t), the blast loading on the cylinder. The maximal chest wall velocity can be calculated for the four gauges located on the cylinder (v<sub>1</sub>, v<sub>2</sub>, v<sub>3</sub>, v<sub>4</sub>). The average velocity V is then calculated (using v<sub>1</sub>, v<sub>2</sub>, v<sub>3</sub>, v<sub>4</sub>) and is used to determine the injury severity expressed by the ASII (Adjusted Injury of Severity Index).

The ASII was developed by Yelverton [Yelverton, 1996] and can be expressed as follow:

$$ASII = (0.124 + 0.117 \cdot V)^{2.63}$$

Based on the injury description given by Axelsson and Yelverton for each of the ‘injury levels’ (designated as negative, trace, slight, moderate and extensive), it was possible to correlate these injury levels with an AIS score. Based on the AIS range given for each injury level, it was possible to establish a ‘global’ AIS range as presented in Table 3.3.

**Table 3.3: Injury Levels with Corresponding AIS Range for Each Body Region\***

<b>Injury Level</b>	<b>Lungs</b>	<b>Pharynx/Larynx and Trachea</b>	<b>GI Tract (Bowel)</b>	<b>Solid Abdominal Organs</b>	<b>Global</b>
Negative (no injury)	0	0	0	0	0
Trace to slight	3 to 4	2 to 3	2 to 4	1 to 2	1 to 4
Slight to moderate	3 to 4	2 to 4	3 to 4	2 to 4	2 to 4
Moderate to extensive	3 to 5	3 to 5	3 to 5	3 to 5	3 to 5

\* Annex C gives more detailed injury descriptions.

Table 3.4 present the ‘injury levels’ with associated ASII and CWVP ranges (given by Axelsson and Yelverton) with the associated global AIS ranges (from Table 3.1).

**Table 3.4: Injury Levels with Corresponding ASII and CWVP, and Estimated AIS Levels**

Injury Level	ASII (-)	V (m/s)	AIS Range
Negative (no injury)	0.0 – 0.2	0.0 – 3.6	0
Trace to slight	0.2 – 1.0	3.6 – 7.5	1 to 4
Slight to moderate	0.3 – 1.9	4.3 – 9.8	2 to 4
Moderate to extensive	1.0 – 7.1	7.5 – 16.9	3 to 5
> 50% lethality	> 3.6	> 12.8	Up to 6

Considering that AIS 4 injuries might occur when the CWVP values is between 3.6 and 7.5 m/s (injury level: trace to slight), the acceptable CWVP tolerance value was set to 3.6 m/s. Based on the summary given in Table 3.3, this value is believed to represent a very low risk of AIS 2 injuries, which is in accordance with the guideline of 10% risk of AIS 2+.

#### 3.6.2.4 Applicability and Limitations of Axelsson Model

Axelsson injury model can be used for the free field as well as the complex blast situation. It should be noted that the Axelsson injury model should be used together with the experimental techniques as described in his paper. However, practical problems are raised when introducing these techniques for the vehicle occupants, and modifications are necessary. This is further discussed in Chapter 4. Finally, the injury model by Axelsson predicts the injury severity, however it does not predict the injury risk.

#### 3.6.3 Conclusions

In conclusion, the Axelsson & Yelverton model is the best available model for non-auditory blast injury assessment occurring during an AV blast mine strike. Considering that there are no risk curves available, it was decided to use a conservative approach and take the no injury level (3.6 m/s) as the limit for the chest wall velocity predictor.

Although it is known that the auditory system is the most vulnerable body region to blast overpressure, no pass/fail criterion has been proposed, because it is assumed that the crew will wear proper hearing protection. This will minimize the risk on temporary and permanent hearing injuries. Besides it should be noted that when the vehicle integrity is guaranteed during a mine strike, the overpressure in the vehicle should be low, resulting into low injury risks for the non-auditory organs.

### 3.7 SUMMARY ON INJURY CRITERIA AND TOLERANCE LEVELS

In this chapter the injury criteria and associated tolerance levels for the different body regions are discussed. The injury criteria and tolerance levels as advised by HFM-090/TG-25 and those to be used for injury assessment for vehicle mine protection are summarized in Table 3.5. More background can be found in the previous sections as well in the appendices.

**Table 3.5: Summary of Injury Criteria and Tolerance Levels Proposed by HFM-090/TG-25 to be Used for Vehicle Mine Protection**

Body Region	Injury Criteria	Tolerance Level	Signification	Specification
Lower leg	Peak lower tibia compression force (-Fz)	5.4 kN	10% risk of AIS 2+	Lower leg position should follow the recommendations of Chapter 4.
Thoraco-lumbar spine	Dynamic Response Index (DRIz)	17.7	10% risk of AIS 2+	Calculated with H3 pelvis vertical upward acceleration.
Neck	Compression force (-Fz)	4 kN @ 0 ms 1.1 kN @ 30 ms (see lower curve in Figure 3.16)	Serious (AIS 3) injuries are unlikely below the tolerance level	Measured at the H3 upper neck.
	Peak flexion bending moment (My)	190 N·m	Significant (AIS 2+) injuries are unlikely below the tolerance level	Measured at the H3 upper neck.
	Peak extension bending moment (-My)	57 N·m	Significant (AIS 2+) injuries are unlikely below the tolerance level	Measured at the H3 upper neck.
Non-auditory internal* organs	Chest wall velocity Predictor (CWVP)	3.6 m/s	No injury	Based on reflected pressure measurement follow the recommendations of Chapter 4.

\* Respiratory system, gastrointestinal tract and solid intra-abdominal organs.

It should be noted again that there is no proposal for assessment of injuries caused by fragments and loose objects. So far, it has been assumed that these injuries will not occur due to preservation of vehicle integrity and prevention of flying objects.

Furthermore, it has been assumed that risk on auditory injuries will be negligible when wearing proper hearing protection. Therefore, injury assessment of auditory injuries has not been proposed.

### 3.8 REFERENCES

AMA (1998), American Medical Association, *Current Procedural Terminology*, Revised 1998 Edition.

AIS (1990), The Abbreviated Injury Scale, Arlington Heights, IL, American Association for Automotive Medicine.

Axelsson, H. and Yelverton, J.T. (1996), Chest Wall Velocity as a Predictor of Nonauditory Blast Injury in Complex Wave Environment, *The Journal of Trauma, Injury, Infection and Critical Care*, 40 (3 (Supplement)): S31-S37.

Bowen, I.G., Holladay, A. and Fletcher, E.R. et al. (1965), A fluid-mechanical model of the thoraco-abdominal system with applications to blast biology, Technical progress report. Washington DC, Defense Atomic Support Agency, Department of Defense.

## INJURY CRITERIA AND TOLERANCE LEVELS

---

Bowen, I.G., Fletcher, E.R. and Richmond, D.R. et al (1966), Biophysical mechanisms and scaling procedures applicable in assessing responses to the thorax energized by air-blast overpressures or by nonpenetrating missiles: Technical progress report, Washington DC, Defense Atomic Support Agency, Department of Defense.

Bowen, I.G., Fletcher, E.R. and Richmond, D.R. (1968), Estimate of Man's Tolerance to the Direct Effects of Air Blast, Headquarters, Defence Atomic Support Agency, Washington, DC. 20305.

Brinkley, J.W. and Shaffer, J.T. (1970), Dynamic Simulation Techniques for the Design of Escape Systems: Current Applications and Future Air Force Requirements, Symposium on Biodynamic Models and their Applications, Report No. AMRL-TR-71-29, Aerospace Medical Research Laboratory, Wright-Patterson Air Force Base, Ohio, USA.

Brinkley, J.W., Specker, L.J. and Mosher, S.E. (1989), Development of Acceleration Exposure Limits for Advanced Escape Systems, Development of Acceleration Exposure Limits for Advanced Escape Systems, Implications of Advanced Technologies for Air and Spacecraft Escape, Advisory Group for Aerospace Research and Development, Conference Proceedings, No. 472, AGARD NATO, pp. 1-1 – 1-14.

Chan, P.C., Ho, K.H., Kan, K.K. and Stuhmiller, J.H. (2001), Evaluation of Impulse Noise Criteria Using Human Volunteer Data, *J. Acoust. Soc. Am.*, 110(4), 1967-1975.

Chandler, R. (1988), Human Injury Criteria Relative to Civil Aircraft Seat and Restraint Systems, 851847, Society of Automotive Engineers, Warrendale, PA, USA.

Dancer, A.L. and Franke, R. (1995), Hearing hazard from impulse noise: a comparative study of two classical criteria for weapon noises (Pfander Criterion and Smoorenburg criterion) and the LAeq8 method, *Acta Acustica*, 3, 539-547.

Devore, J.L. and Farnum, N.R. (1999), *Applied Statistics for Engineers and Scientists*, Duxbury Press.

Dosquet, F. (2003), Thoraco-lumbar Spine and Pelvis Criteria for Vehicular Mine Protection, NATO-RTO-HFM-090, 3<sup>rd</sup> Meeting, TARDEC, Warren, USA.

Dosquet, F. (2004), Analysis of Thoraco-lumbar Spine and Pelvis Criteria for Vehicular Mine Protection, NATO-RTO-HFM-090, 4<sup>th</sup> Meeting, WTD 91, Meppen, Germany.

Fletcher, E.R. (1970), A model to simulate thoracic response to air blast and impact, In: Proceedings of the symposium on biodynamic models and their application, Ohio, Wright Patterson AFB.

Funk, J.R., Crandall, J.R., Tourret, L.J., MacMahon, C.B., Bass, C.R., Patrie, J.T., Khaewpong, N. and Eppinger, R.H. (2002), The Axial Injury Tolerance of the Human Foot/Ankle Complex and the Effect of Achilles Tension, *Journal of Biomechanical Engineering*, Vol. 124, pp. 750-757.

Gadd, C.W. (1966), Use of a weighted-impulse criterion for estimating injury hazard, In proceedings of the 10<sup>th</sup> STAPP Car Crash Conference, SAE Paper No. 660793.

Garth, R.J.N. (1997), Blast Injury of the Ear, Scientific Foundations of Trauma, Jordan Hill, Oxford, Butterworth-Heinemann, 225-235.

Gray, H. (1985), Gray's Anatomy, 30<sup>th</sup> American Edition, Williams & Wilkins, Baltimore, Maryland, USA, pp. 1402-1514.

- Griffin, L.V., Harris, R.M., Hayda, R.A. and Rountree, M.S. (2001), Loading Rate and Torsional Moments Predict Pilon Fractures for Antipersonnel Blast Mine Loading, presented at the International IRCOBI Conference on the Biomechanics of Impacts, Isle of Man, UK.
- Horrocks, C. (2001), Blast Injuries: Biophysics, Pathophysiology and Management Principles, *The Journal of the Royal Army Medical Corps* (147): 28-40.
- Horst, van der, M.J. and Maasdam, van, R., (2004), Numerical study on influence of tibia and foot orientation, Internal TNO memo and presented at fifth HFM-090/TG-25 meeting October 2004, Quebec, Canada.
- Horst, van der, M.J. et al. (2005), Methods for human body response after being exposed to a threat, Phase 1: inventory and future approach, Internal TNO report DV2 2005-IN002 (in Dutch), TNO Defence, Security and Safety, Rijswijk, The Netherlands.
- Horst, van der, M.J. and Deursen, van, J.R. (2005), Injury Assessment for Blast Overpressure Effects. TNO DV2 A239 report. TNO Defence, Security and Safety, Rijswijk, The Netherlands.
- King, A.I. (2000), Fundamentals of Impact Biomechanics: Part I – Biomechanics of the Head, Neck and Thorax. *Annu. Rev. Biomed. Eng.* 2000, 02:55-81.
- King, A.I., Yang, K.H., Zhang, L., Hardy, W. and Viano, D.C. (2003), Is head injury caused by linear or angular acceleration? In Proceedings of International Conference of Biomechanics of Impact (IRCOBI), Portugal.
- Kuppa, S., Klopp, G., Crandall, J., Hall, G., Yoganandan, N., Pintar, F., Eppinger, R., Sun, E., Khaewpong, N. and Kleinberger, M. (1998), Axial Impact Characteristics of Dummy and Cadaver Lower Limbs, 16<sup>th</sup> International Technical Conference on the Enhanced Safety of Vehicles in Windsor, Ontario, Canada, National Highway Traffic Safety Administration, Washington, D.C.
- Kuppa, S. et al. (2001), Lower Extremity Injuries and Associated Injury Criteria, 17<sup>th</sup> International Technical Conference on the Enhanced Safety of Vehicles in Amsterdam, The Netherlands, National Highway Traffic Safety Administration, Washington, D.C.
- Latham, F. (1957), A Study in Body Ballistics, Seat Ejection, Proceedings of the Royal Society of London, Series B – Biologic Sciences, Vol. 147, pp. 121-139.
- Leerdam, P.J.C. (2002), Research experiences on vehicle mine protection, First European Survivability Workshop, Germany.
- Little, A.D. (1993), Safety of High Speed Guided Ground Transportation Systems, Collision Avoidance and Accident Survivability Volume 3, Accident Survivability, U.S. Department of Transportation, Washington D.C., Report No. DOT/FRA/ORD-93/02.III.
- Manseau, J. (2004), MADYMO Numerical Study, Presented at the 5<sup>th</sup> NATO HFM-090/TG-25 meeting, in Quebec City, Canada.
- Maynard, R.L. and Coppel, D.L. (1997), Blast Injury of the Lung, Scientific Foundations of Trauma, Jordan Hill, Oxford, Butterworth-Heinemann: 214-224.
- McElhaney, J.H., Nightingale, R.W., Winkelstein, V.C.C. and Myers, B.S. (2002), Biomechanical Aspects of Cervical Trauma, In: *Accidental Injury – Biomechanics and Prevention*, Second Edition, Edited by Nahum A.M. and Melvin J.W. Springer-Verlag, New York, 2002.

## INJURY CRITERIA AND TOLERANCE LEVELS

---

Medin, A., Axelsson, H. and Suneson, A. (1997), The reaction of the crew in an armoured personnel carrier to an anti-tank mine blast, A Swedish accident in Bosnia 1996, FOA Defence Research Establishment, Weapons and Protection Division.

Medin, A., Axelsson, H. and Suneson, A. (1998), The reactions of the crew in an armoured personnel carrier to an anti-tank mine blast, A Swedish incident in Bosnia 1996, Defence Research Establishment Weapons and Protection Division, SE-147 25 Tumba, Sweden, FOA-R—98-00720-310—SE, ISSN 1104-9154.

Mertz, H.J. and Patrick, L.M. (1971), Strength and Response of the Human Neck, Proc. Stapp Conf. 15th, 710855.

Mertz, H.J., Hodgson, V.R., Murray Thomas, L. and Nyquist, G.W. (1978), An assessment of Compressive Neck Loads Under Injury-Producing Conditions, The Physician and Sport Medicine, November 1978.

Mertz, H.J. (1984), "Injury Assessment Values Used to Evaluate Hybrid III Response Measurements", NHTSA Docket 74-14, Notice 32, Enclosure 2 of Attachment I of Part III of General Motors Submission USG 2284, March 22.

Mertz, J.H., Prasad, P. and Irwin, A.L. (1997), Injury Risk Curves for Children and Adults in Frontal and Rear Collisions, SAE 973318.

MIL-STD-1474D (1997), Design Criteria Standard – Noise Limits, Department of Defense, Report No. AMSC A7245.

Moore, K.L. and Dalley, A.F. (1999), Clinically Oriented Anatomy, Lippincott Williams & Wilkins.

NATO (2003), Reconsideration of the effects of impulse noise RTO Technical report TR-017 AC/323 (HFM-022) TP/17.

Newman, J.A., Shewchenko, N. and Welbourne, E. (2000), A Proposed new biomechanical head injury assessment function- the maximum power index, In Proceedings of 44th STAPP car crash conference, Paper 2000-01-SC16.

Ommaya, A.K. (1985), Biomechanics of Head Injury: Experimental Aspects, In Nahum, A.M. Melvin, J.W., (eds), The Biomechanics of Head Trauma, Appleton-Century-Crofts, Norwalk, CT, pp. 245-269.

Parks, S. (2002), Blast Injury: Biophysics and Modelling, Armed Forces Institute of Pathology.

Patrick, L.M. and Chou, C.C. (1976), Response Of The Human Neck In Flexion, Extension And Lateral Flexion, Veh. Res.Inst. Rep. VRI-7-3, 1976.

Pike, J.A. (2002), Neck Injury – The Use of X-Rays, CTs, and MRI to Study Crash-Related Injury Mechanisms. Society of Automotive Engineers, Inc. Warrendale, PA, USA.

Radonić, V., Giunio, L., Biočić, M., Tripković, A., Lukšić, B. and Primorac, D. (2004), Injuries from Antitank Mines in Southern Croatia, in *Military Medicine*, Vol. 169, April, pp. 320-324.

Richmond, D.R., Yelverton, J.T., Philips, E.R. and Yancy, Y. (1985), Biological Response to Complex Blast Waves, Los Alamos National Laboratory, Life Sciences Division, Los Alamos, NM, New Mexico.

Richmond, D.R. and Axelsson, H. (1990), Airblast and Underwater Blast Studies with Animals, *Journal of Trauma* (China), 6(2), Supplement: 229-234.



- Richmond, D.R. and Jenssen, A. (1992), Compendium on the biological effects of complex blast waves, Oslo Mil/Akershus N-0015, Oslo 1, Norway.
- Richmond, D.R. and Damon, E.G. (1993), Biomedical effects of Impulse Noise. Fortifikatorisk Notat NR 209/93, Norway.
- Richmond (2002), Personal communication, not available up to now, not published.
- Ruff, S. (1950), Brief Acceleration: Less than One Second, German Aviation Medicine in World War II, Vol. I, Chapter VI-C, Department of the Air Force.
- Seipel et al. (2001), Biomechanics of Calcaneal Fractures, *Clinical Orthopaedics and Related Research*, Number 338, pp. 218-224.
- Shanahan, D.F. and Shanahan, M.O. (1989), Injury in U.S. Army Helicopter Crashes October 1979 – September 1985, *Journal of Trauma*, Vol. 29, No. 4.
- Stech, E.L. and Payne, P.R. (1969), Dynamic Models of the Human Body, Aerospace Medical Research Laboratory, Wright Patterson Air Force Base, Ohio, USA.
- Strich, S.J. (1961), Shearing of Nerve Fibers as a Cause of Brain Damage Due to Head Injury. a Pathologic Study of 20 Cases, *Lancet*, 2:443.
- Thibault, L.E., Gennerelli, T.A., Margulies, S.S. and Eppinger, M.J.R. (1990), The strain dependant pathophysiological consequences of inertial loading on central nervous system tissue, In Proceedings of the International Research Council on the Biomechanics of Impact (IRCOBI conference).
- Tortora, G. and Anagnostakos, N. (1984), Principles of Anatomy and Physiology, Fourth Edition, Harper & Row, Publishers, Inc., New York, NY.
- Tortora, G.J. and Reynolds Grabowski, S. (2003), Principles of Anatomy & Physiology, 10<sup>th</sup> edition, John Wiley & Sons, Inc., New York.
- Wismans, W. et al. (1994), Injury Biomechanics (4J610) Course Notes, Eindhoven University of Technology, Mechanical Engineering, The Netherlands.
- Yelverton, J.T. (1996), Pathology scoring system for blast injuries, *Journal of Trauma: Injury, Infection, and Critical Care*, Vol. 40, No. 3.
- Yelverton, J.T. (1993), Blast overpressure studies with animals and man: Final report-Biological response to complex blast waves, US Army Medical Research and Development Command, Fort Detrick.
- Yoganandan, N. et al. (1989), Dynamic response of human cervical ligaments. *Spine*, 14: 1102-1110.
- Yoganandan, N., Pintar, F.A., Boyton M., Begeman, P., Prasad, P., Kuppa, S.M., Morgan, R.M. and Eppinger, R.H. (1996), Dynamic Axial Tolerance of the Human Foot-Ankle Complex, 962426, Society of Automotive Engineers, Warrendale, PA, USA.
- Yorra, A.J. (1956), The Investigation of the Structural Behavior of the Intervertebral Discs, Masters Thesis, Massachusetts Institute of Technology. Yu, J.H.-Y., Vassel, E.J. and Stuhmiller, J.H. (1990), Modelling of the non-auditory response to blast overpressure: Design of a blast overpressure test module – Final report, Fredrick, Md., U.S. Army Medical Research and Development Command, Fort Detrick.

## INJURY CRITERIA AND TOLERANCE LEVELS

---





## Chapter 4 – TEST METHODS AND PROCEDURES

The pass/fail of a vehicle in a qualification test is based on the human body loading aspects. In the previous chapter the criteria and the tolerance levels for the human body loading aspects have been described. This chapter gives an overview of the required measurement tools and equipment, and the test procedure. The following topics will be discussed:

Human surrogates in general

- Hybrid III anthropomorphic test device (ATD);
- Positioning of the Hybrid III ATD;
- Measurements with the Hybrid III ATD;
- Pressure measurement device; and
- Additional measurements.

The above topics are also the background for the test protocol which is included in Annex I. This protocol gives detailed information for the preparation and execution of the mine tests concerning the measurements for the injury assessment. The protocol will be part of the mine test procedure of the STANAG 4569.

### 4.1 HUMAN SURROGATES

To measure the body loads a model or surrogate of the human body is necessary. This surrogate should represent the geometry, the mass and mass distribution to simulate the behaviour (biofidelic response) of the human body. For a geometric surrogate, a simple doll could be used. For a mass surrogate, a sand bag could be used. The combination of a geometric and mass correct surrogate gives the possibility to test safety systems, like a belt. In the last few years, some own developed surrogates, like a steel dummy within the Norwegian Defence, have been used.

The TG-25 stated that the ‘sand bag type of dummies’ are not appropriate for qualification trials according to STANAG 4569. For mine qualification trials a more sophisticated surrogate, which reports information about leg, spine and neck loads as well as the performance of footrest, seat and restraint systems, is required. The surrogate should not only give satisfying biofidelic response in the initial mine loading phase, but also during the whole motion of vehicle and interior parts.

Because the research area Vehicle Mine Protection is very new and of less economical significance, in comparison to the automotive crash research area, no specific surrogate for the anti-vehicle mine detonation process has been developed. Therefore, the most appropriate existing surrogate has been selected, which is the Hybrid III. In the next section this Hybrid III anthropomorphic test device (ATD) is presented.

### 4.2 THE HYBRID III 50<sup>TH</sup> PERCENTILE MALE ANTHROPOMORPHIC TEST DEVICE (ATD)

The Hybrid III 50<sup>th</sup> percentile male ATD (also called a crash test dummy) was developed for frontal crash tests with cars. The ATD provides facilities to be instrumented with a large number of sensors to measure accelerations, forces, moments and displacements in several body parts. The reusable ATD is a robust measurement device and can withstand extreme loading conditions, but it is also an expensive tool,

so handling the ATD should be done with care. As the ATD has been developed for the frontal loading conditions of car crash tests, its biofidelity is also proven for these loading conditions [Jakobsson, 2005]. However, the ATD can also be used for other loading conditions, like the vertical loads in case of an ejection seat escape.

The ATD is a regulated test device in the USA Code of Federal Regulations (49CFR Part 572, subpart E) for frontal car crash tests. This regulation refers to a General Motors drawing package identified by GM Drawing no. 78051-218, revision U, title “Hybrid III Anthropomorphic Test ATD”, date August 30, 1998.

Some other versions of the Hybrid III ATD are available for more specific research purposes. One of them is the FAA-Hybrid III [Gowdy, 1999] for air crashworthiness and ejection seat escape research. This ATD has a straight lumbar spine assembly, which is expected to give a more biofidelic and reproducible response in the vertical loading conditions for pilots sitting in an upright position in their ejection seat and ready to escape.

The standard Hybrid III 50<sup>th</sup> percentile ATD comes with non-instrumented tibias and for mine vehicle qualification tests, both tibias have to be replaced by instrumented tibias made by the Robert A. Denton, Inc. company and will be referred to as the Denton leg [Denton, 2002; Denton 1984]. The instrumented tibias shall be equipped with a lower tibia load cell that records at least the axial force (Fz). Depending on additional desired instrumentation, different models of the lower tibia load cells and also upper tibia load cells are available (Robert A. Denton, Inc. Drawing Number B-3500-D in Ref. 2).

A new mechanical lower leg model is the Thor-Lx, which is the first developed part of the Thor ATD (see Figure 4.1). This model has been developed to improve the biofidelic response in car crash loading conditions. The Thor-Lx is a more complex leg model as it consists of a damper element in the mid tibia shaft and a simulated Achilles tendon. This makes the model more expensive and probably more vulnerable.

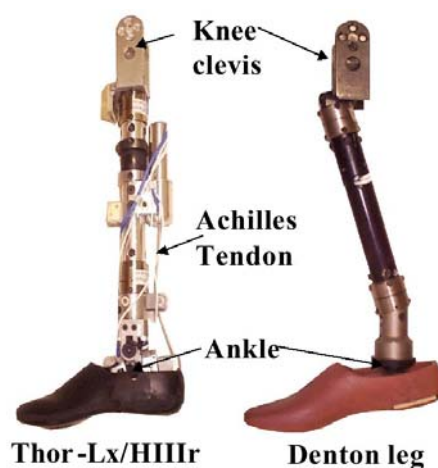


**Figure 4.1: Thor-Lx (left) and Denton Leg Model (right).**

The Hybrid III 50<sup>th</sup> percentile male ATD represents the average male of the USA-population between 1970 and 1980 with the following characteristics:

- Stature (standing position): 1.72 m (67.7 inch);
- Weight: 78 kg (172 lb); and
- Erect sitting height: 0.88 m (34.64 inch).

It is clear that these figures may not accurately represent the current population anymore. For example, in the northern part of Europe, the average man is taller. This is an important issue, because risk of head contact in an AV mine incident depends on head clearance and thus mainly on the height of an occupant. The problem is that even the 95<sup>th</sup> percentile male ATD is not representative. In enclosed figure (Figure 4.2) the size and weights are plotted for a Dutch population in the year 2000 and for the 5<sup>th</sup> percentile female, 50<sup>th</sup> percentile male and 95<sup>th</sup> percentile male ATD. For an equal mixture of Dutch male and female, the original Hybrid III 50<sup>th</sup> percentile matches very well for both the size and mass. In contradiction to the Dutch situation, the Hybrid III 50<sup>th</sup> and 95<sup>th</sup> percentile males are believed representing pretty well the North American 50<sup>th</sup> and 95<sup>th</sup> percentile male soldiers based on an anthropomorphic study of the Canadian Land Forces [Chamberland, 1997]. Only large differences are noted between the 5<sup>th</sup> percentile female soldier and the Hybrid III. Figure 4.3 showed the comparison between Canadian Land Forces anthropomorphic data (in 1997) and different Hybrid III ATDs.

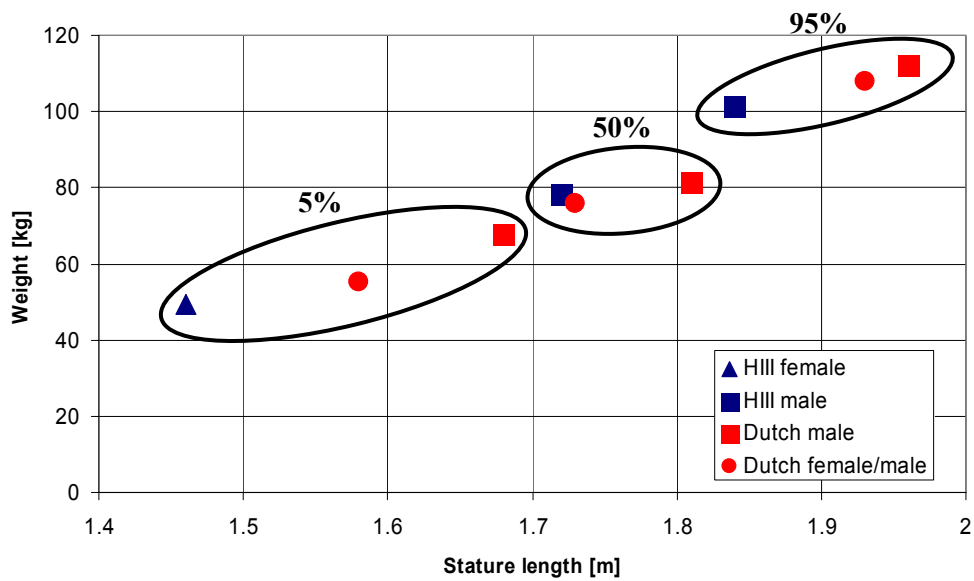
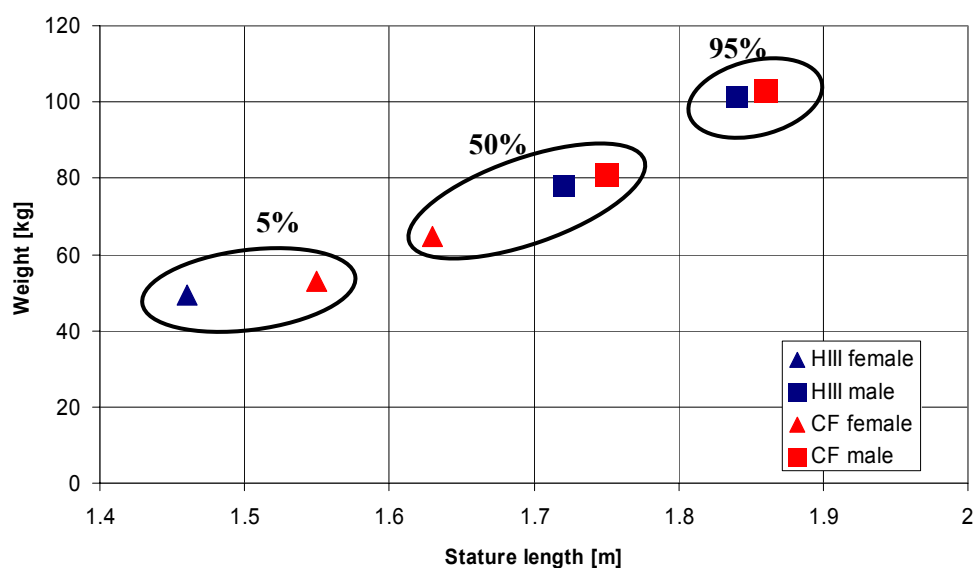


Figure 4.2: Size and Weight for 5<sup>th</sup> Percentile Female and 50<sup>th</sup> and 95<sup>th</sup> Percentile Male Hybrid III ATD and for a Dutch Population in 2000.



**Figure 4.3: Size and Weight for 5<sup>th</sup> Percentile Female and 50<sup>th</sup> and 95<sup>th</sup> Percentile Male Hybrid III ATD and for a Canadian Forces Population in 1997.**

A MADYMO study on the difference in response of the 5<sup>th</sup> percentile female and 50<sup>th</sup> and 95<sup>th</sup> percentile male ATDs showed small differences (<10%) in the human body loads for the same input load (both footplate and seat motion) [Horst, 2004]. However, the 5% ATD showed significantly lower human body loads than the 50<sup>th</sup> percentile dummy.

Summarised, the advantages of the Hybrid III 50<sup>th</sup> percentile ATD are:

- Complete body inclusive head/neck and extremities;
- Well-defined standardized body dimensions;
- Standard measurement equipment;
- All required measurements for injury assessment available (except for overpressure);
- Sufficient realistic biomechanical response; and
- Can be dressed with clothes, boot, and personnel protective equipments.

Its disadvantages are:

- Complex and expensive;
- Risk of damage after high loads with high repairing costs;
- Required handling experience; and
- ATD proportions may not be representative of current population.

The TG-25 decided to use the 50<sup>th</sup> percentile standard (seated) Hybrid III ATD (having a curved spine) for a good representation of most common sitting postures in military vehicles during an unexpected mine incident. Second reason for this choice is the fact that this type is more common in world-wide community. Third reason is that a curved or straight spine has no or very limited influence on the DRI-criterion used for the injury assessment of the lumbar-thoracic spine. The TG-25 decided to use the original instrumented Denton leg for lower leg injury assessment. The use of the more complex instrumented Thor-Lx legs need to be further investigated for the AV-mine loading conditions.

If a standing position is required, a conversion kit can be installed on the standard sitting Hybrid III to make the standing posture possible. In Figure 4.4 a picture is given of the ATD inside a military vehicle.



**Figure 4.4: Hybrid III ATD in a Truck before the Mine Test.**

For a pass/fail test at least one standard Hybrid III 50<sup>th</sup> percentile male ATD has to be used to measure the human body loads in case of a mine detonation under a vehicle.

### **4.3 ANTHROPOMORPHIC TEST DEVICE (ATD) POSITIONING**

For positioning the ATD(s) inside the vehicle, the following aspects are important:

- The position in the vehicle;
- The seating posture of the ATD; and
- The clothing of the ATD.

#### **4.3.1 The Position in the Vehicle**

The ATD has to be placed at one of the original crew positions inside the tested vehicle. This should be the 'worst-case' position: the position that is expected by the 'National Authority' to give the highest loads inside the ATD for a particular mine position under the vehicle.

#### **4.3.2 The Seating Posture**

The seating posture of the ATD should be realistic and representative for an occupant with the same sizes as the 50<sup>th</sup> percentile ATD sitting in an upright position. The straight seating posture should be achieved by placing the pelvis well in the seat cushion and the back of the ATD in contact with the seat back cushion (when available). It should be mentioned that for some seating systems an upright position is not possible for a human. For these cases the most realistic position needs to be checked by a volunteer (preferably with the same sizes as the 50<sup>th</sup> percentile ATD) and imitated with the ATD.

The feet have to be placed in the same way as for a real sitting or standing person. When footrests or protection measures are available, they have to be used. In case of a driver, the right leg should be placed on the accelerator or breaking pedal – the choice of the pedal must be based on the higher expected risk of the transfer of critical loads via the relevant pedal- and the left one on the resting position. For both legs a realistic body posture has to be achieved. By considering this general requirement, the lower leg longitudinal axis should be as good as possible perpendicular to the foot plate to create a worst-case set-up (see Figure 4.5).

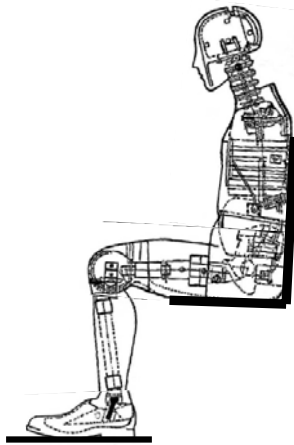


**Figure 4.5: Straight Seating Posture.**

The hands and arms should be placed in a realistic position. In case of steering wheel or joy sticks, the hands should grip these devices; else the hand should be placed in a resting position on the upper leg. The hands should not be fixed to the steering wheel or legs.

The seat has to be adjusted according to the size and weight of a 50<sup>th</sup> percentile man. If different seat positions are possible for different functions and scenarios (e.g. combat vs. driving under homologation conditions in peace keeping operations) the worst-case position of the seat has to be tested. In case of the usage of periscopes or other vision tools, the seat has to be adjusted in such a way that the eye-level of the ATD corresponds to these vision systems.

All available protective measures, such as seat belts and head rests, should be used and installed correctly.

When seat belts are available, they have to be used in the original way. Remove slack in the belts and tighten them as realistic as possible. In case of a belt retractor, allow it to retract the belt to remove slack.

In case of repetitive tests or similar tests at other proving grounds, the same seating posture of the ATD should be kept.

### **4.3.3 The Clothing of the ATD**

The clothing of the ATD should correspond to that of a real crew member or passenger of the tested vehicle. For filming purposes, the uniform can be replaced by an overall with a clear visible colour (contrast with background).

The footwear (shoes or boots) should be the same as normally used by the real personnel of that type of vehicle and the footwear should be in good condition, without any damages. For soldiers, combat boots are recommended.

When the occupants wear personnel protective equipment (helmet, vest, etc.) in normal operational conditions, the ATD should wear the same equipment.

#### 4.4 MEASUREMENTS WITH THE HYBRID III ATD

For a pass/fail test, at least the ATD should be instrumented with the following sensors:

- Lower Tibia Load Cell in both legs: axial force ( $F_z$ );
- Pelvis Accelerometer: vertical acceleration ( $A_z$ ); and
- Upper Neck Load Cell: shear force ( $F_x$ ), axial force ( $F_z$ ), flexion/extension moment ( $M_y$ ).

In Figure 4.6 the position of these sensors are shown.

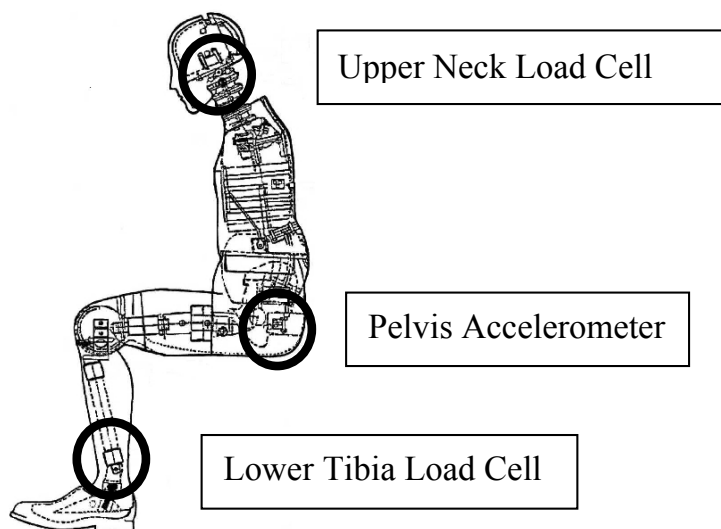


Figure 4.6: Hybrid III ATD with Sensor Positions.

The standard set of instrumentation of the Hybrid III is appropriate for the mine loading conditions.

It is recommended to include more instrumentation to gather additional data about the loading process inside the ATD. This could help to understand the effects and explain unexpected responses observed. When new injury criteria for these additional measured data are available in the future, the injury assessment could be extended.

The following list of additional instrumentation is recommended:

- Five-axis load cell in the lower tibia of both legs ( $F_x$ ,  $F_y$ ,  $F_z$ ,  $M_x$ ,  $M_y$ );
- Five-axis load cell in the upper tibia of both legs ( $F_x$ ,  $F_y$ ,  $F_z$ ,  $M_x$ ,  $M_y$ );
- Tri-axis accelerometers on the mid tibia shaft in both lower legs ( $A_x$ ,  $A_y$ ,  $A_z$ );
- One-axis load cell (shear force) in both femurs ( $F_x$ );
- Tri-axis accelerometers in pelvis, thorax and head: ( $A_x$ ,  $A_y$ ,  $A_z$ );
- Three or five-axis load cell in the lumbar spine ( $F_x$ ,  $F_z$ ,  $M_y$  or  $F_x$ ,  $F_y$ ,  $F_z$ ,  $M_x$ ,  $M_y$ ); and
- Six-axis load cell in the upper neck ( $F_x$ ,  $F_y$ ,  $F_z$ ,  $M_x$ ,  $M_y$ ,  $M_z$ ).



The way to use and maintain the instrumentation and to record and analyse the channels are well described in the SAE regulation J211/1 from December 2003. This document describes:

- The coordinate system;
- The positive polarities of the sensors;
- The certification and calibration aspects;
- Some boundary condition, like the temperature;
- Data acquisition system settings; and
- Signal processing.

The HFM-090/TG-25 recommends to use this standard for the ATD measurements and the processing of the ATD signals. However, since the loading conditions in a mine strike differ from the car crash loading conditions, some other settings are recommended, which are discussed below. More information about the measurement set-up and settings is given in the Test Protocol in Annex I.

### 4.4.1 Certification and Calibration

The ATD consists of a steel skeleton and rubber elements, surrounded by rubber and foam material to simulate the skin and soft tissue. The characteristics, like stiffness and damping, have influence on the internal loads in case of impact or loading transfer. Therefore, the characteristics should meet specific requirements, which are verified in a certification test.

The sensors inside the ATD are mechanical devices, which translate the load into an electric signal. The signal is being recorded by the data-acquisition system, which has to be provided with information about the sensitivity of that particular sensor. Each sensor has to be calibrated to give the relation between load and signal amplitude. Due to repetitive loadings, overloads or aging of the mechanical sensor, re-calibration is necessary on a regular schedule. For certification and calibration, refer the ATD user's manual [SAE, 1998].

It is advised that the ATD will be certified and the sensors be calibrated at least every two years. This advice is based on several years of experience with the use of the ATD in the Vehicle Mine Protection research area and valid for 'normal usage'. This means: 15 to 20 tests, loads within the ranges of the sensors, no structural damage to the ATD and the storage of the ATD in a dark room and at a constant temperature of about 20° C. In case of an overload of a sensor, re-calibration of this sensor is mandatory.

### 4.4.2 Temperature Conditions

Because of the temperature influence on the characteristics of the rubber elements and the skin of the ATD, a constant temperature between 20 and 22° C on the test site is preferred (according to crash test regulations). However, in general, sites for mine tests are outside locations and temperature can hardly be controlled. A temperature of 10° to 30° C inside the vehicle is advised. In winter time, a heater inside the vehicle could prevent too cold conditions and reduce moisture.

## 4.5 PRESSURE MEASUREMENT DEVICE

Inside the vehicle, the overpressure has to be measured to analyse the effects on non auditory internal organs in the thorax and abdomen. The Chest Wall Velocity Predictor (CWVP) model is used to assess injury to these organs (see Chapter 3). As input for this model the reflected overpressure on the thorax has

to be measured. Originally the measurements should take place using a simple blast test device (cylinder) [Axelsson, 1996]. However from a practical point of view (it is not possible to include the cylinder on the same location as the ATD during one test) the following measurement methods are proposed:

- Using the original cylinder described by Axelsson;
- Using the Hybrid III as reflected area instead of the cylinder; and
- Using a flat plate as reflected area instead of the cylinder.

To measure the reflected pressure it is important to have a correct simulation of the body (equal reflected area) and appropriate transducer fixed on this device. The chest of the Hybrid III ATD represents the body dimensions and thus is proposed as mount of a pressure transducer, in case the pressure needs to be measured on the location where an ATD is placed. Based on blast tunnel tests performed by TNO it was shown that the CWVP is similar for a cylinder or when using the Hybrid III as reflected area [Horst, 2005]. During these tests overpressure effects were measured using different types of models, i.e. a simple plate, a simple cylinder as described by Axelsson and a specific developed pressure measurement device on the chest of the ATD (see Figure 4.7). Four pressure transducers were mounted to the cylinder (also called Blast Test Device: BTM). Special brackets were developed for measuring the pressure on the ATD. The mounted pressure transducers on the ATD showed reliable results, which can be used for injury assessment. When neither the BTM, nor the ATD can be used, then a simple reflected area can be used to measure the overpressure effects for injury assessment. However, it needs to be noted that the reflected area need to be close to the reflected area of the BTM in order to prevent early time rarefaction waves, so representative pressure time records are obtained.



**Figure 4.7: BTM (left) and Hybrid III ATD (right) in Blast Tunnel [Horst, 2005].**

For blast overpressure, it is hardly possible to define a worst-case location and the position of the ATD is not always the worst-case position for both the mechanical loads and the pressure loads. Therefore, at least two positions for pressure measurements are mandated:

- One on the chest of the Hybrid III ATD; and
- One on a second Hybrid III ATD (when available) or at the crew location where the highest overpressure loads might be expected.

### 4.5.1 Pressure Measurement Device on the Chest of the ATD

It is recommended to use a flat measurement device strapped on the chest of the ATD as shown in Figure 4.8. The ATD is dressed and the device must be fastened above the clothes. The device should consist of a plate with a flat transducer fixed in or on this plate (see Figure 4.9). To avoid inertia problems for the ATD response, the device should be as light as possible. It is recommended to use hard plastic materials for the mount.

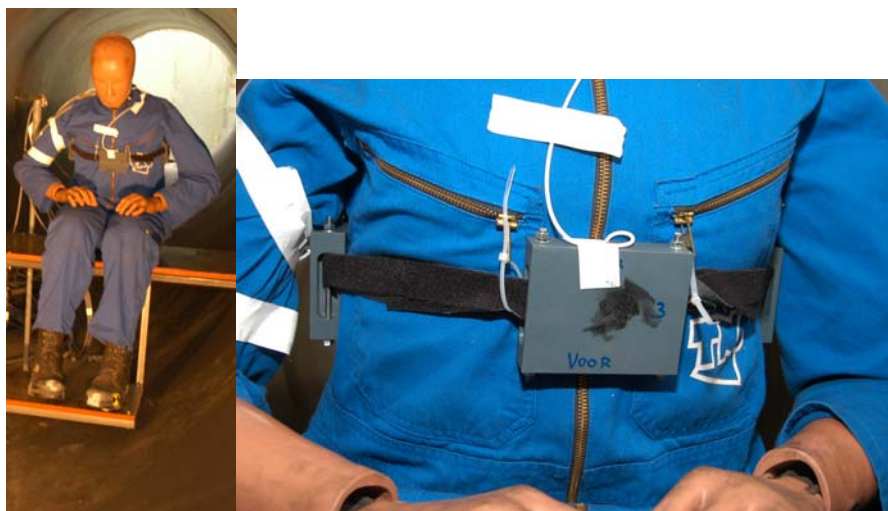


Figure 4.8: Example of Pressure Measurement Device on the Chest of an ATD [Horst, 2005].

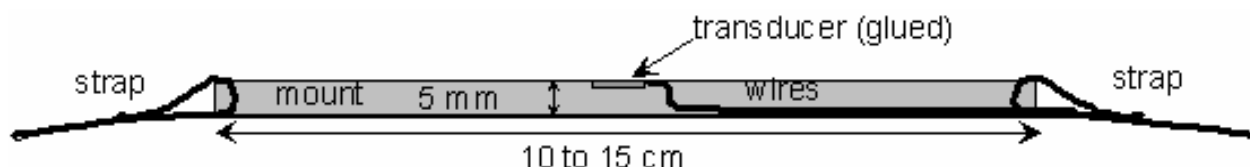
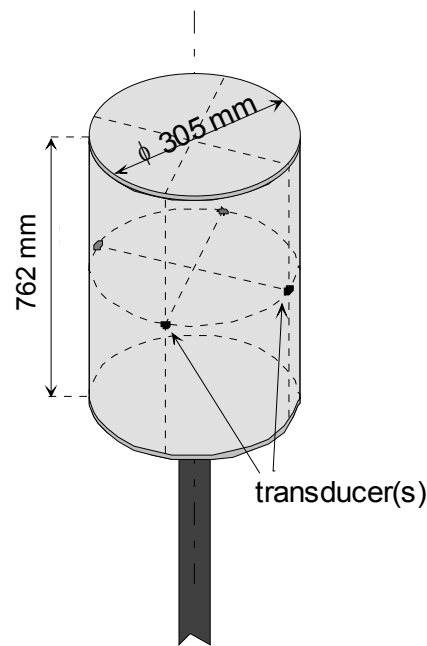


Figure 4.9: Example of a Flat Pressure Measurement Device.

### 4.5.2 Pressure Measurement Device at Another Position

For another measurement position than the chest of the Hybrid III, it is necessary to have a plane as reflected area at or close to a crew position. This should be the position where the highest overpressure is expected. The back of the seat could be used as reflected area in combination with the same pressure measurement device as described for the ATD. The transducer should be orientated in the same direction as the chest of a human being located on that position.

When no appropriate reflecting plane for the pressure measurement device is available, the original blast test device (cylinder) as described by Axelsson & Yelverton [Axelsson, 1996] can be used (see Figure 4.10).



**Figure 4.10: Example of a Cylinder for Pressure Measurements.**

The dimensions of this cylinder are: height of 762 mm, diameter of 305 mm. Although the human thorax has smaller dimensions it is suggested to follow the original blast test device dimensions and stay as close as possible to the original injury model.

The pressure transducer(s) should be fixed in or at the cylinder at half height. The material for the cylinder should be hard enough to protect the transducer and the wires and to reflect sufficiently the incident pressure.

When the frontal direction (chest direction) for the measurement location is known, at least one single transducer in the cylinder is needed in the same frontal direction (like in case with an ATD).

For a standing position and when the crew member at that position can face any direction, four sensors have to be used. For the conservative approach in the injury assessment, the worst-case sensor in terms of peak velocity must be considered.

Note: This is in contradiction with the original method in which the average value of the four peak velocities (from each sensor) was taken. Additional research is necessary to compare above described methods.

### 4.5.3 Pressure Transducer Specifications

For fixation on a plate, a flat transducer (< 1 mm) should be used. This could be glued or screwed on that plate. For fixation in a plate or in the cylinder, other transducers could be used as long as the opening of the sensor is flat with the outer surface (flush). To avoid influence of cylinder deformation on the pressure transducer and the signal, the sensor could be placed in rubber mounts in the cylinder wall.

The following specifications are recommended for the pressure transducer:

- Full scale range > 300 kPa; and
- Resonance frequency > 50 kHz.

## 4.6 ADDITIONAL MEASUREMENTS

In the previous sections the measurement methods have been described for the data, which is required for the mandatory criteria. It is strongly recommended to extend the measurement set-up with extra information, which could be helpful for the assessment.

A list with additional instrumentation in the Hybrid III ATD is already given in Section 4.4. Other additional measurements could consist of belt force measurements, acceleration and displacement measurements on the footrest and seat system or additional pressure measurements.

These measurements are helpful in the understanding of the input loading process. The data is also appropriate for numerical studies of human body loads.

For the assessment of ATD behaviour, normal speed and/or high speed video film recordings give very useful information. For ATD motion only, a high speed recording rate of 1000 frames per second is sufficient. For the high speed video recording of structural response, higher frame rates are recommended.

## 4.7 SUMMARY

This chapter described the test methods and procedures. The following tools are required for a pass/fail of a qualification test of a vehicle against mine strikes:

- Instrumented Hybrid III 50% male anthropomorphic test device; and
- Pressure measurement device(s).

In Annex I the complete test protocol is presented. In Table 4.1 an overview of the required data for the injury assessment is summarized.

**Table 4.1: Overview of Data that Needs to be Measured**

Body Region	Required Data	Measurement Device
Lower leg	Axial compression force (Fz) in the tibia	Load cell in the lower tibia of the Hybrid III ATD
Thoraco-lumbar spine	Vertical acceleration (Az) in the pelvis	Accelerometer in the pelvis of the Hybrid III ATD
Head / neck	Shear force (Fx) and axial compression force (Fz) in the neck Flexion/extension bending moment (My) in the neck	Load cell in the upper neck of the Hybrid III ATD Load cell in the upper neck of the Hybrid III ATD
Non-auditory internal organs	Reflected overpressure p(t)	Two pressure gauges (at least one on the chest of the Hybrid III ATD)

## 4.8 REFERENCES

Axelsson, H. and Yelverton, J.T. (1996), Chest Wall Velocity as a Predictor of Non-Auditory Blast Injury in a Complex Blast Wave Environment, *The Journal of Trauma, Injury, Infection and Critical Care*.

Chamberland, A., Carrier, R., Forest, F. and Hachez, G. (1997), Anthropomorphic Survey of the Land Forces, Final report presented to Defence and Civil Institute of Environmental Medicine (DCIEM), Report number 98-01897, Les Consultants Génicom, Inc., Montréal, Québec, Canada.

Denton, R.A. Inc. (1984), Crash Test Dummy Lower Leg Structure, Patent No. 4, 488, 433.

Denton, R.A. Inc. (2002), Instrumented Lower Leg Assembly.

Gowdy et al. (1999), A lumbar Spine Modification to the Hybrid III ATD for Aircraft Seat Tests, SAE Paper 1999-01-1699.

Horst, van der, M.J. and Maasdam, van, R. (2004), Influence of dummy sizes. Internal TNO memorandum and TNO presentation at third meeting of HFM-090/TG-25, Rijswijk, The Netherlands.

Horst, van der, M.J. and Deursen, van, J.R. (2005), Injury Assessment for Blast Overpressure Effects. TNO DV2 A239 report. TNO Defence, Security and Safety, Rijswijk, The Netherlands.

Jakobsson, L. (2004), Feasibility of Hybrid III for evaluating mine protection of vehicles, TAK report no. TAK2004-018, Volvo Car Corporation, Sponsored by Swedish Defense Materiel Administration, FMV.

NHTSA Title 49 – Transportation Chapter V – National Highway Traffic Safety Administration (NHTSA), Department of Transportation, Part 572 – Anthropomorphic Test Device.

SAE J211/1 (1995), Surface Vehicle Recommended Practice, (R) Instrumentation for Impact Test – Part 1 – Electronic Instrumentation, Rev March.

SAE J1727 (1996), Surface Vehicle Recommended Practice, Injury Calculations Guidelines, Issued August.

SAE (1998), Society of Automotive Engineers, User's Manual for the 50<sup>th</sup> Percentile Male Hybrid III Test ATD, ATD Testing Equipment Subcommittee, SAE Engineering Aid 23, June.





## Chapter 5 – CONCLUSIONS

The NATO/RTO HFM-090/TG-25 was established in response to the NATO/RTO HFM ET 007 which identified the lack of suitable information for injury assessment of the anti-vehicle mine threat. Furthermore, the task group was asked to help the STANAG 4569 TOE to develop an injury assessment methodology for the qualification of the protection of light-armoured and logistic vehicles from (blast) landmines.

The main conclusions and remarks of the HFM-090/TG-25 work are summarized below, while reference is made to the separate chapters for detailed information on the injury assessment and the test methods.

- Injury criteria and tolerance levels were proposed to assess the body regions most vulnerable to a blast mine strike under a vehicle. The tolerance levels established for each body region are considered to represent low risk of life-threatening and disabling injuries (10% risk of AIS 2+). The proposed mandatory injury criteria are summarized per body region:
  - Lower leg and foot/ankle      Peak lower tibia compression force
  - Thoraco-lumbar spine      Dynamic Response Index (DRIZ)
  - Cervical spine (and head)      Compression force  
Peak flexion bending moment  
Peak extension bending moment
  - Non-auditory internal organs      Chest wall velocity predictor (CWVP)

Background information and tolerance levels can be found in Chapter 3.

- The Abbreviated Injury Scale (AIS) is a measure of injury severity (including the risk of fatal injuries) as opposed to a measure of impairment or disabilities. Therefore, the outcome of the injury assessment provides information on the medical condition as opposed to the incapacitation (short or long term) or on the recoverability of the occupants.
- The injury criteria (or injury risk models) proposed herein were originally developed for motor vehicle and aircraft safety and were based on other loading conditions (lower amplitude at longer durations) than those occurring during a mine strike under a vehicle. They were, and still are, however, the most appropriate available for the mine loading conditions.
- The method proposed includes injury criteria for the body regions considered most vulnerable to an AV blast mine strike. These body regions were determined with the best available information (few real incident reports and full-scale testing experience). Of course, other body regions can be injured as well during a real mine strike. Additionally, psychological effects will also occur and influence the incapacitation of the occupant.
- The tolerance levels were determined conservatively.
- There is no proposal for assessment of injuries caused by fragments, detonation products and loose objects. So far, it has been assumed that injury risk constituted by these products was minimal due to vehicle integrity and prevention of flying objects.
- It is assumed that permanent auditory injuries will not occur when wearing proper hearing protection. Therefore, no pass/fail criterion for auditory injuries has been proposed. It is strongly recommended to wear proper hearing protection to minimise risk of temporary or permanent auditory injuries from a mine detonation.
- The TG-25 also discussed a protocol for test set-up and injury assessment, and prescribed the use of the Hybrid III 50th percentile anthropomorphic test device (ATD) together with pressure

## CONCLUSIONS

---

sensors. The test protocol is presented to the STANAG 4569 and more detailed information has been presented in Chapters 4 and 5.

- The standard Hybrid III has been developed for frontal car impact. It is recently the best available surrogate for the vehicle mine protection testing (or research) area as well. The standard Hybrid III lower leg model is stiff and therefore results in higher tibia peak loads than expected in a human. This means that using the standard Hybrid III leg results in a conservative method when used for injury predictions.
- The method described by the TG-25 is to be used as pass/fail assessment for occupant safety in qualification trials of mine protected vehicles, according to the STANAG 4569. It is also possible to estimate the risk of lower leg and spine injury, based on the measured ATD response, since risk curves are available for these body regions.

A new team needs to be assembled to carry the mandate of TG-25 further, but in the meantime, the recommendations made by the TG-25 stand. They reflect the best knowledge available at this point. They are the result of an honest best effort and are the best available at the time of publication.

### What comes after TG-25

TG-25 was assembled by NATO-RTO-HFM ET 007 and STANAG 4569 in response to their need. It brought together a team of professionals from several branches of science, engineering and medicine.

A lot of the TG-25 work was based on information available in literature as well as real accidents and full-scale test data. Some technical and medical assumptions were made to define a simple and realistic injury assessment method for vehicle mine protection testing. Gaps still remain in the method, and further research is required to fill some of them. Based on the current status, recommendations for future work are given below:

- Improvement of lower leg injury assessment (criteria, tolerance level, mechanical models);
- Improvement of spinal injury assessment (criteria and tolerance levels);
- Improvement of neck and head injury assessment (criteria and tolerance levels);
- Improvement of pressure measurement device and injury assessment;
- Expansion validation of experimental and numerical models;
- Improvement of the test methodology; and
- Exploration of actual incidents both from a technical and medical standpoint.

There is also a need to assemble a new team focusing on different types of threats to vehicle occupants such as the improvised explosive devices (IED) and shaped charges. This team, which is already designated as HFM-148/RTG and which will start in 2006, can follow the HFM approach as presented in this report.

## **Annex A – TERMS OF REFERENCE (TOR)**

### **Task Group on Test Methodology for Protection of Vehicle Occupants against Anti-Vehicular Landmine Effects HFM-090/TG-25**

#### **A.1 ORIGIN**

##### **A.1.1 Background**

The threat to military vehicles and their crew from landmines is of urgent and great importance to NATO countries. Currently, NATO STANAG 4569 addresses the anti-vehicular (AV) landmine problem with respect to establishing standards for protection levels for logistic and light armoured vehicles. However, STANAG 4569 does not state how to achieve a particular protection level. Therefore, the creation of a HFM-TG on test methodology for protection of vehicle occupants against anti-vehicular landmine effects is required to establish common NATO landmine test procedures and common injury criteria.

##### **A.1.2 Justification (Relevance to NATO)**

Individual nations or consortia of nations conducted most of the recent development work in anti-vehicular mine protection (AVP). It is recognised that there is a lack of common international procedures to evaluate and assess the performance of AVP systems. A team of subject experts confirmed this during the HFM ET-007 meeting held in Brussels, 22-24 February 2000. The meeting also identified the advantages that would be achieved from pooling knowledge and experience from the participating nations; developing a common and quantitative understanding of the physics of AV mine blast and the resulting injury mechanisms to the human would benefit all participants. It should guide the development of more effective strategies to mitigate the effects of AV mine blast and lead to future AVP system improvements.

#### **A.2 OBJECTIVES**

##### **A.2.1 General Goals**

- Describe blast mine effects resulting human physical injuries based on various countries experiences with mine incidents and tests;
- Propose injury assessment criteria and tolerance levels for occupant injuries during AV mine strike tests;
- Describe test methods and equipment to assess occupant injuries during AV mine strike tests; and
- Produce a comprehensive technical report.

##### **A.2.2 Expected Deliverables**

- Annual progress reports;
- Technical report on the physics of AV mine blast effects on occupants and resulting human injuries;
- Guidelines of procedures, equipment and injury assessment criteria for testing AVP systems; and
- Final administrative report of the activities and results of the Task Group.

## ANNEX A – TERMS OF REFERENCE (TOR)

The duration of the Task Group will be 3 years. See table with the planned meetings.

**Table A-1: Time Schedule**

2002				2003				2004			
Q1	Q2	Q3	Q4	Q1	Q2	Q3	Q4	Q1	Q2	Q3	Q4
	1 <sup>st</sup> meeting (FRA)			2 <sup>nd</sup> meeting (NLD)		3 <sup>rd</sup> meeting (USA)		4 <sup>th</sup> meeting (Europe)		5 <sup>th</sup> meeting (CAN)	Final report

### A.3 RESOURCES

#### A.3.1 Membership

Team leader: P.J.C. Leerdam (NLD).

Participating NATO nations: CAN, USA, DEU, FRA, NLD.

Participating PfP-nations: SWE.

The Task Group members will require expertise in the following areas:

- Medical aspects of shock and acceleration injuries and their consequences;
- Explosive effects related to AV mines;
- Material performance against AV mine blast;
- Protective measures and equipment; and
- Test methods and instrumentation.

#### A.3.2 National and/or NATO Resources Needed

Most of the participating nations already have national programs to develop and test AVPs. The Task Group members need to obtain permission for the release of national test data and experience to the Task Group. Each nation is responsible for its own travel. Invitation of the Task Group members to relevant national AVP tests should be considered.

#### **A.4 SECURITY LEVEL**

NATO Unclassified or NATO Restricted.

#### **A.5 PARTICIPATION BY PARTNER NATIONS**

Partners are invited.

#### **A.6 LIAISON**

- Coordination/collaboration will be established with the proposed TG on protection of dismounted soldiers from anti-personnel landmines. The two TG share some aspects of mine blast protection and close coordination will allow TG members to gain a broader perspective on the subject;
- NL volunteers to act as a central collation and distribution point for TG information/data; and
- In addition to the initial meeting in Brussels, it is expected to hold five additional meetings during the duration of the TG, three meetings will take place in Europe and two in North America.

## ANNEX A – TERMS OF REFERENCE (TOR)

---



## Annex B – EPIDEMIOLOGICAL DATA ON AV MINE INCIDENTS

Epidemiological data are one of the prevalent sources for improving the knowledge of general mechanisms of AV mine incidents. They can include information on four main topics:

- Threats;
- Effects on the vehicle structure;
- Injuries; and
- Boundary conditions (for e.g. soil conditions, depth of burial).

This information can enhance threat analysis, design of vehicular protection systems and test standards by using it as a baseline for further investigations.

WTD 91 created a database on more than 230 military vehicular mine incidents of different nations with information on the threat conditions, effects on the vehicle and especially effects on the occupants beginning in 1990. Figure B.1 shows the number of incidents resulting in casualties and fatalities for the period of 1998 to 2006.

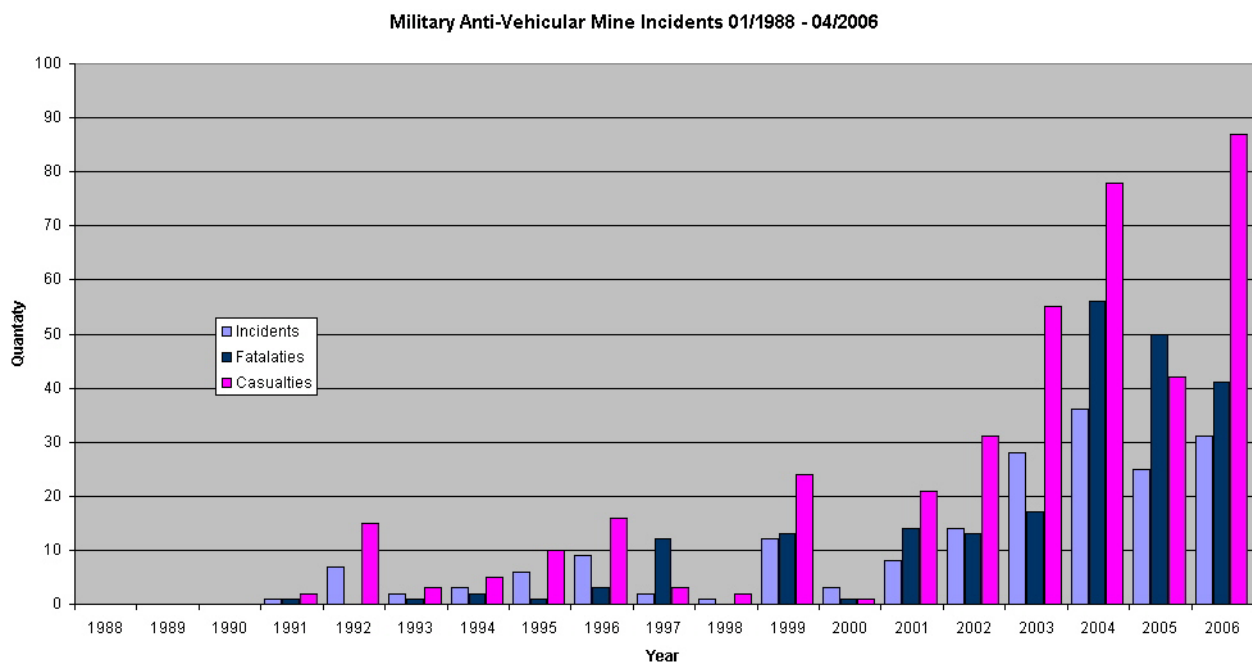


**Figure B.1: Overview of Mine Incidents [WTD 91 Incident Database].**

The press association of the Western world watched military conflicts where western armies were involved. Consequently the number of reported mine incidents increased during such conflicts (e.g. 1995 – 1996 former Yugoslavia, 2001 – today Afghanistan, 2003 – today Iraq). These data are used in the database. However, policies of restricted information influenced the database (Chechnya, Iraq 2004 – today). So the overall number of mine incidents is much higher than illustrated in the diagram. Besides, many nations did not and sometimes still do not want to share detailed data due to the risk of exposing the limits and Achilles' heels of their vehicular protection systems. Hence, only a limited number of comprehensive publications are available.



## ANNEX B – EPIDEMIOLOGICAL DATA ON AV MINE INCIDENTS

---

After the progress and distribution of internet technologies additional information on numerous AV mine incidents could be found in the World Wide Web. These data are mostly not authorized and published by press agencies, which were not familiar with the phenomena of such incidents. Therefore many incidents were described incorrect as well as only on a very low level of detail – e.g. incidents due to attacks with improvised explosive devices were sometimes described as mine incidents. In spite of this problem the analysis of the available data provides a good overview on some general topics, e.g. threat analysis and occupant safety.

The anti-personnel mine-ban convention in 1999 improved the awareness of the mine threat in the society of many nations outside the Western world, which caused an increasing number of publications of mine incidents. Furthermore some nations also took into account effects of the publication of such incidents and used them as a political tool to blame their opponent. Especially mine incidents in Asia (e.g. Sri Lanka and India/Pakistan) and Africa (e.g. Eritrea) were published more often due to these reasons. However, WTD 91 assumes that only at most 25% of all incidents are included in their database.

Additional exploratory data were published from a surgical point of view on injuries from antitank mine strikes in Southern Croatia from 1991 to 1995 [Radonić, 2004]. However, the hit vehicles seem to be quite unprotected against the antitank mine threat. The authors pointed out the high risk of fatalities due to antitank mine strikes and described the AIS and ISS level for the specific casualties and fatalities (42 victims including 12 fatalities). The average AIS was  $3.67 \pm 1.18$  (casualties only:  $2.9 \pm 0.55$ ) and the average ISS was  $31.48 \pm 20.23$  (casualties only:  $17.47 \pm 7.6$ ). Injuries to the brain were the most predominant fatal injury types (50%), followed by vessels injuries (33%) and massive thoracic injuries (16%). The very high portion of fatal brain injuries is most likely due to a lack of available restraint systems in old military vehicles and the seldom usage of these systems in military vehicles, which resulted in head impact with the vehicle roof. Most frequently the lower extremities were injured due to the mine strike. The authors relate the AIS and ISS levels with some of the relevant boundary conditions (crew position, vehicle type) but not with specific injury types. Furthermore the injury distribution is presented by a very rough classification of body regions. Although this paper provides a very good overview on antitank mine strikes from a surgical perspective, it is not possible to derive injury mechanisms and evaluate applicable injury models.

For improving the value of the available data exploration teams including biomechanical experts, engineers and threat analysts should investigate the incidents directly in the operational area. This approach is necessary to understand the load transfer mechanisms from surrounding, threat, vehicle structure and occupant in depth. Data which are reported by non-specialised soldiers in the field cannot guarantee the level of detail and the accuracy which is needed for this kind of analysis.

Examples for the analysis of mine incidents or comparable incidents are given by Medin et al. [Medin, 1997] and Dosquet et al. [Dosquet, 2004].

### B.1 REFERENCES

Dosquet, F., Nies, O. and Lammers, C. (2004), Test Methodology for Protection of Vehicles Occupants against IED, in Proceedings of 18<sup>th</sup> Symposium of Military Aspects of Shock and Blast, Bad Reichenhall, Germany.

Medin, A., Axelsson, H. and Suneson, A. (1997), The reaction of the crew in an armoured personnel carrier to an anti-tank mine blast, A Swedish accident in Bosnia 1996, FOA Defence Research Establishment, Weapons and Protection Division, FOA-R-97-00458-310-SE, March, in Swedish.

Radonić, V., Giunio, L., Biočić, M., Tripković, A., Lukšić, B. and Primorac, D. (2004), Injuries from Antitank Mines in Southern Croatia, in *Military Medicine*, Vol. 169, April, pp. 320-324.

## **Annex C – INFORMATION RELATED TO AV BLAST LANDMINE INJURIES**

### **C.1 INTRODUCTION**

This annex presents the medical aspects of anti-vehicular (AV) blast landmine injuries, which were taken into consideration in the development of the injury assessment method proposed in this report. The information contained in this annex is focused on the **physical** effects on military personnel inside vehicles when subjected to an AV blast landmine. The information contained in this annex does not take into account effects by other types of mines. The structure of this annex is the following:

- Section C.1 – Introduction
- Section C.2 – Injury Risk Assessment/Injury Scaling
- Section C.3 – AV Blast Mine Injuries and Their Consequences
- Section C.4 – Discussion & Conclusions

### **C.2 INJURY SCALING AND INJURY RISK ASSESSMENT**

#### **C.2.1 Injury Scaling**

The injury assessment method proposed in this report (Chapter 3) implies the definition of injury criteria and tolerance levels. Injury criteria refer to parameters or functions of parameters that are related to injury (e.g. the measurements taken during a mine test like forces, moments, acceleration, etc.). Tolerance levels are the maximum acceptable values for each of the injury criterion. To establish injury tolerance levels for each body region of interest, the use of an injury scale was essential. Injury scaling is defined as the numerical classification of the type and severity of an injury. The three main types of injury scaling are [Radonić, 2004]:

- Anatomical scales: Described the injury in terms of anatomical location, type of injury and relative severity.
- Physiologic scales: Described the physiological status of the patient based on the functional change due to injury. This status may change over the duration of the injury's treatment period.
- Impairment, disability and societal loss scales: Rate the long-term consequences and in relation to this, the "quality of life".

Unlike the AP mine injuries [TR-HFM-089, 2004], no specific injury scales were available or developed to classify AV mine injuries. Therefore the HFM-090/TG-25 decided to use the Abbreviated Injury Scale (AIS) [AIS, 1990] to guide the definition of acceptable injury tolerance levels. The AIS is the most well known anatomical scale and has been universally accepted. It was first published in 1971 and has been revised four times (1976, 1980, 1985 and 1990). Although originally intended for impact injuries in motor vehicle accidents, the several updates in the AIS allow now its application for other injuries such as burns and non-penetrating injuries. The AIS was developed to provide researchers with a simple numerical method for ranking and comparing injuries by severity, and to standardize the terminology used to describe injuries. The AIS is based on anatomical injury and in this way, differs from other systems that depend on physiological parameters. The AIS scores injuries and not the consequences of the injuries. It is used as a measure of the severity of the injury itself (including the risk of fatal injuries) and not as a measure of impairments or disabilities that result from the injury. Figure C.1 presents the injury ranking as defined by the AIS [AIS, 1990].

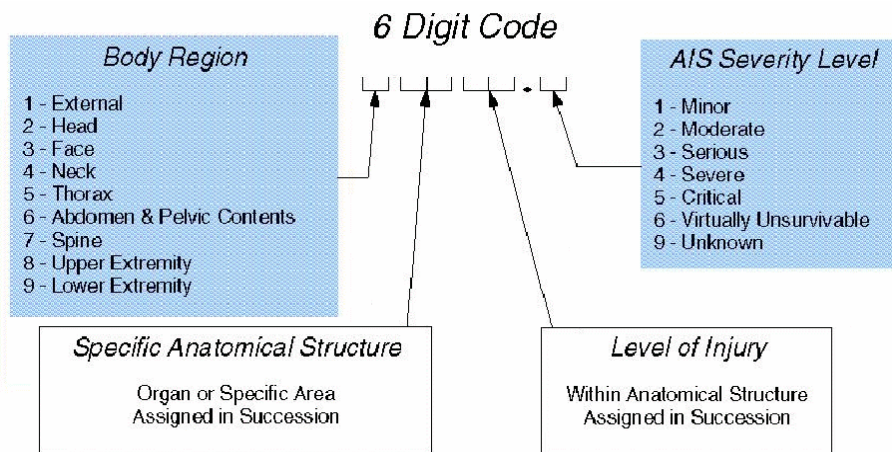


**Figure C.1: AIS Coding Scheme [AIS, 1990].**

An overall parameter for damage to parts of the body (the Injury Severity Score, ISS) can be calculated using the AIS code. The ISS score summarises the damage for the whole body in global terms. The ISS is the sum of the squares of three of the highest AIS codes in each of the most severely injured body parts. Recently, a modification of the ISS that both improves accuracy and simplifies scoring has been discussed in literature [Osler, 1997]. The NISS is the sum of the squares of the AIS scores of a patient's three most severe injuries, regardless of body region. The NISS avoids some shortcomings of the ISS, which leaves some injuries out of the scoring process altogether, such as when a patient sustains multiple injuries to a single body region, in which cases only the single worst injury contributes to the ISS. Also the ISS often ignores some more severe injuries in one body region in favor of less severe injuries to some other body region or regions, such as when multiple body regions are injured. Shortcomings of both, ISS and NISS are that it was designed for blunt trauma only, and it does not take into account physiologic variables. The (N)ISS score ranges from 1 to 75. Any injury code AIS 6 is automatically assigned an (N)ISS score of 75. This implies that 75 means a fatal injury whereas lower values indicate a less serious effect, ranging from critical to minor, in a way similar to that in the AIS code order. The corresponding estimates for survivability go from "highly unlikely" to "full recovery beyond any doubt".

### **C.2.2 Injury Risk Assessment**

Injuries having an AIS score below 3 are generally not life-threatening and are usually not associated with long-term impairment. In order to reduce, as much as possible, the risk of life-threatening as well as disabling injuries, the injury tolerance levels for the pass/fail limits to qualify the protection level were defined by STANAG 4569 based on the research by the HFM-090/TG-25. It has been decided that a 10% risk of AIS 2+ (AIS 2 or more) is acceptable. This guideline was followed, as much as possible, for the determination of the injury tolerance levels. The injury risk assessment for the STANAG 4569 consists of full scale testing using anthropomorphic test devices measuring the injury parameters and comparing the results to the tolerance levels. The procedure is described in the main text of the report, whereas the test protocol is presented in Annex I.

### **C.3 AV BLAST MINE INJURIES AND THEIR CONSEQUENCES**

The analysis of vehicle mine incidents [Medin, 1998; Radonić, 2004] is necessary in understanding the effects on the human body of blast mine detonations under vehicles. However, information is often classified, not/hardly available, or not detailed enough. Information on direct blast injuries caused by AP mines is easier available, because the number of AP mines and therefore the number of incidents is

considerably larger. Besides more civil than military are involved in AP mines incidents, which makes the medical information more accessible for these direct blast injuries. In contrast with antipersonnel (AP) mine strikes [TR-HFM-089, 2004], antivehicular (AV) mine strikes are not associated with specific injury patterns. Depending on a large number of factors, an AV mine blast may result in a full spectrum of physiological effects ranging for example, from a minor scratch to a fatal injury, and may injure all parts of the body. Based on a limited amount of information, coming from incident reports and full-scale testing experience, the lower extremity, the spine, the head and the auditory and non-auditory internal organs/systems (susceptible to overpressure effects), were identified as the most vulnerable body regions to AV blast landmine strikes.

### **C.3.1 Injuries, Recovery and Impairment**

The following tables give examples of injuries that may be sustained by vehicle occupants subjected to an AV blast mine, for the most expected vulnerable body regions: lower leg, spine, head, neck and non-auditory organs. The information is presented here to have an indication of the injuries, recovery and impairment. For each of the injury, the time for recovery is estimated and level of risk of impairment after recovery is indicated. The estimated time for recovery and risk of impairment is in general very sensitive to a number of factors. The information contained in the following tables represents the most expected scenario for a relatively young person in good physical condition.

The term ‘recovery’ refers here to the healing and ‘impairment’ refers to the after-effects and/or limitations caused by the injury. For example, the recovery period for a calcaneus fracture is usually short (3 months), but the risk of impairment associated with this injury is high. Because of the pain, the patient may be not able to walk or run normally anymore.

**Table C.1: Lower Leg Injuries**

<b>Examples of Injuries</b>	<b>AIS</b>	<b>Recovery</b>	<b>Risk of Impairment</b>
Ankle sprain	1	2 to 3 months	Low
Simple fracture of the tibia	2	3 months	Low
Simple or comminuted fracture of the talus	2	3 months or +	Medium
Simple or comminuted fracture of the calcaneus	2	3 months or +	Medium – High
Open fracture of the tibia	3	3 months or +	Low – Medium
Fracture of the fibula with affected artery or nerve	3	3 months or +	Medium – High
Traumatic amputation	4	3 months or +	High

**Table C.2: Cervical and Thoraco-Lumbar Spine Injuries**

<b>Examples of Injuries</b>	<b>AIS</b>	<b>Recovery</b>	<b>Risk of Impairment</b>
Sprain	1	2 to 3 weeks	Low
Disk hernia	2	1 to 3 months	Low – Medium
Stable vertebrae fracture	2	1.5 to 4 months	Low – Medium
Spinal cord simple contusion (with or without fracture)	3	3 months or +	Medium – High
Uncompleted spinal cord syndrome	4	3 months or +	High
Completed spinal cord syndrome	5	6 months or +	High
Unstable vertebrae fracture	5	3 months or +	Medium – High

**Table C.3: Head Injuries**

<b>Examples of Injuries</b>	<b>AIS</b>	<b>Recovery</b>	<b>Risk of Impairment</b>
Skull fracture	2	4 to 6 weeks	Low
Brain concussion	2	1 month	Low
Brain contusion	3	3 months	Low – Medium
Complex or open skull fracture	4	3 months or +	Medium
Intracerebral haemorrhage	4	3 months or +	Medium – High
Brainstem contusion	5	3 months or +	High

**Table C.4: Auditory and Non-Auditory Overpressure Injuries**

<b>Examples of Injuries</b>	<b>AIS</b>	<b>Recovery</b>	<b>Risk of Impairment</b>
Eardrum rupture	1	4 to 6 weeks	Low
Dislocation or rupture of the ossicles (malleus, incus and stapes)	1	1 to 3 months or +	Medium – High
Damage of hair cells of the cochlea	1	1 to 3 months or +	Medium – High
Trachea minor ecchymosis	2	1 month	Low – Medium
Bowel major contusion	3 – 4	2 to 3 months	Medium
Rupture of spleen	3	1 to 3 months	Low – Medium
Unilateral blast lung (1 lung affected)	3	4 to 6 weeks	Medium
Rupture of liver	4	2 to 3 month or +	High
Bilateral blast lung (2 lungs affected)	4	4 to 6 weeks or +	Medium – High
Hemothorax	?	4 to 6 weeks or +	Medium – High
Pneumothorax	?	4 to 6 weeks or +	Medium
Bowel contusion with perforation	5	2 to 3 months	Medium – High

### **C.3.2 Parameters that Influence the Injury Severity**

The extent of damage to the different body regions is related to different human factors like:

- Anthropomorphic data;
- Gender, age; and
- Physical state.

According to [Radonić, 2004] the extent of damage and the localization of the wounds are in direct relation with the type of landmines, the distance between occupant and mine, the strength of explosive charge, the brunt of airwave and the thermal activity. When a vehicle is subjected to a blast landmine, the following factors are believed to be the most influent on the severity of injuries sustained by the occupants:

- Distance between mine and occupant;
- Type of vehicle (including type of protection); and
- Loading conditions.

The severity of the effects of the mine on vehicle occupants is directly correlated with the impact of the mine on the vehicle itself. The mine protection system will then deal with these factors in order to reduce the impact of the mine on the vehicle and thus, on the occupants. The following paragraphs present some examples for these three latter factors.

### **C.3.3 Distance between Mine and Occupant**

The report by Medin et al. [Medin, 1998] describing a blast mine incident on an armoured personnel carrier (APC) in Bosnia, in 1996, shows the important effect of the distance between mine and occupants, on the severity of injuries. Figure C.2 shows the vehicle with the nine passengers (commander, gunner, driver and six rear passengers) and the mine location (red circle). The commander (C), the driver (D) and the passenger Rf did not sustain any physical injury. The gunner (G) and the passengers Lf, Rc and Rr sustained lower extremity injuries. The passengers who were the closest to the mine (Lc and Lr) sustained the most severe lower leg injuries, which unfortunately resulted in surgical amputation for both of them after the incident, (Lc lost both lower legs).

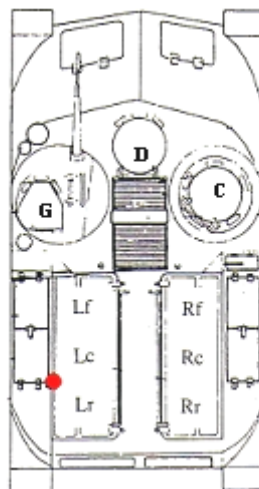


**Figure C.2: APC Subjected to AV Blast Landmines (Modified from [Medin, 1998]).**



### **C.3.4 Type of Vehicle**

The type of vehicle, by its specific geometry, will of course have an influence of the distance between occupants and mine. The vehicle structure solidity (including the type of protection) will affect the extent of damage on the vehicle and thus, on the occupant inside. Figure C.3 shows unprotected light-armored and logistic vehicles both subjected to an equivalent blast mine threat detonated under the front wheel. The light-armored vehicle, being more robust and having a stronger structure, was more resistant than the logistic vehicle. The conditions of the vehicles after detonation (shown on Figure C.3) give a good idea of the impact that may have been transmitted to the vehicle occupants. In these cases, it is expected that the occupants of the logistic vehicle would not survive the blast whereas the probability of survivability is expected to be much higher for the occupants inside the light-armored vehicle.



Light Armoured Vehicle – Before the test



Light Armoured Vehicle – After the tests



Light Logistic Vehicle – Before the test



Light Logistic Vehicle – After the test

**Figure C.3: Light-Armoured and Logistic Vehicles Subjected to Similar Mine Threat (Pictures courtesy of DRDC).**

In the study of Radonić et al. [Radonić, 2004], AV mine strike incidents occurring during the war of Croatia between 1991 and 1995, were analyzed. The vehicles involved in these incidents were light vehicles (lorries, cars, buses, etc.) and six of the seven mine types reported were blast landmines. Of the 464 victims, 42 (9%) were injured and 12 (29%) of the injured victims died. The major cause of death was brain injuries and the most frequent injured body region was the leg. Leg traumatic amputation, leg fracture (especially calcaneus),



eyes injuries and brain injuries (with skull fracture) were the most reported injuries. The severity and types of injuries reported in the study of Radonić would not be necessarily the same expected if heavier vehicles would have been subjected to the same threats. For example, in the vehicle mine incident described by Medin, six of the nine vehicle occupants were injured and none of them died. The injured occupants suffer lower extremity injuries, but none of them suffered traumatic amputation, eye or brain injuries.

Open and closed vehicles subjected to blast mines will not necessarily result in the same severity and type of injuries. In the case of an open vehicle, the occupants are more exposed to detonation products, heat and blast wave. Also, the occupants of an open vehicle may be ejected. The ejection may result in multiple injuries to the whole body when falling on the ground, especially skull, brain and neck injuries. Also fractures to the pelvis and femur have been documented [Medin, 1998]. The severity of the injuries will depend on the height of the fall.

### **C.3.5 Loading Conditions**

The impact of the mine on the vehicle depends on the loading conditions, which are not only related to the mine itself. The following parameters will influence the severity of the loading conditions on the vehicle and its occupants:

- Explosive mass and type;
- Type of soil;
- Depth of burial; and
- Mine location with respect to the vehicle.

More information on this topic can be found in the STANAG 4569 minutes and reports.

## **C.4 DISCUSSION AND CONCLUSIONS**

Antitank blast landmines result in multiple injury mechanisms causing physical injuries to the whole body. The definition of an injury assessment method for protection against AV mines was an important challenge due to the limited information available on AV mine incidents and injuries. However, based on full-scale testing experience and on few incident reports, it was possible to develop a satisfying assessment method. This method includes injury criteria and tolerance levels that were established to protect, as much as possible, against life-threatening and disabling injuries. The Abbreviated Injury Scale (AIS) was the tool used to establish acceptable injury tolerance levels.

Injuries sustained by the vehicle occupants may range from AIS 1 to 6, depending on human, mine and vehicle factors. The Abbreviated Injury Scale has its advantages and limitations. The most important advantage of using the AIS is for its simplicity. Being applicable to individual body regions, the AIS does not reflect the global conditions of a casualty suffering of multiple injuries. Injuries having an AIS score below 3 are generally not life-threatening and are usually not associated with long-term impairment, but they are some exceptions. Ear and lower extremity injuries are examples of AIS 1 (ear) and AIS 2 (leg) injuries resulting in long-term impairment. Ear injuries (even the ones resulting in hearing loss) have a score of AIS 1 and are of course very incapacitating, and represent a considerable loss of quality of life. Calcaneus fracture, having an AIS score of 2, is very painful and is often associated with infection. These complications may result in an amputation of the leg below the knee, which strongly affect the patient quality of life. Finally, different types of fractures may have the same AIS score, but not the same consequence. For example, intra-articular (outside the joint) represent more chances of long-term impairment (loss of joint mobility) than extra-articular (in the joint) fractures. Even if the AIS does not always reflect long-term consequences of injuries, it was believed the best approach for the HFM-090/TG-25 to establish NATO evaluation standards for AV blast landmine protection testing.

As other war injuries, mine injuries are unclean because the explosive brunt carries ground particles, dirt, bacteria, remnants of clothing, metal fragments, etc., besides the inside of the vehicle is never clean. The type of injuries occurring due to the mine blast under the vehicle can require complex and expensive treatments and often result in disability and long-term impairment.

Based on incident reports of Medin and Radonić, it is clear that whatever the type of vehicle striking a mine, the lower leg is the most vulnerable body region, being in direct contact with the vehicle structure. Although usually not lethal, lower leg injuries are very incapacitating because they can result in surgical amputation of the leg. For this reason, the HFM-090/TG-25 participating countries are presently putting a considerable effort on the optimization of the lower leg injury assessment method (see Annex E).

## **C.5 REFERENCES**

AIS (1990), The Abbreviated Injury Scale, Arlington Heights, IL: American Association for Automotive Medicine.

Medin, A., Axelsson, H. and Suneson, A. (1998), The reactions of the crew in an armoured personnel carrier to an anti-tank mine blast, A Swedish incident in Bosnia 1996, Defence Research Establishment Weapons and Protection Division, SE-147 25 Tumba, Sweden, FOA-R—98-00720-310—SE, ISSN 1104-9154.

Osler, T., Baker, S.P. and Long, W. (1997), A modification of the injury severity score that both improves accuracy and simplifies scoring, *Journal of Trauma*; 43 (6), pp. 922-926.

Radonić, V., Giunio, L., Biočić, M., Tripković, A., Lukšić, B. and Primorac, D. (2004), Injuries from Antitank Mines in Southern Croatia, in *Military Medicine*, Vol. 169, April, pp. 320-324.

TR-HFM-089 (2004), RTO Technical Report, No. AC/323 (HFM-089) TP/51, Test Methodologies for Personal Protective Equipment Against Anti-Personnel Mine Blast, Final Report of the RTO Human Factor and Medicine Panel (HFM) Task Group TG-024.

## Annex D – MINE AWARENESS FOR VEHICLE OCCUPANTS

### Human Behaviour – An Important Part of the Protection System

Mine awareness could be described as the knowledge of how to minimize the risk to be injured by a landmine. Mine awareness is often defined in terms of anti personal mines and unprotected personnel. It is based on how to recognise mines and signs of mines and rules of how to handle dangerous situations. In that case, a detonation of a mine is not possible and still remains unharmed.

When it comes to personnel riding a vehicle it is a somewhat different situation. Even an unprotected vehicle often offer some kind of protection and a protected vehicle hopefully gives the crew and the passengers the means to protect themselves in the best possible way. A vehicle, protected and qualified according to the criteria described in this documentation even gives a good chance of no injury at all.

Mine protection of vehicles is often a combination of different measures ranging from reinforced bottom structure to seat belts and holders for weapons and equipment.

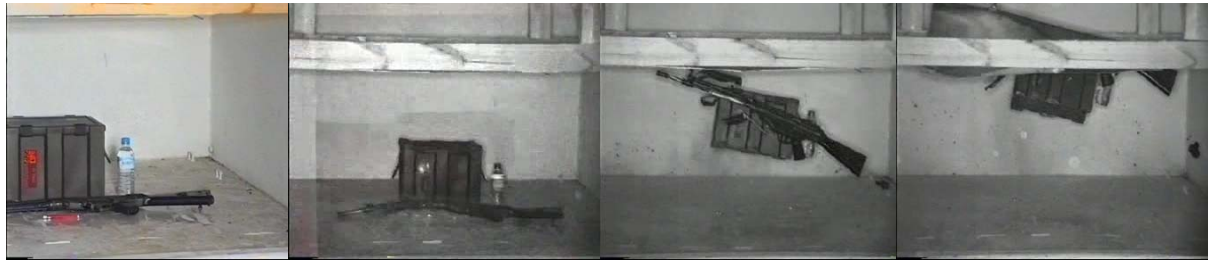
However, the risk for injury of the crew and passengers is not only a function of constructive measures of the vehicle. As described in this document and STANAG 4569 the mine protection level of a vehicle is based on the effects on the human body and qualified according to strict rules. Test equipment is used to evaluate a certain place and even a certain position of the vehicle occupants. Any other place or position could decrease the protection level.

Therefore it is important that the vehicle occupants know how to behave in case of a mine strike to minimize the risk for injury. In fact, the behaviour of the vehicle occupants is a part of the vehicle protective system and thus, education about mine awareness is of great importance. A protected vehicle **and** a well trained crew are the key to maximize the protection.

Below are few examples of recommendations/rules related to mine awareness for vehicle occupants:

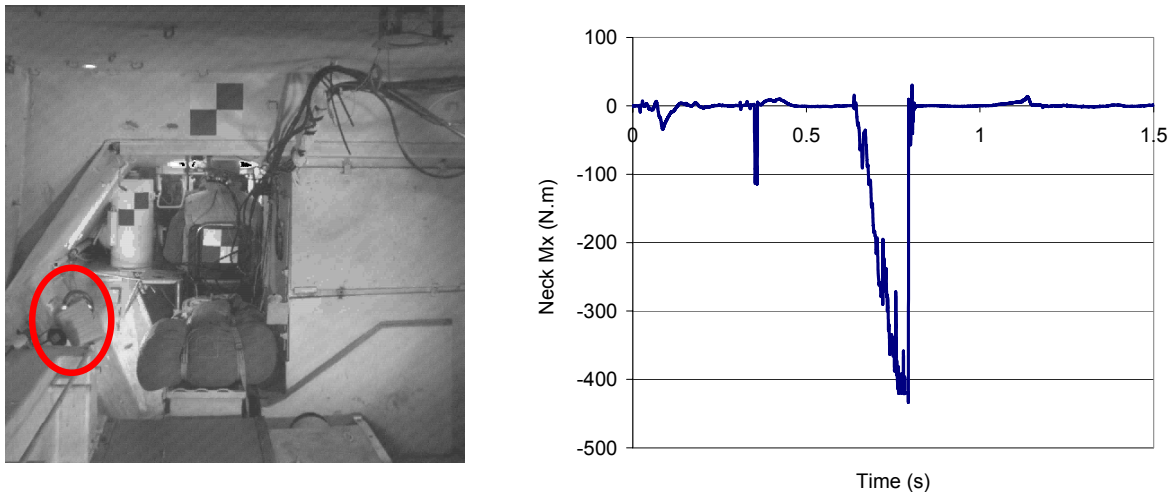
- Wear hearing protection;
- Use only seats that are prescribed and place your feet on the shock absorbing foot rest (if applicable);
- Wear seat restraint system (or seat belt);
- Avoid any loose objects inside the vehicle (see examples below);
- Before mission: Perform inspection of protective measures;
- Do not drive to fast, because of the risk for secondary accidents;
- Keep distance to the vehicle in front in case it strikes a mine; and
- Do not leave the vehicle in case of a mine strike; if there is one mine there could be more (AP or AT mines).

Figure D.1 illustrates what could happen with loose objects when a mine detonates below the bottom of a vehicle (in this case; 0,5 kg TNT placed on the ground at a distance of 0,5 m from a 10 mm steel bottom plate). The equipment (water bottle, gun and ammunition box) gets a velocity of approximately 25 m/s. These loose objects became very dangerous projectiles. A 1 mm soft aluminium plate (placed above the objects) was perforated by the objects.



**Figure D.1: Illustration of Danger of Loose Objects (Picture courtesy of FMV).**

Another example of flying object effects is given in Figure D.2. A fire extinguisher (identified by the red circle) was placed inside a light-armoured vehicle subjected to the detonation of a blast mine. For this specific test, all the measurements did not exceed the injury tolerance levels (as described in Chapter 3), but the neck lateral bending moment (shown on the right side of the figure) was very high (Mx peak value of 420 Nm). This severe impact was caused by the fire extinguisher that hit the side of the driver’s head after hitting the wall beside the driver. This example shows that even if a vehicle is well protected against mines, failure in the other protective procedures might be fatal for occupants. In this case, it is believed that the impact on the driver’s head would probably result in life-threatening neck injuries.



**Figure D.2: Fire Extinguisher Impact on Occupant’s Head during a Mine Test (Picture courtesy of DRDC).**

These two examples show the importance of securing all objects inside the vehicle to prevent loose objects in case of a mine strike.

## **Annex E – SUPPLEMENTAL INFORMATION ON LOWER LEG INJURY ASSESSMENT**

### **E.1 INTRODUCTION**

The loading mechanism acting on the lower leg during an AV blast mine strike is comparable to the ones generated by frontal car crashes or anti-personnel (AP) blast landmines. In these cases, an important axial force is transmitted to the lower leg, which may result in disabling injuries to the foot/ankle complex. A literature review on lower leg injury criteria was performed [Keown, 2003] in order to select the most appropriate one(s) for AV blast landmines testing. A few researchers performed dynamic axial impact tests on Post Mortem Human Surrogate (PMHS) lower legs in order to study the influence of different parameters on foot/ankle injury tolerance. The ones of interest used PMHS data to develop injury risk equations predicting the probability of foot/ankle fracture as a function of tibia axial force response. These models were the ones of Yoganandan et al., [Yoganandan, 1996], Griffin et al., [Griffin, 2001], Kuppa et al., [Kuppa, 2001a], Seipel et al., [Seipel, 2001] and Funk et al., [Funk, 2002b] are described, compared and analysed in the present annex. Other relevant lower leg injury criteria, which are the Tibia Index, the Lower Leg Threshold (LLth) and the ankle moment injury risk models, were found and are briefly described in this document. Finally, this annex also includes lower leg surrogates information and some discussions on the effect of boot, and leg positioning. It should be noted that this annex focus on the 10% risk of AIS 2+ injuries as has been agreed upon by STANAG 456. The reader is referred to the main report (Chapter 3) for anatomy of the lower leg as well as for more general information on the injury assessment method.

The present annex is divided in 8 sections:

- Section E.1 – Introduction
- Section E.2 – Foot/Ankle Injury Risk Models for Pure Axial Loading
- Section E.3 – Other Lower Leg Injury Criteria
- Section E.4 – Lower Leg Surrogates
- Section E.5 – The Effect of the Boot on Lower Leg Protection
- Section E.6 – The Effect of Leg Positioning on Tibia Response
- Section E.7 – Conclusion
- Section E.8 – References

### **E.2 FOOT/ANKLE INJURY RISK MODELS FOR PURE AXIAL LOADING**

#### **E.2.1 Yoganandan Model**

The objective of Yoganandan et al. [Yoganandan, 1996] study was to develop a quantitative relationship between biomechanical parameters such as specimen age, tibia axial force and injury. Dynamic axial impact tests were conducted at the Medical College of Wisconsin (MCW). Twenty-six (26) intact adult lower legs were tested under axial loading using a mini-sled pendulum device. As shown in Figure E.1, the entire lower extremity distal to the knee (lower leg) was installed in a neutral position and ballasted by a 16 kg pendulum. A six-axis load cell was installed behind the potting material in order to record the proximal tibia axial force.

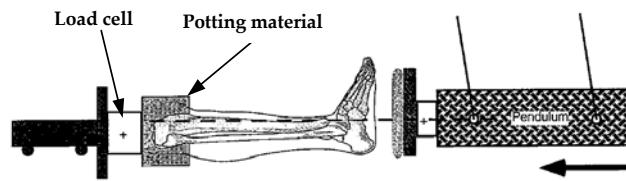


Figure E.1: Yoganandan Experimental Set-up (Modified from [Yoganandan, 1996]).

The results of MCW tests were combined to the ones obtained from similar studies at Wayne State University (WSU) and Calpan Corporation (Caplan), giving a sample size of 52 specimens having an age range of 27 to 85 years old. The whole set of experimental data (MCW, WSU and Caplan) was then used to derive two risk equations using the Weibull technique. The first one expresses the probability of foot/ankle fracture as a function of the tibia axial force and the second one expresses the probability of foot/ankle fracture as a function of tibia axial force as well as the subject age. Because military personnel are relatively young compared to the specimens used in this study (average age was 59 years old), the second injury risk model was the one of interest. Figure E.2 shows the probability distribution for foot/ankle injuries as a function of age and tibia axial force (peak value). Plus/minus one standard deviation limits are shown in dotted lines and solid circles represent the ‘fracture’ and ‘non-fracture’ data points. Fractures of the foot/ankle complex (distal tibia and calcaneus) were reported.

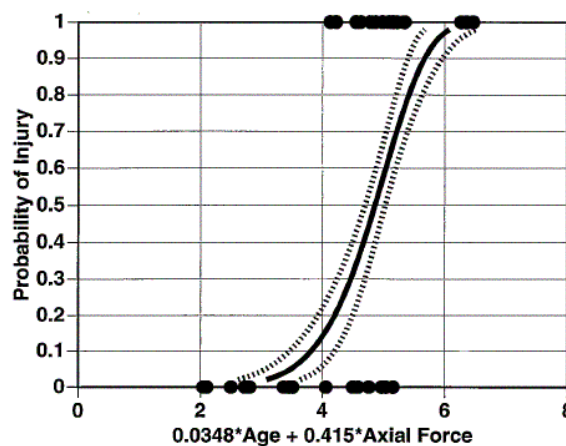


Figure E.2: Risk of Foot/Ankle Injury as a Function of Age and Tibia Axial Force [Yoganandan, 1996]. The injury criterion along the x-axis is expressed in kN.

Based on the relation given on Figure E.2, the probability of foot/ankle fracture can be expressed as follows:

$$P = 1 - \left[ \exp \left\{ - \left( \frac{0.0348 * A + 0.415 * F}{5.13076} \right)^{7.42582} \right\} \right]$$

where:

- P is the probability of foot/ankle fracture;
- A is the age (in years); and
- F is the tibia axial force (in kN).



Using this Weibull probability equation presented above, the risk of foot/ankle fracture, as a function of tibia force, can be computed for any age. Figure E.3 presents foot/ankle injury risk curves for 25, 45 and 65 years old subjects. Based on these curves, the tolerance value for 10% risk of foot/ankle fracture for 25, 45 and 65 years old, are respectively 7.0, 5.4 and 3.8 kN representing 10% risk of foot/ankle fracture (AIS 2+). To protect most of the population in military vehicles (having an estimated age range of 20 to 45 years old), the tolerance value of 5.4 kN (for 45 years old) was chosen by the TG-25. Because most of the specimens used by Yoganandan were male (39 on 52) and the average specimen’s weight was 75 kg, this tolerance value is applicable for mid-size males or large females [see Chapter 4, Figure 4.1 and Figure 4.2].

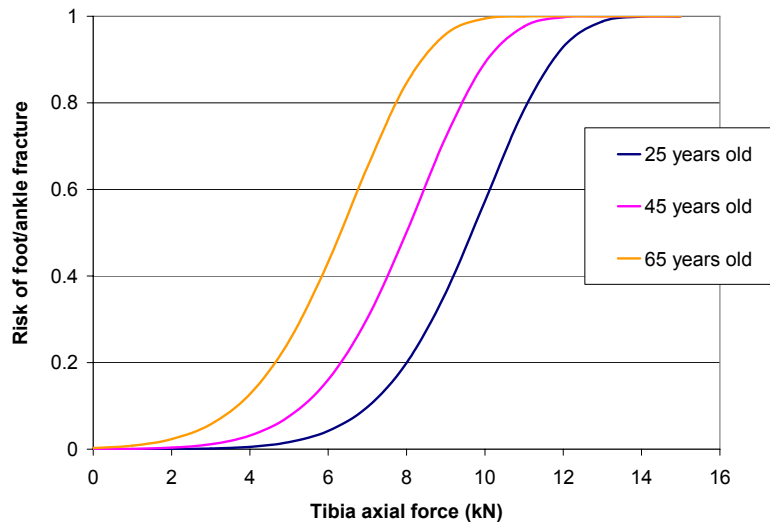


**Figure E.3: Yoganandan Risk Curves for Different Subject Ages.**

### E.2.2 Griffin Model

The objective of Griffin et al., [Griffin, 2001] study was to evaluate the performance of different AP mine protective boot models for a direct contact blast load. Twenty (20) full human cadavers were subjected to the detonation of AP mines, which generated lower extremity injuries. The age range of the cadavers was 37 to 96 years old and the average weight was  $73 \pm 14.1$  kg (close to a mid size male). Specimen gender was not mentioned. A load cell was installed at the proximal end of the tibia to record the axial force transmitted during the mine strike. Fractures in the foot/ankle complex (calcaneus, talus, cuboid, navicular and/or pilon) were reported. It was found that the significant predictors of pilon fracture were the tibia axial force and loading rate. Pilon fracture data points were used to derive the injury following risk equation, expressing the probability of fracture as a function of tibia peak axial force and loading rate.

$$P = \frac{1}{1 + \exp(-8.39 - 0.078R + 0.073W - 5.2 \times 10^{-4} F)}$$

where:

- P is the probability of pilon fracture;
- F is the tibia axial force (in N);
- R is the tibia loading rate (in kN/ms); and
- W is the subject body weight (in lbs).



Based on this risk equation, probability curves were plotted (Figure E.4) for a 75 kg subject submitted to different loading rates.

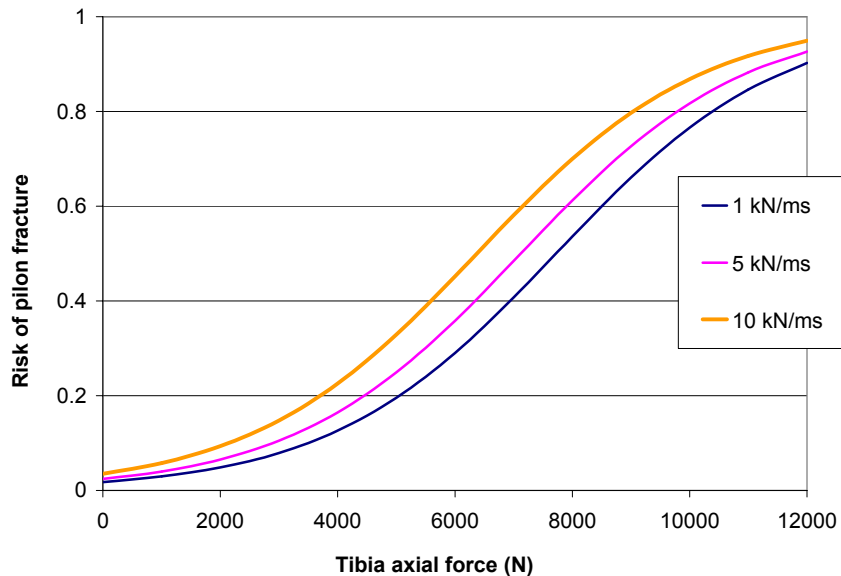


**Figure E.4: Griffin Risk Curves for a 75 kg Subject and Different Loading Rates.**

On 38 tested legs, 37 sustained foot/ankle fractures, but only 25 sustained pilon fractures. All the injured legs had calcaneal fracture. The injury data showed that calcaneal fracture is the primary injury mode under axial impact and may occur without pilon fracture. For this reason, Griffin model is limited for the study of lower leg injuries resulting from AV blast landmine strikes in which calcaneus fracture is a predominant injury. On 38 tests, only 25 were performed with a tibia load cell and used to derive the injury risk equation presented above. The second limitation of the model is that it was developed with tibia loading rate data ranging from 5.2 to 116.8 kN/ms. The validity of the model for loading rates below 5 kN/ms, being more representative of AV blast mine loadings, is then questionable.

### **E.2.3 Kuppa Model**

Kuppa et al., [Kuppa, 2001a], used other authors PMHS experimental data to derive different lower extremity injury risk functions. The data set of Yoganandan et al., [Yoganandan, 1996], was used by Kuppa to develop the following risk equation:

$$P = \frac{1}{1 + \exp(4.572 - 0.670F)}$$

- P is the probability of foot/ankle fracture; and
- F is the tibia axial force (in N).

In contrast to Yoganandan, the risk equation developed by Kuppa does not include the subject age. For example, the tolerance value for 10% risk of fracture is 3.6 kN (Kuppa used Yoganandan data, so same age range) when using Kuppa and 5.4 kN when using Yoganandan for a 45 years old subject. This indicates the need of including the age factor in the definition of the tolerance level.

### E.2.4 Seipel Model

Seipel et al., [Seipel, 2001], simulated axial lower leg injuries secondary to vehicular frontal impacts with the use of a mini-sled pendulum (same set-up as Yoganandan et al., [Yoganandan, 1996], shown in Figure E.1). The study focussed on calcaneus fracture, being the most frequent lower leg injury resulting from an axial impact. The pendulum impacted the surface of the foot of 22 unembalmed cadaver lower extremity specimens. Of the 22 specimens, 21 were males. The specimen age range was 27 to 74 years old. The 16 kg pendulum velocity ranged from 2.2 to 7.6 m/s to produce non-injurious and injurious impacts. A probability distribution was generated with the ‘fracture’ and ‘nonfracture’ data points. Only limited information is available on the injury details. Based on the injury risk curve derived from a logistic regression analysis, the threshold value (based on peak tibia axial force) for 10% and 50% risk of calcaneus fracture are respectively 2.4 and 5.5 kN. The equation developed in this study was not mentioned by the authors, but the probability graph was shown. The first limitation of this study is that the sample size was relatively small (22), which gives a low confidence in the injury risk equation accuracy. The second limitation is that the model does not include the specimen age effect, which, as shown by Yoganandan model, has a significant influence on the foot/ankle injury tolerance. The tolerance values given by Seipel injury model are then too conservative to be applied to military vehicle occupants.

### E.2.5 Funk Model

The objectives of Funk et al., [Funk, 2002b] study were to investigate the effect of Achilles muscle tension on fracture mode and to develop an empirical model of the axial loading tolerance of the foot/ankle complex. Funk developed, using a multivariate Weibull regression model, a risk equation to predict the probability of foot/ankle fracture as a function of the tibia axial force, specimen age, gender and weight, and Achilles tension. Achilles tension was applied on the lower leg specimens to simulate the leg muscle tension prior to a frontal car impact. In the case of AV blast mine detonation, muscle pre-tension is not considered because the vehicle occupants do not ‘expect’ the impact. Also the process is so fast that muscle contraction will probably not respond in time to have any influence on the injury response.

As shown on Figure E.5, thirty (30) cadaveric lower extremity specimens were subjected to dynamic axial impacts by a footplate attached to a transfer piston. The foot was in contact with the footplate prior to the impact and the footplate velocity reached approximately 5 m/s during the impact. The leg specimens were sectioned at mid-femur to preserve knee joint and leg musculature. Fifteen tests (15) over thirty (30) were done without Achilles tension. All the tested legs sustained foot/ankle fracture. Calcaneus, pilon, talus, malleolus, fibula and tibial plateau fractures were reported. On 30 tested legs, 25 sustained calcaneus fractures, showing again that calcaneus is the most vulnerable foot/ankle bone when subjected to axial impact. The tibia load cell, in contrast with the previous studies, was inserted into the tibia.

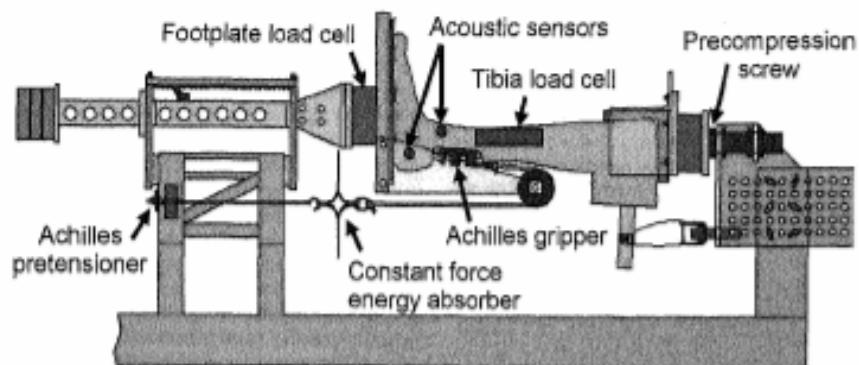


**Figure E.5: Funk Experimental Set-up [Funk, 2002].**

The risk equation developed by Funk is the following:

$$P = 1 - \left[ \exp \left\{ - \exp \left[ \begin{array}{l} 4.99 \ln(F) - 43.7 - 0.964G + 0.0793A \\ - 0.0552W - 0.473AT \end{array} \right] \right\} \right]$$

where:

- P is the probability of foot/ankle fracture;
- F is the tibia axial force (in N);
- G is the subject gender (=1 if male; =0 if female);
- A is the subject age (in years);
- W is the subject body weight (in kg); and
- AT is the Achilles tension (in N).

This model allows the study of the effect of different specimen parameters. For example, the Figure E.6 shows the effect of the age on the tolerance to fracture for mid-size males and females, when there is no Achilles tension. These curves, as the ones of Yoganandan, show the strong effect of the specimen age on the tolerance to fracture. They also show that males have a stronger tolerance to fracture than female. According to Funk model, 45 years old mid-size female lower leg could be less resistant than 65 years old mid-size male lower leg.

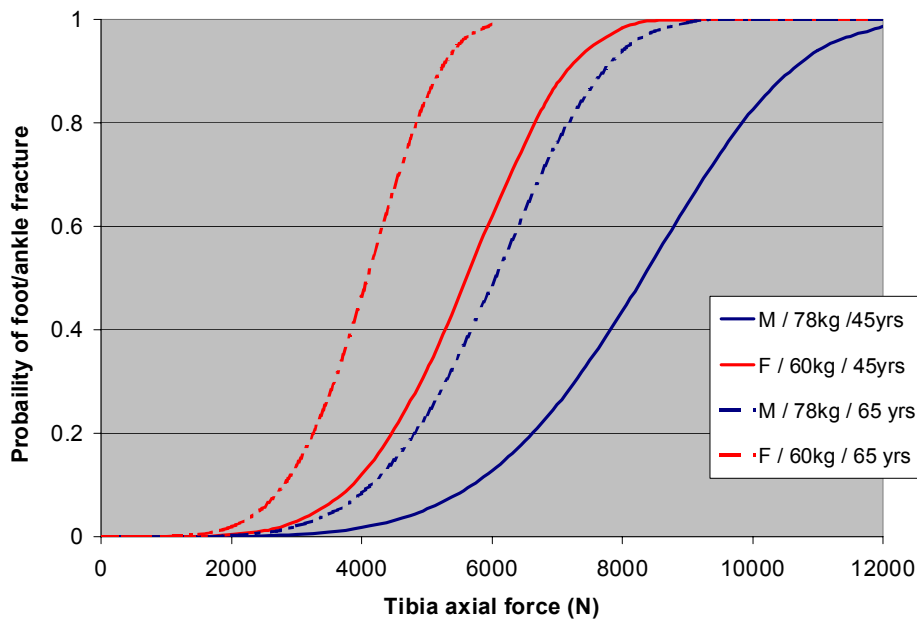


**Figure E.6: Funk Risk Curves for Different Subject Age and Weight.**

The injury risk model developed by Funk is complete because it gives the possibility to predict the risk of fracture for a large range of human population. On the other hand, the model can represent some complications when defining NATO standards because the model requires the specification of gender, weight and age. The average weight and age might be different for the different NATO countries, rendering the definition of these parameters difficult. The second limitation of Funk model is that its validity for age below 40 years old is questionable because the specimen age range was 41 to 74 years old.

### E.2.6 Hirsch

In 1964 Hirsch [Hirsch, 1964] presented a tolerance curve (Figure E.8) for a **standing man** with stiff legs exposed to shock motion of short duration. The shock was represented by an acceleration square pulse with 1 – 100 ms duration and 20 – 800g amplitude. The tolerance curve is a typical “iso-injury” curve meaning that for every point on this curve the same injury/damage will occur (here tolerance). For points over and to the right of the curve more injury/damage will occur and consequently less injury/damage when under and to the left. For other shapes of the acceleration pulse and other targets, different iso-injury curves must be used.

Hirsch has a vertical asymptote for durations of  $> 24$  ms implying that for pulse amplitude of 20g and increasing the pulse duration will have the same tolerance level. The value 20g is based on the crushing load for the two lower legs of 13340N for a 72.5 kg heavy man. A horizontal asymptote of 3 m/s velocity change is for pulse durations  $< 10$  ms. The tolerance level can be something between severe discomfort to fracture on foot or lower leg.

Hirsch gives in his Figure E.7 an example of shock-motion terminology used in the evaluation of a velocity – time history. Assuming that the acceleration – time history is measured at the place on the floor where you can expect to have a man standing stiff-legged with both feet on the floor, the acceleration – time history can be integrated to velocity – time as in his Figure E.8.

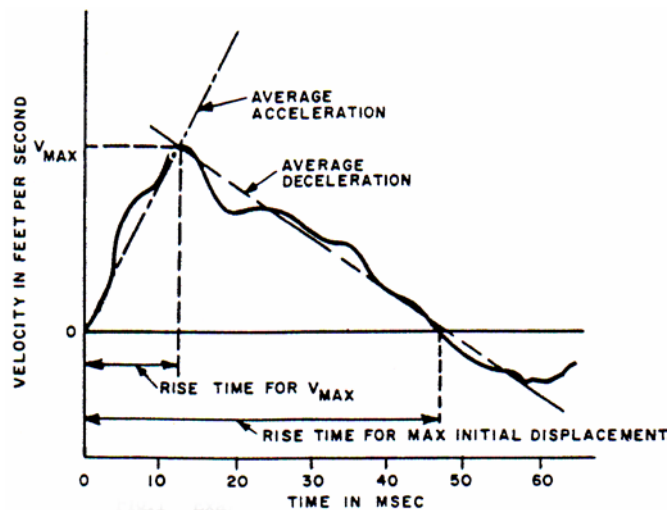


Figure E.7: Example of Shock-Motion Terminology [Hirsch, 1964].

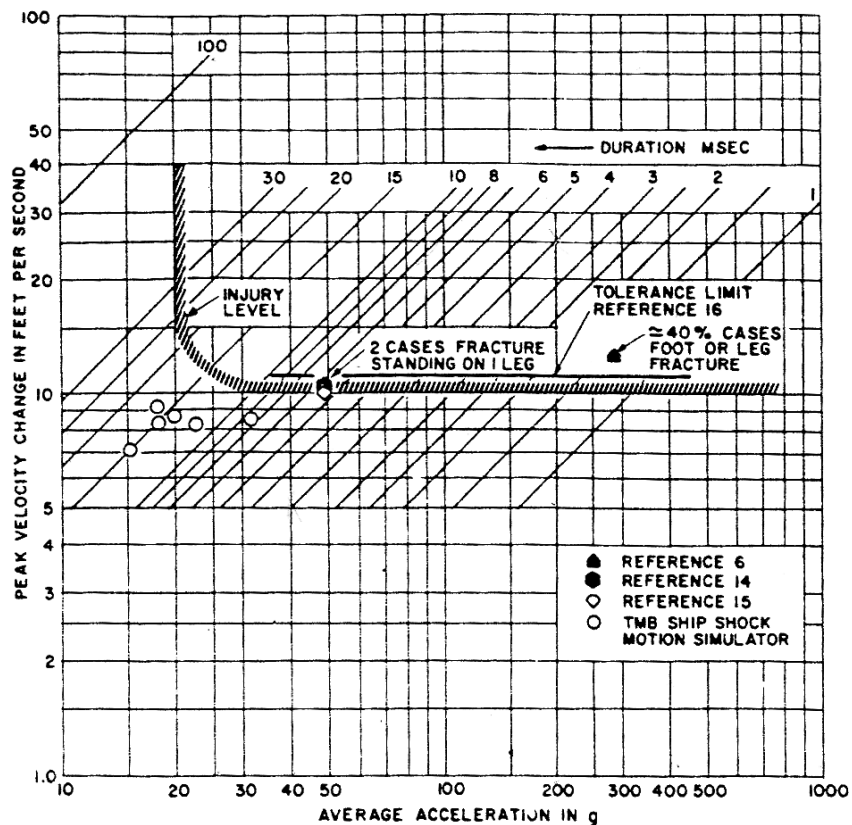


Figure E.8: Tolerance of Stiff-Legged Standing Men to Shock Motion of Short Duration [Hirsch, 1964].

The velocity increases almost linear up to a peak velocity change =  $V_{max}$ , reached after a time  $\Delta t$  (= rise time for  $V_{max}$ ).  $\Delta t$  is called duration in his Figure E.7.  $V_{max}/\Delta t$  = average acceleration and is the constant acceleration level in the square pulse.

Two out of the three quantities

- Max velocity change ( $V_{max}$ )
- Duration/rise time for  $V_{max}$
- Average acceleration

can be used to assess if the shock pulse is on the safe side or not of the tolerance curve.

Some advantages with the Hirsch model are

- Use of PMHS, human volunteers and war experience for evaluation of the tolerance curve;
- Measurements can be made on where the feet are positioned (floor, foot-rest, etc.) and the model is still relevant; and
- Inexpensive method.

Some disadvantages are

- It is still a technical challenge to measure the acceleration on a shock loaded steel plate;
- The model is valid for only one shape of acceleration pulse; and
- The model is not applicable to a sitting man.

Most wanted is a simple mathematical model (like the DRI model) of the lower leg for calculating the response to all kinds of acceleration – time histories.

**E.2.7 The Lower Leg Threshold (LLth)**

The Lower Leg Threshold (LLth) is a foot/ankle injury risk model, which was developed by WTD-91 (DEU). The idea of the model was to correlate the probability of foot/ankle fracture with shock pulse duration and amplitude. Data from Hirsch [Hirsch, 1964], (for the standing man), were used to develop the injury tolerance curve shown in Figure E.9. The tolerance curves implies that any acceleration-duration data points falling below the curve, represents a risk of less than 5% or 10% of sustaining foot/ankle fracture (AIS 2+). Using the acceleration-duration data points of Hirsch, and Yoganandan [Yoganandan, 1997,1998], the force-duration injury tolerance curve (10% risk of foot/ankle fracture) was developed (Figure E.10) without considering the age of the population. In Figure E.10, the actual injury threshold (5.4 kN, representing 10% risk of fracture) is drawn to compare both tolerance curves.

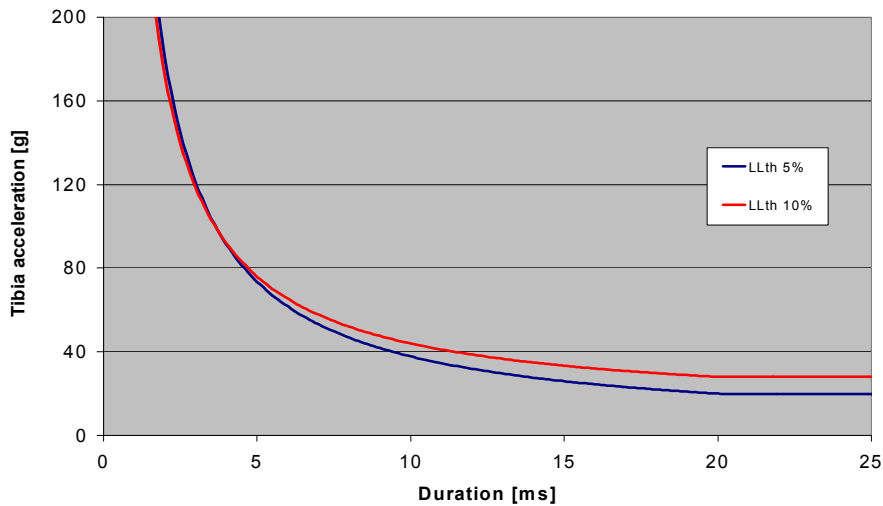


**Figure E.9: The LLth Acceleration-Based Injury Tolerance Curve.**

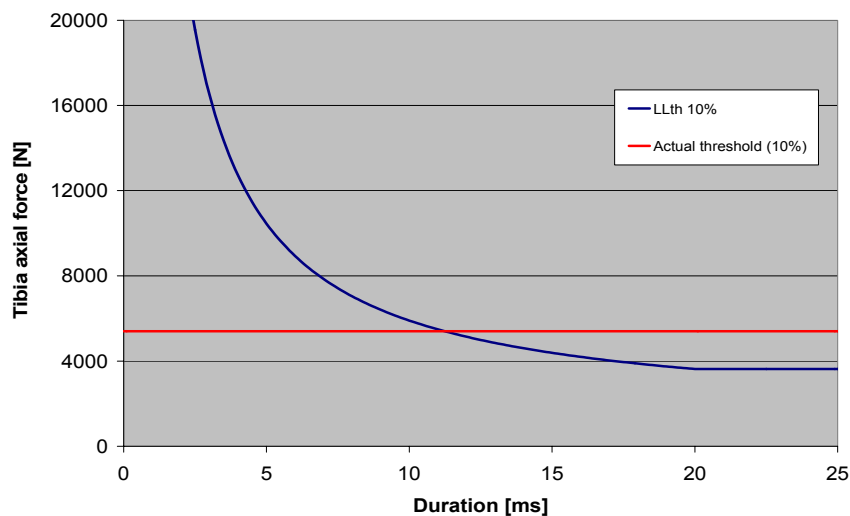


**Figure E.10: The LLth Force-Based Injury Tolerance Curve.**

The typical tibia loading duration expected during a mine strike is approximately 10 msec. As shown on Figure E.9, it can be said that the Lower Leg Threshold is in accordance with the proposed tolerance value for loading durations of approximately 10 to 12.5 ms. For shorter durations, the proposed tolerance value of 5.4 kN would be very conservative compared to the LLth. The LLth gives the possibility to assess risk of foot/ankle fracture as a function of an important parameter, which is the loading duration. This parameter is very important because AV mine strikes are usually shorter events than car crashes, which are the loading simulated to develop most of the injury models presented in the open literature. Additionally to the loading duration, the loading rate, as shown by Griffin model seems to have a significant influence on the tolerance to fracture. The ultimate foot/ankle injury models would take the loading duration, rate and amplitude into consideration, as well as important epidemiologic parameters such as the age and the gender. However, the LLth is a good starting point for the development of injury risk model specific to special loadings such as the ones generated by AV blast landmines.

**E.2.8 Summary, Analysis and Discussion**

The following tables summarize the important information belonging to each foot/ankle injury risk model discussed in this part. Table E.1 presents the specimen characteristics, Table E.2 shows the parameters considered in each study to develop the injury risk equation (Achilles tension is not mentioned) and Table E.3 summarizes the relevant advantages and shortcomings of the models. This information was used to achieve a comparative analysis to select the best model. Table E.4 presents the tolerance value (based on tibia axial force) for 10% and 50% risk of foot/ankle fracture (AIS 2+), for each model. The parameters of the models were specified such that the models can be compared together as best as possible. The age was set to 45 years old for Yoganandan and Funk models. The weight was set to 75 kg for Funk and Griffin based on the average specimen weight of Yoganandan study. The gender was set to ‘male’ for Funk because the majority of the specimens used in the other studies were males. A loading rate of 1 kN/ms was used in Griffin model, which is in the range of the tibia loading rate measured in Seipel and Funk study.

**Table E.1: Specimen Characteristics**

<b>Model</b>	<b>Number of Specimens</b>	<b>Number of Males</b>	<b>Average Weight (kg)</b>	<b>Average Age (range) (yrs)</b>	<b>Force Measurement Location</b>
<b>Yoganandan (and Kuppa)</b>	52	39	75 ± 15	56 ± 15 (27-85)	Proximal tibia
<b>Griffin</b>	25	?	73 ± 14	75 ± 17 (37-96)	Proximal tibia
<b>Seipel</b>	22	21	78 ± 11	49 ± 16 (27-74)	Proximal tibia
<b>Funk</b>	30	15	68 ± 14	63 ± 9 (41-74)	Middle tibia



**Table E.2: Parameters Included in the Injury Risk Equations**

<b>Model</b>	<b>Tibia Axial Force</b>	<b>Tibia Loading Rate</b>	<b>Age</b>	<b>Gender</b>	<b>Weight</b>
<b>Yoganandan</b>	•		•		
<b>Griffin</b>	•	•			•
<b>Kuppa</b>	•				
<b>Seipel</b>	•				
<b>Funk</b>	•		•	•	•

**Table E.3: Relevant Advantages and Shortcomings of the Models**

<b>Models</b>	<b>Advantages</b>	<b>Shortcomings</b>
<b>Yoganandan</b>	Includes subject age.	
<b>Griffin</b>	Includes subject weight and tibia loading rate.	Validity for loading rate < 5 kN/ms is unknown. Only pilon fracture is considered.
<b>Funk</b>	Includes subject age, gender and weight: complete model.	Validity for age < 40 years old is unknown.

**Table E.4: Tolerance Levels for the Different Models**

<b>Model</b>	<b>Injured Region</b>	<b>Tolerance Value (kN)</b>		<b>Specifications or Remarks</b>
		10%	50%	
<b>Yoganandan</b>	Foot/ankle	5.4	8.0	For a 45 years old subject.
<b>Griffin</b>	Tibia pilon	2.7	6.9	For a 75 kg subject and a loading rate of 1 kN/ms.
<b>Kuppa</b>	Foot/ankle	3.6	6.8	
<b>Seipel</b>	Calcaneus	2.4	5.5	Taken from the original graph.
<b>Funk</b>	Foot/ankle	5.5	8.0	For a 75 kg and 45 years old male, no Achilles tension.

The tolerance values presented in Table E.4 quantify the effect of the subject age on the injury tolerance of the foot/ankle complex. Seipel, Kuppa and Griffin models give lower tolerance values than Yoganandan and Funk models for similar conditions. Because military vehicle occupants are relatively young, Funk and Yoganandan models are more suitable for the vehicle mine protection assessment. As shown in Table E.4, both models give almost the same results for a 45 years old mid-size male, but the consistency between both models is not so good for age different from 45 years old (see Figure E.11). The models are

relatively consistent for 65 years old, but are less consistent for 25 years old, which was expected because this age is outside the validity level of Funks model.

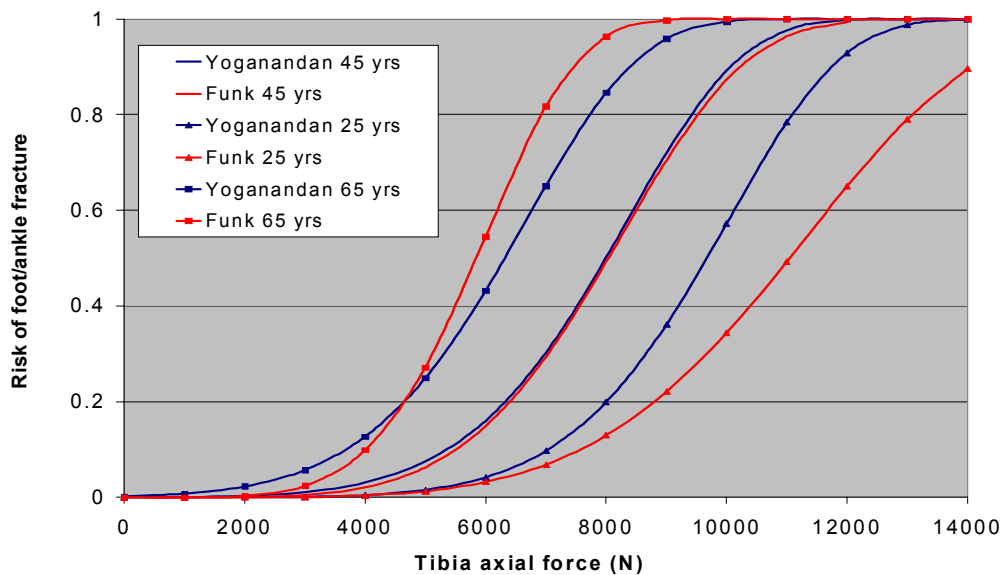


**Figure E.11: Comparison between Yoganandan and Funk Models.**

Based on these findings, the HFM-090/TG-25 has recommended the use of Yoganandan injury risk models to be included in NATO standards for vehicle mine testing assessment. The TG-25 established the lower leg threshold value to 5.4 kN, representing 10% risk of foot/ankle fracture for a 45 years old subject. In order to protect most of the military occupants (having an estimated age range of 20 to 45 years old), the age of 45 was chosen. The Yoganandan model, as well as the other foot/ankle injury models presented above, has four important limitations for the application of AV blast mine testing:

- The model was developed for pure axial impact on the base of the foot. In some cases, the foot may be loaded differently depending on the protection system and seating configuration.
- In some PMHS test conditions the foot is impacted by a mass, whereas in case of an AV mine strike the foot is always in contact with the floor, and this floor will accelerate. It needs to be studied in detail whether this difference in set-up has influence on the injury.
- The loading regime for which the model was developed is not available anymore, but is believed to be different than the one generated by an AV mine strike, being usually faster than the ones generated by frontal car crashes. However, based on other studies the loading conditions for a car crash is not deviating that much from lower legs loads measured in a well protected vehicle.
- The established tolerance level is to be applied to the Hybrid III instrumented tibia, which has different mechanical properties than the one of the human tibia, as discussed in Section E.4.

### **E.3 OTHER LOWER LEG INJURY MODELS**

The previous described injury models focus on a pure axial impact, whereas in reality the lower leg will be subjected to a combination of loadings (compression, bending, shear, etc.), depending on the orientation of the leg on the bottom plate. So far, HFM-090/TG-25 did not study the injury criteria for these different loading conditions. However, a short description of two other injury lower leg models is given below.

### E.3.1 The Tibia Index (TI)

The Tibia Index is used in some qualification trials of car crash safety systems [Kuppa, 2001a]. The TI has been developed to assess tibia and fibula shafts fracture, but does not include foot/ankle injury assessment. The Tibia Index was developed from tests on cadaveric leg specimens (without foot/ankle) that were subjected to a direct impact on the tibia shaft and axially compressed at the same time. The Tibia Index (TI) is expressed as follows:

$$TI = \frac{F_z}{F_c} + \frac{M}{M_c}$$

where:

- $F_z$  is the axial compression force (N);
- $M$  is the resultant bending moment ( $M_x^2 + M_y^2$ )<sup>1/2</sup> (Nm);
- $F_c$  is the critical axial compression force (constant value); and
- $M_c$  is the critical bending moment (constant value).

The Revised Tibia Index (RTI) involves the use of new critical values, established by Kuppa [Kuppa, 2001a] with the use of experimental data from other authors. The axial force and bending moment critical values recommended by Kuppa are respectively 12 kN and 240 Nm. Based on the risk equation developed by Kuppa, the recommended RTI threshold value is 0.75, representing 10% risk of tibia/fibula fracture (AIS 2+). When using the standard Hybrid III instrumented lower leg (described in Section E.4), the bending moment  $M_y$  has to be corrected as specified in [Welbourne, 1998].

The following injury risk equation (developed by Kuppa) can be used:

$$P = 1 - \left[ \exp \left\{ - \exp \left[ \frac{\ln(\text{RTI}) - 0.2728}{0.2468} \right] \right\} \right]$$

where:

- $P$  is the probability of tibia/fibula fracture; and
- RTI is the Revised Tibia Index.

Because direct impact on the tibia is not one of the expected primary injury mechanisms occurring during mine strikes, the Tibia Index was not part of the mandatory injury criteria recommended by the TG-25.

### E.3.2 Ankle Rotation Injury Risk Models

Especially during frontal car crashes, the ankle joint may rotate in dorsiflexion and/or inversion or eversion modes (Figure E.12), which may result in soft tissue injuries and/or ankle bone fractures. Even if this type of loading mechanism is not the first one expected during AV mine, ankle rotation injury assessment may be required in cases where the foot is placed on a pedal or a foot rest, resulting in load transfer via the fore foot. Kuppa et al., [Kuppa, 2001a] developed, with the use of other author experimental data, ankle joint injury risk equations based on dorsiflexion and eversion/inversion moments. Based on the risk equations developed by Kuppa, the recommended ankle moment threshold values are 40 Nm for dorsiflexion and 27 Nm for inversion/eversion, representing 10% risk of AIS 2+ ankle injuries. The ankle moment cannot be directly measured in the dummy lower legs. An equation to calculate the ankle moment, when using the Thor-Lx leg model (described in Section E.4), is given by [Kuppa, 2001b]. Similar relation can be used for the standard Hybrid III leg.

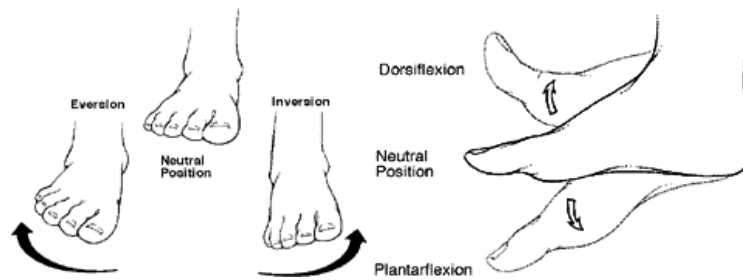


**Figure E.12: Ankle Joint Dorsiflexion and Inversion/Eversion Rotation Modes.**

## **E.4 LOWER LEG SURROGATES**

The injury assessment method proposed by the HFM-090/TG-25 involves the use of the standard Hybrid III instrumented lower leg (see Chapter 4). The standard Hybrid III lower leg model has a 45° rotation foot whereas the original version had a 30° foot. Even if the current Hybrid III lower leg biofidelity has been improved by the 45° foot, its tibia axial force response is not excellent in biofidelity [Owen, 2001]. The standard Hybrid III lower leg is equipped with an instrumented tibia called the Denton leg [Denton, 1984]. The Denton leg (shown in Figure E.13) is a simple steel shaft with lower and/or upper tibia load cells.

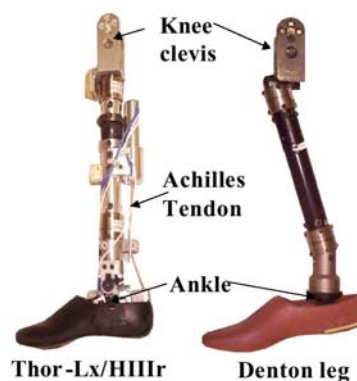


**Figure E.13: Thor-Lx (left) and Standard HIII Denton Lower Leg (right) [Kuppa, 2001b].**

A more biofidelic model of the human lower leg is the Thor-Lx (see Figure E.13), which was designed with the use of recent biomechanical data [Kuppa, 2001b]. It can be used together with the Hybrid III ATD, or with the original THOR frontal ATD (Test device for Human Occupant Restraint).

The Thor-Lx is the more biofidelic mechanical lower leg actually available [Kuppa, 2001b; Owen, 2001]. It is unique in that the design includes an Achilles tendon coupled with the straight tibia shaft to simulate passive resistance of musculature. This was shown to have a considerable influence in axial force response. The tibia includes a rubber element for to improve axial compression biofidelity and the shaft is straight. This is unlike the standard Hybrid III shaft, which is offset at the knee clevis and is known to introduce bending moments under pure axial loading conditions [Kuppa, 2001b; Welbourne, 1998]. The Thor-Lx is available as a retrofit for the Hybrid III 50<sup>th</sup> percentile dummy. More information on Denton leg and Thor-Lx, and their instrumentation is given in [Kuppa, 2001b].

**E.4.1 Frangible Synthetic Lower Legs Surrogates: CLL and FSL**

The Canadian Lower Leg (CLL) was developed by a team including DRDC to evaluate lower leg injuries sustained by anti-personnel (AP) mines and assess protective boot systems [Williams, 2002; Biokinetics, 2003; RTO-TR-HFM-089, 2004]. The CLL, shown in Figure E.14, is comprised of polymeric bones (that represent tibia/fibula, talus, and calcaneus), a nylon tendon, silicone rubber cartilage pads, a silicone rubber heel pad, ballistic gelatin (representing the flesh), and a latex skin. Since the objective of the CLL was to model the injury path up through the heel into the tibia, the forefoot is not considered and the leg has two calcaneus. When subjected to an impact, the CLL sustains damage comparable to real injuries sustained by a human leg. Figure E.15 shows typical CLL damage after AP mine testing (direct blast).

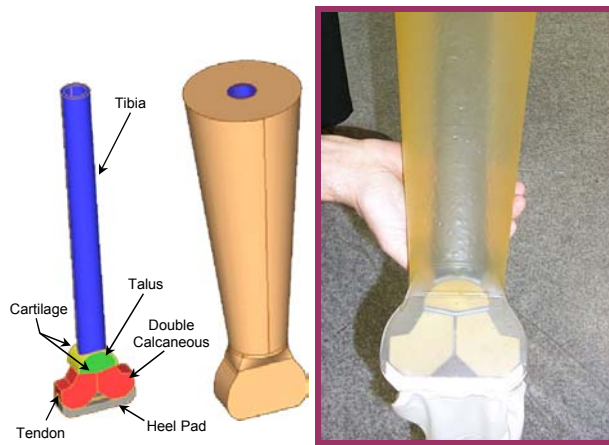


**Figure E.14: The Canadian Lower Leg (Picture courtesy of DRDC).**



**Figure E.15: Typical CLL Injuries (Picture courtesy of DRDC).**

A similar synthetic leg, called the Frangible Synthetic Leg (FSL), was developed at the Defence Science and Technology Organization (DSTO) in Australia to evaluate AP mine protection system performance [RTO-TR-HFM-089, 2004]. The FSL is a geometric reproduction of the human leg using materials that react to blast in a manner similar to human tissue. The bones are made from mineralized plastic and the flesh (soft tissue and muscles) from ballistic gelatin. As opposed to the CLL, which is a below-knee leg surrogate, the FSL is a representation of the whole lower extremity (upper and lower legs). The lower part of the FSL, the FSL (Frangible Synthetic Lower Leg), is shown in Figure E.16.



**Figure E.16: The Frangible Synthetic Lower Leg (FSL),  
Without (left) and With (right) Gelatine.**

The CLL and the FSL are biofidelic frangible human surrogates for axial loading conditions generated by AP mines [RTO-TR-HFM-089, 2004]. Australia performs AV mine strike tests using the FSL [Wang, 2001] and the CLL performance is currently evaluated for axial impacts generated by the vehicle floor intrusion caused by the detonation of AV blast landmines [Manseau, 2005a, 2005b, 2005c]. Both CLL and FSL are considered good research tools for AV mine protection studies when PMHS testing is not available, however so far validation of these models for the AV mine loading conditions are not available.

#### **E.4.2 Post Mortem Human Subjects**

The HFM-090/TG-25 wrote a white paper to perform Post Mortem Human Subjects (PMHS) tests to study the lower leg response during AV mine strikes and to generate validation data for the mechanical, synthetic and numerical models [Bir, 2006; Geurts, 2006a, 2006b]. Recently tests are performed and preliminary results were published [Barbir, 2005, Bir, 2006]. More tests will be performed in the future.

#### **E.4.3 Comparison between Hybrid III Lower Leg and Thor-Lx**

WTD 91 (DEU), IABG (DEU) and TNO (NLD) performed together experimental tests to compare the axial force response measured by the Thor-Lx and the standard Hybrid III lower leg [Nies, 2005]. These tests were done using the TROSS™ (Test Rig for Occupant Safety Systems, developed by IABG), which was designed to assess seat and restraint systems in the field of vehicle mine protection. It also has the capacity to simulate footplate displacement to replicate lower leg loadings seen during full-scale mine trials. The TROSS™ was developed to use scaled detonations and provide the same input to an occupant as during a full-scale test. The loading produced by small charges detonated under the TROSS™ is comparable to a real mine (2 to 10 kg TNT) detonation under a military (light or heavy) vehicle. The TROSS™ offers the possibility to provide well-defined and reproducible loads by the detonation of small explosive charges under an elastic deformable membrane bottom plate. Figure E.17 shows the exterior and interior views of the TROSS™. The test rig is closed by a box (in grey), which is de-coupled from the membrane plate and thus, isolated from the shock of the detonation.





**Figure E.17: Exterior (left) and Interior (right) View of TROSS™ Set-up (Pictures courtesy of IABG).**

Figure E.18 shows the tibia axial force measured by the standard Hybrid III leg (Denton leg) and the THOR-Lx, both subjected at the same time to loadings generated by small charges detonated under the TROSS. The ratio between the tibia axial force measured on the Hybrid III and the Thor ranged from 1.4 to 2.1. These results correlate well with the ones of Owen [Owen, 2001], for which the ratio between Hybrid III and THOR-Lx was approximately 1.43 (Figure E.18).

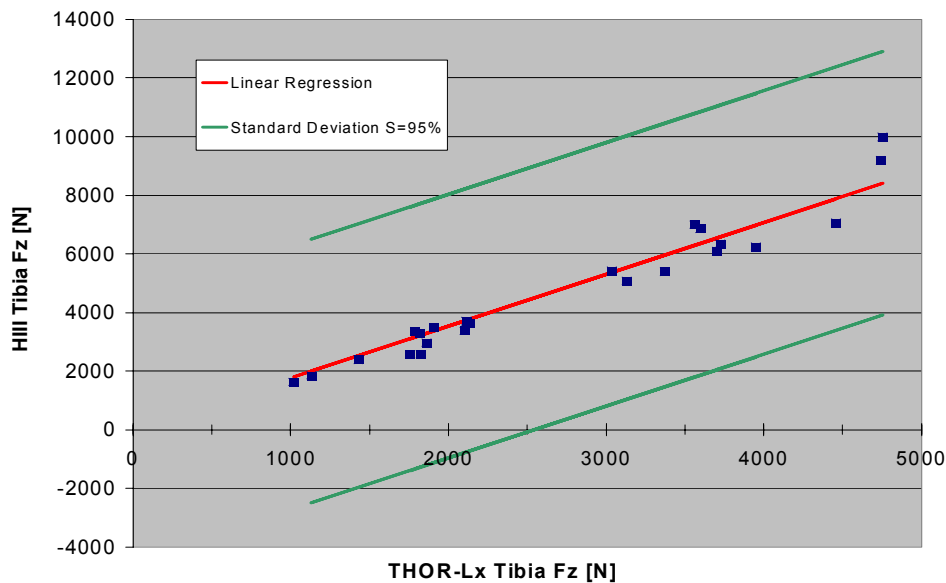


**Figure E.18: Comparison between Hybrid III and Thor-Lx Tibia Axial Forces (TROSS Tests) [Nies, 2005].**

## **E.5 THE EFFECT OF BOOTS ON LOWER LEG PROTECTION**

WTD 91 and IABG (DEU) and TNO (NLD) used the TROSS set-up to perform preliminary tests on the CLL, which was attached to a whole Hybrid III dummy (Figure E.19) [Horst, 2003]. Tests with and without military boot showed that the boot is offering a considerable protection to the foot when subjected to an axial impact [Manseau, 2005a; Nies, 2005, Geurts, 2006a].





**Figure E.19: TROSS Tests on the CLL With (left) and Without (right) Boot (Pictures courtesy of TNO).**

Laboratory axial tests were also performed by CA, on CLL and Hybrid III, in order to evaluate the effect of the military boot on the tibia loading response and the injury severity [Manseau, 2005b]. In both TROSS and laboratory testing, wearing the military boot avoided calcaneal fracture, a disabling lower extremity injury. Figure E.20 shows CLL results after being submitted to laboratory axial impact with and without boot. The CLL with a boot (shown on the left side) only sustain soft injuries (heel pad and talus cartilage damage) and the CLL without boot (shown on the right side) sustained an important calcaneus fracture. Finally, Figure E.21 show Hybrid III tibia loading resulting from tests with and without boot, which quantify the effect of the boot on the injury severity. In that case, the presence of the boot reduced the peak tibia axial force value of approximately 30%.



**Figure E.20: Results of Laboratory Axial Tests on the CLL With (left) and Without (right) Boot [Manseau, 2005b].**

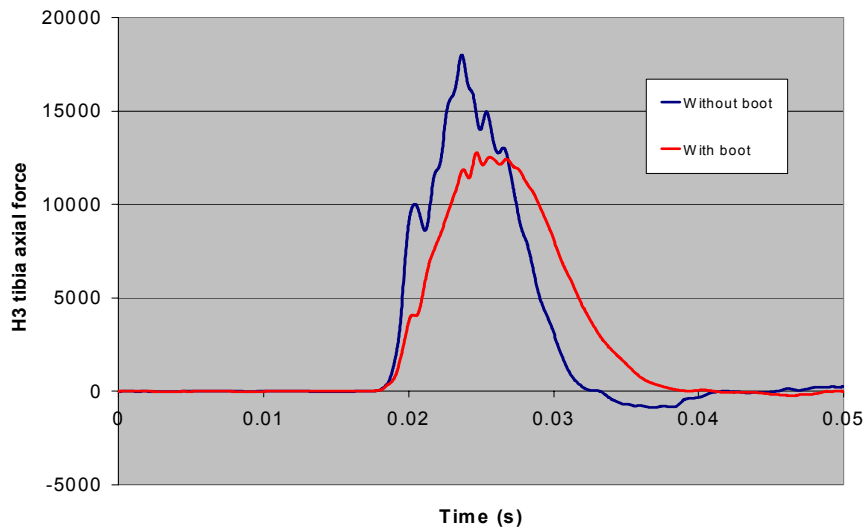


**Figure E.21: Example of Hybrid III Tibia Axial Force for Axial Impact Tests With and Without Boot [Manseau, 2005b].**

## E.6 EFFECT OF LEG POSITIONING

TNO studied the influence of the initial lower leg position on the forces, moment and accelerations using the MADYMO computer model of the Hybrid III 50<sup>th</sup> percentile male ATD [Horst, 2005]. As shown in Figures E.22 and E.23), four initial positions (A, B, C and D) and two loading conditions (db1 and db2) were simulated.

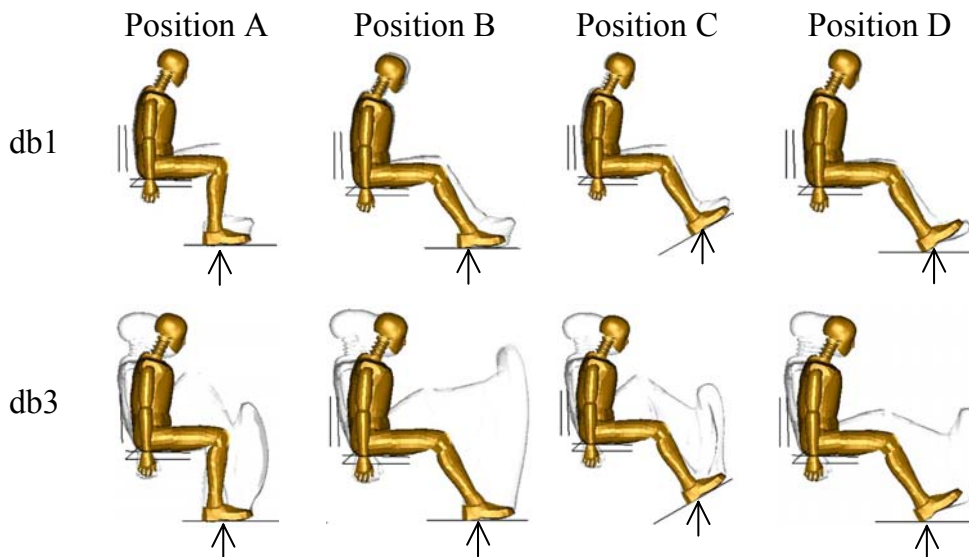


**Figure E.22: Tracing View Using Altair Hyperworks: Crash Dummy Motion during Pure Vertical Footplate Displacement for Four Initial Positions at Two Different Loading Conditions [Horst, 2005].**

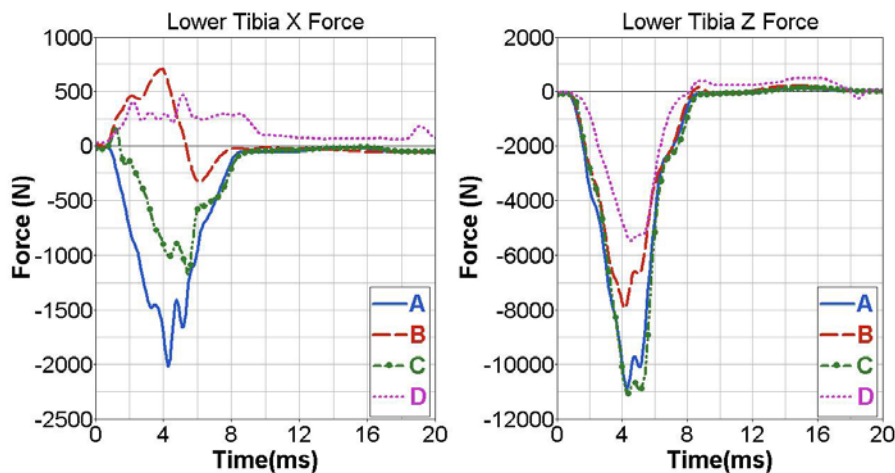


Figure E.23: Lower Tibia Axial Force ( $F_z$ ) for MADYMO Simulation of Test db3 (Vertical Footplate Displacement) for Different Foot Positions [Horst, 2005].

The same trend was seen for the axial tibia forces ( $F_z$ ) and accelerations ( $a_z$ ) for the lower and higher loading conditions [Horst, 2005]. The highest values are seen for position A en C, while D shows the lowest values in all cases. The use of the tibia force as injury indicator is based on pure axial loadings of the lower leg. In case of position B and D the legs are orientated under an angle and there is no pure vertical loading. Although the calculated axial tibia values are low, there may be a risk of foot/ankle injuries for these different orientations.

Recently the numerical research for the lower leg loading conditions has been updated [Geurts, 2006 a,b].

## E.7 CONCLUSION

Over the different injury risk models, [Yoganandan, 1996] and [Funk, 2002] models were the most suitable, since they include age effect. The Yoganandan model was chosen by the HFM-090/TG-25 since it was developed with a larger number of specimens with wider age range.

Actually, the threshold value of 5.4 kN might be too conservative because it is applied to the Hybrid III tibia, which is stiffer than the human tibia. For this reason, work is ongoing to evaluate the biofidelity of different existing mechanical legs [Bir, 2006] under pure axial impacts. Other loading configurations will also need to be studied in the future [Horst, 2005].

Finally, it was shown that the boot offers a considerable protection level and thus, should always be included in the qualification test protocol [Manseau, 2005b].

## E.8 REFERENCES

- Barbir, A. (2005), Validation of lower limb surrogates as injury assessment tools in floor impacts due to anti-vehicular landmine explosions, Masters thesis Wayne State University Detroit, USA (Draft version).
- Biokinetics and Associates Ltd (2003), The Complex Lower Leg (CLL).
- Bir, C., Barbir, A., Wilhelm, M., Horst, van der, M., Dosquet, F. and Wolfe, G. (2006), Validation of lower limb surrogates as injury assessment tools in floor impacts due to anti-vehicular landmine explosions, In Proceedings of International conference of biomechanics of impact (IRCOBI), September, Madrid, Spain.

Denton, R.A. Inc. (1984), Crash Test Dummy Lower Leg Structure, Patent No. 4, 488, 433.

Dosquet, F. (2002), Vehicular Mine Protection, Biomechanical Assessment of Lower Legs and Feet Impact Due to Loads in Mine Protection Tests, WTD 91, Report No. 9-400/67/02, March.

Dosquet, F. and Nies, O. (2004), TROSS tests with Denton/THOR-Lx/CLL – Summary of Results, Presentation given at the 5<sup>th</sup> NATO HFM-090/TG-25 meeting, Quebec, Canada, October.

Funk et al. (2002), The Axial Injury Tolerance of the Human Foot/Ankle Complex and the Effect of Achilles Tension, *Journal of Biomechanical Engineering*, Vol. 124, pp. 750-757, December.

Geurts, J., Horst, van der, M., Leerdam, P.-J., Bir, C., Dommelen, van, H. and Wismans, J. (2006a), Occupant Safety: Mine detonation under vehicles, a numerical lower leg injury assessment, In Proceedings of International conference of biomechanics of impact (IRCOBI), September, Madrid, Spain.

Geurts, J. (2006b), Occupant Safety: Mine detonation under vehicles, a numerical lower leg injury assessment, Masters thesis Eindhoven University of Technology, To be published in December 2006.

Griffin, L.V., Harris, R.M., Hayda, R.A. and Rountree, M.S. (2001), Loading Rate and Torsional Moments Predict Pilon Fractures for Antipersonnel Blast Mine Loading, presented at the International IRCOBI Conference on the Biomechanics of Impacts, Isle of Man, UK.

Hirsch, A.E. (1964), Man's response to Shock Motion, Report 1797, David Taylor Bassin Model, Washington, D.C., USA.

Horst, van der, M.J. and Leerdam, P.J.C. (2003), Preliminary results – Foot plate impact on the Complex Lower Leg caused by an AT-mine detonation, Presentation given at the 3rd NATO HFM-090/TG-25 meeting, Detroit, USA, August.

Horst, van der, M.J., Simms, C.K., Maasdam, van, R. and Leerdam, P.J.C. (2005), Occupant lower leg injury assessment in landmine detonations under a vehicle, Symposium on biomechanics of impact: from fundamental insights to applications, IUTAM, July, Dublin.

Keown, M. and Anctil, B. (2003), Review of Lower Leg Injury Criteria and Physical Surrogates, Report No. R03-15, Biokinetics and Associates Ltd., Ottawa, Canada, October.

Kuppa, S. et al. (2001a), Lower Extremity Injuries and Associated Injury Criteria, Presented at the 17<sup>th</sup> International Technical Conference on the Enhanced Safety of Vehicles in Amsterdam, The Netherlands, National Highway Traffic Safety Administration, Washington, D.C.

Kuppa, S. et al. (2001b), Lower Extremity Response and Trauma Assessment Using the THOR-Lx/HIIIr and the Denton Leg in Frontal Offset Vehicle Crashes, 17<sup>th</sup> International Technical Conference on the Enhanced Safety of Vehicles in Amsterdam, The Netherlands, National Highway Traffic Safety Administration, Washington, D.C.

Manseau, J. and Lapointe, J. (2005a), Evaluation of the Complex Lower Leg (CLL) under anti-vehicular blast landmine loading – TROSS<sup>TM</sup> trials in Germany, July 2003, DRDC Valcartier TM 2004-361.

Manseau, J. and Keown, M. (2005b), Development of an assessment methodology for lower leg injuries resulting from anti-vehicular blast landmines, IUTAM Symposium on Biomechanics of Impact: From Fundamental Insights to Applications, Dublin, 11-15 July.

Manseau, J. and Keown, M. (2005c), Evaluation of the complex lower leg (CLL) for its use in anti-vehicular mine testing applications, In Proceedings of International conference of biomechanics of impact (IRCOBI), September, Prague, Czech Republic.

Nies, O. (2005), Biomechanical Analysis of Lower Leg Surrogates – Comparison between THOR-Lx, Denton Leg and CLL, WTD 91-450 Human Factor, Ergonomics. Report No. 91-400-097/04, May 2005.

Nyquist, G. et al. (1985), Tibia Bending: Strength and Response, SAE No. 851728.

Owen, C. (2001), Requirements for the Evaluation of the Risk of Injury to the Ankle in Car Impact Tests, 17<sup>th</sup> International Technical Conference on the Enhanced Safety of Vehicles in Amsterdam, The Netherlands, National Highway Traffic Safety Administration, Washington, D.C.

RTO-TR-HFM-089 (2004), Test Methodologies for Personal Protective Equipment Against Anti-Personnel Mine Blast, Final Report of the NATO Research and Technology Organization (RTO) Human Factor and Medicine Panel (HFM) Task Group TG-024, Published March.

Schreiber, P., et al. (1997), Static and Dynamic Strength of the Leg, Proceedings of the 1997 IRCOBI Conference, Germany.

Seipel et al. (2001), Biomechanics of Calcaneal Fractures, *Clinical Orthopaedics and Related Research*, Number 338, pp. 218-224, July.

Welbourne, E.R. and Shewchenko, N. (1998), Improved Measured of Foot and Ankle Injury risk from the Hybrid III Tibia, Proceedings of the 16<sup>th</sup> International Technical Conference on the Enhanced Safety Vehicles, Paper Number 98-S7-O-11.

Williams, K., Bourget, D., Cronin, D., Bergeron, D. and Salisbury, C. (2002), Simplified Biofidelic Lower Leg Surrogate, U.S. Provisional Patent 60/406.949, August 30.

Yoganandan, N., Pintar, F.A., Boynton, M., Begeman, P., Prasad, P., Kuppa, S.M., Morgan, R.M. and Eppinger, R.H. (1996), Dynamic Axial Tolerance of the Human Foot-Ankle Complex, 962426, Society of Automotive Engineers, Warrendale, PA, USA, pp. 207-218.

Yoganandan, N., Pintar, F.A., Kumaresan, S. and Boynton, M.D. (1997), Axial Impact Biomechanics of the Human Foot-Ankle Complex, *Journal of Biomechanical Engineering*; Vol. 119, November, pp. 433-437.

Wang, J.J., Bird, R., Swinton, B. and Krstic, A. (2001), Protection of lower limbs against floor impact in army vehicles experiencing landmine explosion. *Journal of Battlefield Technology*, Vol. 4, No. 3, November 2001.

## **Annex F – SUPPLEMENTAL INFORMATION ON THORACO-LUMBAR SPINE INJURY ASSESSMENT**

### **F.1 INTRODUCTION**

The spinal column is one of the vulnerable parts of crew members in vehicular mine incidents due to different loading mechanisms in cranial (axial) direction. Most critical is a direct impact of the elastic structural deformation via the seat system to the spinal column. Furthermore the transfer of the shock wave via the structure and the seat system can cause serious injuries of the spinal region. Although pelvic injuries may also occur due to the high vertical loadings, it was assumed that thoraco-lumbar spine injuries are predominant and hence, are used as an indicator for pelvic injuries [Dosquet, 2003].

The probability of injuries due to loading mechanisms in dorso-ventral and lateral (X, Y) directions are quite low because of the predominance of axial (Z) load scenarios with a mine threat.

There is a lack of available detailed epidemiological data and PMHS data for the specific loading conditions as occur due to a mine strike under a vehicle. Therefore, test results and incidents with similar or at least comparable loading regimes were analyzed. The reader is referred to the main report (Chapter 3) for anatomy of the spinal thoraco-lumbar spine as well as for more general information on the injury assessment method.

The present annex is divided in 6 sections and focuses on the loads and tolerance levels in axial direction:

- Section F.1 – Introduction
- Section F.2 – Quasi-Static Strength
- Section F.3 – Dynamic Strength
- Section F.4 – Miscellaneous
- Section F.5 – Summary
- Section F.6 – References

### **F.2 QUASI-STATIC STRENGTH**

Already in the mid 1920s Junk gave a few values on the compressive strength of vertebrae in his *Tabulae Biologicae* [Junk, 1925 – 1963]. Since detailed data on the boundary conditions (e.g. age) were not mentioned Geertz investigated PMHS between 19 and 46 years during WW II. Geertz tested the strength of individual vertebrae and vertebral complexes by shaping two end vertebrae for a central load transmission of a tension testing machine. The specimens were observed with X-ray pictures to identify the first peak of the stress-strain curve which was determined as an indication for fracture. The strength of the individual vertebrae (Table F.1) increases in caudal direction. As already pointed out in Section 3.3, Ruff summarized the investigations of Geertz [Ruff, 1950]. The lowest tolerance level for acceleration is determined for L1 which is also validated by operational data of US Army helicopter crashes [Shanahan and Shanahan, 1979] which have similar loading directions as Geertz investigations and mine strikes under vehicles.



**Table F.1: Breaking Mass Load ( $m_F$ ) as well as Maximum and Minimum Tolerance Level for Acceleration ( $a_F$ ) [Ruff, 1950]**

	$m_F$ [kg]										$a_F$ [g]	
	age [years]											
	19	21	21	23	33	36	38	43	44	46	min	max
T8	–	640	–	540	–	600	–	–	–	–	20.8	24.9
T9	–	–	–	610	–	720	–	700	–	–	21.0	24.9
T10	–	800	–	–	660	770	–	–	730	–	21.0	25.7
T11	750	–	720	–	–	–	–	860	–	755	20.8	25.1
T12	–	900	690	–	800	–	800	–	–	–	18.6	24.5
L1	720	–	840	–	–	–	–	900	800	800	18.2	23.0
L2	–	990	–	–	800	–	830	–	–	–	19.1	23.9
L3	900	–	–	–	–	–	–	940	–	1100	20.4	25.2
L4	–	–	–	–	1100	–	900	–	950	–	19.7	24.3
L5	–	1020	–	–	–	–	–	1000	–	1200	21.2	25.7

Additionally Ruff analysed the portion of the total weight supported by the individual vertebrae and calculated the tolerance level for acceleration  $a_F$  for each vertebral body with:

$$a_F = \frac{m_F}{\varepsilon \cdot m_G} - 1$$

where  $m_F$  is the breaking mass load,  $\varepsilon$  is the portion of body weight carried by the individual vertebrae and  $m_G$  is the total body weight (75 kg). The minimum and maximum values are listed in Table F.1. The related average breaking force of L1 is 7966 N.

Sonoda [Sonoda, 1962] investigated the vertebral strength by using 22 PMHS with an age between 22 and 79 years old. These investigations are also summarized in Yamada’s Strength of Biological Material [Yamada, 1970]. Sonoda used wet isolated vertebral bodies and lined the deck plates with hard plaster to guarantee a uniform load transfer. The vertebral bodies were compressed with a tensile testing machine so that stress and strain values could be analysed. Table F.2 illustrates the breaking mass loads for specific vertebral bodies dependent on the age. Only the data which are related to an age between 20 and 39 years old are comparable to the data which were published by Ruff due to similar PMHS properties. Both data series show an increase in strength from T8 to L1, although the vertebral strength of Sonoda’s data is round about 15% lower. Furthermore the decrease of vertebral strength from L1 to L5 seems to be questionable due to the geometrical properties of the specific vertebrae and is contradictory to Ruff’s results. The general decrease in vertebral strength with increasing age is strongly correlated with the decrease of mineral density.



**Table F.2: Breaking Mass Load ( $m_F$ ) [Sonoda, 1962]**

	$m_F$ [kg]			
	age [years]			Mean value
	20 – 39	40 – 59	60 – 79	
T8	498	411	253	387
T9	567	431	263	420
T10	625	457	268	450
T11	678	486	273	479
T12	705	469	274	482
L1	755	477	291	508
L2	740	481	289	503
L3	744	484	310	513
L4	719	481	339	513
L5	691	461	311	488

Yoganandan et al investigated the compressive strength of vertebral bodies by using 38 PMHS [Yoganandan et al, 1988]. They positioned isolated vertebrae between two cylinders of a MTS (Material Testing System) device piston and compressed them uniformly to 50% of the original height. The applied load and deformation was recorded as a function of time. The first peak of the stress-strain curve was determined as an indication for fracture. Afterwards the force at failure was analysed by grouping vertebrae of the upper (T1 – T6) and lower thoracic (T7 – T12) as well as the lumbar spine (L1 – L5). The results are presented in Table F.3. The quite low values for failure forces seem to be allegeable due to variations in age of the PMHS and in the testing method. Based on the description of the specimen mounting it is possible that the primarily contact surface was reduced significantly by using a direct contact between the isolated vertebral bodies and the cylinders of the MTS device piston.

**Table F.3: Breaking Force F and Further Properties at Different Regions of the Spine [Yoganandan, 1988]**

	Force [N]	Pressure [MPa]	Deformation [mm]	Strain [%]
T1 – T6	2642 (555)	4.2 (2.7)	6.0 (1.8)	30.8 (9.0)
T7 – T12	3264 (1211)	3.2 (1.4)	4.9 (1.7)	23.4 (9.5)
L1 – L5	4590 (2061)	6.9 (3.2)	6.9 (3.2)	24.4 (9.5)

The focus of the investigations of Vesterby et al [Vesterby et al, 1991] was age-related effects on the compressive strength of the lumbar vertebrae. They compressed individual L2 vertebrae which were sawed 2 mm below the end-plates of 15 male and female PMHS with a material testing machine at a constant rate of 4.5 mm/min. The average breaking force of the vertebrae was 6289 N. The correlation of the compressive strength of the L2 vertebra with age and sex of the PMHS was significant.

Prasad et al [Prasad et al, 1974] focused on the significant weight bearing function of the articular facets during cranial acceleration based on approximately 70 runs with 4 PMHS. The axial force as well as geometrical force eccentricity was measured with a so-called intervertebral load cell between L3 and L4 and compared with the total spine load. Hence, the facet load was deduced. One conclusion of these investigations was the capability of the articular facets bearing compressive and tensile loads. Thus, the cranial load is transmitted via two paths, the vertebral bodies and the articular facets. The vertebral column is initially exposed to a compressive load. The facets tend to unload and cause a tensile load resulting in a forward flexion of head and torso. This flexion affect increasing loading on the anterior components of the vertebra by means anterior wedge fractures. These results are important for designing effective counter measures against cranial compressive loads to the vertebral column.

It is not clear if the aforementioned injury models did consider the effect of facet load during their investigations.

Furthermore Ripple and Mundie [Ripple and Mundie, 1989] proposed bending moment criteria including 1235 Nm for forward-flexion, 370 Nm for rearward-extension, 675 Nm for lateral bending. The only mentioned reference related to these values is Laananen [Laananen, 1980]. However, checking this reference does not give information on these bending moment criteria, but showed the DRIZ criterion (DRIZ is explained in main report Chapter 3, as well as in section Annex F.3). Based on engineering judgement it seemed that the momentum criteria were derived directly from the neck criteria as defined by Mertz and Patrick [Mertz and Patrick, 1967] with a factor of approximately 6.5. The background of this factor is unknown.

Chandler [Chandler, 1988] used the dynamic tolerance levels (see Annex F.3) to define a quasi-static tolerance level. He derived a quasi-static lumbar spine compression force limit of 6700 N (1,500 lb) based on a vertical (axial) DRIZ value of 19 (operational data: 9% injury risk AIS 2+; laboratory data: 20% injury risk AIS 2+) using a Hybrid II ATD with a straight spine [Chandler, 1988]. This transfer from DRIZ to force was done to overcome the general application problems of the DRIZ for development and tests of civil aircraft seat and restraint systems. Chandler stated that the DRIZ does not consider effects of restraint loads which are directly related to the stress in the thoraco-lumbar spine. Although the static compression force criterion is derived by the DRIZ, deviations between DRIZ and static compression force assessment have to be expected due to the fact that the DRIZ analysis considers the dependency of injury risks and acceleration durations. The input for a DRIZ analysis is the acceleration gradient which is directly related to durations. The input for the compression force criterion is only the maximum applied compression force value. This significant limitation has different impacts on air crashworthiness and AV mine protection applications. The impact load to seats in air crashworthiness incidents is characterized by only slight variations. Thus, the air crashworthiness standard provides only a specific standard impact impulse for tests. In opposite to this AV mine strikes provide a huge variation of impact loads due to different materials of the vehicle structure, as well as variations in the threat conditions and deploy conditions (e.g. depth of burial, soil conditions). The variation of this relatively huge number of variables results in significantly different loading regimes. Hence, the duration of the loads becomes more and more important.

The relationship between axial force and DRIZ for full scale mine trails performed in DEU and NLD was studied and compared to data from aerospace [Dosquet, 2003]. In general a quite sufficient linear relationship between DRIZ and measured force was seen. Future work should focus on updating the relationship, using more recent data from several countries.

Rapaport et al [Rapaport et al, 1997] tried to validate the force criterion evaluated by Chandler [Chandler, 1988] for military seat applications. The team used a similar procedure as Chandler and derived a force criterion based on the Eiband tolerance curve [Eiband, 1950] (see Annex F.3) and the DRIZ model by using a FAA-Hybrid III ATD on a sled platform normalized for the occupant weight. The peak acceleration of the crash pulse was varied between 10, 20 and 30 g with a 6.1, 7.6 and 9.1 m/s run each. The proposed values are 8632 N for the 5th percentile Hybrid III, 9656 N for the 50th percentile Hybrid III and 11124 N for the 95th percentile Hybrid III. However, it is not directly stated which DRIZ value is comparable with these values.

### F.3 DYNAMIC STRENGTH

The dynamic properties of the thoraco-lumbar spine are of special interest for mine protection of vehicles properties since the peak accelerations and forces as well as durations vary significantly for various threats and different vehicle structures. This section describes different injury models which take the dynamic strength into account.

The first model which considered the dependency of load tolerance limits on duration was presented by Ruff [Ruff, 1950]. He postulated a tolerance limit for durations between 5 ms and 1 s of 18 to 23 g which reflect the lower and upper limits of the investigations by Geertz for L1 (Figure F.1). The tolerance limit for durations less than 5 ms was approximated on the basis of data acquired in catapult test accidents. The seat acceleration came up to 26 g for 5 ms in these accidents. The tolerance is determined by the dynamic properties of the bones and the intervertebral disks. Hence, the decrease in acceleration is related to an increase of duration due to the fact that some distance must be obtained in a breaking process.

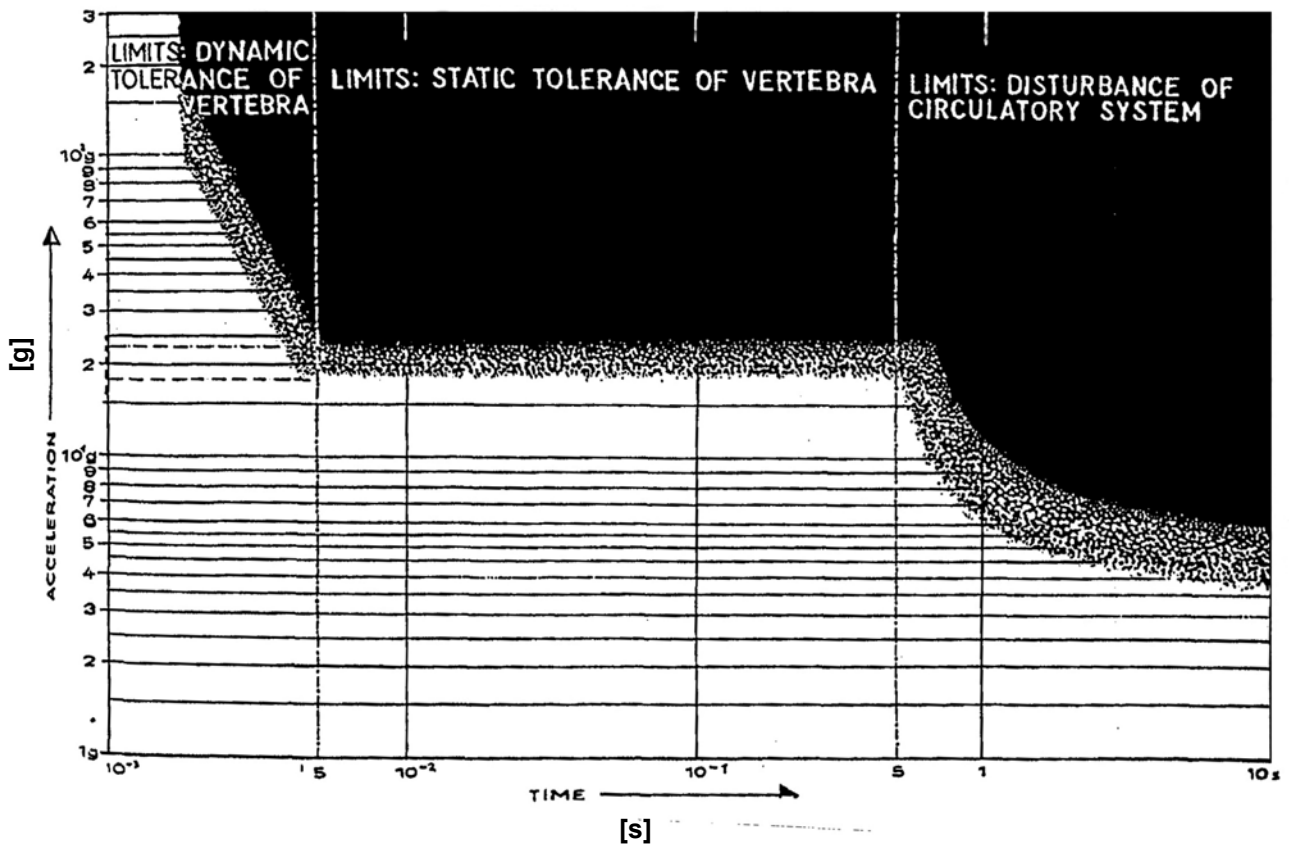
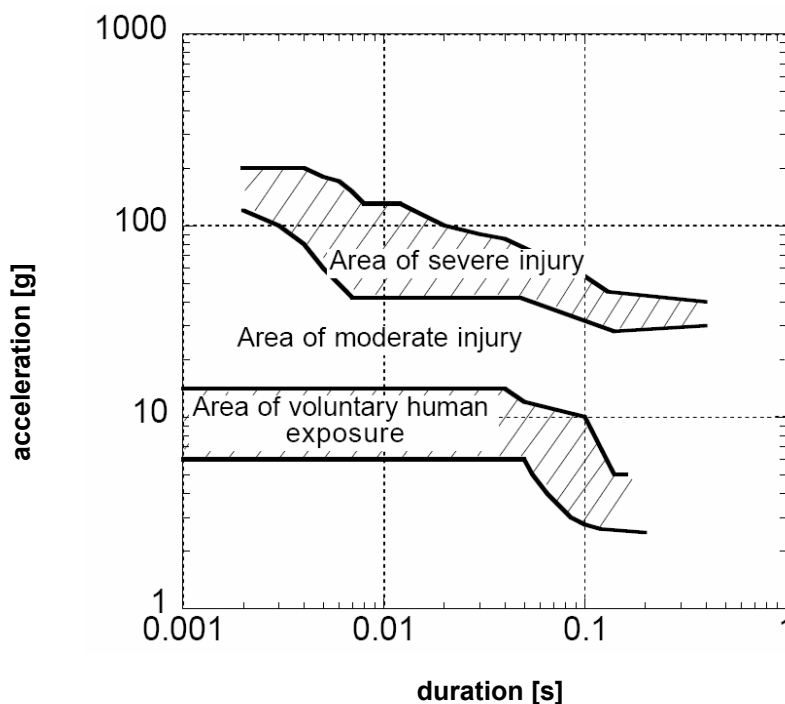


Figure F.1: Tolerance Curve for Vertebrae [Ruff, 1950].

Eiband summarized available acceleration limits related to different durations for a trapezoid pulse of ejection seat experiments in his memorandum to model the spinal strength [Eiband, 1959] (Figure F.2). Human volunteers tolerated uniform seat accelerations of 16 g for durations up to 40 ms in catapult seat experiments. The tolerance levels of human volunteers for longer durations were also confirmed in these experiments. The 110 g limit for 2 ms as well as the 42 g limit for 7 ms was established in hog (domestic pig) experiments. The animals did not suffer any permanent injury. Chimpanzees sustained 42 g for 48 ms and 28 g for 140 ms without permanent injury.



**Figure F.2: Eiband Tolerance Curve [Eiband, 1959].**

In 1964 Hirsch [Hirsch, 1964] presented a tolerance curve of seated unrestrained men in upright position to shock motion of short durations as a design guideline for the protection of ship personnel (Figure F.3). He calculated the tolerance curve on the baseline of Kornhauser's sensitivity analysis approach [Kornhauser, 1954]. Kornhauser assumed that the sensitivity analysis which is valid for inorganic structures is also applicable for animate structures. Hence, the maximum tolerable load of a single degree of freedom mechanical system is related to peak acceleration if the pulse duration is long in comparison to the natural period and to a peak velocity change if the duration is short related to the natural period. The results of Ruff were used to estimate to tolerance curve for long durations. By postulating a uniform strength of the lower vertebral bodies the appropriate load on L5 is 60% of the whole body weight. Thus, using the 1400 lb limit for vertebral strength the acceleration threshold for long durations is 15 g. The threshold will be 30 g by using the 2900 lb upper limit of Ruffs investigations (dashed line). The time when the minimum distance between rib cage and the platform of a ship shock motion simulator occurs was estimated as 40 ms derived by shock tests with volunteers. This time is taken as a quarter period of the natural frequency. Thus, the natural frequency  $f$  is about 6 Hz for a seated man. The peak velocity  $v_0$  was determined by using Kornhauser's equation with the static acceleration sensitivity  $g_0$ :

$$v_0 = 5.13 \cdot \frac{g_0}{f}$$

Hence, the peak velocity change threshold is 13 fps (~ 4 m/s) or 26 fps (~ 8 m/s, dashed line). Overall, the significant assumption in the Hirsch model causes a substantial simplification of the real biomechanical response of a seated man.

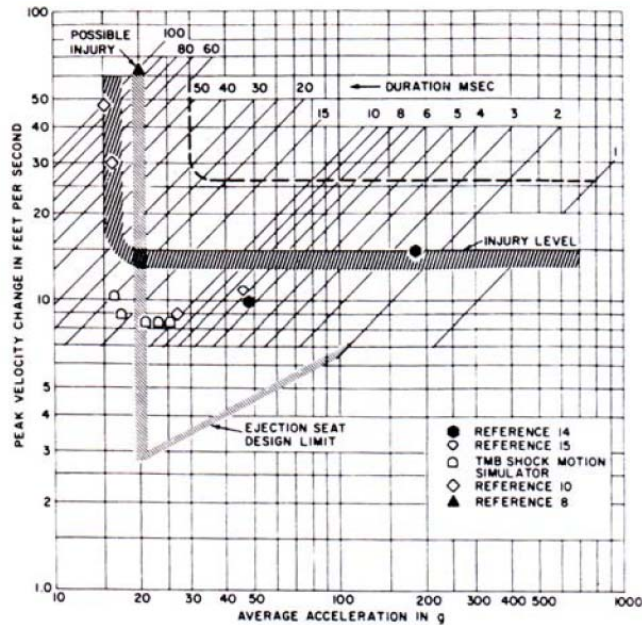


**Figure F.3: Tolerance of Seated Men to Shock Motion of Short Duration [Hirsch, 1964].**

TTCP [Tremblay et al, 1998] proposed a quasi-static value of 3800 N and a linear interpolation between 3800 N ( $t = 30$  ms) and 6673 N ( $t = 0$  ms) for vehicular mine protection applications by referencing the previous mentioned report of Ripple and Mundie [Ripple and Mundie, 1989] (Figure F.4), but the tolerance values are not described in that reference. However, these criteria seem to be derived from the Mertz criteria for neck loads [Mertz and Patrick, 1967] by using a factor of 3.4 – 3.8. This factor reflects the ratio of the geometrical contact surface area of lumbar and cervical vertebrae (~ 1550/420 mm<sup>2</sup>).

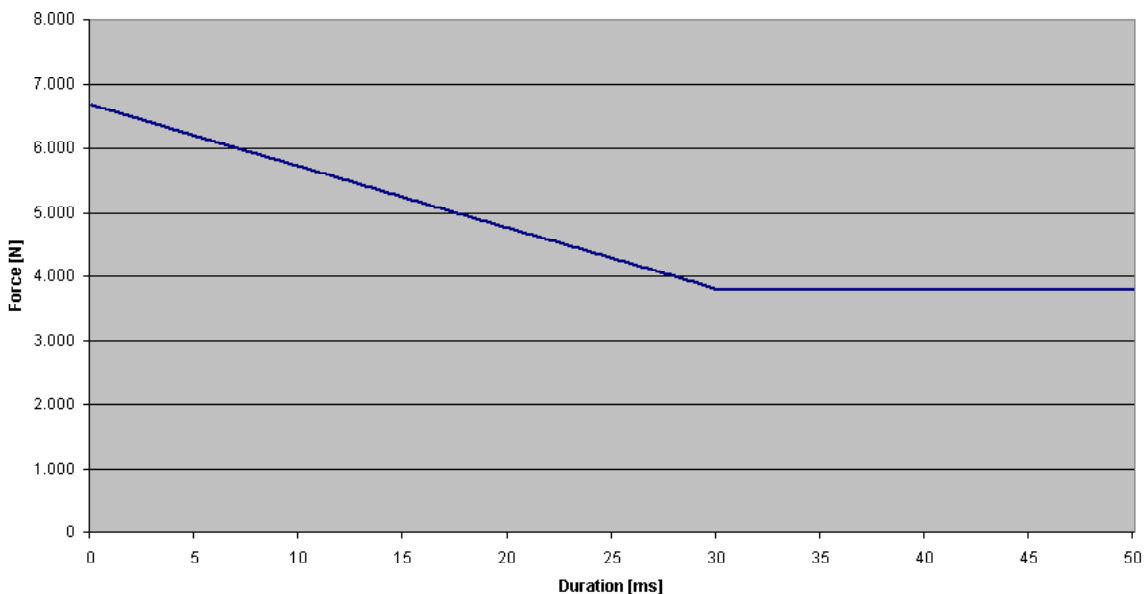


**Figure F.4: Lumbar Spine Compression Force Criterion [TTCP, 1998].**

In 1957, Latham introduced a general model to describe the impact of ejection seat to the human body [Latham, 1957]. Stech and Payne [Stech, 1969] evaluated this model as a general model to simulate the biomechanical response due to human body dynamics by using a single mass-spring-damper system (Figure F.5). The model is called: Dynamic Response Index (DRI). The DRIZ is the DRI model for the vertical direction.

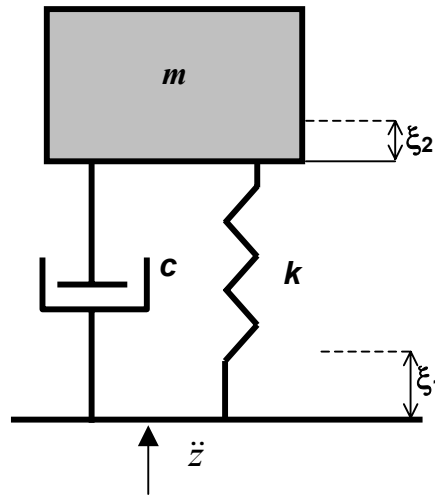


Figure F.5: DRIZ Model [Stech, 1969].

The equation of motion for this model is:

$$\ddot{z}(t) = \ddot{\delta} + 2 \cdot \zeta \cdot \omega_n \cdot \dot{\delta} + \omega_n^2 \cdot \delta$$

where

- $\ddot{z}(t)$  is the acceleration in the vertical direction measured at the position of initiation;
- $\delta$  is the relative displacement of the system with  $\delta = \xi_1 - \xi_2$ ; and  $\delta > 0 \Rightarrow$  compression;
- $\zeta$  is the damping coefficient with  $\zeta = \frac{c}{2 \cdot m \cdot \omega_n}$ ; and
- $\omega_n$  is the natural frequency with  $\omega_n = \sqrt{\frac{k}{m}}$ .

The DRIZ is calculated by the maximum relative displacement  $\delta_{\max}$ ,  $\omega_n$  and the gravity acceleration  $g$ :

$$DRIZ = \frac{\omega_n^2 \cdot \delta_{\max}}{g}$$

The first application was a dynamic model of the human body in spinal direction by Stech and Payne (vertical compression of the spinal column). They selected the values of  $\zeta$  and  $\omega_n$ , 0.224 and 52.9 rad/s respectively, as values for a representative population of Air Force pilots with a mean age of 27.9 years. These values were estimated based on investigations on compressive individual vertebral strength by Geertz [Ruff, 1950] as well as on load-deflection curves [Yorra, 1956]. Ruff [Ruff, 1950] summarized the



investigations by Geertz during WW II. The tests were made either with individual vertebrae or vertebral complexes of PMHS between 19 and 46 years of age. By using Geertz data as an indication for vertebral compression fractures, Stech and Payne related the DRIZ value to an injury risk of 50% depending on the age of the population. For an average age of 27.9 years, they calculated a DRIZ of 21.3. This value was used as a baseline to introduce the function of spinal injury risk due to compressive loads versus DRIZ values by assuming a normal distribution [Brinkley, 1970]. This function is presented in Figure F.6 as the laboratory data curve.

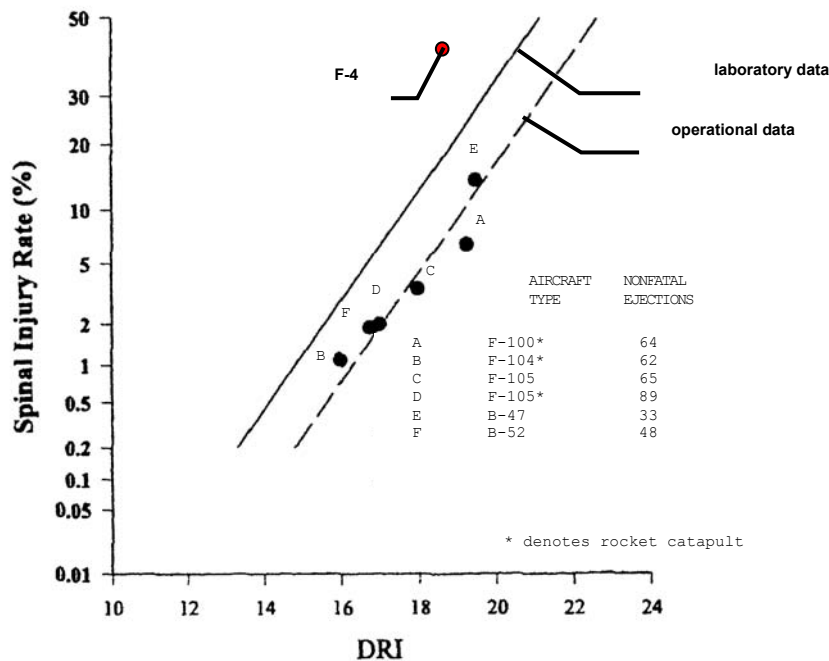


**Figure F.6: Spinal Injury Risk Calculated from Laboratory and Operational Data Supplemented with F-4 Operational Data [Brinkley, 1970] Valid for AIS 2+ Injuries.**

Furthermore, they presented the injury risk as a function of DRIZ based on operationally experienced non-fatal spinal injury probabilities, which were calculated in ejection seat tests (Figure F.6 operational curve). The relation of injury risk and DRIZ is only valid for misalignments of the ejection seat compared to the catapult acceleration vector of less than 5°. Brinkley and Shaffer stated that the seat of an F-4 aircraft did not permit the crewman vertebral column to be aligned with the catapult acceleration vector as in other Air Force ejection seats; therefore, they excluded the F-4 data. When not aware of this misalignments and just using the operational curve, a risk of 9% would be predicted for these F-4 seat. However, when looking at the real data a DRIZ of 19 related to a spinal injury probability of 34% for the F-4 seat, which is much higher. Therefore, it is assumed that for higher misalignments than 5° the tolerance levels decrease, resulting in higher injury risk at the same DRIZ value.

The physical parameter which affects fracture is always force. Using a model which is based on another physical parameter causes less accuracy. However force based injury models taking the visco-elastic properties of the vertebral column into account are not available yet.

#### **F.4 MISCELLANEOUS**

In relation to the cranio-caudal (axial) direction only a little information is available for the lateral and dorso-ventral loading direction of the thoraco-lumbar spine. However, as stated earlier [Dosquet, 2003,



2004], it is expected that the injury risks in these lateral and dorso-ventral directions are low when a vertical load is generated by a mine strike under the vehicle.

Brinkley et al [Brinkley et al, 1989] introduced a general injury-risk criterion based on the DRI values related to lateral (Y), dorso-ventral (X) and cranio-caudal (Z) loading direction. These values have to be calculated with the measurement data and the limit values  $DRI_L$  for specific injury risks (low: 0.5%, moderate: 5%, high: 50%) and the three loading directions:

$$\beta = \sqrt{\left(\frac{DR_x}{DR_{xL}}\right)^2 + \left(\frac{DR_y}{DR_{yL}}\right)^2 + \left(\frac{DR_z}{DR_{zL}}\right)^2}$$

The defined injury risk will be exceeded if  $\beta$  is greater than 1 for the related DRI limits, but this kind of analysis does not consider the different characteristics of the injury risk curves for the three loading directions. The risk curves represent different exponential functions which will have a significant impact on the quotients.

Furthermore the validation of DRI related to lateral and dorso-ventral loading directions is only rudimental. The evaluation of the DRI in dorso-ventral directions is based on tests that were not specifically designed for this purpose. Hence, there is a wide variation in experimental methods and measurements. For example, most of the time to peak acceleration values for the +X direction was between 20 to 50 ms with some data in the range between 8 and 10 ms. The data for the -X direction ranged from 25 to 160 ms. By using a half-sinewave approximation technique the natural frequency and the damping coefficient in -X direction was calculated with 62.8 rad/s and 0.2. These results were confirmed by a transfer function analysis with data from 11 impact tests without dynamic preload (54.5 rad/s and 0.26). By using data of tests with human subjects for evaluating the risk of injury levels the authors choose a conservative approach.

The most critical part of the general injury risk criterion is the calculation and validation in lateral direction. Damping coefficient and natural frequency were calculated by using only one set of data with 13 human subject tests at 8 g deceleration level, an impact velocity of 8.84 m/s and a time to peak acceleration of 22 ms. The injury risk levels were based only on existing expert opinions and available data with a poor applicability.

## **F.5 SUMMARY**

Considering relative low injury risks due to lateral and dorso-ventral loads HFM-090/TG-25 recommended an injury assessment only for the vertical (axial, z) loading direction of the thoraco-lumbar. Loads with durations less than 10 ms presuppose injury risk models which consider the dynamic behaviour of the thoraco-lumbar spine. Hence a dynamic function and not a constant value would reflect the requirements for an assessment criterion for mine related incidents. The Dynamic Response Index (DRIZ) model meets these requirements, whereas other available injury models for the thoraco-lumbar spine disregard the duration dependency or are not validated. The acceleration measurements in the pelvis of the anthropomorphic test device have to be used as input for the DRIZ. This is also the most consistent and practical way of measuring the input accelerations for the DRIZ model. Based on discussions on the risk curves available in literature, TG-25 decided to use the more conservative risk curve derived from laboratory data. When using this curve (Figure F.6) the tolerance level of 17.7 for DRIZ refers to a 10% risk of AIS 2+ injuries.

## **F.6 REFERENCES**

- Brinkley, J.W. and Shaffer, J.T. (1970), Dynamic Simulation Techniques for the Design of Escape Systems: Current Applications and Future Air Force Requirements, Symposium on Biodynamic Models and their Applications, Report No. AMRL-TR-71-29, Aerospace Medical Research Laboratory, Wright-Patterson Air Force Base, Ohio, USA.
- Brinkley, James W., Specker, Lawrence J. and Mosher, Stephen E. (1989), “Development of Acceleration Exposure Limits for Advanced Escape Systems”, in Implications of Advanced Escape Technologies for Air and Spacecraft Escape; AGARD Conference Proceedings 472, pp. 1.1 – 1.14
- Chandler, Richard F. (1988), “Human Injury Criteria Relative to Civil Aircraft Seat and Restraint Systems”, 851847, Society of Automotive Engineers, Warrendale, PA, USA.
- Dosquet, F. (2003), Thoracolumbar Spine and Pelvis Criteria for Vehicular Mine Protection, NATO-RTO-HFM-090, 3<sup>rd</sup> Meeting, TARDEC, Warren, USA.
- Dosquet, Frank. (2004), Analysis of Thoracolumbar Spine and Pelvis Criteria for Vehicular Mine Protection, NATO-RTO-HFM-090, 4<sup>th</sup> Meeting, WTD 91, Meppen, Germany.
- Eiband, A. Martin. (1959), “Human Tolerance to Rapidly Applied Acceleration”, NASA Memorandum 5-19-59E, National Aeronautics and Space Administration, Washington, USA.
- Federal Aviation Administration (Ed.) (1993), “Airworthiness Standards: Transport Category Airplanes”, Federal Aviation Regulation (FAR 25), Aeronautics and Space (Title 14), Code of Federal Regulations.
- Federal Aviation Administration (Ed.) (1990), “Airworthiness Standards: Transport Category Rotorcraft”, Federal Aviation Regulation (FAR 29), Aeronautics and Space (Title 14), Code of Federal Regulations, 1990.
- Hirsch, Arthur E. “Man’s Response to Shock Motions”, Report 1797, David Taylor Model Basin, Structural Mechanics Laboratory, Washington, D.C., USA, 1964.
- Junk, W. (Ed.) (1925 – 1963), “Tabulae Biologicae”, Gravenhage.
- Kornhauser, M. (1954), “Prediction and Evaluation of Sensitivity to Transient Accelerations”, Journal of Applied Mechanics, Vol. 21, pp. 371-380.
- Laananen, D.H. (1980), “Aircraft Crash Survival Design Guide, Volume II – Aircraft Crash Environment and Human Tolerance”, USARTL-TR-79-22B, Simula Inc., Tempe, AZ, USA.
- Latham, F. (1957), A Study in Body Ballistics, Seat Ejection, Proceedings of the Royal Society of London, Series B – Biologic Sciences, Vol. 147, pp. 121-139.
- Mertz, H.J., Jr. and Patrick, L.M. (1967), “Investigation of the Kinematics and Kinetics of Whiplash”, 670919, Society of Automotive Engineers, Warrendale, PA, USA.
- Prasad, P., King, A.I. and Ewing, C.L. (1974), “The Role of Articular Facets During +G<sub>z</sub> Acceleration”, Journal of Applied Mechanics, June 1974, pp. 321-326.
- Rapaport, Martin, Forster, Estrella, Schoenbeck, Ann and Domzalski, Leon. (1997), “Establishing a Spinal Injury Criterion for Military Seats”, Proceedings SAFE 35th Annual Symposium, pp. 156-165.

Ripple, Gary R. and Mundie, Thomas G. (1989), “Medical Evaluation of Nonfragment Injury Effects in Armored Vehicle Live Fire Tests”, AD-A233 058, Walter Reed Army Institute of Research (WRAIR), Washington, D.C., USA.

Ruff, Siegfried. (1950), “Brief Acceleration: Less than One Second”, German Aviation Medicine in World War II, Vol. I, Chapter VI-C, Department of the Air Force.

Shanahan, Dennis F. and Shanahan, Maureen O. (1989), Injury in U.S. Army Helicopter Crashes October 1979 – September 1985, *Journal of Trauma*, Vol. 29, No. 4.

Sonoda, Takeji. (1962), “Studies on the Strength for Compression, Tension and Torsion of the Human Vertebral Column”, *J. Kyoto Pref. Med. University*, Vol. 71, pp. 659-702.

Stech, E.L. and Payne, P.R. (1969), *Dynamic Models of the Human Body*, Aerospace Medical Research Laboratory, Wright Patterson Air Force Base, Ohio, USA.

The Technical Cooperation Program (TTCP). (1998), *Protection of Soft-Skinned Vehicle Occupants from Landmine Effects*, Edited by Tremblay, J., Bergeron, D.M., Gonzalez, R. TTCP, WPN/TP-1, KTA 1-29, Technical Report, August 1998.

Vesterby, A., Modekilde, L., Gundersen, H.J., Melsen, F., Modekilde, L., Holme, K. and Soerensen, S. “Biologically Meaningful Determinants of the in Vitro Strength of Lumbar Vertebrae”, *Bone*, Volume 12, Issue 3, pp. 219-24, 1991.

Yamada, Hiroshi. (1970), “Strength of Biological Materials”, The Williams & Wilkins Company, Baltimore, USA.

Yoganandan, Narayan, Pintar, Frank, Sances, Anthony Jr., Maiman, Dennis, Myklebust, Joel, Harris, Gerlad and Ray, Gautam. (1988), “Biomechanical Investigations to the Human Thoracolumbar Spine”, 881331, Society of Automotive Engineers, Warrendale, PA, USA.

Yorra, A.J. (1956), *The Investigation of the Structural Behavior of the Intervertebral Discs*, Masters Thesis, Massachusetts Institute of Technology. Yu, J.H.-Y., Vassel, E.J. and Stuhmiller, J.H. (1990), *Modelling of the non-auditory response to blast overpressure: Design of a blast overpressure test module – Final report*, Fredrick, Md., U.S. Army Medical Research and Development Command, Fort Detrick.

## Annex G – SUPPLEMENTAL INFORMATION ON NECK INJURY ASSESSMENT

### G.1 INTRODUCTION

This annex gives general information on neck injuries and injury criteria in support to injury assessment for AV mine testing, and is divided in the 8 following sections:

- Section G.1 – Introduction
- Section G.2 – Neck Injuries
- Section G.3 – Axial Compression Injury Criterion
- Section G.4 – Flexion/Extension Injury Criterion
- Section G.5 – The Neck Injury Criterion ( $N_{ij}$ )
- Section G.6 – Other Neck Injury Criteria
- Section G.7 – Summary
- Section G.8 – References

### G.2 NECK INJURIES

Predicting typical AV mine neck injuries is difficult since the nature and the severity of these injuries will depend on a number of factors. The next paragraphs describe some neck injuries which may occur during AV mine strike. For more information on neck injuries, the reader may be referred to [McElhaney et al. 2002] and [Pike, 2002].

Trauma to the cervical spine has been divided into three main categories [Pike, 2002]:

- 1) Osseous (bone) injury;
- 2) Neurological injury; and
- 3) Soft tissue injury.

**Osseous injury** refers to vertebral fractures. The severity level of these fractures will depend on: whether or not the fracture resulted in impingement of the neurological structures, and whether or not the fracture is structurally stable. Axial compressive loading of the erect vertebral column produces a characteristic fracture called *compression or burst fracture* (see Figure G.1) and can occur from C1 through C5 [Pike, 2002]. Burst fracture fragments can also penetrate further into the spinal canal causing life-threatening complications [McElhaney et al. 2002]. The most serious burst fracture is the one of the atlas (C1) commonly called *Jefferson fracture* [Pikes, 2002]. Fatalities and instabilities arising from the *Jefferson fracture* are common and extremely serious. *Wedge compression fracture* (see Figure G.1) is a result of a combination of a flexion bending moment and compressive load resulting in a failure of the anterior of the vertebral body [McElhaney et al. 2002]. Compression-extension loadings produce *posterior elements fractures* of the cervical spine and they may occur throughout the upper and lower parts. They also occur in conjunction with burst fracture and are frequently multiple. They may also be associated with neurological deficit as a result of impingement of the spinal cord by bony or ligament fragments [McElhaney et al. 2002].

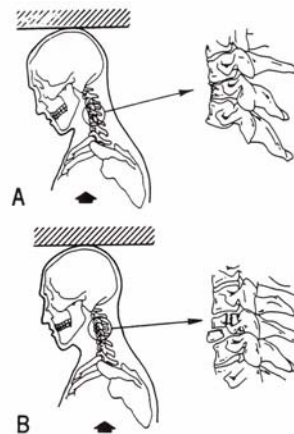


**Figure G.1: Illustration of Wedge Fractures (A) and Burst Fracture (B) (from [McElhaney et al. 2002]).**

**Neurological injury** is the most severe class of neck injuries, which may result in paralysis, long-term pain and even death. They generally are the result of primary osseous or soft tissue injuries [Pike, 2002].

**Soft tissue injury** is the most common type of neck injury in vehicular crash environment. For example, **neck sprain**, in which the ligaments are stretched beyond their normal limits, is a result of flexion-extension (also called ‘whiplash’). Ligamentous injuries are usually minor, but when severe, they can impart severe neurological impairment [Pike, 2002].

### **G.3 AXIAL COMPRESSION INJURY CRITERION**

Mertz et al. undertook a study to develop axial compression neck injury tolerance curves. Impact tests of a spring-loaded tackling block on football helmets [Mertz, 1978] were conducted with a 50<sup>th</sup> percentile male Hybrid III and then compared them to real accidents of high school aged football players. One player (17 years old, 1.88 m, 101 kg) suffered immediate paralysis of the arms and legs and X-rays showed fractures of C3, C4 and C5. A second 17 year old player (1.82 m, 95 kg) suffered fatal injuries including hemorrhages in the brain stem and pons (white matter nerve fibers) and subarachnoid blood (area of brain containing cerebrospinal fluid, cushioning brain from mechanical shock). In a third incident, a high school player was allegedly struck and rendered quadriplegic by the same tackling block used in Mertz’s experiments.

In the tests, the Hybrid III was oriented so that the load was applied to the top of the head, loading the neck structure in compression with minimal head rotation (appropriate figure of the test set-up was not available). The configuration was chosen to produce the maximum value of neck compression force for the impact velocity chosen. The neck compression load measured by the Hybrid III was considered representative of the upper bound of maximum axial compressive load that an equivalent weight human would have experienced for the same impact velocity.

Based on this study, Mertz [Mertz, 1978] derived two injury tolerance curves based on the upper neck axial compression force measured on a 50<sup>th</sup> percentile male Hybrid III (see Figure G.2). The coordinates of the ‘Upper’ curve are 0 ms and 6670 N, 35 ms and 1110 N, and greater than 35 ms, 1110 N. The coordinates of the ‘Lower’ curve are 0 ms and 4000 N, 30 ms and 1110 N, and greater than 30 ms, 1110 N. To evaluate neck load signal, pairs of points (force, duration) are plotted on the graph (shown in Figure G.2) with the two injury assessment curves. The points are connected together by a series of straight lines. If any of the line segments lie above the upper curve (red), the neck axial compression force

is considered to have the potential to produce serious neck injury. If any of the line segments lie above the lower curve (blue), the potential for neck injury from the axial compressive force is considered less likely. If none of the line exceeds the lower curve, the probability of neck injury from axial compressive force is considered remote.

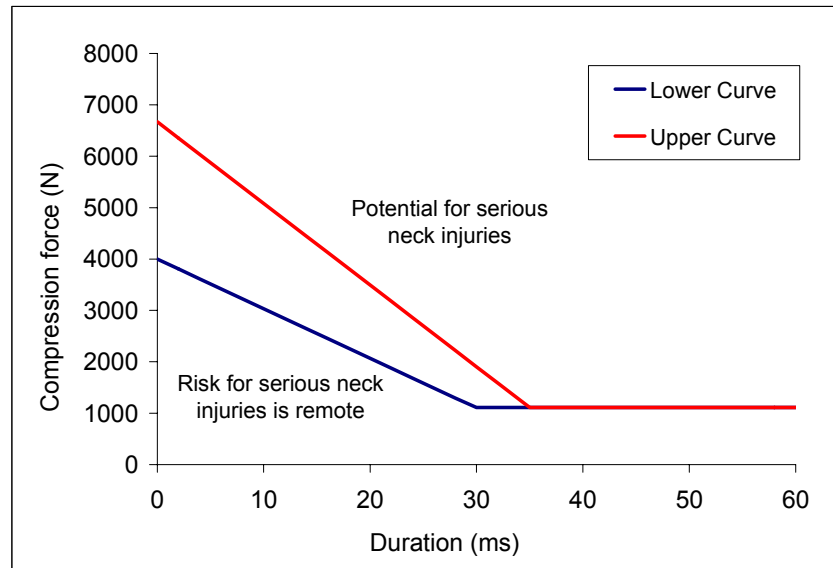


**Figure G.2: Injury Tolerance Curves for Axial Neck Compression Force when Using a Hybrid III 50<sup>th</sup> Percentile Male ATD [Mertz, 1978].**

These levels were proposed for an adult population that was considerably older (exact age range not known) and much less conditioned than a high school football athlete. The time durations were determined from the loading times observed during the experiment, which were on the order of 30-40 ms.

#### **G.4 FLEXION/EXTENSION INJURY CRITERIA**

Mertz and Patrick [Mertz, 1971] as well as Patrick and Chou [Patrick, 1976] conducted tests on volunteers and PMHSs to determine neck reaction on the head under dynamic conditions. Human volunteers were subjected to static and dynamic tests to produce non-injurious response for neck flexion and extension. PMHSs were used to extend the data into the injury region. Their analysis of the data indicated that equivalent moment at the occipital condyles (protusions on the back of the skull which articulate with the cervical vertebra) was the critical injury parameter in flexion (forward) and extension (backward).

The dynamic tests were conducted with one human volunteer and four PMHS. The subjects were restrained in a rigid chair mounted on an impact sled (appropriate figure of the test set-up was not available). The sled was accelerated pneumatically over a distance of 2 meters to a prescribed velocity. A headrest was used to maintain the head in the upright position. After reaching the prescribed velocity the sled was stopped with a hydraulic cylinder, which produced a repeatable stroke. The occupant was restrained with a lap belt and two shoulder harnesses, which crisscrossed at the sternum. The human volunteer was subjected to 46 sled runs of various degrees of severity for four configurations of head weight. The subject attempted to achieve two different degrees of muscle tenseness, relaxed and tensed. With muscles tensed the volunteer was subjected to sled decelerations of 1.9-6.8 g. With weight placed above the center of mass of the head the volunteer was subjected to a 9.6 g deceleration. This particular run resulted in neck and back pain that lasted several days. The PMHS were similarly fixed so as to obtain comparisons of responses to the same sled deceleration pulses for the various configurations and head



weights, and then subjected to more severe conditions. A total of 132 PMHS runs were completed using four subjects.

The volunteer withstood a static flexion moment about his occipital condyles of 35 Nm. This was without contribution from chin contact to the chest. A dynamic tolerance level for the flexion moment about the occipital condyles for the initiation of pain occurred with the maximum equivalent resisting moment of 59 Nm. The maximum dynamic flexion moment generated by the volunteer was measured to be 88 Nm. This level produced a sharp pain in the neck and upper back region with soreness persisting for several days. It was considered non-injurious, but close to the injury threshold. The PMHS were exposed to much greater decelerations. Based on the PMHS data, it was observed that the 50<sup>th</sup> percentile human could withstand equivalent flexion moments of 190 Nm without suffering ligamentous injury (AIS 1 or 2) or bone injury (AIS 2 to 6). However, it is expected that muscle injuries (AIS 1) would occur at a lower value of the flexion moment. Based on these results Mertz [Mertz, 1978] proposed an injury tolerance level of 190 Nm for neck flexion moments measured with a 50<sup>th</sup> percentile male Hybrid III. Similarly from the aforementioned study, corridors for extension were proposed with an injury tolerance level of 57 Nm [Mertz, 1978]. This level was associated with ligamentous damage (AIS 1 or 2), to a PMHS.

## **G.5 THE NECK INJURY CRITERION ( $N_{ij}$ )**

The  $N_{ij}$  (Neck Injury Criterion) was developed to assess performance of frontal airbags during car crashes. The idea of the  $N_{ij}$  came from studies of [Mertz and Weber, 1982] and [Prasad et Daniel, 1984], which lead to the conclusion that linear combination of tensile loads and extension could form the basis for an injury prediction function [Shewchenko, 2001]. This was expanded to include flexion and compression resulting if the four following terms (later referred to  $N_{ij}$ ):

- 1)  $N_{te}$  (for tension/extension);
- 2)  $N_{tf}$  (for tension/flexion);
- 3)  $N_{ce}$  (for compression/extension); and
- 4)  $N_{cf}$  (for compression/flexion).

The  $N_{ij}$  is calculated as follows:

$$N_{ij} = \frac{F_z}{F_{z_c}} + \frac{M_y}{M_{y_c}}$$

where:

- $F_z$  is the tension or compression force;
- $F_{z_c}$  is the critical value for tension or compression;
- $M_y$  is the extension or flexion bending moment; and
- $M_{y_c}$  is the critical value for extension or flexion.

The  $N_{ij}$  calculation then consists in four calculations for the different loading modes ( $N_{te}$ ,  $N_{tf}$ ,  $N_{ce}$  and  $N_{cf}$ ) and the maximum of these values gives the  $N_{ij}$  response. Eppinger et al., 2000 proposed  $N_{ij}$  injury risk equations illustrated in Figure G.3.



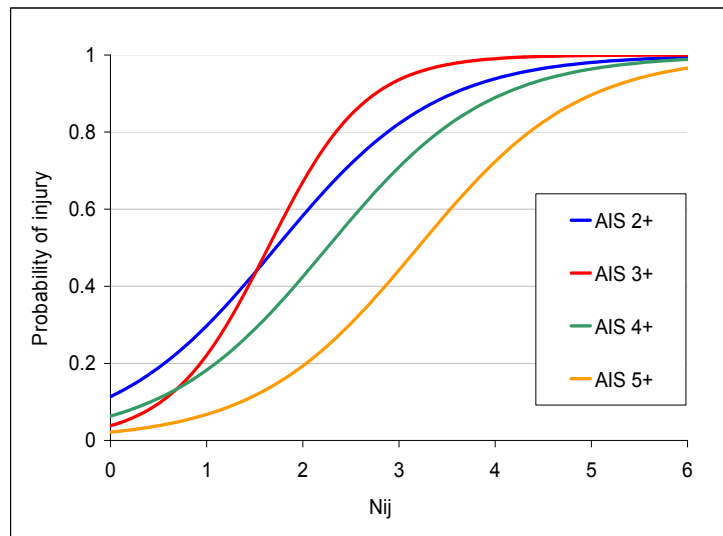


Figure G.3: N<sub>ij</sub> Risk Curves (Proposed by [Eppinger et al., 2000]).

These curves are applicable to various dummy sizes to which different critical values are associated. The following critical values are used for the 50<sup>th</sup> percentile male Hybrid III [CFR 49, 2003]:

$$Fz_c \text{ (for tension)} = 6860 \text{ N}$$

$$Fz_c \text{ (for compression)} = -6160 \text{ N}$$

$$My_c \text{ (for extension)} = -310 \text{ N.m}$$

$$My_c \text{ (for flexion)} = 135 \text{ N.m}$$

The AIS 2+ risk curve presented in Figure G.3 indicates a risk of 11.4% when the N<sub>ij</sub> is zero, which is physically not possible. All other curves also suggest a risk greater than zero when the N<sub>ij</sub> is zero, giving a low confidence in the validity of the curves for low risk value. The N<sub>ij</sub> was primarily based on the results of paired swine and 3-years-old dummy tests, in which they were mainly subjected to tension-extension loadings [Shewchenko, 2001]. The type of loading for which the N<sub>ij</sub> was developed (tension) was not representative of those seen in AV mine situations, where the neck is mainly loaded by axial compression. Also, the N<sub>ij</sub> was first developed for the child dummy and then extrapolated for adult dummies, which introduced other uncertainties in the model. Given the different uncertainties about the N<sub>ij</sub> mentioned above, the HFM-090/TG-25 decided not to use this model and considered each of the loading mechanisms (compression, flexion, extension) separately.

## G.6 OTHER NECK INJURY CRITERIA

[Mertz, 1984] proposed injury tolerance curves, similar to the ones for compression, for neck tension and shear loads and are presented in Figures G.4 and G.5. For shear force, the coordinates of the curve are 0 ms and 3100 N, 25 to 35 ms and 1500 N, and greater than 35 ms, 1110 N. For tension, the coordinates of the curve are 0 ms and 3300 N, 35 ms and 2900 N, and greater than 45 ms, 1110 N. Following the same approach given in Section G.3, if any of the line segments lie above the curve, the neck shear/tension force is considered to have the potential to produce **serious neck injury**. If no line segment lies above the curve, then neck injury caused by shear/tension is considered unlikely.

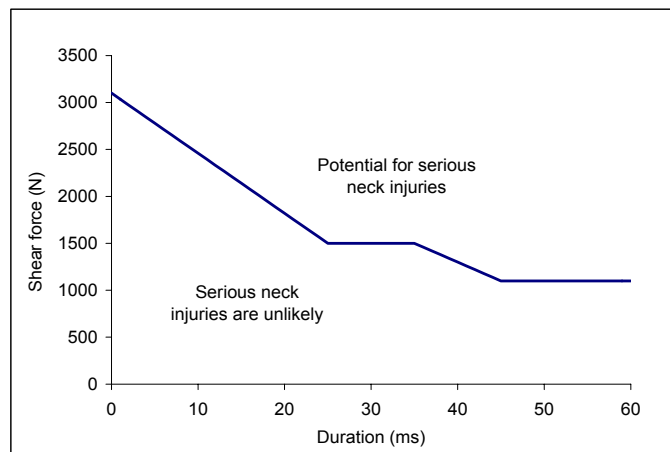


**Figure G.4: Neck Shear Injury Tolerance Curve for the 50<sup>th</sup> Percentile Male Hybrid III (Proposed by [Mertz, 1984]).**

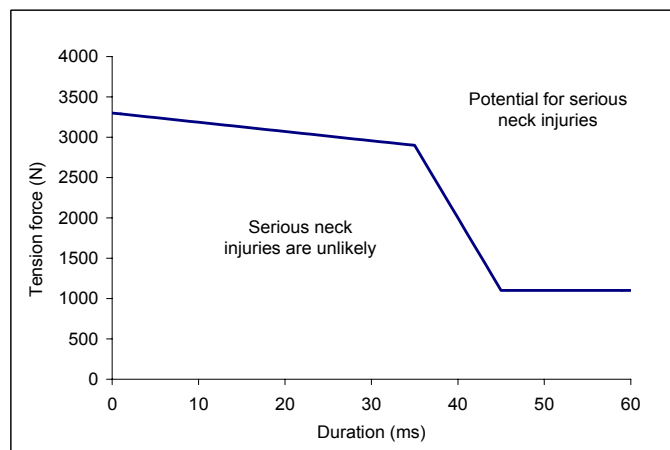


**Figure G.5: Neck Tension Injury Tolerance Curve for the 50<sup>th</sup> Percentile Male Hybrid III (Proposed by [Mertz, 1984]).**

Lateral bending injury tolerance levels were studied in automotive [Patrick and Chou, 1976; Koshiro et al., 2005] and aviation [Soltis et al., 2003] fields with PMHS and human volunteer, as well as with numerical human models. However, no appropriate injury assessment method for AV mine was found for this specific loading regime at this point.

## **G.7 SUMMARY**

The neck injury assessment method proposed in this report includes tolerance levels developed by Mertz and Patrick [Mertz, 1971], Patrick and Chou [Patrick, 1976] and Mertz [Mertz, 1971] for axial compression, flexion and extension. Each of the injury mechanisms is evaluated separately as opposed to what suggests the well known Nij model [Eppinger et al., 2000], which considers combined loading modes on the neck. After evaluation of the Nij model, it appeared that it was not suitable for the current application, in which axial compression is the major loading mode. Since neck injuries may be very severe and life-threatening, it is recommended to extend assessment if appropriate methods exist. Tolerance curves for shear and tension are available [Mertz, 1984] and lateral bending injury assessment is currently being studied for aviation applications [Soltis, 2003].

Although the Hybrid III neck is the most widely used and accepted dummy neck, it possesses major limitations in terms of biofidelity and anthropometry [Shewchenko, 2001]. Some concerns were expressed by the automotive industry regarding the assessment of flexion/extension injuries [Shewchenko, 2001]. As opposed to the axial compression tolerance level, flexion/extension tolerance levels are based on human cadavers and/or volunteers responses, and not the Hybrid III neck response. Since the direct correlation between human and Hybrid III neck response is actually unknown, the accuracy of flexion/extension responses may be questionable. Automotive industry has addressed neck biofidelity improvements with the development of the THOR, however the Hybrid III dummy still remain the standard for car crash testing.

## **G.8 REFERENCES**

CFR 49 (2003), Code of Federal Rules (CFR), Title 49-Transportation. Chapter V – National Highway Traffic Safety Administration (NHTSA), Department of Transportation, Part 571, Federal Motor Vehicle Safety Standard (FMVSS) 208.

McElhaney, J.H., Nightingale, R.W., Winkelstein, V.C.C. and Myers, B.S. (2002), Biomechanical Aspects of Cervical Trauma, In: *Accidental Injury – Biomechanics and Prevention*, Second Edition, Edited by Nahum A.M. and Melvin J.W., Springer-Verlag, New York, 2002.

Mertz, H.J. and Weber, D.A. (1982), Interpretation of the Impact Responses of a 3-Year-Old Child Dummy Relative to Child Injury Potential, Proceedings of the Ninth International Technical Conference on Experimental Safety Vehicles, November 1-4, pp. 368.

Mertz, H.J. (1984), Injury Assessment Values Used to Evaluate Hybrid III Response Measurements, NHTSA Docket 74-14, Notice 32, Enclosure 2 of Attachment I of Part III of General Motors Submission USG 2284, March 22, 1984.

Ono, K., Ejima, S., Kaneoka, K., Fukushima, M., Yamada, S., Ujihashi, S. and Compigne, S. (2005), Biomechanical Response of Head/Neck/Torso to Lateral Impact Loading on Shoulders of Male and Female Volunteers, In: *Proceeding of the 2005 IRCOBI conference*, held in Prague, Czech Republic, 21-23 September, 2005.

Patrick, L.M. and Chou, C.C. (1976), Response of the Human Neck in Flexion, Extension and Lateral Flexion, Vehicle Research Institute Report No. VRI-7.3, Society of Automotive Engineers, Inc.

Prasad, P. and Daniel, R.P. (1984), A biomechanical Analysis of Head, Neck and Torso Injuries to Child Surrogates Due to Sudden Torso Acceleration, Proceedings of the 20<sup>th</sup> Stapp Car Crash Conference, SAE publication P-152, SAE paper no. 841656, p. 25.

Pike, J.A. (2002), Neck Injury – The Use of X-Rays, CTs, and MRI to Study Crash-Related Injury Mechanisms, Society of Automotive Engineers, Inc., Warrendale, PA, USA.

Shewchenko, N. (2001), Review of Neck Injury Criteria in the March 2000 SSNRPM. Biokinetics and Associates, Ltd. Ontario, Canada, Report R01-06, September 2001.

Soltis, S.J., Frings, G., Gowdy, R.V., DeWeese, R., Hoof, van der, J., Meijer, R. and Yang, K.H. (2003), Development of Side Impact Neck Injury Criteria and Tolerances for Occupants of Sideward Facing Aircraft Seats, Presented at the joint RTO AVT/HFM Specialist Meeting, held in Koblenz, Germany, 19-23 May, 2003.



## **Annex H – SUPPLEMENTAL INFORMATION ON OVERPRESSURE INJURY ASSESSMENT**

### **H.1 INTRODUCTION**

Overpressure caused by blast waves can generate life-threatening injuries to non-auditory internal organs/systems and incapacitating (but non life-threatening) auditory injuries. This annex presents background information on the overpressure as well as on the injury assessment for blast overpressure effects.

It should be noted that in case of a mine detonation under a vehicle the risk of high overpressure effects inside the vehicle is small when the vehicle integrity is secured. Although the ears are the most vulnerable body part to blast overpressure, ear injuries have an AIS score of only 1, even when they result in permanent hearing loss. Besides, the risk of permanent auditory injuries can be minimized when proper ear protection is worn. Because of these two reasons HFM-090/TG-25 decided that auditory injury assessment is not a mandatory criterion for the STANAG 4569. The reader is referred to [e.g. Chan, 2001; MIL-STD-1474D, 1997; Richmond, 1992; NATO, 2003; Dancer, 1995] for more background on auditory injury assessment.

The present annex is divided into five sections:

- Section H.1 – Introduction
- Section H.2 – Overpressure
- Section H.3 – Non-Auditory Injury Assessment
- Section H.4 – Conclusion
- Section H.5 – References

### **H.2 OVERPRESSURE**

When an explosive charge detonates, the detonation products will expand and a shock wave will be generated. Figure H.1 shows an example of in a free-field environment. The shock wave is characterized by an instant rise of the pressure, from ambient pressure to peak pressure. After the pressure has reached his peak, it will decay to ambient pressure. Figure H.1 is a typical pressure-time curve for a high explosive (HE). In general, the shock wave will decrease when the distance to the explosive charge increases.

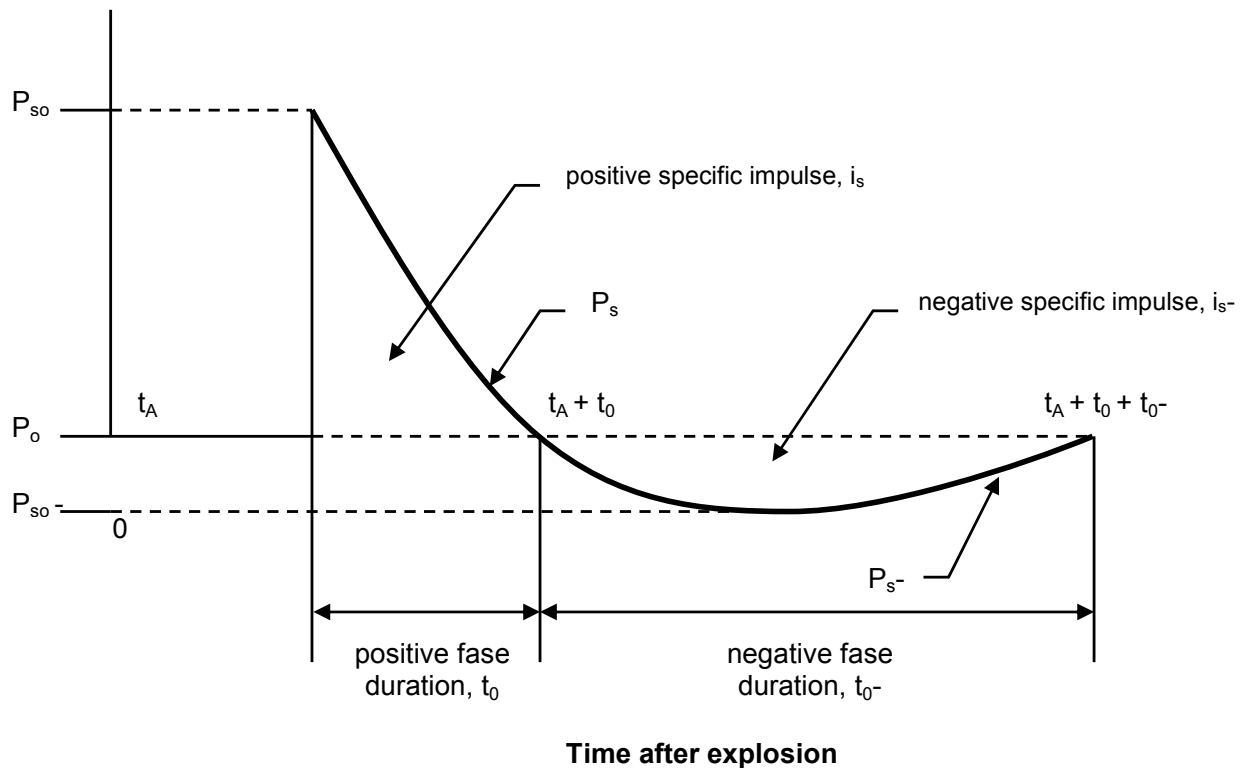


**Figure H.1: Typical Pressure-Time Curve for a High Explosive (Free Field).**

When the shock wave interacts with an object, reflection waves will be generated. The reflected pressure is higher than the incident pressure.

When the overpressure enters a vehicle a complex wave pattern can be generated when the overpressure interacts with the walls. Figure H.2 shows a more complex overpressure pattern.

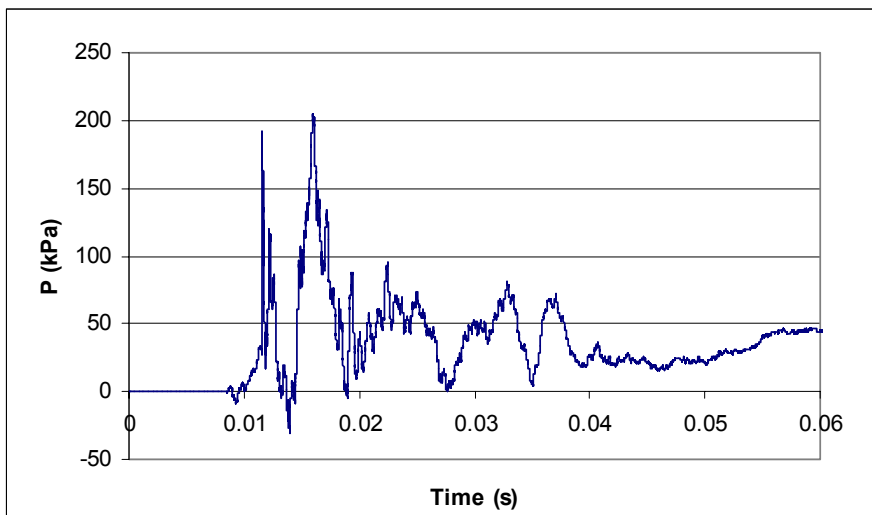


**Figure H.2: Example of Complex Overpressure Pattern inside a Vehicle Subjected to a Blast Mine.**

### H.3 NON AUDITORY INJURY ASSESSMENT

Three different injury assessment models are described here

- 1) Bowen;
- 2) Stuhmiller; and
- 3) Axelsson.

Bowen, Stuhmiller and Axelsson derived their injury models based on animal test data, mainly with sheep. The models of Bowen and Stuhmiller are focused on lung injury, while the injury model of Axelsson includes injury to all vulnerable internal organs/systems.

#### H.3.1 Bowen Model

Bowen derived three curves to predict lethality and lung damage due to free field overpressure (Friedlander wave) [Bowen and Richmond, 1968]. These three curves are derived based on the orientation of the person, see Figure H.3:

- A) Long axis of the body parallel to blast wind (person is only loaded with side-on pressure);
- B) Long axis of the body perpendicular to blast wind (person is loaded with side-on pressure and dynamic pressure); and
- C) Person near a reflected surface (person is loaded with reflected pressure).

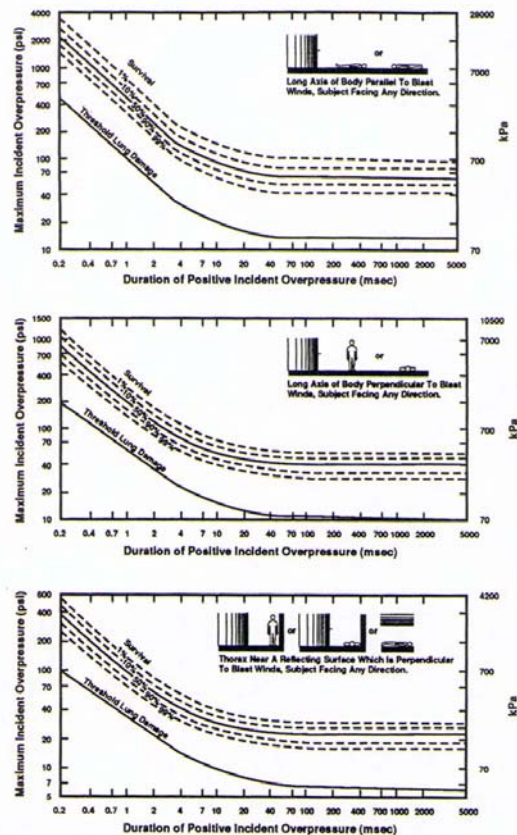


Figure H.3: Survival Curves Predicted for a 70-kg Man, Applicable to a Free-Stream Situation for Different Body Orientations with Respect to the Blast Winds [Richmond and Jenssen, 1992].



These curves were derived for a 70 kg man and in all three curves the incident pressure has to be implemented to predict the survivability. The threshold for lung damage and the survivability curves have lower values for the incident overpressure when a person stands for a reflecting object compared to a person standing in the free field. It should be noted that the survivability curves are based on the survivability of the animals 24 hours after the exposure to the blast. Based on [Richmond, 2004], the lung damage threshold refers to ‘pin head’ damage to the lungs having no physiological effects. The Bowen curves were recently reviewed [Bass, 2006].

The main limitation of the Bowen curves is that they were developed for ideal shock waves whereas complex waves are expected in a vehicle subjected to a mine. The two following models (Stuhmiller and Axelsson) presented were developed for complex waves.

### **H.3.2 Stuhmiller Model**

The lung has initially been identified as the most critical major organ for incapacitation when injured by blast overpressure. Therefore, work was conducted to understand the mechanical properties of lung materials. Stuhmiller et al. has developed a mathematical model of the chest wall dynamics and the subsequent generation of strong pressure waves within the lung, which have been hypothesized as the mediator of injury [Stuhmiller, 1996]. This pleural dynamics model considers the forces on the chest wall due to the blast load, the internal pressure arising from the bulk compression of the lung, and the compression wave generated by the chest motion.

Since the lung behaves as a compressible material, the derivation of Landau and Lifhitz (1959) can be used, which relates the pressure wave in a compressible gas to the motion of a piston.

$$p(t) = p_0 * \left( 1 + \frac{1}{2} (\gamma - 1) \frac{v}{c_0} \right)^{\frac{2\gamma}{\gamma-1}} \quad (1)$$

where:

- p is the pressure
- $p_0$  is the pressure in the undisturbed lung
- $\rho_0$  is the density in the undisturbed lung
- $c_0$  is the speed of sound in undisturbed lung
- v is the velocity of the piston
- $\gamma$  is the ratio of specific heats

If the piston velocity is very small compared with the speed of sound, then the equation can be expanded to give the linear form

$$p(t) \cong p_0 + \rho_0 c_0 v \quad (2)$$

where the adiabatic relation has been used

$$c_0^2 = \gamma \frac{p_0}{\rho_0} \quad (3)$$

If Newton’s law is applied to the local thorax surface, imagining that the chest wall and lung form a rectangular region, the following equation of motion is obtained.

$$m \frac{dv}{dt} = P_{load}(t) - p_0 \left( 1 + \frac{1}{2}(\gamma - 1) \frac{v}{c_0} \right)^{\frac{2\gamma}{\gamma - 1}} - \frac{p_0 L}{L - x} \quad (4)$$

where

v is the velocity

x is the displacement

m is the mass/chest wall area

L is the ratio of the volume of the lung/chest wall area

If the velocity and displacement are small, the equation can be linearized to the form

$$m \frac{dv}{dt} = P_{load}(t) - \rho c_0 v - p_0 \frac{x}{L} \quad (5)$$

Finally, the normalized work,  $W^*$ , defined as total work done to produce the wave divided by the volume of the lung and the ambient pressure, can be computed using the velocity found from the equation (7).

$$W^* = \frac{W}{p_0 V} = \frac{1}{p_0 L} \int_0^{\infty} \rho_0 c_0 v^2 dt \quad (6)$$

Injury is caused by a local excess strain of the tissue, whose details are not described by this model. A correlation of gross pathology, however, may be related to the average energy dissipated in the lung tissue, that is, the normalized work. Normalized, irreversible work done on the lung by the motion of the chest wall has proven to be an excellent correlate of pathology and lethality seen in animal tests [Stuhmiller, 1997]. This method stands for lung injuries due to complex and free field overpressure.

A two dimensional finite element (FE) model was constructed by Stuhmiller et al. that captured the geometric arrangement of four distinct parts: skeletal muscle, rib, lung, and a water filled organ such as the heart [Stuhmiller, 1988]. The results of the FE-model were compared with test data and showed good results.

To assist the process of making health hazards assessments, Stuhmiller has developed a computer program, INJURY [MOMRP, 2004]. The software computes the normalized work from each loading and the total lung injury can be predicted. Figure H.4 shows the layout of the program. The required input is the blast loading, specie, body mass, the number of shots, atmospheric pressure, start and end time. The output of the calculation is the probability of lung injury. There are five injury levels defined; severe, moderate, slight, trace and none.



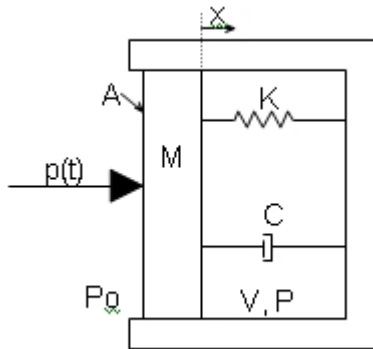
**Figure H.4: Example of INJURY Program [MOMRP, 2004].**

Unfortunately, there is not much information available on how the blast is related to the probability of lung injury.

### **H.3.3 Axelsson Model**

The objective of Axelsson was to understand the effects of complex blast waves on the human body in order to find a simple tool for vulnerability assessment. The model developed by Axelsson is based on experiments performed by Yelverton [Yelverton, 1993], in which 255 sheep and an instrumented cylinder were exposed to complex blast waves in enclosures. The instrumented cylinder (Blast Test Device) was placed where the sheep were positioned. The cylinder was an aluminium tubular test module approximating the size of a sheep. The cylinder was instrumented with four pressure gauges recording the blast loading coming from four different directions. Axelsson used data of 177 of the 255 sheep submitted to complex blast waves in Yelverton study in order to develop a transfer function between injury severity and blast loading recorded on the cylinder.

A mathematical model of the thorax was developed to predict injury severity as a function of the loading recorded by the cylinder submitted by complex blast waves in different enclosures. A mathematical model of a two-chamber spring-mass system (two lungs) was initially developed by Bowen (1965) and Fletcher (1970). The model was then simplified to a single chamber one-lung model (shown in Figure H.5) assuming that the blast load,  $p(t)$ , is acting simultaneously on both lungs.



A is the effective area;  
M is the effective mass;  
V is the initial gaseous volume of the lungs;  
x is the displacement;  
C is the damper coefficient;  
K is the spring constant;  
P<sub>o</sub> is the ambient pressure;  
p(t) is the overpressure over the time; and  
γ is the polytropic exponent for gas in lungs.

**Figure H.5: Single-Chamber One-Lung Model [Axelsson, 1996].**

The model is a single degree of freedom system in which chest wall response (displacement, velocity and acceleration) and intra-thoracic (lung) pressure can be calculated for different complex blast waves and ideal blast waves as well. The equation for the model is the following:

$$M \cdot \frac{d^2x}{dt^2} + C \cdot \frac{dx}{dt} + K \cdot x = A \cdot \left[ p(t) + P_o - \left( \frac{V}{V - A \cdot x} \right)^\gamma \cdot P_o \right] \quad (7)$$

with the model parameters given in Table H.1.

**Table H.1: Model Parameters for a 70 kg Mammal [Axelsson, 1996]**

Parameter	Units	70 kg body*
M	kg	2.03
C	Ns/m	696
K	N/m	989
A	m <sup>2</sup>	0.082
V	m <sup>3</sup>	0.00182
γ	-	1.2

\* For mammal of different body weight, scaling factors can be used as described in [Axelsson, 1996].

The input to the mathematical model is the external overpressure p(t), measured at the four locations (front, back and sides) on the cylinder. The displacement x(t) is then obtained and the maximal chest wall velocity can be determined for the four gauges located on the cylinder (v<sub>1</sub>, v<sub>2</sub>, v<sub>3</sub>, v<sub>4</sub>). The average velocity V is then calculated [V = 0.25 \* (max v<sub>1</sub> + max v<sub>2</sub> + max v<sub>3</sub> + max v<sub>4</sub>)] and is used to determine the injury severity expressed by the ASII (Adjusted Injury of Severity Index). The ASII includes injury to the lungs, upper respiratory tract, gastrointestinal tract and solid intra-abdominal organs and was developed by Yelverton, 1993. The ASII, with its 95% confidence levels, can be expressed as follows:

$$ASII = (0.124 + 0.117 \cdot V)^{2.63} \quad (8)$$

The ASII levels are associated with the velocity V or Chest Wall Velocity Predictor (CWVP).

The following tables (H.2-H.5) present the estimated AIS levels associated with the different ‘injury levels’ defined by Axelsson and Yelverton for the blast overpressure injuries to the lungs, pharynx, larynx and trachea, gastrointestinal tract and solid abdominal organs. In Table H.6 a summary is given of the relation between ASII, CWVP and AIS levels.

**Table H.2: Injury Levels and Associated AIS Levels for the Lungs**

<b>Injury Level</b>	<b>Description or Signification</b>	<b>AIS Level</b>
Negative	No injury.	0
Trace	Scattered surface petechiation or minimal ecchymoses involving less than 10% of the organ.	3
Slight	Areas of extensive petechiation to scattered parenchymal hepatization involving less than 30% of the organ.	3 – 4
Moderate	Areas of hemorrhage ranging from isolated parenchymal contusions to confluent hepatization involving less than 30% of the lungs.	3 – 4
Extensive	Isolated parenchymal contusions and confluent hepatized regions encompassing areas equal to or greater than 30% of the organ.	4 – 5

**Table H.3: Injury Levels and Associated AIS Levels for the Pharynx, Larynx and Trachea**

<b>Level</b>	<b>Injury Description</b>	<b>AIS Level</b>
Negative	No injury.	0
Trace	Scattered surface petechiation to isolated spots of ecchymosis less than one layer deep covering less than 10% of the organ.	2
Slight	Scattered petechiation to confluent contusions one to two layers deep involving less than 30% of the organ.	2 – 3
Moderate	Lesions ranging from ecchymotic spots to confluent contusions two layers deep, encompassing less than 60% of the available surface area.	3 – 4
Extensive	Areas of confluent contusions two or more layers deep, covering 60% or more of the organ.	5

**Table H.4: Injury Levels and Associated AIS Levels for the Gastrointestinal Tract (Gas-Filled Organs)**

Level	Injury Description	AIS Level
Negative	No injury.	0
Trace	Minor contusions with intact mucosa with no more than two gut layers or two organs involved with the contusions distributed over an area of less than 10 cm <sup>2</sup> .	2 – 3
Slight	Scattered contusions generally distributed over an area of 10-20 cm <sup>2</sup> with some mucosal ulcerations.	4
Moderate	Multiple transmural contusions with mucosal ulcerations encompassing an area of 21-30 cm <sup>2</sup> .	3 – 4
Extensive	Areas of more than 30 cm <sup>2</sup> of transmural contusions with concomitant perforation of the gut wall.	4 – 5

**Table H.5: Injury Levels and Associated AIS Levels for the Solid Abdominal Organs**

Level	Injury Description	AIS Level
Negative	No injury.	0
Trace	Small subcapsular contusions of hematomas involving less than 10% of one or two organs.	1
Slight	Subcapsular contusions or hematomas involving less than 30% of one or more organs with slight tears in the organ possible.	2
Moderate	Deep tears in the liver and/or maceration of the spleen with up to 60% of the organ damaged.	3 – 4
Extensive	Deep tears in the liver, maceration of the spleen or both with more than 60% of the organ traumatized.	4 – 5

See Table H.6 for a summary on the injury levels:

**Table H.6: Injury Levels with Corresponding ASII and CWVP and Estimated AIS Levels**

Injury Level	ASII (-)	V (m/s)	AIS Ranges*
Negative (no injury)	0.0 – 0.2	0.0 – 3.6	0
Trace to slight	0.2 – 1.0	3.6 – 7.5	1 to 4
Slight to moderate	0.3 – 1.9	4.3 – 9.8	2 to 4
Moderate to extensive	1.0 – 7.1	7.5 – 16.9	3 to 5
> 50% lethality	> 3.6	> 12.8	Up to 6

Considering that AIS 4 injuries might occur when the CWVP values is between 3.6 and 7.5 m/s (injury level: trace to slight), the acceptable CWVP tolerance value for the pass/fail test was set to 3.6 m/s. Based on the summary given in Table H.6, this value is believed to represent a very low risk of AIS 2 injuries, which is in accordance with the guideline of 10% risk of AIS 2+. However, it should be mentioned that when the blast loading on a body is known, the CWVP and corresponding injuries can be calculated, but that the risk of this type of injury is still unknown. Statistical studies on the injury data are needed to define risk curves.

## **H.4 SUMMARY**

A summary of the available models for non auditory injury assessment is shown in Table H.7.

**Table H.7: Injury Models for Non Auditory Injury Assessment**

<b>Model</b>	<b>Applicable to Ideal Waves</b>	<b>Applicable to Complex Waves</b>	<b>Organs Taken into Consideration</b>
Bowen	Yes	No	Lungs
Stumiller	Yes	Yes	Lungs
Axelsson	Yes	Yes	All internal organs

In conclusion, the Axelsson & Yelverton model is the best available model for non-auditory blast injury assessment occurring during an AV blast mine strike. Considering that there are no risk curves available, it was decided to use a conservative approach and take the no injury level (3.6 m/s) as the limit for the chest wall velocity predictor.

Although it is known that the auditory system is the most vulnerable body region to blast overpressure, no pass/fail criterion has been proposed, because it is assumed that the crew will wear proper hearing protection. This will minimize the risk on temporary and permanent hearing injuries (both AIS 1 injuries). Besides it should be noted that when the vehicle integrity is guaranteed during a mine strike, the overpressure in the vehicle should be low, resulting into low injury risks for the non-auditory organs.

## **H.5 REFERENCES**

- Absil, L.H.J. et al. (2001), Collegedictaat: Pyrotechniek en Beschermingsconstructies, TNO-PML 2001-A27.
- Axelsson, H. and Yelverton, J.T. (1996), Chest Wall Velocity as a Predictor of Nonauditory Blast Injury in a Complex Wave Environment, The journal of trauma, Vol. 40, No 3.
- Bass, C. et al. (2006), Pulmonary Injury Risk Assessment for Short-Duration Blasts, In Proceedings of the Personal Armour Systems Symposium (PASS), Leeds, United Kingdom, September 20-22, 2006.
- Bowen, I.G., Fletcher, E.R. and Richmond, D.R. (1968), Estimate of man’s tolerance to the direct effects of air blast. Headquarters Defense Atomic Support Agency, Washington D.C.
- Dancer, A.L. and Franke, R. (1995), Hearing hazard from impulse noise: a comparative study of twp classical criteria for weapon noises (Pfander Criterion and Smoorenburg criterion) and the LAeq8 method, Acta Acustica, 3, 539-547.



Mayorga, M.A. (1997), The pathology of primary blast overpressure injury, Walter Reed Army Institute of Research, Washington D.C., USA.

Mayorga, M.A. (2005a), A review of thermobaric weapon development, deployment and research, Blast injury consulting service, Maryland, USA.

Mayorga, M.A. (2005b), Primary blast effects to biological systems (presentation), Walter Reed Army Medical Center, Washington D.C., USA.

Military Operational Medicine Research Program (MOMRP) (2004), INJURY8.1. [www.momrp.org](http://www.momrp.org)

NATO (2003), Reconsideration of the effects of impulse noise RTO Technical report TR-017 AC/323 (HFM-022) TP/17.

Richmond, D.R. (2004), Personal communications.

Richmond, D.R. and Jenssen, A. (1992), Compendium on the biological effects of complex blast waves, Oslo Mil/Akershus N-0015, Oslo 1, Norway.

Stuhmiller, J.H., Chuong, C.J., Phillips, Y.Y. and Dodd, K.T. (1988), Computer modeling of thoracic response to blast, The journal of trauma, Volume 28.

Stuhmiller, J.H., Ho, K.H.H., Vander Vorst, M.J., Dodd, K.T., Fitzpatrick, T. and Mayorga, M. (1996), A model of blast overpressure injury to the lung, Biomechanics, Volume 29, No. 2.

Stuhmiller, J.H. (1997), Biological response to blast overpressure: A summary of modeling, Toxicology, 121.

Yelverton, J.T. (1993), Blast overpressure studies with animals and man: Final report – Biological response to complex blast waves, U.S. Army Medical Research and Development Command, Fort Detrick.



## **Annex I – TEST PROTOCOL FOR OCCUPANT SAFETY MEASUREMENTS AND INJURY ASSESSMENT**

### **I.1 DESCRIPTION OF THE TEST SET-UP**

#### **I.1.1 Instrumentation for Injury Assessment**

In order to qualify vehicles according to STANAG 4569 for mine tests (level 1 to 4), the following measurement tools **are required** for injury assessment:

- At least 1 instrumented Hybrid III 50<sup>th</sup> percentile male anthropomorphic test device (ATD).
- At least 2 pressure measurement devices.

A description and instruction of these tools are given in the paragraphs below.

The following tools **are strongly recommended** to include in the qualification tests to get more information on injury mechanisms and to have some redundancy:

- Sensors (displacement, acceleration, force) on seat and foot rest systems, vehicle structure and belts.
- Video cameras, both normal speed and high-speed (approximately 1000 frames per second) inside the vehicle.

These tools are not described in this document.

#### **I.1.2 Description of the Anthropomorphic Test Device (ATD) Measurement**

The following topics will be described in separate sections:

- Type of ATD;
- Instrumentation;
- Coordinate System;
- Certification and Calibration; and
- Boundary Conditions.

##### **I.1.2.1 Type of Anthropomorphic Test Device**

The standard Hybrid III 50<sup>th</sup> percentile male ATD (also called crash test dummy) has to be used to measure the human body biomechanical response in case of a mine detonation under a vehicle. The ATD is a regulated test device in the USA Code of Federal Regulations [CFR, 2003] for frontal car crash tests. This regulation refers to a General Motors drawing package identified by GM Drawing no. 78051-218, revision U, title “Hybrid III Anthropomorphic Test Device”, date August 30, 1998. In Figure I.1 a picture is given of the ATD inside a military vehicle.



**Figure I.1: Examples of Hybrid III ATD in Test Vehicle.**

In the case of a standing position, a conversion kit (e.g. 78051-281-PED-KIT of First Technology Safety Systems) can be installed on the standard sitting Hybrid III to make the standing posture possible.

The standard Hybrid III ATD comes with non-instrumented tibias (part of the lower legs). For mine vehicle qualification tests, both non-instrumented tibias have to be replaced by instrumented tibias called Denton leg [Denton, 1984]. The instrumented tibias need to be equipped with a lower tibia load cell that records the axial force ( $F_z$ ). Depending on additional desired instrumentation, different models of the lower tibia load cells and also upper tibia load cells can be included (Denton, 2002. Drawing Number B-3500-D).

The 50<sup>th</sup> %-tile ATD represents the average male of an USA-population between 1970s and 1980s with the following figures:

- Length (standing position): 1.72 m;
- Weight: 78 kg; and
- Erect sitting height: 0.88 m.

#### **I.1.2.2 Instrumentation of the ATD**

At least the following sensors need to be adapted to the ATD:

- Lower Tibia Load Cell in right and left leg: axial force ( $F_z$ );
- Pelvis Accelerometer: vertical acceleration ( $A_z$ ); and
- Upper Neck Load Cell: shear force ( $F_x$ ), axial force ( $F_z$ ) and flexion/extension moment ( $M_y$ ).

In Figure I.2 the position of these sensors is given.

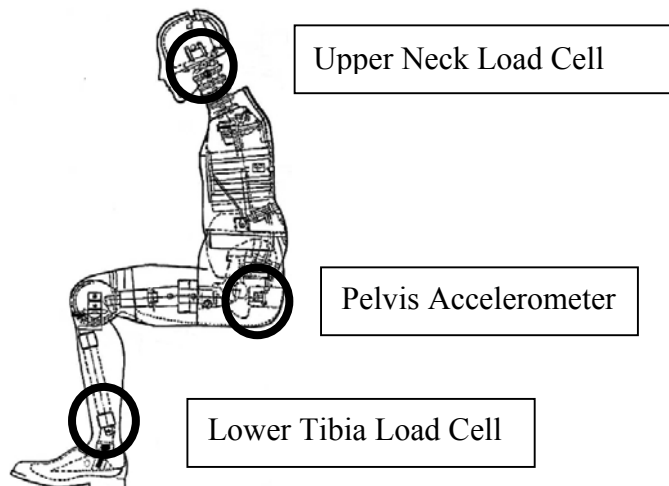


**Figure I.2: Hybrid III ATD with Sensor Positions.**

It is recommended to extend the instrumentation with:

- Five-axis load cell in the lower tibia of both legs (Fx, Fy, Fz, Mx, My);
- Five-axis load cell in the upper tibia of both legs (Fx, Fy, Fz, Mx, My);
- Tri-axial accelerometers on the mid tibia shaft in both lower legs (Ax, Ay, Az);
- One-axis load cell (shear force) in both femurs (Fx);
- Tri-axial accelerometers in pelvis, thorax and head: (Ax, Ay, Az);
- Five-axis load cell in the lumbar spine (Fx, Fz, My or Fx, Fy, Fz, Mx, My); and
- Six-axis load cell in the upper neck (Fx, Fy, Fz, Mx, My, Mz).

Note: The tri-axial accelerometers on the mid tibia shaft is not a standard option in the instrumented Denton leg model for the Hybrid III ATD.

### **I.1.2.3 Coordinate System**

The standard coordinate system as described in SAE J211/1 [SAE, 2003] has to be used. In Figure I.3 this coordinate system is presented for the sitting and standing man. The coordinate systems are local body coordinates and follow the orientation of that specific body part. For the upper leg (femur) the z-axis is along the longitudinal axis of the femur; so it is rotated over 90° for the sitting posture (not shown in Figure I.3).

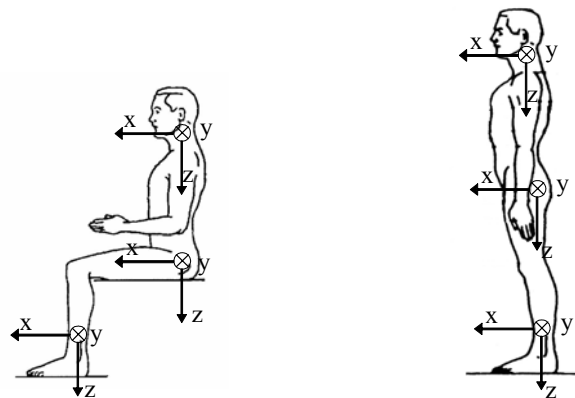


**Figure I.3: ATD Local Body Coordinate System.**

For the positive direction of the moments around the axis the ‘right-hand-rule’ should be followed for the body part **below** the sensor. A positive moment around the y-axis ( $M_y$ ) means a forward bending. The positive polarities of the sensors and the method to check these directions are listed in the SAE J211/1. They are summarised in Table I.1 for the required measurement positions.

**Table I.1: Positive Polarities for the Channels at the Required Measurement Positions**

Sensor	Measurement	ATD Body Part Motion	Polarity
Upper neck load cell	$F_x$	Head rearward, chest forward	+
	$F_y$	Head leftward, chest rightward	+
	$F_z$	Head upward, chest downward	+
	$M_x$	Left ear to left shoulder	+
	$M_y$	Chin toward chest (forward bending)	+
	$M_z$	Chin toward left shoulder	+
Pelvis accelerometers	$A_x$	Pelvis accelerates forward	+
	$A_y$	Pelvis accelerates to the right	+
	$A_z$	Pelvis accelerates downward	+
Lower tibia load cell	$F_x$	Foot forward, knee rearward	+
	$F_y$	Foot rightward, knee leftward	+
	$F_z$	Foot downward, knee upward	+
	$M_x$	Foot leftward, knee in place	+
	$M_y$	Foot toward knee	+

#### **I.1.2.4 Certification and Calibration**

The ATD consists of a steel skeleton and rubber elements and is surrounded by rubber and foam material to simulate the skin and flesh. The characteristics, like stiffness and damping, have influence on the

internal loads in case of impact or loading transfer. Therefore, the characteristics should meet specific requirements, which are verified in a certification test.

The sensors inside the ATD are mechanical devices which translate the load into an electrical signal. The signal is being recorded by the data-acquisition system which has to be provided with information about the sensitivity of that particular sensor. Each sensor has to be calibrated to give the relation between load and signal amplitude. Due to repetitive loadings, overloads or aging of the mechanical sensor, re-calibration is necessary on a regular base. For certification and calibration, refer the ATD user's manual [SAE, 1998].

It is advised that the ATD will be certified and the sensors be calibrated at least each two years. This advice is based on several years of experience with the use of the ATD in the Vehicle Mine Protection research area and valid for 'normal usage'. This means: 15 to 20 tests, loads within the ranges of the sensors, no structural damage to the ATD and the storage of the ATD in a dark room and at a constant temperature of about 20° C.

In case of an overload of a sensor, re-calibration of this sensor is mandatory.

### **I.1.2.5 Boundary Conditions**

The stiffness of the joints in the ATD has to be settled by hand ("one G suspended setting") conform instructions on ATD handling (see the users' manual [SAE, 1998]). After each test, the stiffness settings in the ATD have to be checked.

Because of the temperature influence on the characteristics of the rubber elements and the skin of the ATD, a constant temperature between 20 and 22° C on the test site is preferred (according to crash test regulations). However, in general tests sites are out-side locations and temperature can hardly be controlled. A temperature of 10° to 30° C inside the vehicle is advised. In winter time, a heater inside the vehicle could prevent too cold conditions and reduce moisture.

### **I.1.3 Hybrid III Positioning**

For positioning the Hybrid III inside the vehicle, the following aspects are important:

- Position in the vehicle;
- Seating posture; and
- Clothing.

#### **I.1.3.1 Position in the Vehicle**

The ATD has to be placed at one of the original crew positions inside the tested vehicle. This should be the 'worst-case' position: the position that is expected by the 'National Authority' to give the highest loads inside the ATD for a particular detonation position under the vehicle.

#### **I.1.3.2 Seating Posture**

The seating posture of the ATD should be realistic and representative for a person with the same sizes as the 50<sup>th</sup> percentile ATD sitting in an upright position. The straight seating posture should be achieved by placing the pelvis well in the seat cushion and the back of the ATD in contact with the seat back cushion (when available).



It should be mentioned that for some seating systems an upright position is not possible for a human. For these cases the most realistic position need to be checked by a volunteer (preferably with the same sizes as the 50th percentile ATD) and mimicked with the ATD.

The feet have to be placed in the same way as for a real sitting or standing person. When footrests are available and part of the protection measures, they have to be used. In case of a driver, the right leg should be on the accelerator pedal and the left one on the resting position. For both legs a realistic body posture has to be achieved. By considering this general requirement the lower leg longitudinal axis should be as good as possible perpendicular to the foot plate to provide a worst-case set-up (see Figure I.4).

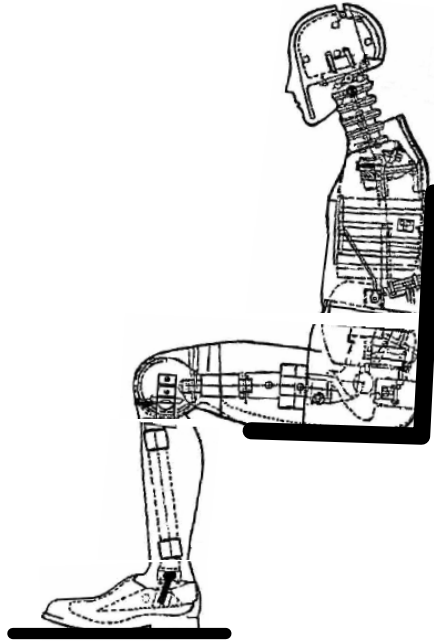


**Figure I.4: Straight Seating Posture.**

The hands and arms should be placed in a realistic position. In case of steering wheel or joy sticks, the hands should grip these devices, else the hand should be placed in a resting position on the upper leg. The hands should not be fixed to the steering wheel or legs, but tape can be used to keep the hands in position prior to the test.

The seat has to be adjusted according to the size and weight of a 50<sup>th</sup> percentile man. If different seat positions are possible for different functions and scenarios (e.g. combat vs. driving under homologation conditions in peace keeping operations) the worst-case position of the seat has to be tested. In case of the usage of periscopes or other vision tools, the seat has to be adjusted in such a way that the eye-level of the ATD corresponds to these vision systems.

All available protective measures, like seat belts and head rests should be used and installed correctly.

When seat belts are available, they have to be used in the original way. Remove slack in the belts and tightened them as realistic as possible. In case of a belt retractor, allow it to retract the belt to remove slack.

In case of repetitive tests or similar tests at other proving grounds, the same seating posture of the ATD should be kept.

### I.1.3.3 Clothing

The clothing of the ATD should correspond to that of a real crew member or passenger of the tested vehicle. For filming purposes, the uniform can be replaced by an overall with a clear visible colour (contrast with background).

The footwear (shoes or boots) should be the same as normally used by the real personnel of that type of vehicle and the footwear should be in good condition, without any damages. For soldiers, combat boots are recommended. Also the use of socks is recommended.

When the occupants wear personnel protective equipment (helmets, vests, etc.) in normal operational conditions, the ATD should wear the same equipment.

### I.1.4 Description of the Pressure Measurement Devices

Inside the vehicle the pressure has to be measured to analyse the effects on the gas filled internal organs in the thorax and abdomen. The Chest Wall Velocity (CWV) model is used to assess injury to these organs. As input for this model the reflected overpressure on the thorax has to be measured.

The overpressure inside the vehicle is caused by the shock wave, which is formed by the mine detonation. Due to reflections a complex blast wave environment exists and the directions of the blast waves could not be predicted. It is assumed that the overpressure on the chest is a dominant factor for injuries to the gas filled organs.

The overpressure could also cause temporary or permanent auditory injuries. This will not be assessed, because the HFM-090/TG-25 stated that hearing protection systems, such as ear plugs or earmuffs, can easily prevent this type of injuries. Therefore, no mandatory criterion on auditory injuries is included.

At least two positions for pressure measurements are mandated:

- One on the chest of the Hybrid III ATD.
- One on a second Hybrid III ATD (when available) or at the crew location where the highest overpressure loads are expected.

To measure the reflected pressure it is important to have a correct simulation of the body (= reflected area) and appropriate transducer fixed on this device. The chest of the Hybrid III ATD represents the body dimensions and thus is proposed as mount of a pressure transducer.

For blast overpressure it is hardly possible to define a worst-case location and the position of the ATD is not always the worst-case position for both the mechanical and the pressure loads. Therefore, at least a second location for pressure measurements is advised. This second location should be on an occupant position also.

#### I.1.4.1 Pressure Measurement Device on the Chest of the ATD

It is **recommended** to use a flat measurement device strapped on the chest of the ATD as shown in Figure I.5. The ATD is dressed and the device must be fastened on the outside of the clothes. The device should consist of a plate with a flat transducer fixed in or on this plate (see Figure I.6). To avoid inertia problems for the ATD response the device should be as light as possible. It is recommended to use hard plastic materials for the mount.

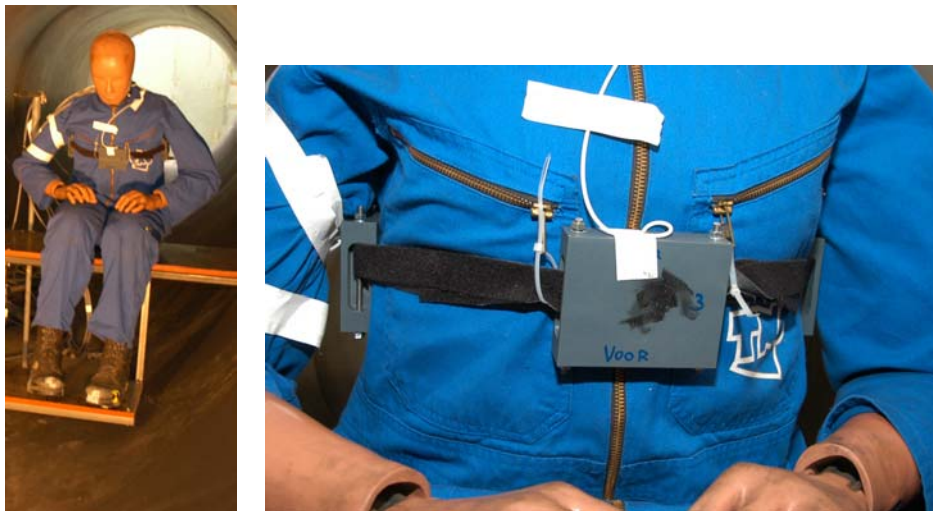


**Figure I.5: Example of Pressure Measurement Device on the Chest of an ATD.**

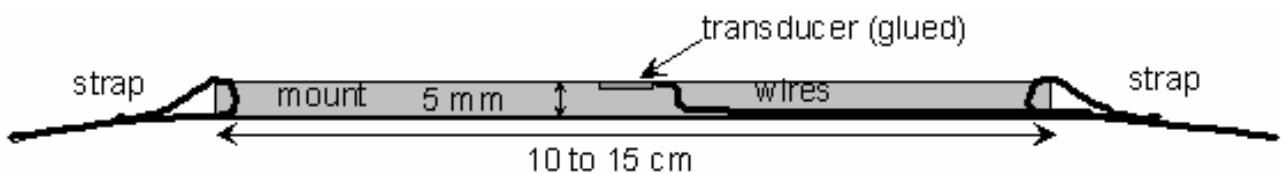


**Figure I.6: Example of a Flat Pressure Measurement Device.**

#### **I.1.4.2 Pressure Measurement Device at Another Position**

For another measurement position than the chest of the Hybrid III, it is necessary to have a plane as reflected area at or close to a crew position. This crew position should be the position where the highest overpressure might be expected. The back of the seat could be used as reflected area in combination with the same pressure measurement device as described above. The transducer should be orientated in the same direction and at the same height as the chest of a human being located on that position.

When no appropriate reflecting plane for the pressure measurement device is available, the original blast test device (cylinder) as described by Axelsson & Yelverton, [Axelsson, 1996], can be used (see Figure I.7).

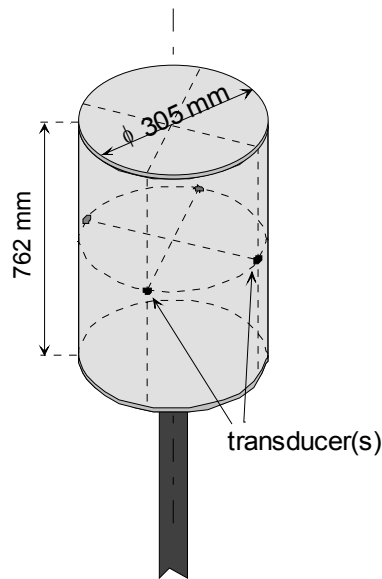


**Figure I.7: Example of a Cylinder for Pressure Measurements.**

The dimensions of this cylinder are: height of 762 mm, diameter of 305 mm. Although the human thorax has smaller dimensions it is suggested to follow the original blast test device dimensions and stay as close as possible to the original injury model.

The pressure transducer(s) should be fixed in or at the cylinder at half height. The material for the cylinder should be hard enough to protect the transducer and the wires and to reflect sufficiently the incident pressure.

When the frontal direction (chest direction) for the measurement location is known, at least one single transducer in the cylinder is needed in the same frontal direction (like in case with an ATD). For a standing position and when the crew member at that position can face any direction 4 sensors have to be used. For the conservative approach in the injury assessment, the worst-case sensor in terms of peak velocity must be considered.

#### **I.1.4.3 Pressure Transducer Specifications**

For fixation on a plate, a flat transducer (< 1 mm) should be used. It can be glued or screwed on that plate.

For fixation in a plate or in the cylinder, other transducers can be used as long as the opening of the sensor is flat with the outer surface.

The following specifications are recommended for the pressure transducer:

- Full scale range > 300 kPa;
- Resonance frequency at least 50 kHz; and
- Time constant (transducer and amplifier) at least 200 ms.

#### **I.1.5 Data Acquisition**

The following parameters are important for the acquisition of the data:

- Trigger;

- Sample rate;
- Anti-aliasing filtering;
- Resolution; and
- Signal duration.

#### **I.1.5.1 Trigger**

It is recommended to use the mine initiation or detonation as trigger time (T<sub>0</sub>) for the data-acquisition systems. In case of more than one data-acquisition system and/or video-system, it is preferred to use the same trigger pulse.

#### **I.1.5.2 Sample Rate**

For ATD measurements only a minimum sampling rate of 10 kHz is specified in the specifications (SAE J211/1, [SAE, 2003]). However, to increase the accuracy of the output (to about 1%) for the mine loading situations, a sampling rate of 200 kHz or higher (at least 10 times the cut-off frequency of the anti-aliasing filter) is advised for ATD measurements. A sampling rate of 200 kHz to 1 MHz is advised for structural and pressure measurements.

#### **I.1.5.3 Anti-Aliasing Filtering**

The ATD-signals have to be filtered by (analogue) filters in the data-acquisition system to avoid aliasing and transducer resonance. It is up to the expertise of the measurement team to define the best filtering method and parameters. It is recommended to use a cut-off frequency of at least 10 kHz.

#### **I.1.5.4 Resolution**

Digital word lengths of at least 12 bits (including sign) should be used according to the standards (SAE J211/1, [SAE, 2003]) for the ATD measurements. However, based on experience in mine tests, higher digital word lengths are recommended for reasonable accuracy in case of low signal amplitude in relation to the maximum range of the sensors.

#### **I.1.5.5 Signal Duration**

The duration of signal measuring depends on the process and should include the initial loading phase and the global vehicle response inclusive the drop-down phase. For light weight vehicles (< 10 tons), this process can take 2 seconds as a maximum. A pre-signal (approximately 100 ms if the trigger origin is known) has to be stored for signal zeroing.

#### **I.1.6 Signal Processing**

After the tests, the measured signals have to be processed for the injury assessment:

- Signal zeroing; and
- Signal filtering.

Both the measured signals (raw data) and the processed signals have to be stored.

##### **I.1.6.1 Signal Zeroing**

The measured signals have to be corrected for zero offset errors before trigger time. For determining the offset, the average zero offset in the stored pre-signal should be taken.

### **I.1.6.2 Signal Filtering**

The signals of the ATD measurements have to be filtered by a low-pass (digital) filter routine according to the Channel Frequency Class (CFC) specifications as described in SAE J211/1 (revision December 2003) [SAE, 2003].

The following CFCs are defined:

- CFC1000, cut-off frequency 1650 Hz;
- CFC600, cut-off frequency 1000 Hz;
- CFC180, cut-off frequency 300 Hz; and
- CFC60, cut-off frequency 100 Hz.

A double 2-pole Butterworth low-pass filter method should be used for filtering. The following steps are prescribed for the phaseless filtering method (SAE J211/1, revision March 1995, [SAE, 1995]):

- Pass the original signal through the 2-pole Butterworth low-pass filter (1.25 \* cut-off frequency);
- Reverse the filtered signal;
- Pass the reversed signal through the 2-pole Butterworth low-pass filter again (1.25 \* cut-off frequency); and
- Reverse the signal again to get the filtered signal without phase shift.

By multiplying the cut-off frequency with the factor of 1.25 and use this in a numerical filter routine, a response is obtained conform the CFC-response as written in the SAE standard.

It is important to use an appropriate tool and computation method to apply above described steps and to choose the best signal parameters, like sample rate, with respect to this computation method.

The use of the Fast Fourier Transform (FFT) of the signals in the computation is recommended in the latest standard (see SAE J211/1, revision December 2003).

The following CFCs are specified for the measured ATD signals (SAE J211/1):

- |   |         |
|---|---------|
| • Head, Thorax and Pelvis accelerations                 | CFC1000 |
| • Neck forces   | CFC1000 |
| • Neck moments  | CFC600  |
| • Lumbar spine forces and moments                       | CFC600  |
| • Leg forces and moments (femur, knee, tibia and ankle) | CFC600  |
| • Belt forces   | CFC60   |

Note: It is recommended to use raw signals for overpressure injury assessment (no filtering).

## **I.2 DESCRIPTION OF INJURY ASSESSMENT**

### **I.2.1 Critical Body Parts**

In case of mine detonations under a military vehicle, the occupants are loaded by the shock, local structural motions and deformations and global vehicle motion. The following body parts are considered as the most vulnerable parts:

- Lower leg (foot/ankle/tibia-complex);

- Thoraco-lumbar spine region;
- Head/neck region; and
- Internal organs/systems (vulnerable to overpressure).

The qualification of a vehicle depends whether the body response for these body parts are below the tolerance levels that are defined. The response of the other body parts may still result in injury, but are assumed to be less critical, and therefore are not included in the mandatory injury criteria list.

**I.2.2 Injury Criteria**

The following list of injury criteria are mandatory and used as pass/fail criteria for the tested vehicle:

- Lower Tibia Axial Compression Force (Fz);
- Dynamic Response Index (DRIZ) for axial direction;
- Upper Neck Axial Compression Force (Fz);
- Upper Neck Flexion and Extension Moment at the occipital condyles (Myoc); and
- Chest Wall Velocity Predictor (CWVP) for non-auditory overpressure injuries.

In Table I.2 information is given about the tolerance values and injury levels for these criteria. The limit values are based on two important parameters in the injury biomechanics: injury severity and injury probability. The tolerance levels were established based on a guideline of a maximum of 10% risk of AIS 2 (moderate injuries). This implies that AIS 1 (minor) injuries are accepted too. Injury risk curves are not available for all body regions, but this guideline (10% risk of AIS 2+) was followed as much as possible to define the tolerance limits.

**Table I.2: Mandatory Criteria and Limit Values**

Body Region	Criteria	Tolerance Value	Signification	Reference
Lower leg	Peak lower tibia axial compression force (-Fz)	5.4 kN	10% risk of AIS 2+	[Yoganandan, 1996]
Thoraco-lumbar spine	Dynamic Response Index (DRIZ), calculated with pelvis Az	17.7	10% risk of AIS 2+	[Brinkley, 1970]
Cervical spine (neck)	Upper neck axial compression force (-Fz)	4.0 kN @ 0 ms 1.1 kN @ 30 ms (see curve in Figure I.8)	Serious (AIS 3) injuries are unlikely*	[Mertz, 1978]
	Upper Neck Moment: Flexion (+My <sub>oc</sub> ) Extension (-My <sub>oc</sub> )	190 Nm 57 Nm	Significant (AIS 2+) injuries are unlikely*	[Mertz, 1984]
Non-auditory internal organs	Chest Wall Velocity Predictor (CWVP)	3.6 m/s	No injury*	[Axelsson, 1996]

\* An injury risk curve is not available.



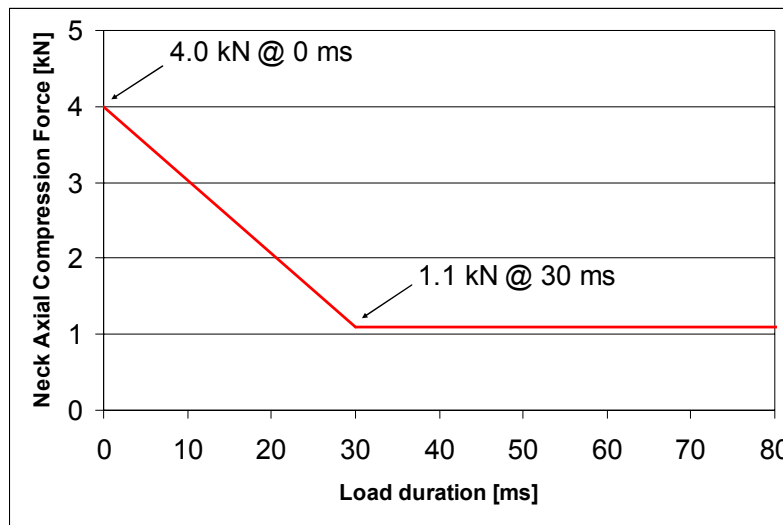


**Figure I.8: Neck Axial Compression Limit Curve.**

A description of the DRIZ and CWVP model is given below.

**I.2.2.1 DRIZ Model Description**

The Dynamic Response Index (DRIZ) is a criterion for axial compression injuries in the thoraco-lumbar spine. The DRIZ is a dimensionless value related to the spine deflection. This deflection is the output of a 2<sup>nd</sup> order mass-spring-damper system (see Figure I.9) with the vertical pelvis acceleration as the input.

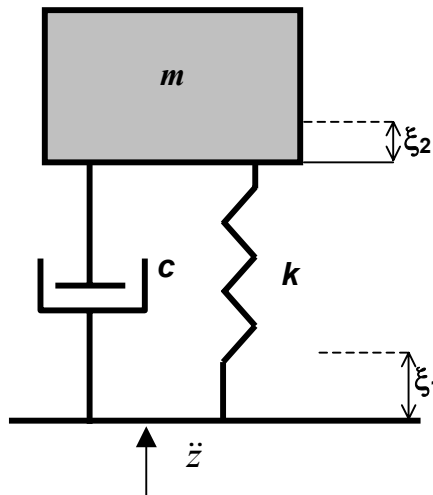


**Figure I.9: Mathematical Spine Model.**

The equation of motion for this model is:

$$\ddot{z}(t) = \ddot{\delta} + 2 \cdot \zeta \cdot \omega_n \cdot \dot{\delta} + \omega_n^2 \cdot \delta$$

where

- $\ddot{z}(t)$  is the acceleration in the vertical direction (in m/s<sup>2</sup>);

- $\delta = \xi_1 - \xi_2$  ( $>0$ ) is the deflection (compression) of the system;
- $\zeta = \frac{c}{2 \cdot m \cdot \omega_n}$  is the damping coefficient (0.224); and
- $\omega_n = \sqrt{\frac{k}{m}}$  is the natural frequency (52.9 rad/s).

The DRIZ is calculated with the maximum compression  $\delta_{\max}$ ,  $\omega_n$  and the gravity acceleration  $g$  (9.81 m/s<sup>2</sup>):

$$DRIZ = \frac{\omega_n^2 \cdot \delta_{\max}}{g}$$

Note: While the DRIZ-model is developed for **compression** injuries to the spine, the input acceleration signal should be positive for the loading direction causing this compression. In the standard coordinate system of the ATD, a negative acceleration signals causes this compression. This means that the output signal of the ATD needs to be multiplied by minus 1, before it can be used for calculating the DRIZ.

### I.2.2.2 CWV Model Description

The measured reflected overpressure ( $p(t)$ ) is used as input for the Chest Wall Velocity model as described below (see Figure I.10).

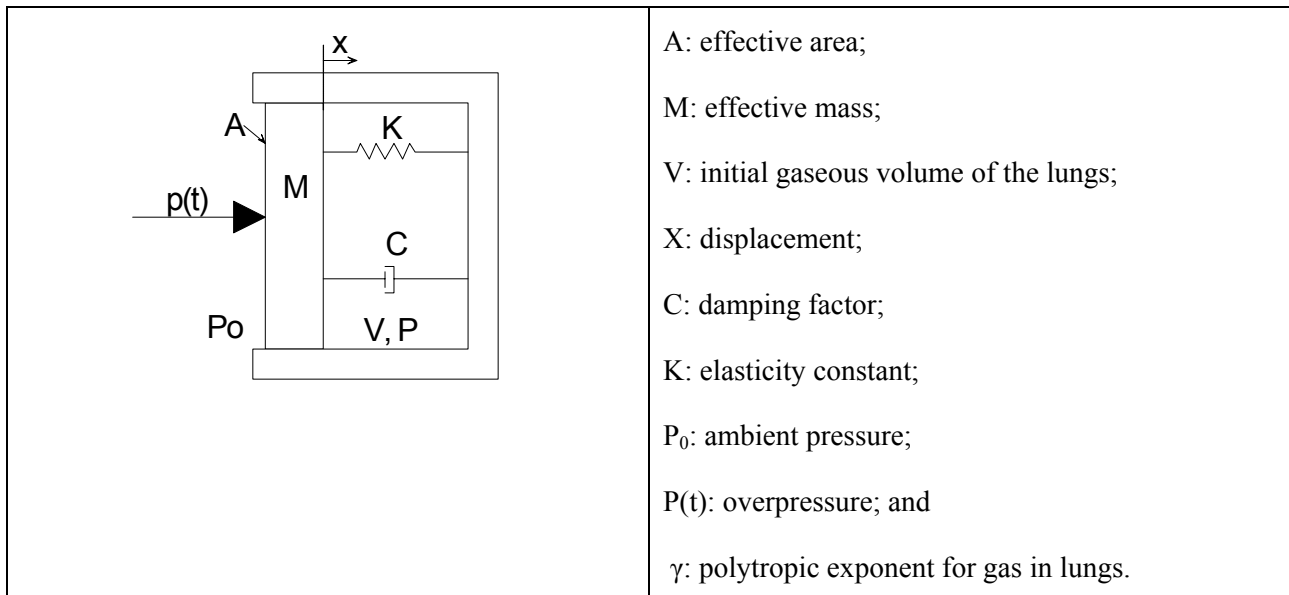


**Figure I.10: Thorax Model.**

$$M \cdot \frac{d^2x}{dt^2} + C \cdot \frac{dx}{dt} + K \cdot x = A \cdot \left[ p(t) + P_0 - \left( \frac{V}{V - A \cdot x} \right)^\gamma \cdot P_0 \right]$$

The model is a second order (nonlinear) differential equation and the following values for the model constants have to be used (based on a 70 kg man):

- $A = 0.082 \text{ m}^2$
- $M = 2.03 \text{ kg}$
- $C = 696 \text{ Ns/m}$
- $K = 989 \text{ N/m}$
- $V = 1.82 * 10^{-3} \text{ m}^3$
- $P_0 = 1.0 * 10^5 \text{ Pa}$
- $\gamma = 1.2$

For the injury assessment, the velocity (dx/dt) profile has to be calculated. This velocity is called the Chest Wall Velocity Predictor (CWVP).

### **I.2.3 Injury Assessment**

The processed signals are input for the injury assessment following the mandatory injury criteria. The outcome is compared to the defined tolerance levels, which results in a pass or a fail of the vehicle.

#### **I.2.3.1 Lower Leg**

For lower leg injury assessment the measured axial force ( $F_z$ ) in the lower tibia has to be used. The peak value for the compression force (negative part) has to be determined.

Pass:  $|F_{z_p}| < F_{z_c}$

Fail:  $|F_{z_p}| \geq F_{z_c}$

- $F_{z_p}$  [kN]: The peak value (maximum amplitude) in the compression (negative) part of the axial force signal in the lower tibia.
- $F_{z_c}$  [kN]: The critical limit value given in Table I.2.

This lower leg injury assessment has to be done for both the left and the right leg.

#### **I.2.3.2 Thoraco-Lumbar Spine**

For the spine injury assessment the measured vertical acceleration ( $A_z$ ) in the pelvis has to be used as input. Note: take care of the polarity of the acceleration system (see Section I.2.1 for the DRIZ-description).

Pass:  $DRIZ_p < DRIZ_c$

Fail:  $DRIZ_p \geq DRIZ_c$

- $DRIZ_p$  [-]: The peak value (maximum amplitude) in the compression (positive) part of the output of the DRI-routine.
- $DRIZ_c$  [-]: The critical limit value for the DRIZ given in Table I.2.

The complete acceleration signal has to be used as input for the routine to calculate the Dynamic Response Index. It is expected to find the maximum DRIZ value in the initial phase (in general within 100 ms). The DRIZ-value in the drop-down phase when the vehicle hits the ground surface should be checked and compared with the DRIZ in the initial phase to see which one is the highest. It is advised to use a plot of

the simulated spine deflection as check for the time-step at which the maximum spine compression (in the initial phase) and thus the maximum DRIZ-value is reached. Take care of drift in the pelvis acceleration signal, while this could give too high DRIZ-values at other time steps.

### I.2.3.3 Neck Injury

The measured axial force ( $F_z$ ) and the measured flexion/extension bending moment ( $M_y$ ) in the upper neck should be used as input for the neck injury assessment.

#### I.2.3.3.1 Axial Compression Force Criterion

Both the peak value of the compression force (negative part) and the duration of the compression force levels have to be determined. The method to determine the duration is given in the standard SAE J1727, [SAE, 1996], and described below.

Pass:  $|F_z(\delta)| < F_{z_c}\text{-curve}$

Fail:  $|F_z(\delta)| \geq F_{z_c}\text{-curve}$

- $F_z(\delta)$  [kN]: The compression force as function of the load duration.
- $F_{z_c}$  [kN]: The critical limit curve given in Figure I.11.

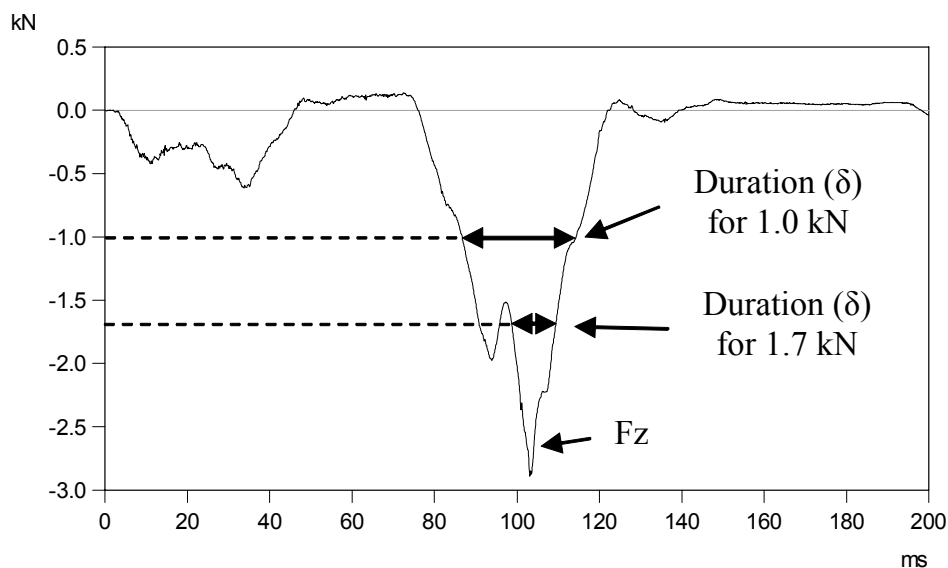


**Figure I.11: Example of Defining the Maximum Duration for Two Load Levels.**

The duration of the load does not need to be calculated when:

Pass:  $|F_{z_p}| < \text{lowest limit value of the } F_{z_c}\text{-curve (1.1 kN)}$

Fail:  $|F_{z_p}| \geq \text{highest limit value of the } F_{z_c}\text{-curve (4.0 kN)}$

- $F_{z_p}$  [kN]: The peak value (maximum amplitude) in the compression (negative) part of the axial force signal in the upper neck.

The following steps have to be followed to determine the duration of the loading, as described in SAE J1727 [SAE, 1996]:

- Determine the maximum value of the compression load and assign a duration of zero to it.

- Create a matrix of two columns and 101 rows. In the first column the load levels from maximum to zero will be stored. Each subsequent load value will be equal to the previous minus 1/100 of the peak value.
- For each load level, determine the maximum continuous time interval that the measured load exceeds this level and store this in the second column, see Figure I.11.
- Plot the points of the matrix in the criterion graph, see Figure I.8.

#### *I.2.3.3.2 Flexion/Extension Moment Criterion*

The flexion- extension moment at the occipital condyles is calculated using the formula:

$$My_{oc} = My - Fx * d$$

- $My_{oc}$  [Nm]: The flexion-extension moment around the occipital condyles;
- $My$  [Nm]: The measured flexion-extension moment in the Hybrid III upper neck;
- $Fx$  [N]: The measured shear force in x-direction in the Hybrid III upper neck;
- $d$  [m]: The lever arm of the upper load cell, see [Vehicle safety workgroup, 2005]  
 $d = 0.01778$  (for the 6-axis load cell, 50%-tile Hybrid III).

The peak value in the flexion moment (positive part of the  $My_{oc}$ -signal) has to be determined.

Pass:  $My_{oc\_p+} < My_{oc\_c+}$

Fail:  $My_{oc\_p+} \geq My_{oc\_c+}$

- $My_{oc\_p+}$  [Nm]: The peak value (maximum amplitude) in the flexion moment in the upper neck;
- $My_{oc\_c+}$  [Nm]: The critical limit value for flexion as given in Table I.2.

The peak value in the extension moment (negative part of the  $My_{oc}$ -signal) has to be determined.

Pass:  $|My_{oc\_p-}| < My_{oc\_c-}$

Fail:  $|My_{oc\_p-}| \geq My_{oc\_c-}$

- $My_{oc\_p-}$  [Nm]: The peak value (maximum amplitude) in the extension moment in the upper neck;
- $My_{oc\_c-}$  [Nm]: The critical limit value for extension as given in Table I.2.

#### **I.2.3.4 Overpressure Injury**

The peak value of the Chest Wall Velocity Predictor (CWVP), which is the output of the CWV model for a measured pressure signal, has to be determined.

Pass:  $|CWVP_p| < CWVP_c$

Fail:  $|CWVP_p| \geq CWVP_c$

- $CWVP_p$  [m/s]: The peak value (maximum amplitude) of the Chest Wall Velocity Predictor calculated by the numerical model for a measured overpressure signal.
- $CWVP_c$  [m/s]: The critical limit value of the CWVP given in Table I.2.

### **I.3 REFERENCES**

- Axelsson, H. and Yelverton, J.T. (1996), Chest Wall Velocity as a Predictor of Non-Auditory Blast Injury in a Complex Blast Wave Environment, *The Journal of Trauma, Injury, Infection and Critical Care*.
- Brinkley, J.W. and Shaffer, J.T. (1970), Dynamic Simulation Techniques for the Design of Escape Systems: Current Applications and Future Air Force Requirements, Symposium on Biodynamic Models and their Applications, Report No. AMRL-TR-71-29, Aerospace Medical Research Laboratory, Wright-Patterson Air Force Base, Ohio, USA.
- CFR 49 (2003), Code of Federal Rules (CFR), Title 49-Transportation, Chapter V – National Highway Traffic Safety Administration (NHTSA), Department of Transportation, Part 571, Federal Motor Vehicle Safety Standard (FMVSS) 208.
- Denton, R.A. Inc. (2002), Instrumented Lower Leg Assembly, Patent No. 4, 488, 433.
- Denton, R.A. Inc. (1984), Crash Test Dummy Lower Leg Structure, Patent No. 4, 488, 433.
- Mertz, H.J., Hodgson, V.R., Murray Thomas, L. and Nyquist, G.W. (1978), An assessment of Compressive Neck Loads Under Injury-Producing Conditions, *The Physician and Sport Medicine*, November.
- Mertz, H.J. (1984), Injury Assessment Values Used to Evaluate Hybrid III Response Measurements, NHTSA Docket 74-14, Notice 32, Enclosure 2 of Attachment I of Part III of General Motors Submission USG 2284, March 22.
- SAE J1727 (1996), Surface Vehicle Recommended Practice, Injury Calculations Guidelines, Issued August.
- SAE J211/1 (1995), Surface Vehicle Recommended Practice, (R) Instrumentation for Impact Test – Part 1 – Electronic Instrumentation, Revision March.
- SAE J211/1 (2003), Surface Vehicle Recommended Practice, (R) Instrumentation for Impact Test – Part 1 – Electronic Instrumentation, Revision December.
- SAE (1998), Society of Automotive Engineers, User’s Manual for the 50<sup>th</sup> Percentile Male Hybrid III Test Dummy, Dummy Testing Equipment Subcommittee, SAE Engineering Aid 23, June.
- Title 49 – Transportation Chapter V – National Highway Traffic Safety Administration (NHTSA), Department of Transportation, Part 572 – Anthropomorphic Test Device.
- Vehicle Safety Workgroup, (2005), Crash Analysis Criteria Version 1.6.2, Arbeitskreis Messdatenverarbeitung Fahrzeugsicherheit, April 2005.
- Yoganandan, N., Pintar, F.A., Boyton, M., Begeman, P., Prasad, P., Kuppa, S.M., Morgan, R.M. and Eppinger, R.H. (1996), Dynamic Axial Tolerance of the Human Foot-Ankle Complex, 962426, Society of Automotive Engineers, Warrendale, PA, USA.

<b>REPORT DOCUMENTATION PAGE</b>			
<b>1. Recipient's Reference</b>	<b>2. Originator's References</b>	<b>3. Further Reference</b>	<b>4. Security Classification of Document</b>
	RTO-TR-HFM-090 AC/323(HFM-090)TP/72	ISBN 978-92-837-0068-5	UNCLASSIFIED/ UNLIMITED
<b>5. Originator</b>	Research and Technology Organisation North Atlantic Treaty Organisation BP 25, F-92201 Neuilly-sur-Seine Cedex, France		
<b>6. Title</b>	Test Methodology for Protection of Vehicle Occupants against Anti-Vehicular Landmine Effects		
<b>7. Presented at/Sponsored by</b>	Final Report of HFM-090 Task Group 25.		
<b>8. Author(s)/Editor(s)</b>	Multiple	<b>9. Date</b>	April 2007
<b>10. Author's/Editor's Address</b>	Multiple	<b>11. Pages</b>	176
<b>12. Distribution Statement</b>	There are no restrictions on the distribution of this document. Information about the availability of this and other RTO unclassified publications is given on the back cover.		
<b>13. Keywords/Descriptors</b>	Antitank mines Anti-vehicular mines Armoured vehicles Blast effects Blast loads Computer modelling Damage assessment Design Dynamic response	Experimental data Explosion effects Field tests Ground vehicles Human factors engineering Land mines Methodology Mine countermeasures	Protection Simulators Soft-skinned vehicles Specifications Standards Survivability Trucks Vulnerability
<b>14. Abstract</b>	<p>In 2001, the NATO/RTO HFM-090/TG-25 was created in response to the NATO/RTO HFM ET-007, which identified the lack of suitable information for injury assessment of the anti-vehicle mine threat. Furthermore, the Task Group was asked to help the STANAG 4569 Team of Experts to develop an injury assessment methodology for the qualification of light-armoured and logistic vehicles (blast) landmines protection systems.</p> <p>Injury criteria, tolerance levels and measurement methods were proposed to assess the most vulnerable body regions to a blast mine strike under a vehicle. The tolerance levels established for these body regions are considered to represent low risk of life-threatening and disabling injuries. The results, conclusions and recommendations of the HFM-090/TG-25 work are presented in the technical report.</p>		







BP 25  
F-92201 NEUILLY-SUR-SEINE CEDEX • FRANCE  
Télécopie 0(1)55.61.22.99 • E-mail [mailbox@rta.nato.int](mailto:mailbox@rta.nato.int)



**DIFFUSION DES PUBLICATIONS**  
**RTO NON CLASSIFIEES**

Les publications de l'AGARD et de la RTO peuvent parfois être obtenues auprès des centres nationaux de distribution indiqués ci-dessous. Si vous souhaitez recevoir toutes les publications de la RTO, ou simplement celles qui concernent certains Panels, vous pouvez demander d'être inclus soit à titre personnel, soit au nom de votre organisation, sur la liste d'envoi.

Les publications de la RTO et de l'AGARD sont également en vente auprès des agences de vente indiquées ci-dessous.

Les demandes de documents RTO ou AGARD doivent comporter la dénomination « RTO » ou « AGARD » selon le cas, suivi du numéro de série. Des informations analogues, telles que le titre et la date de publication sont souhaitables.

Si vous souhaitez recevoir une notification électronique de la disponibilité des rapports de la RTO au fur et à mesure de leur publication, vous pouvez consulter notre site Web ([www.rta.nato.int](http://www.rta.nato.int)) et vous abonner à ce service.

### CENTRES DE DIFFUSION NATIONAUX

#### ALLEMAGNE

Streitkräfteamt / Abteilung III  
Fachinformationszentrum der  
Bundeswehr (FIZBw)  
Gorch-Fock-Straße 7, D-53229 Bonn

#### BELGIQUE

Etat-Major de la Défense  
Département d'Etat-Major Stratégie  
ACOS-STRAT – Coord. RTO  
Quartier Reine Elisabeth  
Rue d'Evère, B-1140 Bruxelles

#### CANADA

DSIGRD2 – Bibliothécaire des ressources du savoir  
R et D pour la défense Canada  
Ministère de la Défense nationale  
305, rue Rideau, 9<sup>e</sup> étage  
Ottawa, Ontario K1A 0K2

#### DANEMARK

Danish Acquisition and Logistics  
Organization (DALO)  
Lautrupbjerg 1-5  
2750 Ballerup

#### ESPAGNE

SDG TECEN / DGAM  
C/ Arturo Soria 289  
Madrid 28033

#### ETATS-UNIS

NASA Center for AeroSpace Information (CASI)  
7115 Standard Drive  
Hanover, MD 21076-1320

#### FRANCE

O.N.E.R.A. (ISP)  
29, Avenue de la Division Leclerc  
BP 72, 92322 Châtillon Cedex

#### GRECE (Correspondant)

Defence Industry & Research  
General Directorate  
Research Directorate  
Fakinos Base Camp, S.T.G. 1020  
Holargos, Athens

#### HONGRIE

Department for Scientific Analysis  
Institute of Military Technology  
Ministry of Defence  
P O Box 26  
H-1525 Budapest

#### ISLANDE

Director of Aviation  
c/o Flugrad  
Reykjavik

#### ITALIE

Centro di Documentazione  
Tecnico-Scientifica della Difesa  
Via XX Settembre 123  
00187 Roma

#### LUXEMBOURG

*Voir Belgique*

#### NORVEGE

Norwegian Defence Research  
Establishment  
Attn: Biblioteket  
P.O. Box 25  
NO-2007 Kjeller

#### PAYS-BAS

Royal Netherlands Military  
Academy Library  
P.O. Box 90.002  
4800 PA Breda

#### POLOGNE

Centralny Ośrodek Naukowej  
Informacji Wojskowej  
Al. Jerozolimskie 97  
00-909 Warszawa

#### PORTUGAL

Estado Maior da Força Aérea  
SDFA – Centro de Documentação  
Alfragide  
P-2720 Amadora

#### REPUBLIQUE TCHEQUE

LOM PRAHA s. p.  
o. z. VTÚLaPVO  
Mladoboleslavská 944  
PO Box 18  
197 21 Praha 9

#### ROUMANIE

Romanian National Distribution  
Centre  
Armaments Department  
9-11, Drumul Taberei Street  
Sector 6, 061353, Bucharest

#### ROYAUME-UNI

Dstl Knowledge Services  
Information Centre  
Building 247  
Dstl Porton Down  
Salisbury  
Wiltshire SP4 0JQ

#### TURQUIE

Milli Savunma Bakanlığı (MSB)  
ARGE ve Teknoloji Dairesi  
Başkanlığı  
06650 Bakanlıklar – Ankara

### AGENCES DE VENTE

#### NASA Center for AeroSpace Information (CASI)

7115 Standard Drive  
Hanover, MD 21076-1320  
ETATS-UNIS

#### The British Library Document Supply Centre

Boston Spa, Wetherby  
West Yorkshire LS23 7BQ  
ROYAUME-UNI

#### Canada Institute for Scientific and Technical Information (CISTI)

National Research Council Acquisitions  
Montreal Road, Building M-55  
Ottawa K1A 0S2, CANADA

Les demandes de documents RTO ou AGARD doivent comporter la dénomination « RTO » ou « AGARD » selon le cas, suivie du numéro de série (par exemple AGARD-AG-315). Des informations analogues, telles que le titre et la date de publication sont souhaitables. Des références bibliographiques complètes ainsi que des résumés des publications RTO et AGARD figurent dans les journaux suivants :

#### Scientific and Technical Aerospace Reports (STAR)

STAR peut être consulté en ligne au localisateur de ressources uniformes (URL) suivant :

<http://www.sti.nasa.gov/Pubs/star/Star.html>

STAR est édité par CASI dans le cadre du programme NASA d'information scientifique et technique (STI)  
STI Program Office, MS 157A  
NASA Langley Research Center  
Hampton, Virginia 23681-0001  
ETATS-UNIS

#### Government Reports Announcements & Index (GRA&I)

publié par le National Technical Information Service  
Springfield

Virginia 2216

ETATS-UNIS

(accessible également en mode interactif dans la base de données bibliographiques en ligne du NTIS, et sur CD-ROM)



BP 25

F-92201 NEUILLY-SUR-SEINE CEDEX • FRANCE  
Télécopie 0(1)55.61.22.99 • E-mail [mailbox@rta.nato.int](mailto:mailbox@rta.nato.int)



**DISTRIBUTION OF UNCLASSIFIED  
RTO PUBLICATIONS**

AGARD & RTO publications are sometimes available from the National Distribution Centres listed below. If you wish to receive all RTO reports, or just those relating to one or more specific RTO Panels, they may be willing to include you (or your Organisation) in their distribution.

RTO and AGARD reports may also be purchased from the Sales Agencies listed below.

Requests for RTO or AGARD documents should include the word 'RTO' or 'AGARD', as appropriate, followed by the serial number. Collateral information such as title and publication date is desirable.

If you wish to receive electronic notification of RTO reports as they are published, please visit our website ([www.rta.nato.int](http://www.rta.nato.int)) from where you can register for this service.

**NATIONAL DISTRIBUTION CENTRES**

**BELGIUM**

Etat-Major de la Défense  
Département d'Etat-Major Stratégie  
ACOS-STRAT – Coord. RTO  
Quartier Reine Elisabeth  
Rue d'Evère  
B-1140 Bruxelles

**CANADA**

DRDKIM2  
Knowledge Resources Librarian  
Defence R&D Canada  
Department of National Defence  
305 Rideau Street, 9<sup>th</sup> Floor  
Ottawa, Ontario K1A 0K2

**CZECH REPUBLIC**

LOM PRAHA s. p.  
o. z. VTÚLaPVO  
Mladoboleslavská 944  
PO Box 18  
197 21 Praha 9

**DENMARK**

Danish Acquisition and Logistics  
Organization (DALO)  
Lautrupbjerg 1-5  
2750 Ballerup

**FRANCE**

O.N.E.R.A. (ISP)  
29, Avenue de la Division Leclerc  
BP 72  
92322 Châtillon Cedex

**GERMANY**

Streitkräfteamt / Abteilung III  
Fachinformationszentrum der  
Bundeswehr (FIZBw)  
Gorch-Fock-Straße 7  
D-53229 Bonn

**GREECE (Point of Contact)**

Defence Industry & Research  
General Directorate  
Research Directorate  
Fakinos Base Camp  
S.T.G. 1020  
Holargos, Athens

**HUNGARY**

Department for Scientific Analysis  
Institute of Military Technology  
Ministry of Defence  
P O Box 26  
H-1525 Budapest

**ICELAND**

Director of Aviation  
c/o Flugrad, Reykjavik

**ITALY**

Centro di Documentazione  
Tecnico-Scientifica della Difesa  
Via XX Settembre 123  
00187 Roma

**LUXEMBOURG**

See Belgium

**NETHERLANDS**

Royal Netherlands Military  
Academy Library  
P.O. Box 90.002  
4800 PA Breda

**NORWAY**

Norwegian Defence Research  
Establishment  
Attn: Biblioteket  
P.O. Box 25  
NO-2007 Kjeller

**POLAND**

Centralny Ośrodek Naukowej  
Informacji Wojskowej  
Al. Jerozolimskie 97  
00-909 Warszawa

**PORTUGAL**

Estado Maior da Força Aérea  
SDFA – Centro de Documentação  
Alfragide  
P-2720 Amadora

**ROMANIA**

Romanian National Distribution Centre  
Armaments Department  
9-11, Drumul Taberei Street  
Sector 6, 061353, Bucharest

**SPAIN**

SDG TECEN / DGAM  
C/ Arturo Soria 289  
Madrid 28033

**TURKEY**

Milli Savunma Bakanlığı (MSB)  
ARGE ve Teknoloji Dairesi Başkanlığı  
06650 Bakanlıklar – Ankara

**UNITED KINGDOM**

Dstl Knowledge Services  
Information Centre  
Building 247  
Dstl Porton Down  
Salisbury, Wiltshire SP4 0JQ

**UNITED STATES**

NASA Center for AeroSpace  
Information (CASI)  
Parkway Center  
7121 Standard Drive  
Hanover, MD 21076-1320

**SALES AGENCIES**

**NASA Center for AeroSpace  
Information (CASI)**

Parkway Center  
7121 Standard Drive  
Hanover, MD 21076-1320  
UNITED STATES

**The British Library Document  
Supply Centre**

Boston Spa, Wetherby  
West Yorkshire LS23 7BQ  
UNITED KINGDOM

**Canada Institute for Scientific and  
Technical Information (CISTI)**

National Research Council  
Acquisitions  
Montreal Road, Building M-55  
Ottawa K1A 0S2, CANADA

Requests for RTO or AGARD documents should include the word 'RTO' or 'AGARD', as appropriate, followed by the serial number (for example AGARD-AG-315). Collateral information such as title and publication date is desirable. Full bibliographical references and abstracts of RTO and AGARD publications are given in the following journals:

**Scientific and Technical Aerospace Reports (STAR)**

STAR is available on-line at the following uniform resource locator:

<http://www.sti.nasa.gov/Pubs/star/Star.html>

STAR is published by CASI for the NASA Scientific and Technical Information (STI) Program  
STI Program Office, MS 157A  
NASA Langley Research Center  
Hampton, Virginia 23681-0001  
UNITED STATES

**Government Reports Announcements & Index (GRA&I)**

published by the National Technical Information Service  
Springfield  
Virginia 2216  
UNITED STATES  
(also available online in the NTIS Bibliographic Database or on CD-ROM)